Isospin Breaking in Kaon Decays to Pions

Fredrik Borg

Department of Theoretical Physics
Lund University, Sweden

Thesis for the degree of Doctor of Philosophy

Thesis Advisor: Johan Bijnens

Faculty Opponent: Antonio Pich

To be presented, with the permission of the Faculty of Natural Sciences of Lund University, for public criticism in Lecture Hall F of the Department of Theoretical Physics on Friday, the 28th of January 2005, at 10.30 a.m.

DOKUMENTDATABLAD
enl SIS 61 41 21

Organization

LUND UNIVERSITY
Department of Theoretical Physics
Sölvegatan 14A
SE-223 62 LUND

Document Name
DOCTORAL DISSERTATION

Date of issue
January 2005

CODEN:

Author(s)
Fredrik Borg

Sponsoring organization

Title and subtitle

Isospin Breaking in Kaon Decays to Pions

Abstract

The five different K -> 3 Pi and the three K -> 2 Pi decays are calculated in Chiral Perturbation Theory.
The calculation is done using different approximations, to study whether this changes the result significantly. First the isospin approximation is used. Discrepancies are then found between theory and experiment. Further calculations without the isospin approximation are then done to see if this solves the found problems. The purpose is two-fold. To test the validity of Chiral Perturbation Theory and to fix some of the unknown parameters in the theory.

Summary in Swedish

Amplituden för fem olika processer av typen K -> 3 Pi och tre olika av K -> 2 Pi har beräknats i kiral störningsteori.
Beräkningen har genomförts flera gånger med olika approximationer. Först används isospin-approximationen, men detta resulterar i diskrepanser mellan teori och experiment. I följande beräkningar tas isospin-approximationen bort i två steg, för att se om denna är förklaringen till uppkomna diskrepanser.
Arbetet motiveras dels genom dess kontroll av den kirala störnings-teorin och dels genom resulterande bestämning av några fria parametrar i teorin.

Key words
Strong interactions, weak interactions, pseudoscalar mesons, Chiral Perturbation Theory, decays, isospin breaking.

Classification system and/or index terms (if any)

Supplementary bibliographical information

Language
English

ISSN and key title

ISBN
91-628-6347-9

Recipient's notes

Number of pages
165

Price

Security classification

Distribution by (name and address)
Fredrik Borg, Dept. of Theoretical Physics,
Sölveg. 14A, SE-223 62 Lund

Signature ______________________ **Date** 2004-XX-XX

To my family

This thesis is based on the following publications:

I Johan Bijnens, Pierre Dhonte and Fredrik Persson,
$K \to 3\pi$ **Decays in Chiral Perturbation Theory**,
Nucl. Phys. B **648** (2003) 317,
LU TP 02-21.

II Johan Bijnens and Fredrik Borg,
Isospin Breaking in $K \to 3\pi$ **Decays I: Strong Isospin Breaking**,
Nucl. Phys. B **697** (2004) 319,
LU TP 04-20.

III Johan Bijnens and Fredrik Borg,
Isospin Breaking in $K \to 3\pi$ **Decays II: Radiative Corrections**,
Accepted for publication in The European Physical Journal C,
LU TP 04-37.

IV Johan Bijnens and Fredrik Borg,
Isospin Breaking in $K \to 3\pi$ **Decays III: Bremsstrahlung and Fit to Experiment**,
LU TP 04-40.

Contents

Outlook

> From the moment I picked up your book until I laid it down, I was convulsed with laughter. Some day I intend reading it.
>
> *Groucho Marx*

There are at least two reasons to write an introduction to this thesis. One of them is of course to provide the scientific background needed to be able to understand the papers presented in the later part of the thesis. In scientific papers there is usually not much room to go into the background information, which means that they are very hard to read for anyone not in the field themselves. In a thesis the restrictions are not the same, and I will use this to provide a more elaborate background. This is presented in the Introduction part II.

The other, and just as important, reason is that some people may only be interested in reading the introduction and not continuing to the details in the papers. These people have a very varying knowledge of physics and mathematics but may still find it interesting to try to understand something of what I have been doing over the last four years. Therefore, I will start with writing Introduction part I where the intention is that it should be accessible to someone with little or no physics or mathematics education.

However, those people should be aware that it will not be an easy read. It will require motivation and concentration, and some parts may have to be read more than once. My hope is however that they will find this experience satisfying and well worth the effort, because along the way they will indeed learn something of how the universe works.

Introduction part I

The beginning of knowledge is the discovery of something we do not understand.

Frank Herbert

For some reason, understanding how things work has always fascinated me. This has over the years been obvious in many ways, but maybe most so through my obsession with rules. I want to immediately make clear that this has absolutely nothing to do with rules or principles of life, since such can easily be over-used. What I mean is rules of various games, e.g. board games. I have always found playing such games highly entertaining, and although this is in no way uncommon, my interest in reading and knowing the rules very well has never been equaled by other people in my surroundings. Therefore, it is very natural for me to look at particle physics as *"The Game of the Universe"*, and I will use this idea as a tool to describe it.

When you open a newly-bought board game, usually a lot of weird cards and pieces fall out. To understand how to play the game you have to understand what those pieces are, how they work and the way in which they affect each other. It is exactly the same with understanding the world of particle physics; you just have to know the pieces (the different particles) and how they influence each other (their interactions).

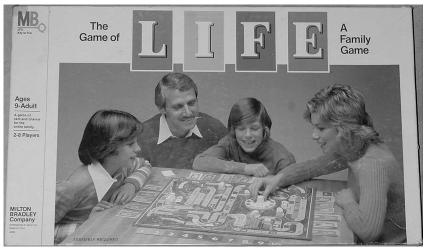

In the rest of this introduction I will try to describe how to play *"The Game of the Universe"*, and if there are some rules that are unclear, don't hesitate to try to find complementary information elsewhere.

The physics described can be found in many places. Some references are [1–5]. Many of the pictures are taken from The Particle Adventure, Lawrence Berkeley National Lab (`http://particleadventure.org/`).

The Particles

> Get your facts first, and then you can distort them as much as you please.
>
> *Mark Twain*

In describing *"The Game of the Universe"* I will start with the particles. They can be seen as the many different pieces in the game, all with different shape and colour. Of course, during the game some of these may combine to form bigger and more complicated pieces, but to understand how everything works it is best to start with understanding the basic building blocks, i.e. the smallest pieces in the universe.

In a very complicated universe there may be thousands of different building blocks and that would then be considered a very difficult game. On the other hand some games may only have one type of particle, and that would probably be very easy to understand. Our game lies somewhere in between; in the universe there are 12 basic building blocks corresponding to 12 different pieces in the game.

These pieces all look different, e.g. some are big and some are small, but there are some similarities and based on that it would be natural to group them together in various ways. Half of the pieces look almost like pieces of a puzzle. They seem to be constructed to fit together two or three at a time. The other six don't have this feature so one might expect that they enter the game one at a time. That is obviously an important difference so let's understand them separately six at a time.

I start with the puzzle-pieces (*the quarks*) and then the stand-alones (*the leptons*).

The Quarks

There are six different pieces that look like they can be fitted together two or three at a time. We call them collectively the quarks. But since they are all different we have to give them individual names and starting with the lightest one they are called up-quark (u), down-quark (d), strange-quark (s), charm-quark (c), bottom-quark (b) and top-quark (t), with top being the heaviest one. These quarks are very important in the universe. As the game proceeds bigger pieces will be built from the smaller ones and the quarks are the main building blocks , i.e. they are the pieces that build up the universe and most things in it.

It turns out that there is a very important reason that they are puzzle-shaped; they simply can not enter the game on their own, but always have to be put together first. In other words there are no free quarks in the universe, they always appear two or three together. This is indeed interesting and a very important rule to remember. The bigger particles, consisting of two or three quarks, are called *hadrons*.

Even if there are only six of them one can put them together in very many different ways, creating most of the different things in the universe. One can e.g. put together two up-quarks and a down-quark (uud) and the resulting hadron we call a proton, or two down-quarks and one up-quark (udd) which is a neutron. You might remember that protons and neutrons are what all the different materials on earth are made of, and that is part of the game of course.

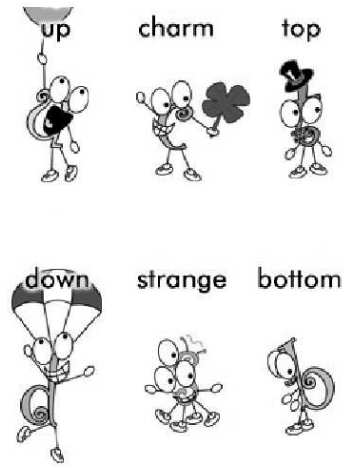

But quarks can also come together as a pair. However, before going on and giving the rules for quark-pairs, I have to admit that I have been cheating. There are more than six quarks in the game, in fact there are twelve. This sounds horrible since that might mean that we have to learn six new rules. Fortunately it is not that bad. The six additional ones are just the exact opposite of the ones that I already mentioned. We don't have to learn new rules, instead we just remember to treat them in exactly the opposite way. For example if the up-quark (u) piece would be black and move to the left, the anti-up ($\bar{u}$) would be white and move to the right and so on. As indicated, the six *anti-quarks* are denoted ($\bar{u}, \bar{d}, \bar{s}, \bar{c}, \bar{b}, \bar{t}$).

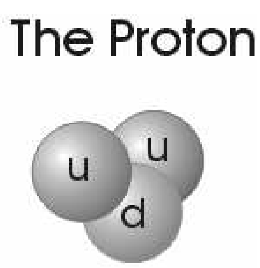

The reason for this introduction of the anti-quarks is that they are needed to explain how quarks form pairs. It is in fact not two quarks that form a hadron, but instead one quark and one anti-quark. One can e.g. put together an up-quark and an anti-strange-quark ($u\bar{s}$) to create a hadron called K^+ and an anti-up-quark and a down-quark ($\bar{u}d$) to form another hadron named π^- (this has nothing to do with 3.14159, it is just the name of the particle).

In fact there are a whole group of particles called K (kaons) and another group called π (pions), and as you might guess from the title of this thesis, those two types of particles are very important for the work presented in the papers in the latter part. Because, when you dig a little deeper in the rules, you realize that there are lots of small details, which take a lot of time to find out and understand, and that is what the papers are about. Luckily we don't have to worry about that here. Let's instead continue with the other six particles (the leptons).

The Leptons

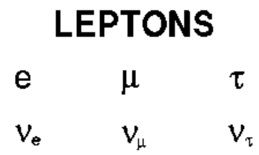

The pieces in the game representing the leptons enter the game on their own. The most famous lepton is the electron (e), which most people have heard of, but there are five more. The electron piece seems to be somehow connected with the electron-neutrino (ν_e), which is one of the other leptons. The reason for this is not obvious right now but will be covered in a later section of the rules. The remaining four leptons are also grouped in pairs: the muon (μ) and the muon-neutrino (ν_μ) and the tau (τ) and the tau-neutrino (ν_τ).

My research doesn't have much to do with the leptons so I will not talk too much about them here. However, I can mention that there are in fact six *anti-leptons* as well, but just as with the quarks, they just behave exactly opposite to the ordinary leptons.

We have now described all of the pieces (particles) in *"The Game of the Universe"*. What is left to understand is what can happen to those particles during the game.

The Interactions

The trouble with facts is that there are so many of them.

Samuel McChord Crothers

The interactions can be seen as the various cards that are included in the game. During the game you can play a card and depending on what card you play, something happens to the pieces (particles). In *"The Game of the Universe"* there are four types of cards. i.e. there are four types of interactions that can affect the particles. That is all that is needed to explain everything in the universe: twelve different particles (and their anti-particles) and four types of interactions. The names of the cards are "The Electromagnetic Interaction", "The Gravitational Interaction", "The Weak Interaction" and "The Strong Interaction". I will now describe what each of these do to the particles.

The Electromagnetic Interaction

This is more or less the electric and magnetic forces that most people have heard of. When you play this card all particles that have electric charge are affected. We haven't mentioned anything about electric charge but in fact all the quarks and half of the leptons (e, μ, τ) have electric charge.

When the electric force comes into play the particles are differently affected depending on whether they have positive or negative charge. As most people have heard, different charges attract each other and equal charges repel each other. So, for example an electron (negative charge) is attracted to a proton (positive charge) resulting in a hydrogen atom. In the same way all other atoms can be created and from that bigger structures like molecules, proteins, humans, motorcycles and the sun.

The Gravitational Interaction

Once again this is an interaction that most people know of. Gravity affects *all* particles, and its effect is to pull particles together. This is a very important interaction in ordinary life. It keeps people from falling of the earth, it keeps earth in its orbit, the solar system in the galaxy and so on.

However, its effect on individual particles is much more complicated. In fact, the exact rules for this card are not known. It's one of the biggest challenges for present and future particle physicists to figure out how it works. Fortunately though, gravity has a very *small* effect on understanding particle physics in general, or my work in particular. So, in the part of the game where you put together two or three particles, this card can be neglected; but to understand the complete universe it is of course very important.

The Weak Interaction

The weak interaction is not as famous as the electromagnetic interaction or gravity (in fact it is almost infamous since it leads to radioactivity). It also has a completely different effect. It doesn't attract or repel particles but instead it replaces one particle with one or more other particles. So, you can use the weak interaction to exchange one piece in the game with other pieces.

However, you can not exchange *any* particles. You can e.g. replace a strange-quark with an up-quark but not with a down-quark. I am not going to go through exactly which types of exchanges that can be made but an s-quark transforming into the $(u\bar{u}d)$-quarks is very important for the work in my papers so that is definitely allowed.

Since quarks are always grouped together into hadrons, changing a quark means changing from one type of hadron into another. So if you start with e.g. K^- $(\bar{u}s)$ and by the weak interaction change the strange-quark into an up-quark, an anti-up-quark and a down-quark you end up with π^- $(\bar{u}d)$ and π^0 $(\bar{u}u)$. In a similar way, using more advanced rules, you can exchange a K with *three* different π's. Such exchanges are what the papers in this thesis are about and that explains the phrase "Kaon Decays to Pions" in the title.

The effect of the weak interaction on the leptons is easier. There one can replace one particle in a pair like (e, ν_e) with the other one in the same pair. That is in fact the whole explanation of why they are grouped in pairs in the first place.

The Strong Interaction

The last interaction to describe is the strong interaction. It affects the quarks but not the leptons. When it comes into play all the quarks group together to form hadrons, either three quarks (qqq) or one quark and one anti-quark $(q\bar{q})$.

As I mentioned before the quarks are never in the game alone, and the strong interaction is the reason. It binds the quarks together and the effect is very strong (hence the name). In fact it is so strong that it is completely impossible to separate the quarks, and they are bound together forever.

However, even though one knows that the quarks are bound together in hadrons, one doesn't understand exactly how it works. There are obviously some really difficult rules for the strong interaction that nobody completely knows, and in fact this is what my work is about.

As I mentioned, the reactions I study are $K \to 2\pi$ and $K \to 3\pi$, which we know happens because of the weak interaction. However, since the quarks are grouped together, the strong interaction also plays a part in the process. The weak interaction changes the strange-quark into other quarks but the strange-quark is bound inside the hadron by the strong interaction. So to understand exactly what is going on one has to know the rules for both the weak and the strong interaction. Since all the rules for the strong interaction aren't known, this is ongoing research and my contribution to this research is presented in the papers in the second part of this thesis.

Summary

> Education's purpose is to replace an empty mind with an open one.
>
> *Malcolm Forbes*

I have now tried to describe the basic rules of *"The Game of the Universe"*, or in other words the basic facts of the universe. The universe consists of 12 different particles and their 12 corresponding anti-particles. The way in which the particles combine to create everything we see in the universe is through the four different interactions: the electromagnetic, the gravitational, the weak and the strong interaction. To know and understand this is to know the fundamental structure of the universe.

As a side remark, it can be noted that with a deeper understanding of the rules the difference between the pieces and the cards is not that big. Some of the particles then act like interactions and some of the interactions like particles. Fascinating!

This ends Introduction part I and part II follows. There I intend to give a more detailed background of the method I have been using to describe the effect of the strong interaction in the processes $K \to 2\pi$ and $K \to 3\pi$. The method is called Chiral Perturbation Theory, and to follow the description of it some knowledge of mathematics and particle physics will probably be needed.

References

[1] S. F. Novaes, "Standard model: An introduction," hep-ph/0001283.

[2] P. Aurenche, "The standard model of particle physics," hep-ph/9712342.

[3] Z. Kunszt, "Bread and butter standard model," hep-ph/0004103.

[4] H-U. Bengtsson, G. Gustafson, L. Gustafson, "Kvarken och universum", Corona AB, Malmö, Sweden (1994).

[5] G. Kane, "Modern Elementary Particle Physics", Perseus Books, Reading MA, USA (1993).

Introduction part II

> Education is a progressive discovery of our own ignorance.
>
> *Will Durant*

As mentioned in Introduction part I, the processes of interest in my research are $K \to 2\pi$ and $K \to 3\pi$, a kaon decaying into two or three pions. The underlying process in that decay is that the strange-quark in the kaon changes into an up-quark via the weak interaction. The weak interaction is very well known and the way in which the quarks change into each other is understood.

However, since the quarks are bound into hadrons by the strong interaction, the theory of the strong interaction also comes into play. That theory is known, but one doesn't understand well enough how to do calculations based on it. My research can therefore be considered to explore the strong interaction even though it concerns a weak decay.

I will start by describing briefly the strong interaction and the problems that arise when trying to understand how quarks are bound into hadrons. I will then describe how similar problems can be addressed in general (Effective Theories) followed by the specific theory used in our case (Chiral Perturbation Theory). However, even though there exists a method that works, research still has to be done to check the consistency of the method and to determine the details (free parameters) in the theory. I will end by trying to describe how my research fits in this picture.

More details of the physics described in this section can be found in [1–10] and references therein.

The Theory of the Strong Interaction

When you know a thing, to hold that you know it; and when you do not know a thing, to allow that you do not know it - this is knowledge.

Confucius, The Confucian Analects

The theory of the strong interaction is called QCD, Quantum Chromo Dynamics. The starting point of all calculations in QCD is the QCD *Lagrangian*, in which all the information of the strong interaction is described. The Lagrangian (or Lagrangian density to be precise) contains mass-, kinetic- and interaction-terms for the particles affected by the strong interaction, namely quarks (q) and gluons (G), and can be written

$$\mathcal{L}_{\text{QCD}} = -\frac{1}{4}\, G^a_{\mu\nu} G_a^{\mu\nu} + i\bar{q}_L \gamma^\mu D_\mu q_L + i\bar{q}_R \gamma^\mu D_\mu q_R - m_q\, \bar{q}q\,. \tag{1}$$

In the very successful theories for the electromagnetic and weak interaction the way to calculate explicit physical observables from the Lagrangians is through the use of perturbation theory. One realizes that the coupling constants, α, in those theories are small and orders the different contributions to physical observables, e.g. decay rates, in terms of *increasing* powers of α and therefore, since α is numerically small, in *decreasing* order of importance. This means that although the Lagrangians generate in principle an infinite number of contributions for any physical observable, it is enough to consider a finite number in a calculation to some given accuracy. Furthermore, one can get a good estimate of the theoretical error induced by this finite order calculation and this makes “standard” perturbation theory, i.e. an expansion in α, very useful.

Naturally one would like to do something similar in QCD. However, a problem arises which is not present in the other two theories. The coupling constant, α_s, is not small for all processes. If the energy in the process is too small, α_s can be much bigger than 1 and this obviously leads to the breakdown of perturbation theory. Unfortunately this turns out to affect most QCD processes since the quarks are confined into hadrons. The hadronization process itself is a low-energy process implying that perturbation theory fails to describe processes including hadrons, e.g. $K \to 3\pi$.

This means that new ideas are needed and a lot of different non-perturbative methods exist. One way is to construct an effective theory, i.e. a theory which doesn't describe all of QCD but just tries to solve the low-energy problem. Chiral Perturbation Theory (ChPT) [11–13], which is used in my research, is an effective theory for low-energy strong interactions, but before describing it in more detail let's talk more about effective theories in general.

Effective Theories

> Education is the ability to listen to almost anything without losing your temper or your self-confidence.
>
> *Robert Frost*

The goal of physics is often stated as a search for the *"Theory of Everything"*. By that one means achieving a simple understanding of all observed phenomena in terms of some fundamental dynamics among the basic constituents of nature. However, even if such a theory is ever found, quantative analysis at the most elementary level will be of little or no use for describing nature at all physical scales. Using the quantum field theory for the electromagnetic interactions, QED, to describe e.g. the way in which dice roll along a table will never be very fruitful [1, 2].

The point is that, even though it is of course very important to search for the *fundamental* underlying theory, effective theories, which use the *most relevant* ingredients to describe a problem, will always be needed as well. Furthermore, most field theories seen are not complete up to arbitrarily high energies. They are effective theories, valid up to some cut-off.

The basic idea with effective theories is not to attempt to construct "a theory of everything", but instead to construct a theory that is appropriate to the energy scale of the experiments one is interested in. In order to understand a particular physical system in the impressive richness of the world, it is necessary to isolate the most relevant pieces from the rest. In this way one can obtain a simple description without having to understand everything.

The first thing to do is to choose the appropriate variables to capture the physics most important for the problem under investigation. Then one should look at the energy scales involved. Often, a problem involves widely separated energy scales and this allows one to understand the low-energy interactions independently of the details of the high-energy interactions.

The idea is to start with an approximation where parameters which are very large compared to the relevant energy scale are put to infinity. In the same way one puts parameters that are very small to zero. This approximation can then be improved by taking into account the corrections induced by the neglected parameters as small perturbations.

This means that effective field theories are great theoretical tools to describe low-energy physics, where low is defined with respect to some energy scale. They only take into account the relevant light degrees of freedom, while the heavier excitations are integrated out from the action. The information on the heavier degrees of freedom is instead contained in the couplings of the resulting low-energy Lagrangian.

Since the original problem described in the section about the strong interaction was exactly a low-energy problem, an effective theory might be the solution. Chiral Perturbation Theory, which is used in my research, is exactly a low-energy effective theory of the strong interaction. I will now try to describe it in more detail.

Chiral Perturbation Theory

I never have found the perfect quote. At best I have been able to find a string of quotations which merely circle the ineffable idea I seek to express.

Caldwell O'Keefe

Starting Point

Chiral Perturbation Theory (ChPT) is a low-energy effective theory of QCD, the theory of the strong interaction. To construct ChPT we should start by looking at QCD to get some ideas of how to do it. As mentioned before the basis of QCD is the QCD Lagrangian, which looks like

$$\mathcal{L}_{\text{QCD}} = -\frac{1}{4}\, G^a_{\mu\nu} G^{\mu\nu}_a + i\bar{q}_L \gamma^\mu D_\mu q_L + i\bar{q}_R \gamma^\mu D_\mu q_R - m_q\, \bar{q}q\,,$$

where $q = q_L + q_R$ and a summation over the six different quarks is implicit.

Just as in perturbation theory, it is useful to search for something "small" in the Lagrangian because a good starting point might be to put small quantities to zero and then add their effects later as perturbations. The masses of the three lightest quarks are rather small so a possible starting point is to look at the Lagrangian with those set to zero,

$$\mathcal{L}^0_{\text{QCD}} = -\frac{1}{4}\, G^a_{\mu\nu} G^{\mu\nu}_a + i\bar{q}_L \gamma^\mu D_\mu q_L + i\bar{q}_R \gamma^\mu D_\mu q_R - \sum_{c,b,t} m_q\, \bar{q}q\,, \tag{2}$$

where the sum indicates that only the mass terms for c, b and t are present.

Furthermore, since we are trying to describe low-energy interactions it is a good guess that the three heavy quarks don't play an important part. Their contribution must be proportional to some negative power of their masses, since in the limit where they are infinitely heavy their contribution should be zero. Those terms are then also neglected, resulting in the Lagrangian

$$\mathcal{L}^0_{\text{QCD}} = -\frac{1}{4}\, G^a_{\mu\nu} G^{\mu\nu}_a + i\bar{q}_L \gamma^\mu D_\mu q_L + i\bar{q}_R \gamma^\mu D_\mu q_R\,, \tag{3}$$

where the implicit sum is now only over the three light quarks.

Chiral Symmetry

To look for invariances, or *symmetries*, of the Lagrangian is usually very fruitful [6]. If there are such symmetries they often provide a lot of information of how the theory works and therefore, if the theory is good, of how nature works.

A first obvious symmetry is a global $U(1)_V$ phase transformation, $q \to q\, e^{i\alpha}$ (the similar $U(1)_A$ symmetry is broken by the anomaly). If you do this field-redefinition the Lagrangian remains unchanged, and it is therefore said to be invariant with respect to this symmetry. This symmetry corresponds to quark number conservation which is an important fact of the theory and of the world. However, this symmetry was there even before we set $m_u = m_d = m_s = 0$, so it is not a consequence of our approximation and will therefore probably not help us solve the underlying problem in low-energy QCD.

However, the new approximate Lagrangian is also invariant with respect to a set of *chiral* transformations, i.e. independent rotations of the right- and left-handed components of u, d and s,

$$\begin{pmatrix} u_{\mathrm{R}} \\ d_{\mathrm{R}} \\ s_{\mathrm{R}} \end{pmatrix} \to V_{\mathrm{R}} \begin{pmatrix} u_{\mathrm{R}} \\ d_{\mathrm{R}} \\ s_{\mathrm{R}} \end{pmatrix} \quad , \quad \begin{pmatrix} u_{\mathrm{L}} \\ d_{\mathrm{L}} \\ s_{\mathrm{L}} \end{pmatrix} \to V_{\mathrm{L}} \begin{pmatrix} u_{\mathrm{L}} \\ d_{\mathrm{L}} \\ s_{\mathrm{L}} \end{pmatrix} \quad , \qquad V_{\mathrm{R}},\, V_{\mathrm{L}} \in \mathrm{SU}(3) \ . \quad (4)$$

The objects V_{R} and V_{L} can be thought of as complex matrices and SU(3) then means that these matrices should be three-dimensional, unitary and that $\det V = 1$.

The corresponding total symmetry group is thus the direct product of the two groups, $\mathrm{SU}(3)_{\mathrm{R}}\times\mathrm{SU}(3)_{\mathrm{L}}$. Of course, in reality chiral symmetry is broken, because m_u, m_d and m_s do not vanish. We hope however that this symmetry might be a good starting point for an approximate low-energy effective theory.

We can write the QCD Lagrangian as a chirally symmetric part and a symmetry breaking part

$$\mathcal{L}_{QCD} = \mathcal{L}^0_{QCD} + \mathcal{L}^{\mathrm{sb}}_{QCD} \ \ , \ \ \mathcal{L}^{\mathrm{sb}}_{QCD} = -(m_u\, \bar{u}u + m_d\, \bar{d}d + m_s\, \bar{s}s) \ . \qquad (5)$$

We will start by making an approximate theory of the first part and then add effects of the second part as perturbations to this theory.

Spontaneous Symmetry Breaking

Even though we have this far only taken $\mathcal{L}^0_{QCD}$ into account, we hope that the theory is a good approximation to the real world. Since $\mathcal{L}^0_{QCD}$ is chirally symmetric this means that nature should be chirally symmetric as well. The effects of this would be the existence of groups (multiplets) of particles, connected by chiral symmetry, with nearly the same mass (exactly the same mass if $\mathcal{L}^0_{QCD}$ was the whole truth). However, this is *not* seen in nature. This seems to suggest that our starting point was wrong, but before we throw it away we should explore all possible solutions to the puzzle.

In fact there exist strong indications from both theory and phenomenology that chiral symmetry is *spontaneously broken* [4]. A spontaneously broken symmetry is not broken by terms in the Lagrangian (which is called explicit symmetry breaking), but instead broken by the ground state (the vacuum) of the theory.

An intuitive example is the Lagrangian describing magnetism. The Lagrangian is invariant under rotations of the spin directions, but the ground state is not. Even though the spins in a magnet can choose *any* direction in the ground state, in practice they have to choose *one* direction, and thereby they spontaneously break the symmetry.

In the same way the QCD vacuum chooses a specific *chiral direction.* One way this can happen is through a non-vanishing quark condensate

$$\langle 0|\bar{q}q|0\rangle \neq 0\,. \tag{6}$$

Since $q = q_L + q_R$ this can be written as

$$\langle 0|(\bar{q}_L + \bar{q}_R)(q_L + q_R)|0\rangle = \langle 0|(\bar{q}_L q_R + \bar{q}_R q_L)|0\rangle\,, \tag{7}$$

and those two terms, mixing q_R and q_L, break chiral symmetry. However, they don't break the symmetry completely. There is still a symmetry left of the form

$$\begin{pmatrix} u \\ d \\ s \end{pmatrix} \to V \begin{pmatrix} u \\ d \\ s \end{pmatrix} \quad , \qquad V_L = V_R = V \in \mathrm{SU}(3) \ \ . \tag{8}$$

So the vacuum breaks the $\mathrm{SU}(3)_\mathrm{R}\times\mathrm{SU}(3)_\mathrm{L}$ symmetry of $\mathcal{L}^0_{QCD}$ down to just SU(3). This remaining SU(3) is called the Gell-Mann Ne'eman octet symmetry.

Goldstone Bosons

The spontaneous breaking of a symmetry, like chiral symmetry, has some implications. According to the Goldstone theorem, the breaking implies the existence of *massless* so called Goldstone particles.

One way to understand this is through considering the potentials of two different theories, one with exact symmetry and the other with a spontaneously broken symmetry. The potential of the first theory looks like a bowl; it has a single well defined lowest point which corresponds to the vacuum. The potential of the theory with the spontaneously broken symmetry has another shape, usually referred to as a Mexican hat potential, see Fig. 1. This potential has a continuous line of vacua corresponding to the different choices of the symmetry direction.

The dynamical fields of the theory, i.e. the particles, are the excitations from the vacuum. In the first theory any excitation from the ground state means that you move uphill in the potential and this corresponds to your particles being massive. On the other hand, in the second theory there is a possibility to have

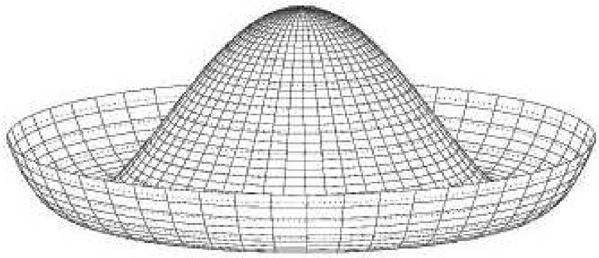

Figure 1: The potential of a theory with a spontaneously broken symmetry.

excitations along the vacuum line. These excitations do not have a higher energy than the vacuum, which means that they are massless.

But the Goldstone theorem also states how many of these massless particles that should exist. It's the same amount as the number of spontaneously broken *generators*, i.e. the dimensionality of the bottom of the potential. The number of generators of a SU(N) symmetry is $N^2 - 1$ and since one SU(3) symmetry is broken this means eight broken generators, corresponding to eight massless Goldstone particles.

Prediction

The consequences of the spontaneous breaking of chiral symmetry, as described in the Goldstone theorem, are a very strong prediction of our theory. The theorem predicts both the existence of eight massless hadrons in nature as well as the way in which they interact (their interactions should vanish when their momenta go to zero). This can easily be checked. However, before looking for such particles we should remember that we neglected the symmetry breaking part $\mathcal{L}^{\mathrm{sb}}_{QCD}$ in our analysis.

In our approximation we treat the u, d and s quarks as massless even though we know that they have a small mass in the real world. The resulting theory predicts that we should see some massless particles. It is then probably a good guess that this corresponds to light (instead of massless) particles in nature.

In other words, the group $\mathrm{SU(3)_R \times SU(3)_L}$ represents an *exact* symmetry of the approximate theory only considering $\mathcal{L}^{0}_{QCD}$, which is then spontaneously broken leading to eight strictly massless Goldstone particles. When the quark masses are introduced via $\mathcal{L}^{\mathrm{sb}}_{QCD}$, the Goldstone particles get a mass M_i, with $M_i^2 \sim m_u, m_d, m_s$. The Goldstone particles remain light, provided m_u, m_d and m_s are small. The quark mass term of the Lagrangian then amounts to a small perturbation, such that $\mathrm{SU(3)_R \times SU(3)_L}$ still represents an *approximate* symmetry, with approximately massless Goldstone particles.

So instead of eight massless hadrons we should look for eight very light hadrons. And in fact there do exist eight hadrons in nature which are significantly lighter than all other hadrons. These eight light hadrons are called π^0, π^+, π^-, K^+, K^-, K^0, $\bar{K}^0$ and η, and the spontaneous breaking of chiral symmetry could be the reason that these particles are lighter than the other hadrons. Moreover, they interact in the way predicted from the theory.

This mass-gap, between the eight lightest hadrons and the rest, is suitable for constructing an effective theory. As stated before, in an effective theory you (to a first approximation) neglect the effects of particles that are heavier than the particles in the effective theory. Those effects are later added as perturbations and if the difference in mass is large between the particles in the theory and the neglected ones, the perturbations will be smaller and one can expect a nice convergence in the theory.

This is the motivation to construct Chiral Perturbation Theory, the effective theory of low energy QCD, describing the interactions of π^0, π^+, π^-, K^+, K^-, K^0, $\bar{K}^0$ and η.

Comparison with Perturbative QCD

The decomposition of the QCD Lagrangian in eq. (5) may be compared with the standard perturbative splitting

$$\mathcal{L}_{QCD} = \mathcal{L}_{\text{free}} + \mathcal{L}_{\text{int}} \,, \tag{9}$$

where the first term accounts for the free quarks and gluons, while the second describes their interaction. The corresponding expansion parameter is the coupling constant α_S. Since QCD is *asymptotically free*, the effective coupling becomes weak at large energies and this means that processes which *exclusively* involve high energies may be analyzed by treating the interaction as a perturbation.

Perturbation theory fails however in the low-energy domain, where the effective coupling constant is too large, such that it is not meaningful to stop the expansion of $\mathcal{L}_{\text{int}}$ after the first few terms. In particular, the structure of the ground state can not be analyzed in this way.

On the other hand, the decomposition in eq. (5), which retains the interaction among the quarks and gluons in the unperturbed Lagrangian $\mathcal{L}^0_{QCD}$ and only treats m_u, m_d and m_s as perturbations, is perfectly suitable as a starting point for studying the low-energy interactions among the hadrons.

The Search for an Effective Lagrangian

The idea is now to find a new *effective* Lagrangian, describing the interactions of the eight Goldstone particles, which has the properties we learnt from $\mathcal{L}^0_{QCD}$, i.e. a spontaneously broken SU(3)×SU(3) symmetry. If such a Lagrangian can be constructed we later add the effects of $\mathcal{L}_{QCD}^{sb}$, i.e. the small non-zero masses of m_u, m_d and m_s as a perturbation to it. To learn how to create an effective theory from an underlying one, we will start by studying the linear σ-model. It is a model with the same chiral symmetry as QCD, but formulated in terms of hadrons instead of quarks.

The σ-model is very useful since it provides an example where explicit calculations can be done both in the underlying theory, the linear σ-model, and in the effective field theory approximation to it. In QCD, we can *only* use the low-energy effective theory for calculations. The problem with calculations in low-energy QCD is the reason to construct ChPT in the first place.

Important note: To describe the ideas behind the construction of Chiral Perturbation Theory I will only work with *two* light flavours instead of three. This means setting only $m_u = m_d = 0$ in the QCD Lagrangian, which will then have $\mathrm{SU(2)_R \times SU(2)_L}$ symmetry spontaneously broken by the ground state. This breaking leads to the appearance of *three* massless Goldstone particles, identified as π^0, π^+ and π^-. This is in itself an interesting theory sometimes referred to as *two-flavour* ChPT, and it then describes the interactions of the three pions.

The rest of this section will motivate the construction of an effective Lagrangian describing this symmetry breaking. One can follow exactly the same reasoning for three light flavours, but in this way the formulae get shorter.

The Linear σ-model

A Lagrangian consists of a kinetic part (T) and a potential part (U), $\mathcal{L} \equiv T - U$. The kinetic part is determined by the spin of the particles you want to describe, whether they are fermions or bosons, and Goldstone particles are always bosons. The potential part is where the interactions sit and there one has to try various forms and analyze the outcome.

One starting point to describe the effects of spontaneous symmetry breaking is the potential in the so called linear σ-model,

$$U = -\frac{1}{2}\mu^2(\vec{\phi}\cdot\vec{\phi}) + \frac{\lambda}{4}(\vec{\phi}\cdot\vec{\phi})^2,\ \mu^2 > 0\,, \tag{10}$$

where $\vec{\phi} = (\phi_1, \phi_2, \phi_3, \phi_4)$ is a set of four scalar fields. This results in the Lagrangian

$$\mathcal{L} = \frac{1}{2}\partial_\mu\vec{\phi}\cdot\partial^\mu\vec{\phi} + \frac{1}{2}\mu^2(\vec{\phi}\cdot\vec{\phi}) - \frac{\lambda}{4}(\vec{\phi}\cdot\vec{\phi})^2\,, \tag{11}$$

with a kinetic term, a mass term and an interaction term. This Lagrangian is symmetric under transformations of $\vec{\phi}$ using a matrix V of the group O(4) $\simeq$ SU(2)×SU(2)

$$\vec{\phi} \to V\vec{\phi},\ \ V \in O(4) \simeq SU(2)\times SU(2)\ \ . \tag{12}$$

To investigate whether this symmetry is spontaneously broken we have to find the ground state, i.e. the state which minimizes the potential part of the Lagrangian. One can see that the set of ground states are those with

$$\vec{\phi} \cdot \vec{\phi} = \frac{\mu^2}{\lambda}\,, \tag{13}$$

indicating that the ground state is degenerate. But in practice nature has to choose *one* particular ground state, ϕ_0, and thereby it breaks the symmetry spontaneously. The exact choice doesn't matter for the result, but to show the effects we take

$$\vec{\phi_0} = (0,0,0,v),\;\; v = \sqrt{\frac{\mu^2}{\lambda}}\,. \tag{14}$$

To see the effects of this in the Lagrangian we redefine the field $\vec{\phi}$

$$\vec{\phi} \to \vec{\phi}\,' = (\phi_1, \phi_2, \phi_3, \sigma + v)\,, \tag{15}$$

where the change of name, from ϕ_4 to σ, in the last field component is done to indicate that σ is the field with a nonzero expectation value in the ground state. The *new* Lagrangian then looks like

$$\mathcal{L}\,' = \frac{1}{2}\left(\partial_\mu\sigma\partial^\mu\sigma - 2\mu^2\,\sigma^2\right) + \frac{1}{2}\,\partial_\mu\phi_i\,\partial^\mu\phi_i - \lambda v\sigma(\sigma^2 + \phi_i^2) - \frac{\lambda}{4}\,(\sigma^2 + \phi_i^2)^2 \tag{16}$$

where we dropped the constant terms (they don't have any effect) and a summation over $i = 1,2,3$ is implicit.

The important thing to note is that the three ϕ_i-fields are now *massless* fields, since their mass-terms vanishes. This explicitly breaks the SU(2)×SU(2) symmetry of the original Lagrangian and instead we are left with a smaller symmetry, O(3) $\simeq$ SU(2), of the ϕ_i fields.

In other words this new Lagrangian now explicitly describes the interactions of the massless Goldstone particles: ϕ_1, ϕ_2 and ϕ_3, appearing after the spontaneous breaking of the symmetry in the Lagrangian.

That is exactly what we are looking for, so we use the linear σ-model as a starting point to construct a new model of π^0, π^+ and π^-. However, the model also describes an unwanted massive σ-particle and its interactions with the pions. In a low-energy process this particle will play a very small part, and the idea is now to create an effective theory without the σ-particle.

Different Representations

Before dealing with the unwanted σ-particle, there is an important thing to notice. The *representation* chosen for the fields, $\vec{\phi} = (\phi_1, \phi_2, \phi_3, \phi_4)$, is just one choice of many. The physics shouldn't depend on which representation is chosen so one should try different ones to find the one most suitable for calculations.

The first change we make is to rename the fields. We know that after the symmetry breaking the first three fields correspond to the massless Goldstone particles, i.e. the pions, and the last one to the massive σ. Therefore the four fields are named $(\pi_1, \pi_2, \pi_3, \sigma + v)$.

To put the fields, as above, in a vector is one type of representation, but they could just as well be put into a matrix. One way to construct such a matrix (Σ) is

$$\Sigma \equiv \sigma + i\,\vec{\pi} \cdot \vec{\tau}\,, \tag{17}$$

where $\vec{\pi} = (\pi_1, \pi_2, \pi_3)$ and $\vec{\tau}$ is a vector of the three Pauli matrices. The resulting Lagrangian is then

$$\mathcal{L} = \frac{1}{4}\,\mathrm{Tr}\left(\partial_\mu \Sigma\, \partial^\mu \Sigma^\dagger\right) + \frac{\mu^2}{4}\,\mathrm{Tr}\left(\Sigma\,\Sigma^\dagger\right) - \frac{\lambda}{16}\,\left[\mathrm{Tr}\,\Sigma\,\Sigma^\dagger\right]^2\,, \tag{18}$$

where Tr means the trace. This Lagrangian is, after the symmetry breaking ($\sigma \to \sigma + v$), exactly equivalent to the Lagrangian presented in eq. (16), and all the interactions are still simple non-derivative polynomial couplings.

As will soon be apparent, this form of the interactions is not good for calculations. We are trying to find a low energy effective theory for the hadrons, and since we don't have any explicit prescription of how to do that we have to write down the *most general* effective Lagrangian consistent with chiral symmetry. This leads to an infinite number of terms, and the linear σ-model we have studied includes just a few of those terms, in order to see how it works. This generalization to an infinite number of terms seems like a big problem, and it would be if there was no way to order the terms by importance.

Since we are aiming for a low-energy theory it would be great if the Lagrangian could be written as an energy expansion. This means that each term would have a coefficient of the type q^n/M^n, where q is the low momentum of the process and M some heavier scale in the theory. In that case the terms with smaller n would be more important than those with large n, and one could work with a finite number of terms in a calculation to a given accuracy.

The momenta of a particle enters the calculation through the derivative of the corresponding field. This means that if the interactions were described only by derivative terms in the Lagrangian, it would result in an energy expansion with a finite number of *dominant* terms.

The question one would like to answer is therefore whether there exist a representation which results in terms with different (non-zero) number of derivatives. The answer to that question is yes.

It turns out that one can write Σ, defined in eq. (17), as

$$\Sigma = (v + S)\,U\,, \tag{19}$$

where

$$S \equiv \sqrt{(\sigma + v)^2 + \vec{\pi}^2} - v = \sigma + \ldots \tag{20}$$

and

$$U \equiv \exp\left(i\,(\vec{\tau}\cdot\vec{\pi}\,')\,/\,v\right), \quad \vec{\pi}\,' = \vec{\pi} + \ldots \,. \tag{21}$$

The resulting Lagrangian then looks like

$$\mathcal{L} = \frac{1}{2}(\partial_\mu S)^2 - \mu^2\, S^2 - \lambda v\, S^3 - \frac{\lambda}{4} S^4 + \frac{(v+S)^2}{4}\mathrm{Tr}\big(\partial_\mu U \partial^\mu U^\dagger\big)\,, \tag{22}$$

which once again describes one massive field, now called S, and three massless pions ($\vec{\pi}\,'$). Although this looks a bit more complicated, no longer having simple polynomial interactions, it is nothing more than a renaming of the fields.

The new form has several interesting features. The pion fields no longer occur in the potential part of the Lagrangian, but instead appear with derivative interactions. This is in fact, as mentioned above, the main reason to choose this representation. The meaning of this is that the pions are massless and that their interactions vanish in the limit $q \to 0$, as expected since they are Goldstone particles.

However, the issue still remains with the σ-field; it is not a Goldstone particle, and its interactions are therefore not described by derivative terms. This leads to the next step, to create an effective theory based on the linear σ-model, but without σ itself.

Integrating Out Heavy Fields

When studying physics at some energy scale E, one must explicitly include all the particles which can be produced at that energy. But somehow the effects of the heavier particles must be taken into account as well, since they may still be felt through virtual effects, such as loops. In a low energy effective theory, one does not include the heavy fields in the Lagrangian, but their effects are represented by the various coupling constants used to describe the interactions between the light fields. The process of removing the heavy fields from the Lagrangian is called *integrating out* the fields.

The idea comes from the path integral formalism, where the path integral of the action is the central concept

$$Z = \int \mathcal{D}\phi_H D\phi_L\, \exp\left[i\int d^4x\, \mathcal{L}(\phi_H,\phi_L)\right], \tag{23}$$

where ϕ_H and ϕ_L denotes the heavy and light fields respectively. This can then be written as

$$Z = \int D\phi_L\, \exp\left[i\int d^4x\, \mathcal{L}'_{eff}(\phi_L)\right], \tag{24}$$

with

$$\exp\left[i\int d^4x\, \mathcal{L}'_{eff}(\phi_L)\right] = \int D\phi_H\, \exp\left[i\int d^4x\, \mathcal{L}(\phi_H,\phi_L)\right]. \tag{25}$$

The effective Lagrangian, $\mathcal{L}_{eff}(\phi_L)$, with the heavy fields, ϕ_H, integrated out is now defined by the relation

$$\exp\left[i\int d^4x\,\mathcal{L}_{eff}(\phi_L)\right] = \frac{\exp\left[i\int d^4x\,\mathcal{L}'_{eff}(\phi_L)\right]}{\int D\phi_H\,\exp\left[i\int d^4x\,\mathcal{L}(\phi_H,0)\right]}\,, \tag{26}$$

where $\int D\phi_H\,\exp\left[i\int d^4x\,\mathcal{L}(\phi_H,0)\right]$ is just the normalization.

In practice, one constructs the effective Lagrangian, expressed in the massless fields only, from symmetry considerations alone and then only use eq. (26) to fix the coefficients in the theory. Since the symmetries have already been taken care of in the σ-model, there it just corresponds to setting $S = 0$ in the Lagrangian, resulting in

$$\mathcal{L} = \frac{v^2}{4}\,\mathrm{Tr}\big(\partial_\mu U\partial^\mu U^\dagger\big) = \frac{m_\sigma^2}{\sqrt{\lambda}}\,\mathrm{Tr}\big(\partial_\mu U\partial^\mu U^\dagger\big)\,. \tag{27}$$

This is the new effective Lagrangian (the *non-linear* σ-model), only expressed in the massless fields, where the effects of the particles integrated out are coefficients proportional to the mass of the heavy particle, in this case m_σ^2. Higher order terms will then be suppressed by further factors of $1/m_\sigma^2$ as described below.

Since we are interested in processes with an energy smaller than m_σ, this solves the problem from before. All the pion interaction terms are sorted according to the number of derivatives and the power n of $1/m_\sigma^{2n}$. This means that all the terms in the effective Lagrangian can be assigned an order of importance, and in this way the problem with an infinite number of terms vanishes.

In summary, the idea is to generate candidate interactions which are invariant under SU(2)×SU(2) transformations. Examples of two-derivative and four-derivative terms in the exponential representation are

$$\mathrm{Tr}\big(\partial_\mu U\partial^\mu U^\dagger\big) \quad\text{and}\quad \mathrm{Tr}\big(\partial_\mu U\partial_\nu U^\dagger\big)\times\mathrm{Tr}\big(\partial^\mu U\partial^\nu U^\dagger\big)\,, \tag{28}$$

where the important thing is that there can be no derivative-free terms in the list since $\mathrm{Tr}\big(UU^\dagger\big) = 2$ is a constant. It is then clear that one can generate an infinite amount of similar terms with arbitrary numbers of derivatives. The resulting general Lagrangian can be organized by the dimensionality of the operators,

$$\mathcal{L} = \mathcal{L}_2 + \mathcal{L}_4 + \mathcal{L}_6 + \mathcal{L}_8 + \ldots \tag{29}$$

The key point is now that, at sufficiently low energies, the resulting matrix elements of most of these terms are very small, since each derivative becomes a factor of the momentum q when matrix elements are taken. It then follows from dimensional analysis that the coefficient of an operator with n derivatives behaves as $1/M^{n-4}$, where M is the mass scale in the theory, i.e. m_σ in this case. Therefore, the effect of an n-derivative vertex is of order q^n/M^{n-4}, and at an energy small compared to M, large n-terms have a very small effect, and can often be neglected.

The Explicit Symmetry Breaking

The σ-model discussed above corresponds to the chirally symmetric $\mathcal{L}^0_{QCD}$ alone, where

$$\mathcal{L}^0_{\mathrm{QCD}} = -\frac{1}{4}\, G^a_{\mu\nu} G_a^{\mu\nu} + i\bar{q}_L \gamma^\mu D_\mu q_L + i\bar{q}_R \gamma^\mu D_\mu q_R \,. \tag{30}$$

But that is only one part of the QCD Lagrangian. The other part is the symmetry breaking part

$$\mathcal{L}^{\mathrm{sb}}_{QCD} = -(m_u\, \bar{u}u + m_d\, \bar{d}d)\,, \tag{31}$$

and the effects of this part will now be described.

To incorporate this, we still want to use the idea of effective Lagrangians, but now to analyze the effect of a small *explicit* symmetry breaking. Studying this effect in the language of the σ-model will again be fruitful.

The SU(2)$\times$SU(2) symmetry of the non-linear σ-model should be explicitly broken and we do that by adding to the potential a small symmetry breaking term

$$\mathcal{L}_{breaking} = a\,\sigma = \frac{a}{4}\, v\, \mathrm{Tr}(U + U^\dagger), \tag{32}$$

where a is a small breaking parameter. Just like the mass terms in QCD, this term breaks SU(2)$\times$SU(2) but is invariant under SU(2). Here this term is just used to study the consequences of the symmetry breaking. Later however, it will be seen that in fact it is the only lowest order term possible, which has all the symmetries we require.

The addition of $\mathcal{L}_{breaking}$ results in a shift in the minimum of the potential

$$v\,' = \sqrt{\frac{\mu^2}{\lambda}} + \frac{a}{2\mu^2}\,, \tag{33}$$

and produces a small pion mass

$$m_\pi^2 = \frac{a}{v}\,. \tag{34}$$

The new Lagrangian, based on the linear σ-model but slightly changed according to $\mathcal{L}_{breaking}$, now looks like

$$\mathcal{L} = \frac{v^2}{4}\, \mathrm{Tr}\big(\partial_\mu U \partial^\mu U^\dagger\big) + \frac{m_\pi^2}{4}\, v^2\, \mathrm{Tr}(U + U^\dagger)\,, \tag{35}$$

and this is the starting point for a description of the interactions of the three pions.

It is important to realize that the symmetry breaking Lagrangian can have higher-order contributions, where each factor of m_π^2 corresponds to two derivatives (since $p^2 = m^2$) when counting the orders. This means that if m_π^2 is small, the resulting expansion is an expansion in *both* the momenta and mass.

The Chiral Perturbation Theory we use in the papers is the generalization of this to three flavours.

Constructing ChPT

We have now gone through all the tools needed to understand the construction of Chiral Perturbation Theory. The Chiral Lagrangian is an effective Lagrangian describing the interactions of the massless Goldstone particles , π^0, π^+, π^-, K^+, K^-, K^0, $\bar{K}^0$ and η, appearing when the $\mathrm{SU(3)_R{\times}SU(3)_L}$ symmetry of $\mathcal{L}^0_{QCD}$ is *spontaneously* broken down to SU(3).

The starting point is to write down *all* terms, using the exponential representation, symmetric under $\mathrm{SU(3)_R{\times}SU(3)_L}$. The terms are then sorted according to their number of derivatives, where *increasing* number of derivatives means *decreasing* order of importance.

One then adds to this an *explicit* breaking of $\mathrm{SU(3)_R{\times}SU(3)_L}$ in terms of the masses of the Goldstone particles, as described above in the σ-model.

The results is the lowest order chiral Lagrangian

$$\mathcal{L}_2 = \frac{F_0^2}{4}\left\{\mathrm{Tr}\big(\partial_\mu U \partial^\mu U^\dagger\big) + \mathrm{Tr}\left(U\chi^\dagger + \chi U^\dagger\right)\right\}, \tag{36}$$

where U is changed according to

$$U = \exp\left(i\frac{\vec{\tau}\cdot\vec{\pi}}{v}\right) \to U = \exp\left(\frac{i\sqrt{2}}{F_0}\,M\right) \tag{37}$$

with

$$M = \begin{pmatrix} \frac{1}{\sqrt{2}}\pi^0 + \frac{1}{\sqrt{6}}\eta & \pi^+ & K^+ \\ \pi^- & \frac{-1}{\sqrt{2}}\pi^0 + \frac{1}{\sqrt{6}}\eta & K^0 \\ K^- & \bar{K}^0 & \frac{-2}{\sqrt{6}}\eta \end{pmatrix}. \tag{38}$$

This is the generalization of the σ-model into three flavours, and the constant F_0 corresponds to v from before.

The explicit symmetry breaking part is generalized using

$$\chi \equiv 2B_0 \begin{pmatrix} m_u & & \\ & m_d & \\ & & m_s \end{pmatrix} \tag{39}$$

where B_0 is an unknown constant (corresponding to a) with the dimension of mass. Just as $\mathcal{L}^{\mathrm{sb}}_{QCD}$ it breaks the $\mathrm{SU(3)_R{\times}SU(3)_L}$ down to SU(3).

The two unknown parameters, F_0 and B_0, reflect our lack of knowledge of low-energy QCD, but they can be related to experimental observables. The lowest-order mass of e.g. the neutral pion is in the theory given by

$$m^2_{\pi^0} = B_0\left(m_u + m_d\right), \tag{40}$$

but this mass can instead be taken from experiment.

Weak Interactions

Up to now we have just described the building of an effective theory for the strong interaction. However, as mentioned before the interactions under study in the papers are $K \to 2\pi$ and $K \to 3\pi$, two *weak* decays. To describe these decays, one has to add new pieces to Chiral Perturbation Theory. I will now briefly describe how this is done.

The $K \to 3\pi$ (and $K \to 2\pi$) weak decay is a strangeness-changing transition with $\Delta S = 1$. In the Standard Model this happens via the exchange of a W-boson, as described in the weak Lagrangian. However, since W is very heavy, it can be integrated out together with the heavy quarks c, b and t.

The idea is then, just as in the strong case, to construct the most general effective Lagrangian. This Lagrangian should be written directly in the meson fields and should have all the symmetry properties of the weak Lagrangian (with the heavy fields integrated out).

This results in the lowest order Lagrangian

$$\mathcal{L}_{W2} = C\, F_0^4 \left[G_8 \langle \Delta_{32} u_\mu u^\mu \rangle + G_8' \langle \Delta_{32} \chi_+ \rangle + G_{27} t^{ij,kl}\, \langle \Delta_{ij} u_\mu \rangle \langle \Delta_{kl} u^\mu \rangle \right] + \text{ h.c.}\,, \tag{41}$$

where

$$u_\mu = i u^\dagger\, \partial_\mu U\, u^\dagger\,, \quad u^2 = U\,. \tag{42}$$

The tensor $t^{ij,kl}$ has as nonzero components

$$\begin{aligned} t^{21,13} = t^{13,21} &= \frac{1}{3}\,, \qquad & t^{22,23} = t^{23,22} &= -\frac{1}{6}\,, \\ t^{23,33} = t^{33,23} &= -\frac{1}{6}\,, \qquad & t^{23,11} = t^{11,23} &= \frac{1}{3}\,, \end{aligned} \tag{43}$$

and the matrix Δ_{ij} is defined as

$$\Delta_{ij} \equiv u \lambda_{ij} u^\dagger\,, \quad (\lambda_{ij})_{ab} \equiv \delta_{ia}\, \delta_{jb}\,. \tag{44}$$

The coefficient C, coming from the underlying weak Lagrangian, is defined as

$$C = -\frac{3}{5} \frac{G_F}{\sqrt{2}} V_{ud}\, V_{us}^*\,, \tag{45}$$

where G_F is the Fermi-constant and V_{ij} are elements of the CKM matrix, describing the mixing of the quarks. Three new unknown parameters are introduced, G_8, G_{27} and G_8'.

Higher Orders

When calculating amplitudes to next-to-leading order, there are two new features that enter. First, one has to calculate loop-diagrams constructed using

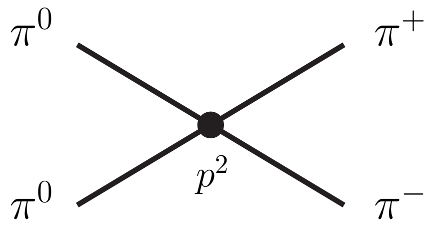

Figure 2: $\pi\pi$-scattering diagram at order p^2.

vertices from the lowest order Lagrangians. But, additionally, one has to take into account effects from *next-to-leading order Lagrangians*, $\mathcal{L}_4$ and $\mathcal{L}_{W4}$. These two effects are equally important and next-to-leading order calculations are meaningless without the inclusion of both.

Since ChPT loop amplitudes are divergent, the theory has to be regularized and renormalized. Renormalization is essential for getting cut-off independent results. The procedure amounts to absorbing the divergences from the loops in the unknown coupling constants in $\mathcal{L}_4$ and $\mathcal{L}_{W4}$.

Calculating Amplitudes

I will end this introduction by showing how to calculate an amplitude using the Chiral Lagrangian. The process will be $\pi^0\pi^0 \to \pi^+\pi^-$, and the calculation will be to first order in the isospin limit. The isospin limit means using the approximation $m_u = m_d = \hat{m}$.

The starting point is to find the lowest order diagrams contributing to the process. In this case there is only one, see Fig. 2

The lowest order amplitude corresponding to this diagram is

$$\langle \pi^+(p_1)\pi^-(p_2) \left| \mathcal{L}_2 \right| \pi^0(p_3)\pi^0(p_4) \rangle \, , \tag{46}$$

and the next step is to find terms in the Lagrangian that gives a non-zero contribution to this. After expanding U

$$U = \exp\left(\frac{i\sqrt{2}}{F_0} M\right) = 1 + \frac{i\sqrt{2}}{F_0} M - \frac{1}{F_0^2} M M - \frac{i\sqrt{2}}{3 F_0^3} M M M + \dots \tag{47}$$

in eq. (36), we pick out all terms containing four fields M

$$\mathcal{L}_2 = \dots + \frac{1}{6F_0^2} \mathrm{Tr}\left(\partial_\mu M M \partial^\mu M M - \partial_\mu M \partial^\mu M M^2\right) + \frac{1}{12F_0^2} \mathrm{Tr}\left(\chi M^4\right) + \dots \tag{48}$$

Then one expands the traces of M, see eq. (38), and keeps only the relevant pion terms

$$\begin{aligned}
\mathcal{L}_2 = \quad & \ldots \\
& + \frac{1}{6F_0} 2B_0 \hat{m} (\pi^0)^2 \pi^+ \pi^- \\
& - \frac{1}{3F_0} (\pi^0)^2 \partial_\mu \pi^+ \partial^\mu \pi^- \\
& - \frac{1}{3F_0} (\partial_\mu \pi^0)^2 \pi^+ \pi^- \\
& + \frac{1}{3F_0} (\pi^0 \partial_\mu \pi^0 \partial^\mu \pi^+ \pi^-) \\
& + \frac{1}{3F_0} (\pi^0 \partial_\mu \pi^0 \pi^+ \partial^\mu \pi^-) \\
& + \ldots
\end{aligned} \tag{49}$$

This is all the terms necessary to calculate the amplitude and the next step is to contract the fields. Remembering the different possible permutations, and that the derivative of a scalar field $\partial_\mu \phi$ produces momentum factors ip_μ and $-ip_\mu$ (on incoming and outgoing states respectively), the result is

$$\begin{aligned}
\langle \pi^+(p_1) \pi^-(p_2) | \mathcal{L}_2 | \pi^0(p_3) \pi^0(p_4) \rangle \quad = \quad & + \frac{1}{3F_0} 2B_0 \hat{m} \\
& + \frac{1}{3F_0}\, 2\, p_1 \cdot p_2 \\
& + \frac{1}{3F_0}\, 2\, p_3 \cdot p_4 \\
& + \frac{1}{3F_0}\, p_1 \cdot (p_3 + p_4) \\
& + \frac{1}{3F_0}\, p_2 \cdot (p_3 + p_4).
\end{aligned} \tag{50}$$

To write it in a simpler form, one can define

$$s \equiv (p_1 + p_2)^2 = (p_3 + p_4)^2 = (2p_1.p_2 + 2m_\pi^2) = (2p_3.p_4 + 2m_\pi^2)\,, \tag{51}$$

and the result for the process $\pi^0\pi^0 \to \pi^+\pi^-$ in the isospin limit, where $m_\pi^2 = 2B_0\hat{m}$, can then be written

$$\langle \pi^+(p_1) \pi^-(p_2) | \mathcal{L}_2 | \pi^0(p_3) \pi^0(p_4) \rangle = \frac{s - m_\pi^2}{F_0^2}\,. \tag{52}$$

This well-known result was calculated first by Weinberg in 1966 [14].

Summary

I have tried to present the ideas behind the creation of Chiral Perturbation Theory. Since it describes the low-energy strong interactions, the starting point is the QCD Lagrangian. In the limit $m_u = m_d = m_s = 0$, it is chirally symmetric, i.e. symmetric under rotation of the left- and right-handed quarks separately.

This symmetry turns out to be spontaneously broken, explaining the existence of eight nearly massless Goldstone particles: π^0, π^+, π^-, K^+, K^-, K^0, $\bar{K}^0$ and η. ChPT tries to describe their interactions, and is based on the idea of spontaneous symmetry breaking.

To get an effective theory, one writes down *all* possible terms, consistent with the symmetries of the QCD Lagrangian. Using the exponential representation, these terms are *ordered* according to their number of derivatives. These derivatives correspond to momenta and since it is a low-energy theory, the momenta are small. Therefore, even though one starts out with an infinite amount of terms, only a finite number of them need to be used in a calculation to a given accuracy.

The effects of the explicit symmetry breaking, $m_u, m_d, m_s \neq 0$, are added as a perturbation, leading to extra terms in the Lagrangian. These terms are proportional to the masses of the Goldstone particles to various orders, and since these masses are small, again only a finite number of terms need to be taken into account. Chiral Perturbation Theory is then a *double* expansion in the momenta and masses of the Goldstone Particles.

The Papers

The papers are all about the decays $K \to 2\pi$ and $K \to 3\pi$. For $K \to 2\pi$, there are three different CP-conserving decays:

$$\begin{aligned} K_S &\to \pi^0\,\pi^0\,, \\ K_S &\to \pi^+\,\pi^-\,, \\ K^+ &\to \pi^+\,\pi^0\,, \end{aligned} \tag{53}$$

and for $K \to 3\pi$, there are five different decay modes:

$$\begin{aligned} K_L &\to \pi^0\,\pi^0\,\pi^0\,, \\ K_L &\to \pi^+\,\pi^-\,\pi^0\,, \\ K_S &\to \pi^+\,\pi^-\,\pi^0\,, \\ K^+ &\to \pi^0\,\pi^0\,\pi^+\,, \\ K^+ &\to \pi^+\,\pi^+\,\pi^-\,. \end{aligned} \tag{54}$$

These decay rates are calculated to next-to-leading order, using different approximations. Some of the calculations in the isospin limit have already been carried through by Kambor, Missimer and Wyler [15], but the analytical results were never published and eventually lost by the authors. A lot of new data have also become available since 1991, so a recalculation was motivated.

Paper I

Here the calculation is performed in the isospin limit, i.e. setting $m_u = m_d = \hat{m}$. The total Lagrangian used for the calculation can be written

$$\mathcal{L} = \mathcal{L}_{S2} + \mathcal{L}_{S4} + \mathcal{L}_{W2} + \mathcal{L}_{W4} \,, \tag{55}$$

where the subscripts refer to strong, weak and the order.

The expressions found are fitted to all available data. Agreement is found for the decay widths and linear slopes, but a small discrepancy is observed for the quadratic slopes.

The discrepancy found can have several different origins. It could be an experimental problem or it could have a theoretical origin. In the latter case the corrections to the amplitude are threefold: strong isospin breaking, electromagnetic isospin breaking or higher order corrections.

Paper II

In this paper effects from the *strong isospin breaking* and part of the electromagnetic isospin breaking are added. This means effects of the quark mass difference $m_u - m_d$ as well as the *local electromagnetic effects*. The difference between m_u and m_d leads to mixing between π and η. This means changes in the formulas for both the physical masses of π and η as well as the amplitude for any process involving either of the two. For a detailed discussion see [16].

Including the local EM part means introducing new Lagrangians at each order, proportional to e^2 and $p^2\, e^2$ respectively. The total Lagrangian is then

$$\mathcal{L} = \mathcal{L}_{S2} + \mathcal{L}_{S4} + \mathcal{L}_{W2} + \mathcal{L}_{W4} + \mathcal{L}_{E2} + \mathcal{L}_{S2E2} + \mathcal{L}_{W2E2} \,. \tag{56}$$

To estimate the effects of the strong breaking, a comparison is made between the squared amplitudes with and without isospin violation. The effect is at a few percent level.

Paper III

In this paper the effects of radiative corrections, or *explicit* electromagnetic isospin breaking, are added which means that the total (first order) isospin breaking amplitude to next-to-leading chiral order is calculated.

The motivations for this are both because it is interesting in general to see the importance of isospin breaking, and also to investigate whether isospin violation will improve the fit to experimental data.

The radiative corrections, or non-local electromagnetic effects, are taken into account by adding new diagrams at each order. In total 40 new topologies are added.

Once again, the effects of the isospin breaking are estimated by comparing the squared amplitudes with and without isospin violation. The effect seems to be at a 5–10 percent level.

Paper IV

This is the final paper in the series, and we once again perform a fit to experimental data. This time the theoretical amplitudes include full isospin breaking. The resulting fit has changed somewhat due to this as well as the additions of new data. We also try fitting with additional model assumptions, like factorization and vector dominance.

To be complete we also calculate $K \to 2\pi$, $K \to 2\pi\gamma$ and $K \to 3\pi\gamma$ to the same order as $K \to 3\pi$. Some of these were calculated before, and we agree with previous results.

References

[1] D. B. Kaplan, "Effective field theories," nucl-th/9506035.

[2] J. Polchinski, "Effective field theory and the Fermi surface," hep-th/9210046.

[3] H. Leutwyler, "Foundations and scope of chiral perturbation theory," hep-ph/9409423.

[4] G. Ecker, "Strong interactions of light flavours," hep-ph/0011026.

[5] A. Pich, "Effective field theory," hep-ph/9806303.

[6] J. Donoghue, E. Golowich, B. Holstein, "Dynamics of the Standard Model", Cambridge University Press, Cambridge, Great Britain (1992).

[7] P. Dhonte, "Pion and Kaon Dynamics at Higher Orders in Chiral Perturbation Theory", Ph. D. Thesis, KFS AB, Lund, Sweden (2004).

[8] F. Mandl, G. Shaw, "Quantum Field Theory", John Wiley & Sons, Chichester, Great Britain (1984).

[9] M. Peskin and D. Schroeder, "An Introduction to quantum field theory," Perseus Books, Reading MA, USA (1995).

[10] S. Weinberg, "The Quantum Theory of Fields, Vol. 2: Modern Applications", Cambridge University Press, Cambridge, Great Britain (1996).

[11] S. Weinberg, "Phenomenological Lagrangians," Physica A **96** (1979) 327.

[12] J. Gasser and H. Leutwyler, "Chiral Perturbation Theory To One Loop," Annals Phys. **158** (1984) 142.

[13] J. Gasser and H. Leutwyler, "Chiral Perturbation Theory: Expansions In The Mass Of The Strange Quark," Nucl. Phys. B **250** (1985) 465.

[14] S. Weinberg, "Pion Scattering Lengths," Phys. Rev. Lett. **17** (1966) 616.

[15] J. Kambor, J. Missimer and D. Wyler, "K $\to$ 2 pi and K $\to$ 3 pi decays in next-to-leading order chiral perturbation theory," Phys. Lett. B **261** (1991) 496.

[16] G. Amorós, J. Bijnens, P. Talavera "QCD Isospin Breaking in Meson Masses, Decay Constants and Quark Mass Ratios" Nucl. Phys. B 602 (2001) 87, [hep-ph/0101127].

Acknowledgments

I've learned that all a person has in life is family and friends. If you lose those, you have nothing, so friends are to be treasured more than anything else in the world.

Trey Parker and Matt Stone, South Park

First of all I would like to thank Hans, without whom none of this work would have been possible. Even though he is a very busy man, he always seems happy to answer all my questions. Our cooperation has worked perfectly.

I would also like to thank the rest of the people at the department. Even though I am not such a big talker myself (in groups consisting of more than two people), I do appreciate when others have interesting and fun things to say, and I haven't felt a lack of either during the years at the department. Especially Samuel Andersson, Linus Göransson and Peter Mörck have contributed with many "interesting" discussions during the coffee breaks. A special thanks also goes to my roommates, Fredrik Söderberg and Niclas Danielsson, for making the office a very pleasant place indeed.

I want to thank my mother, my father and my two sisters for always being there. During the time of this work a lot of things have happened, some good and some bad, but I think that we have come out nice and safe on the other side.

Thanks also to all my friends who make my life so much more interesting and entertaining. In particular the members of the board game group (Christian Nilsson, Fredrik Söderberg, Jimmy Strömberg, Kristofer Bengtsson and Niclas Danielsson) for making a Monday evening something to look forward to.

Last, but of course not least, I want to thank my wife Åsa. She has during the last ten years shown an enormous loyalty and a willingness beyond what can be expected to put up with all the weird things I have made us go through. She is the most important person in my life.

Thanks.

$K \to 3\pi$ Decays in Chiral Perturbation Theory

Paper I

$K \to 3\pi$ Decays in Chiral Perturbation Theory[1,2]

Johan Bijnens, Pierre Dhonte and Fredrik Persson

Department of Theoretical Physics, Lund University
Sölvegatan 14A, S 22362 Lund, Sweden

Abstract:

The CP conserving amplitudes for the decays $K \to 3\pi$ are calculated in Chiral Perturbation Theory at the next-to-leading order. We present the expressions in a compact form with single parameter functions only. These expressions are then fitted to all available $K \to 2\pi$ and $K \to 3\pi$ data to obtain a fit of the parameters that occur. We compare with the work of Kambor, Missimer and Wyler.

[1]Reprinted from Nucl. Phys. B 648 (2003) 317, Johan Bijnens, Pierre Dhonte and Fredrik Persson, $K \to 3\pi$ Decays in Chiral Perturbation Theory, Copyright (2003), with permission from Elsevier.

[2]LU TP 02-21, hep-ph/0205341, October 2002

1.1 Introduction

Chiral Perturbation Theory (ChPT) is the low-energy effective field theory of the strong interactions. It was introduced in its modern form by Weinberg, Gasser and Leutwyler [1–3]. It has had many successes and applications. A pedagogical introduction can be found in [4]. The method has been used as well for nonleptonic weak decays. The main work of extending ChPT to the nonleptonic weak interaction was done long ago by Kambor, Missimer and Wyler who worked out the general formalism [5] and applied it to $K \to 2\pi, 3\pi$ decays [6]. These results were then used to obtain directly relations between physical observables in [7]. Reviews of applications of ChPT to nonleptonic weak interactions are [8].

Earlier work using current algebra methods or tree level Lagrangians relevant for $K \to 3\pi$ are [9, 10] and references therein. Many new measurements in $K \to 3\pi$ have become available since the work of [6] so an update of the fits of the parameters done there became necessary. The analytical expressions of [6] were never published and have since been lost. This forced us to reevaluate these decays and we present the analytical results here using a simplified form derived using the arguments first used for $\pi\pi$-scattering by Knecht et al. [11]. We then perform a detailed comparison of the expressions with the data and find a reasonable agreement. We point out some directions for future work.

The next section defines our notation and gives a unique list of possible terms at next-to-leading order in ChPT. Section 1.3 gives the list of decays and the isospin constraints as well as the simplified analytical form valid up till order p^6 in ChPT. The ambiguities in this simplified form are discussed in detail in App. 1.A. This section also discusses the isospin constraints on the various amplitudes. Our main result, the recalculation of the $K \to 3\pi$ amplitudes is discussed in section 1.4 where we present the tree level result and work out the independent combinations of the weak p^4 parameters that occur. The expressions at order p^4 are still rather cumbersome and are listed in App. 1.B. Section 1.5 contains a short review of the available data and presents in detail the various fits we have performed to the data. Our conclusions are summarized in the final section.

1.2 The ChPT Lagrangian

The Lagrangian of ChPT in the strong sector was worked out at next-to-leading order (NLO) in [2] and is given by

$$\mathcal{L}_S = \mathcal{L}_{S2} + \mathcal{L}_{S4}\,, \tag{1.1}$$

with

$$\mathcal{L}_{S2} = \frac{F_0^2}{4}\{\langle D_\mu U^\dagger D^\mu U\rangle + \langle \chi^\dagger U + \chi U^\dagger\rangle\}\,, \tag{1.2}$$

$$\begin{aligned}
\mathcal{L}_{S4} = \; & L_1\langle D_\mu U^\dagger D^\mu U\rangle^2 + L_2\langle D_\mu U^\dagger D_\nu U\rangle\langle D^\mu U^\dagger D^\nu U\rangle \\
& +L_3\langle D^\mu U^\dagger D_\mu U D^\nu U^\dagger D_\nu U\rangle + L_4\langle D^\mu U^\dagger D_\mu U\rangle\langle \chi^\dagger U + \chi U^\dagger\rangle \\
& +L_5\langle D^\mu U^\dagger D_\mu U(\chi^\dagger U + U^\dagger\chi)\rangle + L_6\langle \chi^\dagger U + \chi U^\dagger\rangle^2 \\
& +L_7\langle \chi^\dagger U - \chi U^\dagger\rangle^2 + L_8\langle \chi^\dagger U\chi^\dagger U + \chi U^\dagger \chi U^\dagger\rangle \\
& -iL_9\langle F^R_{\mu\nu} D^\mu U D^\nu U^\dagger + F^L_{\mu\nu} D^\mu U^\dagger D^\nu U\rangle \\
& +L_{10}\langle U^\dagger F^R_{\mu\nu} U F^{L\mu\nu}\rangle \,.
\end{aligned} \tag{1.3}$$

$\langle A\rangle$ stands for the flavour trace of the matrix A, and F_0 is the pion decay constant in the chiral limit. The special unitary matrix U contains the Goldstone boson fields

$$U = \exp\left(\frac{i\sqrt{2}}{F_0}M\right)\,, \quad M = \begin{pmatrix} \frac{1}{\sqrt{2}}\pi^0 + \frac{1}{\sqrt{6}}\eta & \pi^+ & K^+ \\ \pi^- & \frac{-1}{\sqrt{2}}\pi^0 + \frac{1}{\sqrt{6}}\eta & K^0 \\ K^- & \overline{K^0} & \frac{-2}{\sqrt{6}}\eta \end{pmatrix}\,. \tag{1.4}$$

The formalism we use is the external field method of [2] with s, p, l_μ and r_μ matrix valued scalar, pseudo-scalar, left-handed and right handed vector external fields respectively. These show up in

$$\chi = 2B_0\,(s+ip)\,, \tag{1.5}$$

in the covariant derivative

$$D_\mu U = \partial_\mu U - ir_\mu U + iUl_\mu\,, \tag{1.6}$$

and in the field strength tensor

$$F^{L(R)}_{\mu\nu} = \partial_\mu l(r)_\nu - \partial_\nu l(r)_\mu - i\left[l(r)_\mu, l(r)_\nu\right]\,. \tag{1.7}$$

For our purpose it suffices to set

$$s = \begin{pmatrix} m_u & & \\ & m_d & \\ & & m_s \end{pmatrix}\,, \quad p = 0\,, \quad l_\mu = r_\mu = 0\,. \tag{1.8}$$

We also define the matrices u, u_μ and $\chi_\pm$,

$$u_\mu = iu^\dagger D_\mu U u^\dagger = u_\mu^\dagger\,, \quad u^2 = U, \quad \chi_\pm = u^\dagger\chi u^\dagger \pm u\chi^\dagger u\,. \tag{1.9}$$

The ChPT Lagrangian for the weak nonleptonic interactions at lowest order dates back to current algebra days [9] and is

$$\mathcal{L}_{W2} = C\,F_0^4\left[G_8\langle\Delta_{32}u_\mu u^\mu\rangle + G_8'\langle\Delta_{32}\chi_+\rangle + G_{27}t^{ij,kl}\,\langle\Delta_{ij}u_\mu\rangle\langle\Delta_{kl}u^\mu\rangle\right] + \text{ h.c.} \tag{1.10}$$

The tensor $t^{ij,kl}$ has as nonzero components

$$
\begin{aligned}
t^{21,13} = t^{13,21} = \frac{1}{3} \quad &; \quad t^{22,23} = t^{23,22} = -\frac{1}{6}\,; \\
t^{23,33} = t^{33,23} = -\frac{1}{6} \quad &; \quad t^{23,11} = t^{11,23} = \frac{1}{3}\,.
\end{aligned}
\tag{1.11}
$$

The matrix Δ_{ij} is defined as

$$
\Delta_{ij} \equiv u\lambda_{ij}u^\dagger\,, \quad (\lambda_{ij})_{ab} \equiv \delta_{ia}\,\delta_{jb}\,. \tag{1.12}
$$

We only quote the $|\Delta S| = 1$ part here but the others can be obtained by changing the indices in Δ_{32} and $t^{ij,kl}$ appropriately. The parts with G_8 and G_8' transforms as an octet under $SU(3)_L$ while the G_{27} part transforms as a 27 under the same group. The term with G_8' is often referred to as the weak mass term.

The coefficient C is defined such that in the chiral and large N_c limits $G_8 = G_{27} = 1$,

$$
C = -\frac{3}{5}\,\frac{G_F}{\sqrt{2}} V_{ud}\,V_{us}^*\,. \tag{1.13}
$$

The correspondence with the parameters c_2 and c_3 of [5,6] is

$$
c_2 = CF_0^4 G_8 \quad c_3 = -\frac{1}{6} CF_0^4 G_{27}\,. \tag{1.14}
$$

The NLO nonleptonic weak Lagrangian was first worked out in [5] but the basis given there was redundant. Subsequent work on a less redundant basis was [12]. A fully nonredundant basis for the octet part was presented in [13]. We will use the basis of [13] for the octet part and use the notation of [5] for the 27 part, but keep only the nonredundant terms as derived in [12]. The NLO weak ChPT Lagrangian, quoting only the terms relevant for $K \to 2\pi$ and $K \to 3\pi$ decays, is

$$
\begin{aligned}
\mathcal{L}^{(4)}_{\Delta S=1} \;=\; & C\,F_0^2 \Big\{ G_8 \Big[N_1\mathcal{O}_1^8 + N_2\mathcal{O}_2^8 + N_3\mathcal{O}_3^8 + N_4\mathcal{O}_4^8 N_5\mathcal{O}_5^8 + N_6\mathcal{O}_6^8 + N_7\mathcal{O}_7^8 \\
& + N_8\mathcal{O}_8^8 + N_9\mathcal{O}_9^8 + N_{10}\mathcal{O}_{10}^8 + N_{11}\mathcal{O}_{11}^8 + N_{12}\mathcal{O}_{12}^8 + N_{13}\mathcal{O}_{13}^8 \Big] \\
& + G_{27} \Big[D_1\mathcal{O}_1^{27} + D_2\mathcal{O}_2^{27} + D_4\mathcal{O}_4^{27} + D_5\mathcal{O}_5^{27} + D_6\mathcal{O}_6^{27} + D_7\mathcal{O}_7^{27} \\
& + D_{26}\mathcal{O}_{26}^{27} + D_{27}\mathcal{O}_{27}^{27} + D_{28}\mathcal{O}_{28}^{27} + D_{29}\mathcal{O}_{29}^{27} + D_{30}\mathcal{O}_{30}^{27} + D_{31}\mathcal{O}_{31}^{27} \Big] \Big\} \\
& + \text{h.c.}\,.
\end{aligned}
\tag{1.15}
$$

The octet operators are

$$
\begin{aligned}
\mathcal{O}^8_1 &= \langle \Delta_{32} u_\mu u^\mu u_\nu u^\nu \rangle\,,\\
\mathcal{O}^8_2 &= \langle \Delta_{32} u_\mu u_\nu u^\nu u^\mu \rangle\,,\\
\mathcal{O}^8_3 &= \langle \Delta_{32} u_\mu u_\nu \rangle \langle u^\mu u^\nu \rangle\,,\\
\mathcal{O}^8_4 &= \langle \Delta_{32} u_\mu \rangle \langle u_\nu u^\mu u^\nu \rangle\,,\\
\mathcal{O}^8_5 &= \langle \Delta_{32} (\chi_+ u_\mu u^\mu + u_\mu u^\mu \chi_+) \rangle\,,\\
\mathcal{O}^8_6 &= \langle \Delta_{32} u_\mu \rangle \langle u^\mu \chi_+ \rangle\,,\\
\mathcal{O}^8_7 &= \langle \Delta_{32} \chi_+ \rangle \langle u_\mu u^\mu \rangle\,,\\
\mathcal{O}^8_8 &= \langle \Delta_{32} u_\mu u^\mu \rangle \langle \chi_+ \rangle\,,\\
\mathcal{O}^8_9 &= \langle \Delta_{32} (\chi_- u_\mu u^\mu - u_\mu u^\mu \chi_-) \rangle\,,\\
\mathcal{O}^8_{10} &= \langle \Delta_{32} \chi_+ \chi_+ \rangle\,,\\
\mathcal{O}^8_{11} &= \langle \Delta_{32} \chi_+ \rangle \langle \chi_+ \rangle\,,\\
\mathcal{O}^8_{12} &= \langle \Delta_{32} \chi_- \chi_- \rangle\,,\\
\mathcal{O}^8_{13} &= \langle \Delta_{32} \chi_- \rangle \langle \chi_- \rangle\,.
\end{aligned}
\tag{1.16}
$$

The 27 operators are

$$
\begin{aligned}
\mathcal{O}^{27}_1 &= t^{ij,kl} \langle \Delta_{ij} \chi_+ \rangle \langle \Delta_{kl} \chi_+ \rangle\,,\\
\mathcal{O}^{27}_2 &= t^{ij,kl} \langle \Delta_{ij} \chi_- \rangle \langle \Delta_{kl} \chi_- \rangle\,,\\
\mathcal{O}^{27}_4 &= t^{ij,kl} \langle \Delta_{ij} u_\mu \rangle \langle \Delta_{kl} (u^\mu \chi_+ + \chi_+ u^\mu) \rangle\,,\\
\mathcal{O}^{27}_5 &= t^{ij,kl} \langle \Delta_{ij} u_\mu \rangle \langle \Delta_{kl} (u^\mu \chi_- - \chi_- u^\mu) \rangle\,,\\
\mathcal{O}^{27}_6 &= t^{ij,kl} \langle \Delta_{ij} \chi_+ \rangle \langle \Delta_{kl} u_\mu u^\mu \rangle\,,\\
\mathcal{O}^{27}_7 &= t^{ij,kl} \langle \Delta_{ij} u_\mu \rangle \langle \Delta_{kl} u^\mu \rangle \langle \chi_+ \rangle\,,\\
\mathcal{O}^{27}_{26} &= t^{ij,kl} \langle \Delta_{ij} u_\mu u^\mu \rangle \langle \Delta_{kl} u_\nu u^\nu \rangle\,,\\
\mathcal{O}^{27}_{27} &= t^{ij,kl} \langle \Delta_{ij} (u_\mu u_\nu + u_\nu u_\mu) \rangle \langle \Delta_{kl} (u^\mu u^\nu + u^\nu u^\mu) \rangle\,,\\
\mathcal{O}^{27}_{28} &= t^{ij,kl} \langle \Delta_{ij} (u_\mu u_\nu - u_\nu u_\mu) \rangle \langle \Delta_{kl} (u^\mu u^\nu - u^\nu u^\mu) \rangle\,,\\
\mathcal{O}^{27}_{29} &= t^{ij,kl} \langle \Delta_{ij} u_\mu \rangle \langle \Delta_{kl} u_\nu u^\mu u^\nu \rangle\,,\\
\mathcal{O}^{27}_{30} &= t^{ij,kl} \langle \Delta_{ij} u_\mu \rangle \langle \Delta_{kl} (u^\mu u_\nu u^\nu + u_\nu u^\nu u^\mu) \rangle\,,\\
\mathcal{O}^{27}_{31} &= t^{ij,kl} \langle \Delta_{ij} u_\mu \rangle \langle \Delta_{kl} u^\mu \rangle \langle u_\nu u^\nu \rangle\,.
\end{aligned}
\tag{1.17}
$$

Notice that some have the opposite sign compared to [5], because of the difference in the definition of χ_i and P of that reference. The basis used in [14] for the octet case is slightly different but related to the one here by

$$
\begin{array}{lll}
N_5 = E_{10} - E_{11}\,; & N_6 = E_{11} + 2E_{12}\,; & N_7 = \frac{1}{2}E_{11} + E_{13}\,;\\
N_8 = E_{11}\,; & N_9 = E_{15}\,; & N_{10} = E_1 - E_5\,;\\
N_{11} = E_2\,; & N_{12} = -E_3 + E_5\,; & N_{13} = E_4\,;\\
N_{36} = E_5\,. & &
\end{array}
\tag{1.18}
$$

L_i	ℓ_i	N_i	n_i	D_i	d_i
1	$-3/64$	1	-1	1	$1/12$
2	$-3/32$	2	$1/4$	2	0
3	0	3	0	4	$-3/2$
4	$-1/16$	4	$-1/2$	5	$-1/2$
5	$-3/16$	5	$-3/4 - 3/8\,(G_8'/G_8)$	6	$3/4$
6	$-11/288$	6	$1/8$	7	$-1/2$
7	0	7	$9/16 - 1/4\,(G_8'/G_8)$	26	$1/2$
8	$-5/96$	8	$1/4$	27	$1/4$
9	$-1/8$	9	$-3/8 + 3/8\,(G_8'/G_8)$	28	$5/6$
10	$1/8$	10	$-1/3 - 5/24\,(G_8'/G_8)$	29	$-19/$
		11	$13/36 - 11/36\,(G_8'/G_8)$	30	$-5/3$
		12	$5/24 - 5/24\,(G_8'/G_8)$	31	0
		13	0		

Table 1.1: The coefficients of the subtraction of the infinite parts defined in Eq. (1.19).

Notice that there is a small misprint in the relation between the E_i and N_i in (2.19) of [14] in the relation between N_{13} and E_4.

The infinities appearing in the loop diagrams are canceled by replacing the coefficients in (1.3) and (1.15) by the renormalized coefficients and a subtraction part. The infinities needed in the strong sector were calculated first in [3] and those for the weak sector in [5] and confirmed in [12]. For the terms in Eqs. (1.3) and (1.15) they are all of the type

$$X_i = (e^c \mu)^{-2\epsilon} \left(X_i^r + x_i \frac{1}{16\pi^2 \epsilon} \right) , \tag{1.19}$$

with the dimension of space-time $d = 4 - 2\epsilon$ and

$$c = -\frac{1}{2} \left(\ln(4\pi) + \Gamma'(1) + 1 \right) , \tag{1.20}$$

for $X = L, N, D$. The coefficients are listed in Table 1.1 [3,5,12].

1.3 Kinematics and Isospin

There are five CP-conserving decays of the type $K \to 3\pi$:

$$\begin{array}{lcll} K_L(k) & \to & \pi^0(p_1)\pi^0(p_2)\pi^0(p_3)\,, & [A^L_{000}]\,, \\ K_L(k) & \to & \pi^+(p_1)\pi^-(p_2)\pi^0(p_3)\,, & [A^L_{+-0}]\,, \end{array}$$

$$\begin{aligned} K_S(k) &\rightarrow \pi^+(p_1)\pi^-(p_2)\pi^0(p_3)\,, \quad [A^S_{+-0}]\,, \\ K^+(k) &\rightarrow \pi^0(p_1)\pi^0(p_2)\pi^+(p_3)\,, \quad [A_{00+}]\,, \\ K^+(k) &\rightarrow \pi^+(p_1)\pi^+(p_2)\pi^-(p_3)\,, \quad [A_{++-}]\,, \end{aligned} \tag{1.21}$$

where we have indicated the four momentum defined for each particle and the symbol we will use for the amplitude. The K^+ decays have an obvious counterpart in K^- decays.

The kinematics is normally treated using

$$s_1 = (k-p_1)^2\,, \quad s_2 = (k-p_2)^2\,, \quad s_3 = (k-p_3)^2\,. \tag{1.22}$$

The amplitudes are often expanded in terms of the Dalitz plot variables x and y defined via

$$x = \frac{s_2 - s_1}{m^2_{\pi^+}}\,, \quad y = \frac{s_3 - s_0}{m^2_{\pi^+}}\,, \quad s_0 = \frac{1}{3}\left(m_K^2 + m^2_{\pi^1} + m^2_{\pi^2} + m^2_{\pi^3}\right)\,, \tag{1.23}$$

where the kaon mass and the pion masses in s_0 are those from the particles appearing in the decay under consideration.

The amplitudes for $K_L \rightarrow \pi^+\pi^-\pi^0, K^+ \rightarrow \pi^+\pi^+\pi^-$ and $K^+ \rightarrow \pi^0\pi^0\pi^+$ are symmetric under the interchange of the first two pions because of CP or Bose-symmetry. The amplitude for $K_L \rightarrow \pi^0\pi^0\pi^0$ is obviously symmetric under the interchange of all three final state particles and the one for $K_S \rightarrow \pi^+\pi^-\pi^0$ is antisymmetric under the interchange of π^+ and π^- because of CP.

Isospin invariance does give some constraints on the amplitudes [15–17]. These can be written as

$$\begin{aligned} A^L_{000}(s_1,s_2,s_3) &= 3A_n(s_1,s_2,s_3)\,, \\ A^L_{+-0}(s_1,s_2,s_3) &= A_n(s_1,s_2,s_3) - B_n(s_1,s_2,s_3)\,, \\ A^S_{+-0}(s_1,s_2,s_3) &= C_0(s_1,s_2,s_3) + \frac{2}{3}\left[B_t(s_3,s_2,s_1) - B_t(s_3,s_1,s_2)\right]\,, \\ A_{00+}(s_1,s_2,s_3) &= A_c(s_1,s_2,s_3) - B_c(s_1,s_2,s_3) + B_t(s_1,s_2,s_3)\,, \\ A_{++-}(s_1,s_2,s_3) &= 2A_c(s_1,s_2,s_3) + B_c(s_1,s_2,s_3) + B_t(s_1,s_2,s_3)\,. \end{aligned} \tag{1.24}$$

The functions $A_{c,n}$ are fully symmetric in s_1, s_2, s_3. C_0 is fully antisymmetric and $B_{c,n,t}(s_1,s_2,s_3)$ is symmetric under the interchange $s_1 \leftrightarrow s_2$ and satisfies the relation

$$B_i(s_1,s_2,s_3) + B_i(s_2,s_3,s_1) + B_i(s_3,s_1,s_2) = 0\,. \tag{1.25}$$

$A_{c,n}$ and $B_{c,n}$ belong to the $I=1$ final state, B_t to the $I=2$ final state and C_0 to the $I=0$ final state.

A further simplification can be obtained by observing that the imaginary parts of loop diagrams in ChPT do not contain $\ell \geq 2$ until at least $\mathcal{O}(p^8)$. This allows to rewrite the amplitudes in a way that only contains functions of single variables and is fully correct up to $\mathcal{O}(p^6)$. The underlying arguments are the same as the ones used for a similar decomposition for $\pi\pi$ scattering by [11].

$$\begin{aligned}
A^L_{000}(s_1,s_2,s_3) &= M_0(s_1)+M_0(s_2)+M_0(s_3)\,,\\
A^L_{+-0}(s_1,s_2,s_3) &= M_1(s_3)+M_2(s_1)+M_2(s_2)+M_3(s_1)(s_2-s_3)\\
&\quad +M_3(s_2)(s_1-s_3)\,,\\
A^S_{+-0}(s_1,s_2,s_3) &= M_4(s_1)-M_4(s_2)+M_5(s_1)(s_2-s_3)-M_5(s_2)(s_1-s_3)\\
&\quad +M_6(s_3)(s_1-s_2)\,,\\
A_{00+}(s_1,s_2,s_3) &= M_7(s_3)+M_8(s_1)+M_8(s_2)+M_9(s_1)(s_2-s_3)\\
&\quad +M_9(s_2)(s_1-s_3)\,,\\
A_{++-}(s_1,s_2,s_3) &= M_{10}(s_3)+M_{11}(s_1)+M_{11}(s_2)+M_{12}(s_1)(s_2-s_3)\\
&\quad +M_{12}(s_2)(s_1-s_3)\,. \qquad (1.26)
\end{aligned}$$

The expressions for the various amplitudes become significantly shorter when written explicitly in this form. Comparing (1.24) and (1.26) gives

$$\begin{aligned}
A_n(s_1,s_2,s_3) &= \sum_{i=1,3}\frac{1}{3}M_0(s_i)\,,\\
A_c(s_1,s_2,s_3) &= \sum_{i=1,3}\frac{1}{3}\left(M_7(s_i)+2M_8(s_i)\right)\,,\\
B_n(s_1,s_2,s_3) &= B_{n1}(s_1)+B_{n1}(s_2)-2B_{n1}(s_3)+B_{n2}(s_1)(s_2-s_3)\\
&\quad +B_{n2}(s_2)(s_1-s_3)\,,\\
B_{n1}(s) &= \frac{1}{3}\left(M_1(s)-M_2(s)\right)\,,\\
B_{n2}(s) &= -M_3(s)\,,\\
B_c(s_1,s_2,s_3) &= B_{c1}(s_1)+B_{c1}(s_2)-2B_{c1}(s_3)+B_{c2}(s_1)(s_2-s_3)\\
&\quad +B_{c2}(s_2)(s_1-s_3)\,,\\
B_{c1}(s) &= \frac{1}{6}\left(M_7(s)-M_8(s)-M_{10}(s)+M_{11}(s)\right)\\
B_{c2}(s) &= \frac{1}{2}\left(-M_9(s)+M_{12}(s)\right)\,,\\
B_t(s_1,s_2,s_3) &= B_{t1}(s_1)+B_{t1}(s_2)-2B_{t1}(s_3)+B_{t2}(s_1)(s_2-s_3)\\
&\quad +B_{t2}(s_2)(s_1-s_3)\,,\\
B_{t1}(s) &= \frac{1}{6}\left(-M_7(s)+M_8(s)-M_{10}(s)+M_{11}(s)\right)\\
B_{t2}(s) &= \frac{1}{2}\left(M_9(s)+M_{12}(s)\right)\,,\\
C_0(s_1,s_2,s_3) &= C_{01}(s_3)(s_1-s_2)+C_{01}(s_1)(s_2-s_3)+C_{01}(s_2)(s_3-s_1)\,,
\end{aligned}$$

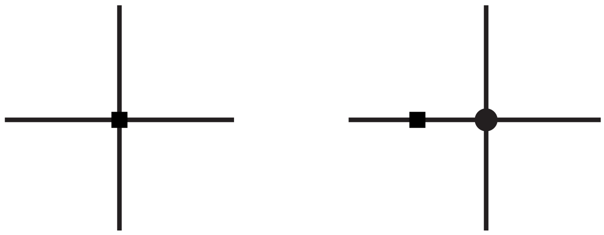

Figure 1.1: The tree level diagrams for $K \to 3\pi$. A filled square is a vertex from $\mathcal{L}_{W2}$ and a filled circle from $\mathcal{L}_{S2}$.

$$C_{01}(s) = \frac{1}{3}\left(2M_5(s) + M_6(s)\right) \tag{1.27}$$

and the relations

$$\begin{aligned} M_0(s) &= M_1(s) + 2M_2(s)\,, \\ 2M_7(s) + 4M_8(s) &= M_{10}(s) + 2M_{11}(s)\,, \\ M_4(s) &= \frac{1}{3}\left(M_7(s) - M_8(s) + M_{10}(s) - M_{11}(s)\right) \\ M_5(s) - M_6(s) &= M_9(s) + M_{12}(s)\,. \end{aligned} \tag{1.28}$$

The split-up between the polynomial parts in (1.26) has some ambiguity as discussed in App. 1.A. The same ambiguity appears in the rewriting of the B_{cnt} functions in single variable parts and can affect the last two relations in (1.28). The results given explicitly in App. 1.B are brought in a form satisfying the relations (1.28) using this freedom.

1.4 Analytical Results

The lowest order result is well known and follows from the diagrams in Fig.1.1. The Feynman amplitude at tree level for A^L_{000} is

$$M_0(s)|_{p^2} = i\frac{CF_0^4}{F_\pi^3 F_K}\,\frac{1}{3}\,(G_8 - G_{27})\,m_K^2\,. \tag{1.29}$$

A choice for A^L_{+-0} compatible with the relations (1.28) and (1.29) is

$$\begin{aligned} M_1(s)|_{p^2} &= i\frac{CF_0^4}{F_\pi^3 F_K}\,\frac{1}{3}\,(G_8 - G_{27})\,m_K^2\,, \\ M_2(s)|_{p^2} &= 0\,, \\ M_3(s)|_{p^2} &= i\frac{CF_0^4}{F_\pi^3 F_K}\left\{-\frac{G_8}{3} + \frac{G_{27}}{6}\,\frac{-3m_K^2 + 8m_\pi^2}{m_K^2 - m_\pi^2}\right\} \end{aligned} \tag{1.30}$$

The tree level result for A^S_{+-0} allows very much of reshuffling between M_4, M_5 and M_6. A choice is

$$\begin{aligned}
M_4(s)|_{p^2} &= i\frac{CF_0^4}{F_\pi^3 F_K}\,\frac{G_{27}}{m_K^2-m_\pi^2}\,\frac{5}{6}\left(2m_\pi^2-3m_K^2\right)s\,,\\
M_5(s)|_{p^2} &= i\frac{CF_0^4}{F_\pi^3 F_K}\,\frac{G_{27}}{m_K^2-m_\pi^2}\,\frac{5}{6}\left(2m_\pi^2-3m_K^2\right)\,,\\
M_6(s)|_{p^2} &= i\frac{CF_0^4}{F_\pi^3 F_K}\,\frac{G_{27}}{m_K^2-m_\pi^2}\,\frac{5}{6}\left(2m_\pi^2-3m_K^2\right)\,. \qquad (1.31)
\end{aligned}$$

A_{00+} leads to

$$\begin{aligned}
M_7(s)|_{p^2} &= i\frac{CF_0^4}{F_\pi^3 F_K}\left\{\frac{G_8}{2}\left(m_\pi^2+m_K^2-s\right)\right.\\
&\left.+\frac{G_{27}}{m_K^2-m_\pi^2}\left(\frac{-5}{3}m_\pi^2 m_K^2+\frac{13}{6}m_\pi^4-\frac{1}{2}m_K^4+\frac{7}{6}m_\pi^2 s-\frac{17}{6}m_K^2 s\right)\right\},\\
M_8(s)|_{p^2} &= -\,M_7(s)|_{p^2}+i\frac{CF_0^4}{F_\pi^3 F_K}\,\frac{G_{27}}{m_K^2-m_\pi^2}\,\frac{5}{6}\left(2m_\pi^2-3m_K^2\right)s\,,\\
M_9(s)|_{p^2} &= 0\,. \qquad (1.32)
\end{aligned}$$

The amplitude for A_{++-} can be written as

$$\begin{aligned}
M_{10}(s)|_{p^2} &= i\frac{CF_0^4}{F_\pi^3 F_K}\left\{G_8\left(s-m_\pi^2-m_K^2\right)\right.\\
&\left.+G_{27}\left(-\frac{13}{3}\,s+m_K^2+\frac{13}{3}m_\pi^2\right)\right\},\\
M_{11}(s)|_{p^2} &= 0\,,\\
M_{12}(s)|_{p^2} &= 0\,. \qquad (1.33)
\end{aligned}$$

The result at order p^4 is significantly longer. The diagrams that contribute are shown in Fig. 1.2. Using the decomposition of all the amplitudes in the $M_i(s)$, and using the freedom in choosing the functions $M_i(s)$, relatively compact expressions can be obtained and we have given them explicitly in App. 1.B. Our results for $K \to \pi\pi$ are in full agreement with [14].

In order to do the data fits it is important to see how many combinations of the 25 unknown parameters appearing in (1.15) actually matter. Taking the various independent coefficients from the amplitudes $M_i(s)$, it turns out that only 11 linear combinations of the 25 parameters show up. Of these seven appear in the amplitudes multiplied by coefficients of order m_K^4 while the remaining four have coefficients of order $m_\pi^2 m_K^2$.

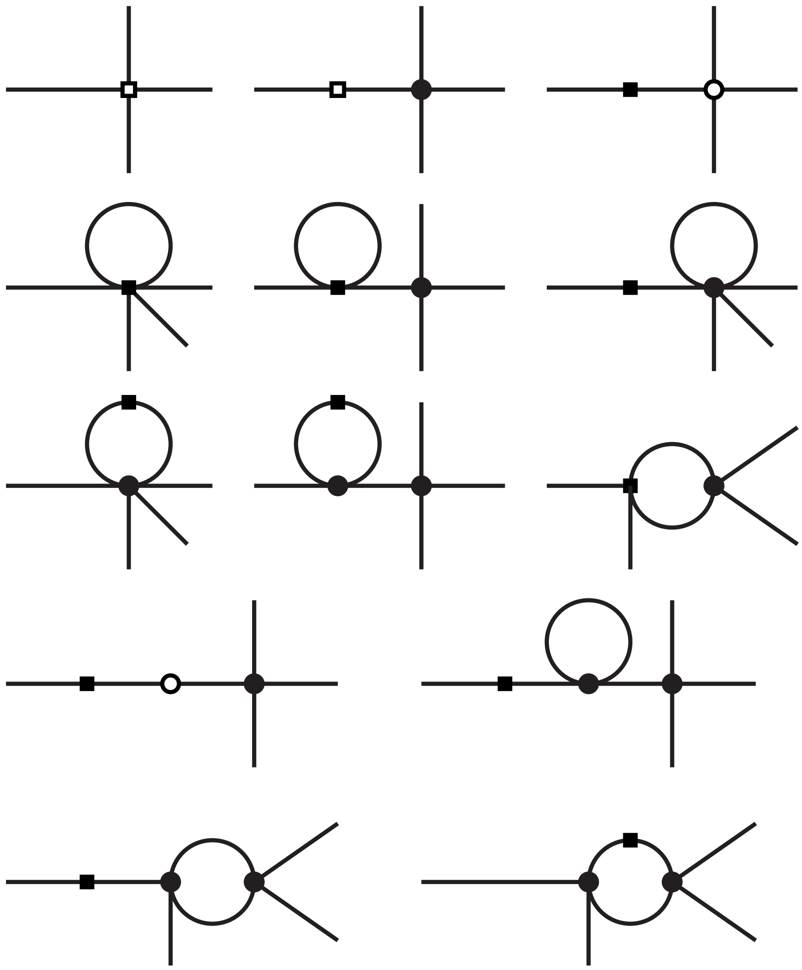

Figure 1.2: The diagrams of order p^4. An open square is a vertex from $\mathcal{L}_{W4}$, an open circle a vertex from $\mathcal{L}_{S4}$, a filled square a vertex from $\mathcal{L}_{W2}$ and a filled circle a vertex from $\mathcal{L}_{S2}$. Diagrams contributing to strong interaction wave function renormalization are not shown.

The measurable combinations are displayed in table 1.2. Any linear combination of them is of course also allowed. The choice displayed in the table was made to have all combinations to be orthogonal to the non-measurable ones when possible. The remainder was then chosen simply to have somewhat

$\tilde{K}_1$	$G_8\left(N_5^r - 2N_7^r + 2N_8^r + N_9^r\right) + G_{27}\left(-\frac{1}{2}D_6^r\right)$
$\tilde{K}_2$	$G_8\left(N_1^r + N_2^r\right) + G_{27}\left(\frac{1}{3}D_{26}^r - \frac{4}{3}D_{28}^r\right)$
$\tilde{K}_3$	$G_8\left(N_3^r\right) + G_{27}\left(\frac{2}{3}D_{27}^r + \frac{2}{3}D_{28}^r\right)$
$\tilde{K}_4$	$G_{27}\left(D_4^r - D_5^r + 4D_7^r\right)$
$\tilde{K}_5$	$G_{27}\left(D_{30}^r + D_{31}^r + 2D_{28}^r\right)$
$\tilde{K}_6$	$G_{27}\left(8D_{28}^r - D_{29}^r + D_{30}^r\right)$
$\tilde{K}_7$	$G_{27}\left(-4D_{28}^r + D_{29}^r\right)$
$\tilde{K}_8$	$G_8\left(2N_5^r + 4N_7^r + N_8^r - 2N_{10}^r - 4N_{11}^r - 2N_{12}^r\right) + G_{27}\left(-\frac{2}{3}D_1^r + \frac{2}{3}D_6^r\right)$
$\tilde{K}_9$	$G_8\left(N_5^r + N_8^r + N_9^r\right) + G_{27}\left(-\frac{1}{6}D_6^r\right)$
$\tilde{K}_{10}$	$G_{27}\left(2D_2^r - 2D_4^r - D_7^r\right)$
$\tilde{K}_{11}$	$G_{27}\left(D_7^r\right)$

Table 1.2: The independent linear combinations of the N_i^r and D_i^r that appear in the amplitudes.

compact expressions for their contributions to the $M_i(s)$ and the A_0 and A_2 amplitude for $K \to \pi\pi$. $\tilde{K}_4$ is the combination multiplying m_K^4 in the A_2 amplitude. $\tilde{K}_1$ is the octet part of the A_0 amplitude proportional to m_K^4 plus the part of the 27 multiplying m_K^4 that cannot be written in terms of $\tilde{K}_4$. $\tilde{K}_{10}$ and $\tilde{K}_8$ are the equivalent parts of the coefficients of m_π^4 in A_2 and A_0. The numbering is chosen such that $\tilde{K}_1$ to $\tilde{K}_7$ contribute leading in m_K^2 and inside those categories the ones with octet contributions are listed first. There are 5 combinations with octet contributions of which three leading in m_K^2.

The amplitudes we calculated are at one loop in ChPT. They thus include final state rescattering effects. A partial analysis of this type of effects was done in [17]. They derived the relations

$$\begin{aligned}
\begin{pmatrix} A_c(s_1,s_2,s_3) \\ B_c(s_1,s_2,s_3) \end{pmatrix}_R &= R(s_1,s_2,s_3)\begin{pmatrix} A_c(s_1,s_2,s_3) \\ B_c(s_1,s_2,s_3) \end{pmatrix}_{NR} \\
\begin{pmatrix} A_n(s_1,s_2,s_3) \\ B_n(s_1,s_2,s_3) \end{pmatrix}_R &= R(s_1,s_2,s_3)\begin{pmatrix} A_n(s_1,s_2,s_3) \\ B_n(s_1,s_2,s_3) \end{pmatrix}_{NR} \\
B_2(s_1,s_2,s_3)_R &= \delta(s_1,s_2,s_3)B_2(s_1,s_2,s_3)_{NR} \qquad (1.34)
\end{aligned}$$

for the amplitudes defined in (1.24). The subscript R on the l.h.s. means that rescattering effects have been included and NR on the r.h.s. that they are not included. The expressions for the matrix function $R(s_1,s_2,s_3)$ and the function $\delta(s_1,s_2,s_3)$ to lowest order in ChPT can be found in [17]. We have checked numerically that our amplitudes satisfy those relations to the order required. The approach to the various thresholds ($s_i \to 4m_\pi^2$) is as expected to this order in ChPT. The effects of the thresholds can be seen in Fig. 1.3. The plot shows $\mathrm{Im}(A_{++-})$ as a function of x and y normalized to $-|A_{++-}(s_0,s_0,s_0)|$

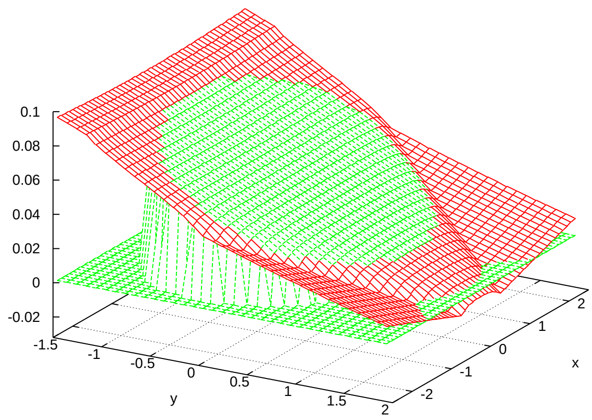

Figure 1.3: $\mathrm{Im}(A_{++-})$ as a function of x and y normalized to $-|A_{++-}(s_0,s_0,s_0)|$. The curve with the plateau at zero indicates the phasespace. The thresholds in the various $\pi\pi$ channels are clearly visible.

1.5 Experimental Data and Fits

At the end of the seventies a review was written incorporating the then finished precision experiments on the charged kaon decays [18]. Since then there have been many new results on $K \to 3\pi$ decays. A recent attempt to refit the data using some of the partial numerics of [6] is [19]. We have in this paper recalculated the full expressions and will do a full fit to the data contrary to [19]. We analyze the data in terms of the widths given in Table 1.3. The numbers are taken from the review of particle properties [20]. We do not directly use the data for Γ^S_{+-0} but instead fit directly to the measured quantity λ as discussed below.

In addition several slope parameters are measured in the various decays. The distributions in the Dalitz plot are conventionally described in terms of x and y defined in (1.23).

The decay amplitudes squared are now expanded as

$$\left|\frac{A(s_1,s_2,s_3)}{A(s_0,s_0,s_0)}\right|^2 = 1 + gy + hy^2 + kx^2 \tag{1.35}$$

where we have used CP invariance and the symmetries in the decays. For $K_L \to \pi^0\pi^0\pi^0$ $g = 0$ and $k = h/3$. For $K_S \to \pi^+\pi^-\pi^0$ one defines the ratio λ

Decay	Width [GeV]	CHPT fit [GeV]
$K^+ \to \pi^+\pi^0$	$(1.1245 \pm 0.0078) \cdot 10^{-17}$	$1.124 \cdot 10^{-17}$
$K_S \to \pi^0\pi^0$	$(2.3124 \pm 0.0207) \cdot 10^{-15}$	$2.312 \cdot 10^{-15}$
$K_S \to \pi^+\pi^-$	$(5.0543 \pm 0.0211) \cdot 10^{-15}$	$5.054 \cdot 10^{-15}$
$K_L \to \pi^0\pi^0\pi^0$	$(2.6901 \pm 0.0402) \cdot 10^{-18}$	$2.655 \cdot 10^{-18}$
$K_L \to \pi^+\pi^-\pi^0$	$(1.5978 \pm 0.0283) \cdot 10^{-18}$	$1.626 \cdot 10^{-18}$
$K_S \to \pi^+\pi^-\pi^0$	$(2.36 \pm 0.81) \cdot 10^{-21}$	$3.1 \cdot 10^{-21}$
$K^+ \to \pi^0\pi^0\pi^+$	$(0.9194 \pm 0.0426) \cdot 10^{-18}$	$0.911 \cdot 10^{-18}$
$K^+ \to \pi^+\pi^+\pi^-$	$(2.9706 \pm 0.0272) \cdot 10^{-18}$	$2.973 \cdot 10^{-18}$

Table 1.3: The various decay widths from the PDG tables [20].

or measures directly the expansion of the amplitude [21]

$$\begin{aligned}
\lambda &= \frac{\displaystyle\int_{y_{min}}^{y_{max}} dy \int_0^{x_{lim}(y)} dx A^{L*}_{+-0} A^S_{+-0}}{\displaystyle\int_{y_{min}}^{y_{max}} dy \int_0^{x_{lim}(y)} dx A^{L*}_{+-0} A^L_{+-0}} \\
A^S_{+-0} &= \gamma_S x - \xi_S xy\,.
\end{aligned} \tag{1.36}$$

The various measurements are given in Table 1.4. Experiments after 1980 have been cited explicitly. Earlier references can be found in the PDG [20] or in the comprehensive review [18]. Notice that there are significant discrepancies between the various experiments indicated by the fairly large scale factors.

The data have been analyzed previously in terms of expansions in x and y of the amplitudes.

$$\begin{aligned}
A^L_{000} &= 3(\alpha_1+\alpha_3) + 3(\zeta_1 - 2\zeta_3)\left(y^2 + \frac{1}{3}x^2\right)\,, \\
A^L_{+-0} &= (\alpha_1+\alpha_3) - (\beta_1+\beta_3)y + (\zeta_1 - 2\zeta_3)\left(y^2 + \frac{1}{3}x^2\right) \\
&\quad + (\xi_1 - 2\xi_3)\left(y^2 - \frac{1}{3}x^2\right)\,, \\
A^S_{+-0} &= \frac{2}{3}\sqrt{3}\,\gamma_3 x - \frac{4}{3}\xi'_3 xy\,, \\
A_{00+} &= \left(-\alpha_1 + \frac{1}{2}\alpha_3\right) + \left(\beta_1 - \frac{1}{2}\beta_3 - \sqrt{3}\gamma_3\right) y + (-\zeta_1 - \zeta_3)\left(y^2 + \frac{1}{3}x^2\right) \\
&\quad + (-\xi_1 - \xi_3 - \xi'_3)\left(y^2 - \frac{1}{3}x^2\right)\,,
\end{aligned}$$

Decay	Quantity		S	Ref.	CHPT fit
$K_L \to$	h	-0.0033 ± 0.0013		[22]	
$\pi^0\pi^0\pi^0$	h	-0.0061 ± 0.0010		[23]	
	h	-0.00506 ± 0.00135	1.7	average	-0.0072
$K_L \to$	g	0.678 ± 0.008	1.5	[20, 21]	0.677
$\pi^+\pi^-\pi^0$	h	0.076 ± 0.006		[20, 21]	0.085
	k	0.0099 ± 0.0015		[20, 21]	0.0055
$K_S \to$	$\mathrm{Re}(\lambda)$	0.0316 ± 0.0062		[21, 24]	0.0359
$\pi^+\pi^-\pi^0$	$\mathrm{Im}(\lambda)$	-0.0088 ± 0.0068		[21, 24]	-0.003
	γ_S	$(3.3 \pm 0.5) \cdot 10^{-8}$		[21]	$3.4 \cdot 10^{-8}$
	ξ_S	$(0.4 \pm 0.8) \cdot 10^{-8}$		[21]	$-0.2 \cdot 10^{-8}$
$K^\pm \to$	g	0.652 ± 0.031	2.7	[20, 25, 26]	0.638
$\pi^0\pi^0\pi^\pm$	h	0.057 ± 0.018	1.4	[20, 25, 26]	0.074
	k	0.0197 ± 0.0054		[20, 25]	0.0045
$K^+ \to$	g	-0.2154 ± 0.0035	1.4	[20]	-0.216
$\pi^+\pi^+\pi^-$	h	0.012 ± 0.008	1.4	[20]	0.012
	k	-0.0101 ± 0.0034	2.1	[20]	-0.0052
$K^- \to$	g	-0.217 ± 0.007	2.5	[20]	
$\pi^-\pi^-\pi^+$	h	0.010 ± 0.006		[20]	
	k	-0.0084 ± 0.0019	2.1	[20]	

Table 1.4: The measurements of the Dalitz plot distributions. Notice that in many cases the scale factors calculated with the PDG [20] method are sizable. The references refer to the most recent measurements and the PDG. S is the scale factor calculated using the prescription of [20].

$$\begin{aligned} A_{++-} \;&=\; (-2\alpha_1 + \alpha_3) + \left(-\beta_1 + \frac{1}{2}\beta_3 - \sqrt{3}\gamma_3\right) y \\ &\quad + (-2\zeta_1 - 2\zeta_3)\left(y^2 + \frac{1}{3}x^2\right) + (\xi_1 + \xi_3 - \xi_3')\left(y^2 - \frac{1}{3}x^2\right) . \end{aligned} \tag{1.37}$$

A main problem in dealing with the data fitting is the question of how to deal with the isospin breaking effects. The phase-space itself is very sensitive to the precise masses of the pions and kaons which are used. There are several ways to deal with this problem. One is to first fit the expressions (1.37) to the data where x and y are defined with s_0 calculated with the physical masses but otherwise the charged pion mass as in (1.23). The result of this fit is shown in Table 1.5. Here we have assumed that the only complex phase appearing is the relative phase between A_0 and A_2. The errors quoted are the MINUIT errors. For the K_S-measurements only $\mathrm{Re}(\lambda)$ is included. Leaving it out changes the χ^2/DOF to 3.9/4 but all parameters stay within the errors given.

Qty	Ref. [18]	Ref. [6]	Our fit	p^2	$\tilde{K}_i = 0$
$\lvert A_0 \rvert$	0.4687 ± 0.0006	0.4699 ± 0.0012	0.4622 ± 0.0014	input	input
$\lvert A_2 \rvert$	0.0210 ± 0.0001	0.0211 ± 0.0001	0.0212 ± 0.0001	input	input
$\delta_2 - \delta_0$	$(-45.6 \pm 5)^o$	$(-61.5 \pm 4)^o$	$(-58.2 \pm 4)^o$	—	—
α_1	91.4 ± 0.24	91.71 ± 0.32	93.16 ± 0.36	74.0(73.5)	59.4
α_3	-7.14 ± 0.36	-7.36 ± 0.47	-6.72 ± 0.46	$-4.8(4.8)$	-6.5
β_1	-25.83 ± 0.41	-25.68 ± 0.27	-27.06 ± 0.43	$-17.7(16.2)$	-21.9
β_3	-2.48 ± 0.48	-2.43 ± 0.41	-2.22 ± 0.47	$-1.2(1.1)$	-1.0
γ_3	2.51 ± 0.36	2.26 ± 0.23	2.95 ± 0.32	2.3(2.1)	2.5
ζ_1	-0.37 ± 0.11	-0.47 ± 0.15	-0.40 ± 0.19	—	0.26
ζ_3	—	-0.21 ± 0.08	-0.09 ± 0.10	—	-0.01
ξ_1	-1.25 ± 0.12	-1.51 ± 0.30	-1.83 ± 0.30	—	-0.46
ξ_3	—	-0.12 ± 0.17	-0.17 ± 0.16	—	-0.01
ξ'_3	—	-0.21 ± 0.51	-0.56 ± 0.42	—	-0.06
χ^2/DOF	12.8/3	10.3/2	5.4/5	—	—

Table 1.5: The values of the parameters in the expansion in x and y of the $K \to 3\pi$ amplitudes and the $K \to \pi\pi$ amplitudes. The χ^2 quoted are for the fits with the then used data. $|A_0|$ and $|A_2|$ are in units of 10^{-6} GeV. $\alpha_1,\ldots,\xi'_3$ are in units of 10^{-8}.

In the column labeled p^2 in Table 1.5 we fixed G_8 and G_{27} from the result for A_0 and A_2 at tree level and show the predictions for the linear slopes in the amplitude at this order. The source of the differences with [6] is not obvious but could be due to a different pion and kaon mass. The numbers in the table were calculated using the charged pion and kaon masses, using the neutral ones instead leads to the numbers in brackets. As can be seen a general reasonable agreement within about 40% is obtained. The input here determines $G_8 = 10.4$ and $G_{27} = 0.61$ when we used for F_0 the pion decay constant F_π and used F_π and F_K in the tree level amplitude with the physical values.

Going to the next order, we first show also in Table 1.5 in the column labeled $\tilde{K}_i = 0$ the p^4 results with G_8 and G_{27} fixed to fit $|A_0|$ and $|A_2|$. These were calculated with charged pion and kaon mass. The input here determines $G_8 = 5.47$ and $G_{27} = 0.39$. The change compared to the previous is an indication of the size of the p^4 effect. It should be kept in mind that we have chosen to normalize the lowest order including one factor of $1/F_K$, changing that to $1/F_\pi$ changes the relative size of the p^2 and p^4 contributions significantly. There is as well a mild dependence on the value of the L_i^r used. We use in general a scale of $\mu = 0.77$ GeV and the L_i^r values of the one-loop fit of [27], the p^4 fit including the latest $K_{\ell 4}$ data. These values are (all at $\mu = 0.77$ GeV.)

$$L_1^r = 0.38 \cdot 10^{-3}, \quad L_2^r = 1.59 \cdot 10^{-3}, \quad L_3^r = -2.91 \cdot 10^{-3}, \quad L_4^r = 0,$$
$$L_5^r = 1.46 \cdot 10^{-3}, \quad L_6^r = 0, \quad L_7^r = -0.49 \cdot 10^{-3}, \quad L_8^r = 1.0 \cdot 10^{-3}\,. \tag{1.38}$$

It is not possible to determine all 13 quantities G_8, G_{27} and $\tilde{K}_1,\ldots,\tilde{K}_{11}$. In principle it cannot be done if we try to fit to the 12 quantities listed in Table 1.5,[3] but in practice the situation is even worse, simply fitting the possible parameters without constraints leads to fits with negligible tree level contributions. We have therefore chosen a two-step process, first we study the variation of fitting subsets of G_8, G_{27} and $\tilde{K}_1,\ldots,\tilde{K}_{11}$ to $|A_0|,\ldots,\xi_3'$. This allows for a more direct study of the various dependencies on parameters. Finally we present the direct fit where we compare directly to the data, but allowing in addition for a variable phase $\delta_2 - \delta_0$ between A_0 and A_2

The various relations advocated in [7] follow if one sets

$$\tilde{K}_1 = \tilde{K}_4 = 0 \quad \text{and} \quad \tilde{K}_8 = \cdots = \tilde{K}_{11} = 0\,. \tag{1.39}$$

The resulting fit values are in Table 1.6, column 2. Several of the $\tilde{K}_i$ are uncomfortably large but inspection of the size of the p^2 versus p^4 contributions shows nothing conspicuous. The source of the problem turned out to be γ_3 which with the constraints of Eq. (1.39) can only be fitted by varying $\tilde{K}_6$ but it comes multiplied with a small factor. It then produces fairly large other $\tilde{K}_i$ in order to minimize the effect of $\tilde{K}_7$ on the other quantities. We have therefore also fitted using the constraints

$$\tilde{K}_1 = \tilde{K}_4 = \tilde{K}_6 = 0 \quad \text{and} \quad \tilde{K}_8 = \cdots = \tilde{K}_{11} = 0\,. \tag{1.40}$$

We can now attempt to also determine somewhat the combinations $\tilde{K}_1$ and $\tilde{K}_4$. Leaving $\tilde{K}_1$ free hardly changes the quality of the fit but shows that the actual value of G_8 can change over a fairly wide range. The results are shown in the fourth column of Table 1.6 with constraints

$$\tilde{K}_4 = 0 \quad \text{and} \quad \tilde{K}_8 = \cdots = \tilde{K}_{11} = 0\,. \tag{1.41}$$

The same type of correlation occurs for G_{27} and $\tilde{K}_4$ as shown with the results in column 5 of the Table where we fitted with constraints

$$\tilde{K}_1 = 0, \quad \tilde{K}_4 = 0.1 \quad \text{and} \quad \tilde{K}_8 = \cdots = \tilde{K}_{11} = 0\,. \tag{1.42}$$

The reason we have picked a fixed value for $\tilde{K}_4$ is because there is very long, narrow and extremely shallow fitting region that moves in the end to a very small G_{27} and values for $\tilde{K}_4$, $\tilde{K}_5$, $\tilde{K}_6$ and $\tilde{K}_7$ that are simply enormous but a total χ^2 which is only marginally smaller than the one shown, 11.7 rather than 11.9.

How well do the relations proposed in [7] stand up to the new data. In practice, for the octet which dominates the $\Delta I = 1/2$ part, it means that α_1 determines ζ_1, β_1 determines ξ_1. The first of these relations is extremely well

[3] $\delta_2 - \delta_0$ cannot be fitted at this order.

constraints	Eq. (1.39)	Eq. (1.40)	Eq. (1.41)	Eq. (1.42)	Eq. (1.39)
Fitted	$\lvert A_0\rvert, \ldots, \xi_3'$				experiment
G_8	5.47(2)	5.47(2)	7.24(2.04)	5.49	5.45(2)
G_{27}	0.392(2)	0.392(2)	0.392(2)	0.139	0.392(2)
$10^3\tilde{K}_1/G_8$	$\equiv 0$	$\equiv 0$	$-8.5(7.5)$	$\equiv 0$	$\equiv 0$
$10^3\tilde{K}_2/G_8$	54.7(2.8)	53.6(2.7)	41.3(11.4)	53.7	51.9(3.2)
$10^3\tilde{K}_3/G_8$	3.0(1.4)	3.5(1.3)	10.0(6.3)	3.2	3.8(1.5)
$10^3\tilde{K}_4/G_{27}$	$\equiv 0$	$\equiv 0$	$\equiv 0$	$\equiv 100$	$\equiv 0$
$10^3\tilde{K}_5/G_{27}$	$-54.5(23.4)$	$-19.8(9.6)$	$-54.5(23.1)$	-49.4	$-42.5(16.6)$
$10^3\tilde{K}_6/G_{27}$	$-185(114)$	$\equiv 0$	$-184(113)$	-366	$-166(113)$
$10^3\tilde{K}_7/G_{27}$	114(46)	45.1(18.2)	114(46)	199	120(32)
χ^2/DOF	12.3/5	14.9/6	11.8/4	11.9/4	26.8/10

Table 1.6: The results for G_8, G_{27} and the $\tilde{K}_i$ for the various constraints discussed in the text. In brackets are the MINUIT errors.

satisfied, but it is hard to get ξ_1 to better than about 2.5 standard deviations, the value obtained from the various above fits is

$$\xi_1 \approx (-0.98 - i0.13) \cdot 10^{-8} \,. \tag{1.43}$$

Inspection of the numerical coefficients for the octet parameters that only contribute suppressed by powers of m_π^2 reveals that some of them show up with large numerical coefficients. One can then instead choose to leave K_8 or $\tilde{K}_9$ free rather than $\tilde{K}_1$. The resulting fits are of similar quality to the one with $\tilde{K}_1$ free and do not significantly improve the prediction for ξ_1 given in (1.43). The possible variation is less than 10%.

There is no similar single value with significant discrepancies for the $\Delta I = 3/2$ parameters. The above named problem with γ_3 does not lead to a major discrepancy but typically the quadratic quantities are the ones with a deviation of about 0.5 to 1.4 σ.

Varying the masses of the pion and kaon or the eta mass used in the loops does not change the results of the fits significantly.

The fit via the intermediate step of $|A_0|, \ldots, \xi_3'$ is fairly fast and allows an easy study of the variation with the inputs. We have also done the fit directly to all the experimental data listed in Tables 1.3 and 1.4 with only the use of $\mathrm{Re}(\lambda)$ for the $K_S \to \pi^+\pi^-\pi^0$ data. The masses used in the phase space were the physical masses occurring in the decays. The masses used in the amplitudes are the physical kaon mass and the pion mass such that $3m_\pi^2 = \sum_{i=1,3} m_{\pi^i}^2$ is satisfied. The eta mass in the loops we then calculated using the GMO relation. The resulting values for the $\tilde{K}_i$ are given in the last column of Table 1.6 and the values for the widths and Dalitz plot distribution variables are in the column labeled CHPT fit in Tables 1.3 and 1.4. We have allowed an extra phase between

A_0 and A_2 in this fit. Otherwise this fit corresponds to the constraints (1.39). The higher χ^2 is mainly due to the fact that ξ_1 has been fitted to more than one quantity, and here we have the discrepancy with the slope k in $K_L \to \pi^+\pi^-\pi^0$ and $K^+ \to \pi^0\pi^0\pi^+$. These together account for 16.4 of χ^2.

The fact that the last fit and the fit via the intermediate step of $|A_0|, \ldots, \xi_3'$ agree very well is an indication that the isospin breaking effects at the amplitude level are small. An estimate can be done by calculating the amplitudes and the slopes with the masses of K^0, π^0 and comparing them with the amplitudes calculated with m_{K^+}, m_{π^+}. Since often factors of $m_K^2 - m_\pi^2$ appear this is the worst case. The changes are typically 2% for the amplitudes, 5-8% for the linear slopes and up to 20% for the quadratic slopes.

1.6 Conclusions

In this paper we have recalculated the $K \to \pi\pi$ and $K \to \pi\pi\pi$ amplitudes to next-to-leading order in CHPT in the isospin limit and presented the amplitudes in a simple form suitable for dispersive estimates of higher orders.

We have performed a new global fit to all available kaon data at this level taking into account the isospin breaking in the phase space. Work is under progress to include isospin breaking also in the amplitudes.

At present the situation is that a satisfactory agreement is obtained with the predictions keeping in mind that for the quadratic slopes higher order corrections could be sizable as happened with the analogous results in $\eta \to 3\pi$ results. A discussion of the latter together with references can be found in [28]. Some work exists on dispersive corrections in $K \to 3\pi$ [17], but more study is needed to fit their results in this framework.

Now the isospin breaking corrections, including possible electromagnetic radiative corrections, need to be studied to see if they are the cause of the differences in the quadratic Dalitz plot parameters. Work exists to a large extent for the $K \to 2\pi$ decays [29], but little has been done using modern methods for $K \to 3\pi$ decays.

Acknowledgments

This work is supported by the Swedish Research Council and the European Union TMR network, Contract No. ERBFMRX–CT980169 (EURODAPHNE).

1.A Ambiguity in the Definition of M_i

The functions $M_i(s)$ defined in Eq. (1.26) are not unique for two reasons. The variables s_1, s_2 and s_3 are not independent, they satisfy the relation (1.23), and low powers of s_1, s_2 and s_3 can be fitted in more than one of the M_i functions.

As a simple example, we could have added

$$\delta M_0(s) = \alpha\,(s - s_0)\ , \tag{A.1}$$

with α any constant, without changing the result, for A^L_{000}. The full set of these ambiguities can be derived by checking the total number of independent terms that exist in the polynomial expansion of the amplitudes and comparing it with the the same expansion of the $M_i(s)$.

The changes of the functions that leave all amplitudes unchanged are

$$
\begin{aligned}
M_0(s) &\longrightarrow M_0(s) + \delta_1\,(s - s_0) && \text{(A.2)}\\
M_1(s) &\longrightarrow M_1(s) + \delta_2, \quad M_2(s) \longrightarrow M_2(s) - \frac{1}{2}\delta_2\,; && \text{(A.3)}\\
M_1(s) &\longrightarrow M_1(s) + \delta_3\,(s - s_0))\,, \quad M_2(s) \longrightarrow M_2(s) + \delta_3\,(s - s_0))\ ; && \text{(A.4)}\\
M_1(s) &\longrightarrow M_1(s) + 2\delta_4 s, \quad M_2(s) \longrightarrow M_2(s) - \delta_4 s, &&\\
M_3(s) &\longrightarrow M_3(s) + \delta_4\,; && \text{(A.5)}\\
M_1(s) &\longrightarrow M_1(s) - 2\delta_5 s\,(s - 3s_0)\,, \quad M_2(s) \longrightarrow M_2(s) + \delta_5 s\,(s - 3s_0)\,, &&\\
M_3(s) &\longrightarrow M_3(s) + \delta_5 s\,; && \text{(A.6)}\\
M_1(s) &\longrightarrow M_1(s) + \frac{2}{3}\delta_6\,(s - 3s_0)^3\,, \quad M_2(s) \longrightarrow M_2(s) - \frac{1}{3}\delta_6 s^2\,(s - 9s_0)\,, &&\\
M_3(s) &\longrightarrow M_3(s) + \delta_6 s^2\,; && \text{(A.7)}\\
M_4(s) &\longrightarrow M_4(s) + \delta_7\,; && \text{(A.8)}\\
M_4(s) &\longrightarrow M_4(s) + \delta_8 s\,, \quad M_5(s) \longrightarrow M_5(s) + \delta_8; && \text{(A.9)}\\
M_5(s) &\longrightarrow M_5(s) + \delta_9, \quad M_6(s) \longrightarrow M_5(s) + \delta_9; && \text{(A.10)}\\
M_4(s) &\longrightarrow M_4(s) - \delta_{10} s\,(s - 3s_0)\ , \quad M_5(s) \longrightarrow M_5(s) + \delta_{10} s; && \text{(A.11)}\\
M_5(s) &\longrightarrow M_5(s) + \delta_{11} s, \quad M_6(s) \longrightarrow M_5(s) + \delta_{11} s; && \text{(A.12)}\\
M_4(s) &\longrightarrow M_4(s) + \delta_{12}\left(s^3 - 9s_0 s^2 + 18 s_0^2 s\right), \quad M_5(s) \longrightarrow M_5(s) + \delta_{12} s^2; &&\\
M_6(s) &\longrightarrow M_6(s) - 2\delta_{12} s^2; && \text{(A.13)}\\
M_4(s) &\longrightarrow M_4(s) + \delta_{13} 3s_0\left(s^3 - 9s_0 s^2 + 18 s_0^2 s\right), \quad M_5(s) \longrightarrow M_5(s) + \delta_{13} s^3, &&\\
M_6(s) &\longrightarrow M_6(s) - 2\delta_{13}\left(s^2 - 9s_0 s^2\right)\ . && \text{(A.14)}
\end{aligned}
$$

The triplets (M_7, M_8, M_9) and (M_{10}, M_{11}, M_{12}) have an ambiguity similar to (A.3)-(A.7), leading to a total ambiguity of 23 free parameters.

1.B Explicit Expressions for the $M_i(s)$ in $K \to 3\pi$

We write the $M_i(s)$ functions defined in Eq. (1.26) as

$$M_i(s) = M_i(s)|_{p^2} + i\frac{CF_0^4}{F_\pi^3 F_K}\left\{\frac{G_8}{F_\pi^2}M_i^8(s) + \frac{G_8'}{F_\pi^2}M_i^{8\prime}(s) + \frac{G_{27}}{F_\pi^2}M_i^{27}(s)\right\}\ . \tag{B.1}$$

The effect of G_8' cannot be distinguished from higher order coefficients in decays not involving external fields. This was known at tree level earlier and has been proven to one-loop in [5]. The effect of $M_i^{8\prime}(s)$ can be reconstructed from $M_i^8(s)$ by the changes

$$\begin{aligned} N_{10}^r + 2N_{11}^r + N_{12}^r &\longrightarrow N_{10}^r + 2N_{11}^r + N_{12}^r + \frac{G_8'}{G_8}\left(2L_5^r - 16L_6^r - 8L_8^r\right) , \\ N_7^r &\longrightarrow N_7^r + \frac{G_8'}{G_8}\left(-4L_4^r\right) . \end{aligned} \tag{B.2}$$

The results for the $K \to \pi\pi$ amplitudes are in full agreement with [14] and can be found there.

We have brought the $M_i^j(s)$ in a form that satisfies the isospin relations (1.28). These can be used in the form

$$\begin{aligned} M_1^j(s) &= M_0^j(s) - 2M_2^j(s)\,, \\ M_6^j(s) &= M_5^j(s) - M_9^j(s) - M_{12}^j(s)\,, \\ M_7^j(s) &= 2M_4^j(s) - \frac{1}{2}M_{10}^j(s) + M_{11}^j(s)\,, \\ M_8^j(s) &= -M_4^j(s) + \frac{1}{2}M_{10}^j(s) \end{aligned} \tag{B.3}$$

to reconstruct these. We have extensively used the GMO relation in writing them in this form.

The explicit expressions for $\overline{A}$, $\overline{B}$ and $\overline{B}_1$, the finite part of the loop functions, can be found in many places, e.g. [30].

The octet ones are:

$$\begin{aligned} &M_0^8(s) = \\ &\quad +(N_1^r + N_2^r)\,(-2\,m_\pi^2\,m_K^2 + 3\,m_\pi^2\,s - 2\,m_\pi^4 + m_K^2\,s - s^2) \\ &\quad +N_3^r\,(2\,m_\pi^2\,m_K^2 - 3\,m_\pi^2\,s + 5\,m_\pi^4 - m_K^2\,s + m_K^4 - 2\,s^2) \\ &\quad +N_5^r\,(2\,m_\pi^2\,m_K^2 - 2\,m_\pi^2\,s + 2\,m_\pi^4 + 2\,m_K^2\,s) + N_7^r\,(8\,m_\pi^2\,m_K^2 - 4\,m_K^2\,s) \\ &\quad +N_8^r\,(-2\,m_\pi^2\,s + 2\,m_\pi^4 + 4\,m_K^2\,s) \\ &\quad +N_9^r\,(-2\,m_\pi^2\,m_K^2 - 2\,m_\pi^2\,s + 2\,m_\pi^4 + 2\,m_K^2\,s) \\ &\quad +(N_{10}^r + 2N_{11}^r + N_{12}^r)\,(-4\,m_\pi^2\,m_K^2) \\ &\quad +L_1^r\,(32\,m_\pi^2\,m_K^2 - 48\,m_\pi^2\,s + 32\,m_\pi^4 - 16\,m_K^2\,s + 16\,s^2) \\ &\quad +L_2^r\,(-16\,m_\pi^2\,m_K^2 + 24\,m_\pi^2\,s - 40\,m_\pi^4 + 8\,m_K^2\,s - 8\,m_K^4 + 16\,s^2) \\ &\quad +L_3^r\,(16\,m_\pi^2\,m_K^2 - 24\,m_\pi^2\,s + 16\,m_\pi^4 - 8\,m_K^2\,s + 8\,s^2) \\ &\quad +L_4^r\,(-16\,m_\pi^2\,m_K^2 + 16\,m_\pi^2\,s - 16\,m_\pi^4) + L_5^r\,(-8\,m_\pi^2\,m_K^2 + 16\,m_\pi^2\,s - 16\,m_\pi^4) \\ &\quad +(1/(16\pi^2))\,(4/3\,m_\pi^2\,m_K^2 + 1/2\,m_\pi^2\,s - 1/2\,m_\pi^4 - 3/2\,m_K^2\,s + 1/2\,m_K^4) \\ &\quad +\overline{A}(m_\pi^2)\,(-19/8\,m_\pi^2 - 2/3\,m_K^2 + 21/8\,s) \end{aligned}$$

$$
\begin{aligned}
&+\overline{A}(m_K^2)\,(-13/4\,m_\pi^2 - 1/3\,m_K^2 + 3\,s)\\
&+\overline{A}(m_\eta^2)\,(-3/8\,m_\pi^2 + 3/8\,s)\\
&+\overline{B}(m_\pi^2, m_\pi^2, s)\,(1/2\,m_\pi^2\,m_K^2 - 2\,m_\pi^2\,s + m_\pi^4 + s^2)\\
&+\overline{B}(m_\pi^2, m_K^2, s)\,(13/8\,m_\pi^2\,m_K^2 - 5/4\,m_\pi^2\,s - 5/8\,m_K^2\,s - 1/8\,m_K^4 + 3/4\,s^2)\\
&+\overline{B}(m_K^2, m_K^2, s)\,(1/4\,m_\pi^2\,s + 1/4\,m_K^2\,s - 1/4\,s^2)\\
&+\overline{B}(m_\eta^2, m_K^2, s)\,(-5/24\,m_\pi^2\,m_K^2 + 1/8\,m_K^2\,s + 1/24\,m_K^4)\\
&+\overline{B}(m_\eta^2, m_\eta^2, s)\,(1/18\,m_\pi^2\,m_K^2)\\
&+\overline{B_1}(m_\pi^2, m_K^2, s)\,(-3/4\,m_\pi^2\,m_K^2 + 1/2\,m_\pi^4 + 1/4\,m_K^4)\\
&+\overline{B_1}(m_\eta^2, m_K^2, s)\,(1/4\,m_\pi^2\,m_K^2 - 1/4\,m_K^4)\,. \qquad \text{(B.4)}
\end{aligned}
$$

$$
\begin{aligned}
&M_2^8(s) =\\
&\quad +N_3^r\,(-s^2) + L_2^r\,(8\,s^2) + (1/(16\pi^2))\,(1/6\,s^2)\\
&\quad +\overline{B}(m_\pi^2, m_\pi^2, s)\,(1/2\,m_\pi^2\,m_K^2 - 3/4\,m_\pi^2\,s + 1/2\,m_\pi^4 - 1/4\,m_K^2\,s + 1/4\,s^2)\\
&\quad +\overline{B}(m_\pi^2, m_K^2, s)\,(1/2\,m_\pi^2\,m_K^2 - 1/2\,m_\pi^2\,s + 1/4\,m_\pi^4\\
&\quad -1/2\,m_K^2\,s + 1/4\,m_K^4 + 1/4\,s^2). \qquad \text{(B.5)}
\end{aligned}
$$

$$
\begin{aligned}
&M_3^8(s) =\\
&\quad +\overline{B}(m_\pi^2, m_\pi^2, s)\,(1/3\,m_\pi^2 - 1/12\,s)\\
&\quad +\overline{B}(m_\pi^2, m_K^2, s)\,(1/8\,m_\pi^2 + 1/24\,m_K^2 - 1/24\,s)\\
&\quad +\overline{B}(m_\eta^2, m_K^2, s)\,(-1/8\,m_\pi^2 + 5/8\,m_K^2 - 1/8\,s)\\
&\quad +\overline{B_1}(m_\pi^2, m_K^2, s)\,(-1/12\,m_\pi^2 + 1/12\,m_K^2)\\
&\quad +\overline{B_1}(m_\eta^2, m_K^2, s)\,(1/12\,m_\pi^2 - 1/12\,m_K^2). \qquad \text{(B.6)}
\end{aligned}
$$

$$
M_4^8(s) \quad = \quad 0. \qquad \text{(B.7)}
$$

$$
\begin{aligned}
&M_5^8(s) =\\
&\quad +\overline{B}(m_\pi^2, m_K^2, s)\,(-1/8\,m_\pi^2 - 1/24\,m_K^2 + 1/24\,s)\\
&\quad +\overline{B}(m_K^2, m_K^2, s)\,(-1/3\,m_K^2 + 1/12\,s)\\
&\quad +\overline{B}(m_\eta^2, m_K^2, s)\,(1/8\,m_\pi^2 - 5/8\,m_K^2 + 1/8\,s)\\
&\quad +\overline{B_1}(m_\pi^2, m_K^2, s)\,(1/12\,m_\pi^2 - 1/12\,m_K^2)\\
&\quad +\overline{B_1}(m_\eta^2, m_K^2, s)\,(-1/12\,m_\pi^2 + 1/12\,m_K^2); \qquad \text{(B.8)}
\end{aligned}
$$

$$
M_9^8(s) \quad = \quad -M_3^8(s). \qquad \text{(B.9)}
$$

$$
\begin{aligned}
&M_{10}^8(s) = \\
&\quad +(N_1^r + N_2^r)\,(-2\,m_\pi^2\,m_K^2 + 3\,m_\pi^2\,s - 5\,m_\pi^4 + m_K^2\,s - m_K^4) \\
&\quad +N_3^r\,(2\,m_\pi^2\,m_K^2 - 3\,m_\pi^2\,s - m_\pi^4 - m_K^2\,s - m_K^4 + 2\,s^2) \\
&\quad +N_5^r\,(-8\,m_\pi^2\,m_K^2 - 2\,m_\pi^2\,s + 2\,m_\pi^4 + 2\,m_K^2\,s - 2\,m_K^4) \\
&\quad +N_7^r\,(-4\,m_\pi^2\,m_K^2 - 4\,m_K^2\,s + 4\,m_K^4) \\
&\quad +N_8^r\,(-10\,m_\pi^2\,m_K^2 - 2\,m_\pi^2\,s + 2\,m_\pi^4 + 4\,m_K^2\,s - 4\,m_K^4) \\
&\quad +N_9^r\,(-2\,m_\pi^2\,s + 2\,m_\pi^4 + 2\,m_K^2\,s - 2\,m_K^4) + (N_{10}^r + 2N_{11}^r + N_{12}^r)\,(8\,m_\pi^2\,m_K^2) \\
&\quad +L_1^r\,(32\,m_\pi^2\,m_K^2 - 48\,m_\pi^2\,s + 80\,m_\pi^4 - 16\,m_K^2\,s + 16\,m_K^4) \\
&\quad +L_2^r\,(-16\,m_\pi^2\,m_K^2 + 24\,m_\pi^2\,s + 8\,m_\pi^4 + 8\,m_K^2\,s + 8\,m_K^4 - 16\,s^2) \\
&\quad +L_3^r\,(16\,m_\pi^2\,m_K^2 - 24\,m_\pi^2\,s + 40\,m_\pi^4 - 8\,m_K^2\,s + 8\,m_K^4) \\
&\quad +L_4^r\,(16\,m_\pi^2\,m_K^2 + 16\,m_\pi^2\,s - 16\,m_\pi^4) + L_5^r\,(16\,m_\pi^2\,s - 16\,m_\pi^4) \\
&\quad +(1/(16\pi^2))\,(11/9\,m_\pi^2\,m_K^2 + 4/9\,m_\pi^2\,s - 1/3\,m_\pi^4 - 13/9\,m_K^2\,s \\
&\quad +4/9\,m_K^4 - 1/3\,s^2) \\
&\quad +\overline{A}(m_\pi^2)\,(-25/8\,m_\pi^2 - 31/24\,m_K^2 + 21/8\,s) \\
&\quad +\overline{A}(m_K^2)\,(-5/2\,m_\pi^2 - 7/3\,m_K^2 + 3\,s) \\
&\quad +\overline{A}(m_\eta^2)\,(-3/8\,m_\pi^2 - 3/8\,m_K^2 + 3/8\,s) \\
&\quad +\overline{B}(m_\pi^2, m_\pi^2, s)\,(-m_\pi^2\,m_K^2 + 3/2\,m_\pi^2\,s - m_\pi^4 + 1/2\,m_K^2\,s - 1/2\,s^2) \\
&\quad +\overline{B}(m_\pi^2, m_K^2, s)\,(-m_\pi^2\,m_K^2 + m_\pi^2\,s - 1/2\,m_\pi^4 \\
&\quad +m_K^2\,s - 1/2\,m_K^4 - 1/2\,s^2).
\end{aligned} \tag{B.10}
$$

$$
\begin{aligned}
&M_{11}^8(s) = \\
&\quad +(N_1^r + N_2^r + N_3^r - 16L_1^r - 8L_2^r - 8L_3^r)\,(s^2) \\
&\quad +(1/(16\pi^2))\,(-1/18\,m_\pi^2\,s + 1/18\,m_K^2\,s + 1/6\,s^2) \\
&\quad +\overline{B}(m_\pi^2, m_\pi^2, s)\,(5/4\,m_\pi^2\,s - 1/2\,m_\pi^4 - 1/4\,m_K^2\,s - 3/4\,s^2) \\
&\quad +\overline{B}(m_\pi^2, m_K^2, s)\,(-9/8\,m_\pi^2\,m_K^2 + 3/4\,m_\pi^2\,s + 1/4\,m_\pi^4 \\
&\quad +1/8\,m_K^2\,s + 3/8\,m_K^4 - 1/2\,s^2) \\
&\quad +\overline{B}(m_K^2, m_K^2, s)\,(-1/4\,m_\pi^2\,s - 1/4\,m_K^2\,s + 1/4\,s^2) \\
&\quad +\overline{B}(m_\eta^2, m_K^2, s)\,(5/24\,m_\pi^2\,m_K^2 - 1/8\,m_K^2\,s - 1/24\,m_K^4) \\
&\quad +\overline{B}(m_\eta^2, m_\eta^2, s)\,(-1/18\,m_\pi^2\,m_K^2) \\
&\quad +\overline{B_1}(m_\pi^2, m_K^2, s)\,(3/4\,m_\pi^2\,m_K^2 - 1/2\,m_\pi^4 - 1/4\,m_K^4) \\
&\quad +\overline{B_1}(m_\eta^2, m_K^2, s)\,(-1/4\,m_\pi^2\,m_K^2 + 1/4\,m_K^4).
\end{aligned} \tag{B.11}
$$

$$
M_{12}^8(s) \quad = \quad M_3^8(s) = -M_9^8(s). \tag{B.12}
$$

The 27 plet ones depend as well on the quantity

$$P_{K\pi} = \frac{1}{m_K^2 - m_\pi^2}\,. \tag{B.13}$$

$$\begin{aligned}
&M_0^{27}(s) = \\
&\quad +D_1^r\,(-4/3\,m_\pi^2\,m_K^2) \\
&\quad +D_2^r\,((2/3\,m_\pi^2\,m_K^2 + 10\,m_\pi^2\,s - 40/3\,m_\pi^4) + P_{K\pi}(10\,m_\pi^4\,s - 40/3\,m_\pi^6)) \\
&\quad +D_4^r\,((-11/2\,m_\pi^2\,m_K^2 + m_\pi^2\,s + 7/3\,m_\pi^4 + 3/2\,m_K^2\,s - 5/6\,m_K^4) \\
&\qquad +P_{K\pi}\,(-10\,m_\pi^4\,s + 40/3\,m_\pi^6)) \\
&\quad +D_5^r\,(29/6\,m_\pi^2\,m_K^2 - 11\,m_\pi^2\,s + 11\,m_\pi^4 - 3/2\,m_K^2\,s + 5/6\,m_K^4) \\
&\quad +D_6^r\,(5/3\,m_\pi^2\,m_K^2 + 1/3\,m_\pi^2\,s - 1/3\,m_\pi^4 - m_K^2\,s) \\
&\quad +D_7^r\,((-25/3\,m_\pi^2\,m_K^2 - 3\,m_\pi^2\,s + 8\,m_\pi^4 + 6\,m_K^2\,s - 10/3\,m_K^4) \\
&\qquad +P_{K\pi}\,D_7^r\,(-15\,m_\pi^4\,s + 20\,m_\pi^6)) \\
&\quad +D_{26}^r\,(-2/3\,m_\pi^2\,m_K^2 + m_\pi^2\,s - 2/3\,m_\pi^4 + 1/3\,m_K^2\,s - 1/3\,s^2) \\
&\quad +D_{27}^r\,(4/3\,m_\pi^2\,m_K^2 - 2\,m_\pi^2\,s + 10/3\,m_\pi^4 - 2/3\,m_K^2\,s + 2/3\,m_K^4 - 4/3\,s^2) \\
&\quad +D_{28}^r\,(8\,m_\pi^2\,m_K^2 - 12\,m_\pi^2\,s + 12\,m_\pi^4 - 4\,m_K^2\,s + 4/3\,m_K^4) \\
&\quad +D_{29}^r\,(-3/2\,m_\pi^2\,m_K^2 + 9/4\,m_\pi^2\,s - 13/4\,m_\pi^4 + 3/4\,m_K^2\,s - 7/12\,m_K^4 + s^2) \\
&\quad +D_{30}^r\,(3/2\,m_\pi^2\,m_K^2 - 9/4\,m_\pi^2\,s + 1/4\,m_\pi^4 - 3/4\,m_K^2\,s - 5/12\,m_K^4 + 2\,s^2) \\
&\quad +D_{31}^r\,(4\,m_\pi^2\,m_K^2 - 6\,m_\pi^2\,s + 4\,m_\pi^4 - 2\,m_K^2\,s + 2\,s^2) \\
&\quad +L_1^r\,(-32\,m_\pi^2\,m_K^2 + 48\,m_\pi^2\,s - 32\,m_\pi^4 + 16\,m_K^2\,s - 16\,s^2) \\
&\quad +L_2^r\,(16\,m_\pi^2\,m_K^2 - 24\,m_\pi^2\,s + 40\,m_\pi^4 - 8\,m_K^2\,s + 8\,m_K^4 - 16\,s^2) \\
&\quad +L_3^r\,((-58/3\,m_\pi^2\,m_K^2 + 34\,m_\pi^2\,s - 118/3\,m_\pi^4 + 8\,m_K^2\,s - 8\,s^2) \\
&\qquad +P_{K\pi}\,(40\,m_\pi^4\,s - 160/3\,m_\pi^6)) \\
&\quad +L_4^r\,(16\,m_\pi^2\,m_K^2 - 16\,m_\pi^2\,s + 16\,m_\pi^4) \\
&\quad +L_5^r\,((8\,m_\pi^2\,m_K^2 - 16\,m_\pi^2\,s + 68/3\,m_\pi^4) + P_{K\pi}\,(-20\,m_\pi^4\,s + 80/3\,m_\pi^6)) \\
&\quad +(1/(16\pi^2))\,((503/324\,m_\pi^2\,m_K^2 + 197/216\,m_\pi^2\,s - 287/216\,m_\pi^4 \\
&\quad -401/216\,m_K^2\,s + 401/648\,m_K^4) + P_{K\pi}\,(1/(16\pi^2))\,(5/4\,m_\pi^4\,s - 5/3\,m_\pi^6)) \\
&\quad +\overline{A}(m_\pi^2)\,((-409/72\,m_\pi^2 - 49/9\,m_K^2 + 29/3\,s) \\
&\quad +P_{K\pi}\,(-215/24\,m_\pi^2\,s + 215/18\,m_\pi^4) \\
&\qquad +P_{K\pi}^2\,(5/2\,m_\pi^4\,s - 10/3\,m_\pi^6)) \\
&\quad +\overline{A}(m_K^2)\,((-191/72\,m_\pi^2 - 19/8\,m_K^2 + 37/6\,s) \\
&\quad +P_{K\pi}\,(-325/24\,m_\pi^2\,s + 325/18\,m_\pi^4) \\
&\qquad +P_{K\pi}^2\,(-5/2\,m_\pi^4\,s + 10/3\,m_\pi^6)) \\
&\quad +\overline{A}(m_\eta^2)\,((-13/12\,m_\pi^2 - 5/8\,m_K^2 + 3/2\,s) + P_{K\pi}\,(-5/4\,m_\pi^2\,s + 5/3\,m_\pi^4))
\end{aligned}$$

$$
\begin{aligned}
&+\overline{B}(m_\pi^2,m_\pi^2,s)\,((1/3\,m_\pi^2\,m_K^2-13/6\,m_\pi^2\,s+2/3\,m_\pi^4-5/6\,m_K^2\,s+3/2\,s^2)\\
&\quad+P_{K\pi}\,(-5/2\,m_\pi^2\,s^2+35/6\,m_\pi^4\,s-10/3\,m_\pi^6))\\
&+\overline{B}(m_\pi^2,m_K^2,s)\,((91/24\,m_\pi^2\,m_K^2-35/6\,m_\pi^2\,s+10/3\,m_\pi^4\\
&-25/12\,m_K^2\,s-7/24\,m_K^4+19/8\,s^2)\\
&+P_{K\pi}\,(15/8\,m_\pi^2\,s^2-5\,m_\pi^4\,s+10/3\,m_\pi^6))\\
&+\overline{B}(m_K^2,m_K^2,s)\,((-13/12\,m_\pi^2\,s-7/8\,m_K^2\,s+7/8\,s^2)\\
&+P_{K\pi}\,(5/8\,m_\pi^2\,s^2-5/6\,m_\pi^4\,s))\\
&+\overline{B}(m_\eta^2,m_K^2,s)\,(5/24\,m_\pi^2\,m_K^2-1/8\,m_K^2\,s-1/24\,m_K^4)\\
&+\overline{B}(m_\eta^2,m_\eta^2,s)\,(-1/18\,m_\pi^2\,m_K^2)\\
&+\overline{B_1}(m_\pi^2,m_K^2,s)\,(-4/3\,m_\pi^2\,m_K^2+1/3\,m_\pi^4-2/3\,m_K^4)\\
&+\overline{B_1}(m_\eta^2,m_K^2,s)\,(-1/4\,m_\pi^2\,m_K^2+1/4\,m_K^4).
\end{aligned}
\tag{B.14}
$$

$$
\begin{aligned}
M_2^{27}(s) =&\\
&+D_{27}^r\,(-2/3\,s^2)+D_{28}^r\,(-4/3\,s^2)+D_{29}^r\,(7/12\,s^2)+D_{30}^r\,(5/12\,s^2)\\
&+L_2^r\,(-8\,s^2)+P_{K\pi}\,L_3^r\,(10/3\,m_\pi^2\,s^2)\\
&+(1/(16\pi^2))\,((-55/648\,m_\pi^2\,s+55/648\,m_K^2\,s+8/27\,s^2)\\
&+P_{K\pi}\,(-5/24\,m_\pi^2\,s^2))\\
&+\overline{B}(m_\pi^2,m_\pi^2,s)\,((-1/12\,m_\pi^2\,m_K^2-11/12\,m_\pi^2\,s+1/3\,m_\pi^4\\
&+1/24\,m_K^2\,s+3/8\,s^2)\\
&+P_{K\pi}\,\overline{B}(m_\pi^2,m_\pi^2,s)\,(-5/8\,m_\pi^2\,s^2+25/12\,m_\pi^4\,s-5/3\,m_\pi^6))\\
&+\overline{B}(m_\pi^2,m_K^2,s)\,((13/4\,m_\pi^2\,m_K^2-67/16\,m_\pi^2\,s+11/6\,m_\pi^4\\
&-217/96\,m_K^2\,s+1/6\,m_K^4+67/32\,s^2)\\
&+P_{K\pi}\,\overline{B}(m_\pi^2,m_K^2,s)\,(25/32\,m_\pi^2\,s^2-5/3\,m_\pi^4\,s+5/6\,m_\pi^6))\\
&+\overline{B}(m_\eta^2,m_K^2,s)\,((5/72\,m_\pi^2\,m_K^2-5/12\,m_\pi^2\,s+5/18\,m_\pi^4\\
&-5/32\,m_K^2\,s-5/72\,m_K^4\\
&\quad+5/32\,s^2)+P_{K\pi}\,(5/32\,m_\pi^2\,s^2-5/12\,m_\pi^4\,s+5/18\,m_\pi^6))\\
&+\overline{B_1}(m_\pi^2,m_K^2,s)\,(-15/16\,m_\pi^2\,m_K^2+5/24\,m_\pi^4-25/48\,m_K^4)\\
&+\overline{B_1}(m_\eta^2,m_K^2,s)\,(5/16\,m_\pi^2\,m_K^2+5/48\,m_K^4).
\end{aligned}
\tag{B.15}
$$

$$
\begin{aligned}
M_3^{27}(s) =&\\
&+\overline{B}(m_\pi^2,m_\pi^2,s)\,((1/2\,m_\pi^2-1/8\,s)+P_{K\pi}\,(5/24\,m_\pi^2\,s-5/6\,m_\pi^4))\\
&+\overline{B}(m_\pi^2,m_K^2,s)\,(67/144\,m_\pi^2+43/288\,m_K^2-43/288\,s\\
&+P_{K\pi}\,(-5/288\,m_\pi^2\,s+5/72\,m_\pi^4))\\
&+\overline{B}(m_K^2,m_K^2,s)\,((-5/18\,m_\pi^2+5/9\,m_K^2-5/36\,s)
\end{aligned}
$$

$$
\begin{aligned}
&+P_{K\pi}\,(5/72\,m_\pi^2\,s - 5/18\,m_\pi^4))\\
&+\overline{B}(m_\eta^2, m_K^2, s)\,((-7/24\,m_\pi^2 + 5/32\,m_K^2 - 1/32\,s)\\
&+P_{K\pi}\,(5/96\,m_\pi^2\,s - 5/24\,m_\pi^4))\\
&+\overline{B_1}(m_\pi^2, m_K^2, s)\,(-19/72\,m_\pi^2 + 43/144\,m_K^2)\\
&+\overline{B_1}(m_\eta^2, m_K^2, s)\,(1/18\,m_\pi^2 - 1/48\,m_K^2).
\end{aligned}
\tag{B.16}
$$

$$
\begin{aligned}
M_4^{27}(s) =&\\
&+D_2^r\,(10/3\,m_\pi^2\,s) + P_{K\pi}\,(10/3\,m_\pi^4\,s)) + D_4^r\,(-10\,m_\pi^2\,s - 5/2\,m_K^2\,s)\\
&+P_{K\pi}\,(-10/3\,m_\pi^4\,s))\\
&+D_5^r\,(20/3\,m_\pi^2\,s + 5/2\,m_K^2\,s) + D_7^r\,((-25/3\,m_\pi^2\,s - 10\,m_K^2\,s)\\
&+P_{K\pi}\,(-5\,m_\pi^4\,s)) + D_{28}^r(10\,m_\pi^2\,s + 10/3\,m_K^2\,s - 10/3\,s^2)\\
&+(D_{29}^r - D_{30}^r)(-5/4\,m_\pi^2 s - 5/12\,m_K^2 s + 5/12\,s^2)\\
&+L_3^r\,((10/3\,m_\pi^2\,s) + P_{K\pi}\,(-10/3\,m_\pi^2\,s^2 + 40/3\,m_\pi^4\,s))\\
&+L_4^r\,(64/9\,m_\pi^2\,m_K^2) + L_5^r\,(P_{K\pi}\,(-20/3\,m_\pi^4\,s))\\
&+(1/(16\pi^2))\,(5/18\,m_\pi^2\,s + 205/108\,m_K^2\,s + 55/54\,s^2)\\
&+P_{K\pi}\,(5/24\,m_\pi^2\,s^2 + 5/12\,m_\pi^4\,s))\\
&+\overline{A}(m_\pi^2)\,((-1105/72\,s) + P_{K\pi}\,(-95/24\,m_\pi^2\,s) + P_{K\pi}^2\,(5/6\,m_\pi^4\,s))\\
&+\overline{A}(m_K^2)\,((-335/36\,s) + P_{K\pi}\,(-85/24\,m_\pi^2\,s) + P_{K\pi}^2\,(-5/6\,m_\pi^4\,s))\\
&+\overline{A}(m_\eta^2)\,((-35/24\,s) + P_{K\pi}\,(-5/12\,m_\pi^2\,s))\\
&+\overline{B}(m_\pi^2, m_\pi^2, s)\,((5/4\,m_\pi^2\,m_K^2 - 35/6\,m_\pi^2\,s + 25/6\,m_\pi^4\\
&-5/8\,m_K^2\,s + 15/8\,s^2) + P_{K\pi}\,(5/8\,m_\pi^2\,s^2 - 25/12\,m_\pi^4\,s + 5/3\,m_\pi^6))\\
&+\overline{B}(m_\pi^2, m_K^2, s)\,((-5/12\,m_\pi^2\,m_K^2 - 5/16\,m_\pi^2\,s + 5/12\,m_\pi^4\\
&-55/96\,m_K^2\,s + 5/12\,m_K^4 + 5/32\,s^2)\\
&+P_{K\pi}\,(-25/32\,m_\pi^2\,s^2 + 5/3\,m_\pi^4\,s - 5/6\,m_\pi^6))\\
&+\overline{B}(m_\eta^2, m_K^2, s)\,(-5/72\,m_\pi^2\,m_K^2 + 5/12\,m_\pi^2\,s - 5/18\,m_\pi^4\\
&+5/32\,m_K^2\,s + 5/72\,m_K^4 - 5/32\,s^2)\\
&+P_{K\pi}\,(-5/32\,m_\pi^2\,s^2 + 5/12\,m_\pi^4\,s - 5/18\,m_\pi^6))\\
&+\overline{B_1}(m_\pi^2, m_K^2, s)\,(15/16\,m_\pi^2\,m_K^2 - 5/24\,m_\pi^4 + 25/48\,m_K^4)\\
&+\overline{B_1}(m_\eta^2, m_K^2, s)\,(-5/16\,m_\pi^2\,m_K^2 - 5/48\,m_K^4).
\end{aligned}
\tag{B.17}
$$

$$
\begin{aligned}
M_5^{27}(s) =&\\
&+D_2^r\,((10/3\,m_\pi^2) + P_{K\pi}\,(10/3\,m_\pi^4)) + D_4^r\,((-10\,m_\pi^2 - 5/2\,m_K^2)\\
&+P_{K\pi}\,(-10/3\,m_\pi^4)) + D_5^r\,(20/3\,m_\pi^2 + 5/2\,m_K^2) + D_7^r\,((-25/3\,m_\pi^2 - 10\,m_K^2)
\end{aligned}
$$

$$
\begin{aligned}
&+P_{K\pi}\,(-5\,m_\pi^4)) + D_{28}^r\,(10/3\,s) + D_{29}^r\,(-5/12\,s) + D_{30}^r\,(5/12\,s)\\
&+P_{K\pi}\,(L_3^r - 2L_5^r)\,(10/3\,m_\pi^2\,s)\\
&+(1/(16\pi^2))\,((280/81\,m_\pi^2 + 1945/648\,m_K^2 - 55/54\,s)\\
&+P_{K\pi}\,(-5/24\,m_\pi^2\,s + 5/4\,m_\pi^4))\\
&+\overline{A}(m_\pi^2)\,((-1105/72) + P_{K\pi}\,(-95/24\,m_\pi^2) + P_{K\pi}^2\,(5/6\,m_\pi^4))\\
&+\overline{A}(m_K^2)\,((-335/36) + P_{K\pi}\,(-85/24\,m_\pi^2) + P_{K\pi}^2\,(-5/6\,m_\pi^4))\\
&+\overline{A}(m_\eta^2)\,((-35/24) + P_{K\pi}\,(-5/12\,m_\pi^2))\\
&+\overline{B}(m_\pi^2, m_\pi^2, s)\,(-5/6\,m_\pi^2 + 5/24\,s) + P_{K\pi}\,(5/72\,m_\pi^2\,s - 5/18\,m_\pi^4))\\
&+\overline{B}(m_\pi^2, m_K^2, s)\,(-67/144\,m_\pi^2 - 43/288\,m_K^2 + 43/288\,s\\
&+P_{K\pi}\,(5/288\,m_\pi^2\,s - 5/72\,m_\pi^4))\\
&+\overline{B}(m_K^2, m_K^2, s)\,((-5/18\,m_\pi^2 - 7/9\,m_K^2 + 7/36\,s)\\
&+P_{K\pi}\,(5/72\,m_\pi^2\,s - 5/18\,m_\pi^4))\\
&+\overline{B}(m_\eta^2, m_K^2, s)\,((7/24\,m_\pi^2 - 5/32\,m_K^2 + 1/32\,s)\\
&+P_{K\pi}\,(-5/96\,m_\pi^2\,s + 5/24\,m_\pi^4))\\
&+\overline{B_1}(m_\pi^2, m_K^2, s)\,(19/72\,m_\pi^2 - 43/144\,m_K^2)\\
&+\overline{B_1}(m_\eta^2, m_K^2, s)\,(-1/18\,m_\pi^2 + 1/48\,m_K^2).
\end{aligned}
\tag{B.18}
$$

$$
\begin{aligned}
M_9^{27}(s) = {}&\\
&+\overline{B}(m_\pi^2, m_\pi^2, s)\,((-19/18\,m_\pi^2 + 19/72\,s) + P_{K\pi}\,(5/24\,m_\pi^2\,s - 5/6\,m_\pi^4))\\
&+\overline{B}(m_\pi^2, m_K^2, s)\,(-67/144\,m_\pi^2 - 43/288\,m_K^2 + 43/288\,s\\
&+P_{K\pi}\,(5/288\,m_\pi^2\,s - 5/72\,m_\pi^4))\\
&+\overline{B}(m_K^2, m_K^2, s)\,((-5/9\,m_\pi^2 - 5/9\,m_K^2 + 5/36\,s)\\
&+P_{K\pi}\,(5/36\,m_\pi^2\,s - 5/9\,m_\pi^4))\\
&+\overline{B}(m_\eta^2, m_K^2, s)\,((7/24\,m_\pi^2 - 5/32\,m_K^2 + 1/32\,s)\\
&+P_{K\pi}\,(-5/96\,m_\pi^2\,s + 5/24\,m_\pi^4))\\
&+\overline{B_1}(m_\pi^2, m_K^2, s)\,(19/72\,m_\pi^2 - 43/144\,m_K^2)\\
&+\overline{B_1}(m_\eta^2, m_K^2, s)\,(-1/18\,m_\pi^2 + 1/48\,m_K^2).
\end{aligned}
\tag{B.19}
$$

$$
\begin{aligned}
M_{10}^{27}(s) = {}&\\
&(D_1^r + 2D_2^r)(8/3\,m_\pi^2\,m_K^2)\\
&+D_4^r(14/3\,m_\pi^2 m_K^2 - 47/3\,m_\pi^2 s + 47/3\,m_\pi^4 - 13/3\,m_K^2\,s + m_K^4)\\
&+D_5^r\,(-10\,m_\pi^2\,m_K^2 + 47/3\,m_\pi^2\,s - 47/3\,m_\pi^4 + 13/3\,m_K^2\,s - m_K^4)
\end{aligned}
$$

$$
\begin{aligned}
&+D_6^r\,(-2/3\,m_\pi^2\,m_K^2 + 1/3\,m_\pi^2\,s - 1/3\,m_\pi^4 - m_K^2\,s + m_K^4)\\
&+D_7^r\,(50/3\,m_\pi^2\,m_K^2 - 34/3\,m_\pi^2\,s + 34/3\,m_\pi^4 - 52/3\,m_K^2\,s + 4\,m_K^4)\\
&+D_{26}^r\,(-2/3\,m_\pi^2\,m_K^2 + m_\pi^2\,s - 5/3\,m_\pi^4 + 1/3\,m_K^2\,s - 1/3\,m_K^4)\\
&+D_{27}^r\,(4/3\,m_\pi^2\,m_K^2 - 2\,m_\pi^2\,s - 2/3\,m_\pi^4 - 2/3\,m_K^2\,s - 2/3\,m_K^4 + 4/3\,s^2)\\
&+D_{28}^r\,(-12\,m_\pi^2\,m_K^2 + 18\,m_\pi^2\,s - 18\,m_\pi^4 + 6\,m_K^2\,s - 2\,m_K^4 - 4\,s^2)\\
&+D_{29}^r\,(8/3\,m_\pi^2\,m_K^2 - 4\,m_\pi^2\,s + 8/3\,m_\pi^4 - 4/3\,m_K^2\,s + 4/3\,s^2)\\
&+D_{30}^r\,(-8/3\,m_\pi^2\,m_K^2 + 4\,m_\pi^2\,s - 20/3\,m_\pi^4 + 4/3\,m_K^2\,s - 4/3\,m_K^4)\\
&+D_{31}^r\,(-8/3\,m_\pi^2\,m_K^2 + 4\,m_\pi^2\,s - 20/3\,m_\pi^4 + 4/3\,m_K^2\,s - 4/3\,m_K^4)\\
&+L_1^r\,(64/3\,m_\pi^2\,m_K^2 - 32\,m_\pi^2\,s + 160/3\,m_\pi^4 - 32/3\,m_K^2\,s + 32/3\,m_K^4)\\
&+L_2^r\,(-32/3\,m_\pi^2\,m_K^2 + 16\,m_\pi^2\,s + 16/3\,m_\pi^4\\
&+16/3\,m_K^2\,s + 16/3\,m_K^4 - 32/3\,s^2)\\
&+L_3^r\,(32/3\,m_\pi^2\,m_K^2 - 16\,m_\pi^2\,s + 80/3\,m_\pi^4 - 16/3\,m_K^2\,s + 16/3\,m_K^4)\\
&+L_4^r\,(32/3\,m_\pi^2\,m_K^2 + 32/3\,m_\pi^2\,s - 32/3\,m_\pi^4) + L_5^r\,(32/3\,m_\pi^2\,s - 32/3\,m_\pi^4)\\
&+(1/(16\pi^2))\,(-643/162\,m_\pi^2\,m_K^2 - 49/324\,m_\pi^2\,s + 31/108\,m_\pi^4\\
&+1273/324\,m_K^2\,s - 439/324\,m_K^4 + 34/27\,s^2)\\
&+\overline{A}(m_\pi^2)\,((2075/72\,m_\pi^2 + 493/72\,m_K^2 - 329/12\,s)\\
&+P_{K\pi}\,(-35/24\,m_\pi^2\,s + 25/9\,m_\pi^4))\\
&+\overline{A}(m_K^2)\,((575/36\,m_\pi^2 + 149/36\,m_K^2 - 49/3\,s)\\
&+P_{K\pi}\,(5/6\,m_\pi^2\,s - 10/9\,m_\pi^4))\\
&+\overline{A}(m_\eta^2)\,((29/24\,m_\pi^2 + 19/24\,m_K^2 - 9/4\,s) + P_{K\pi}\,(5/8\,m_\pi^2\,s - 5/3\,m_\pi^4))\\
&+\overline{B}(m_\pi^2, m_\pi^2, s)\,(m_\pi^2\,m_K^2 - 13/2\,m_\pi^2\,s + 13/3\,m_\pi^4 - 1/2\,m_K^2\,s + 13/6\,s^2)\\
&+\overline{B}(m_\pi^2, m_K^2, s)\,(8/3\,m_\pi^2\,m_K^2 - 13/3\,m_\pi^2\,s + 13/6\,m_\pi^4\\
&-8/3\,m_K^2\,s + 1/2\,m_K^4 + 13/6\,s^2).
\end{aligned}
\tag{B.20}
$$

$$
\begin{aligned}
M_{11}^{27}(s) =&\\
&+(D_{26}^r + 2D_{27}^r + 6D_{28}^r + 4D_{30}^r + 4D_{31}^r)\,(1/3\,s^2)\\
&+(2L_1^r + L_2^r + L_3^r)\,(-16/3\,s^2)\\
&+(1/(16\pi^2))\,(-11/162\,m_\pi^2\,s + 11/162\,m_K^2\,s - 17/27\,s^2)\\
&+\overline{B}(m_\pi^2, m_\pi^2, s)\,((-5/12\,m_\pi^2\,m_K^2 + 5/2\,m_\pi^2\,s - 2\,m_\pi^4 - 1/6\,m_K^2\,s - 1/2\,s^2)\\
&\quad+P_{K\pi}\,(-5/4\,m_\pi^2\,s^2 + 35/12\,m_\pi^4\,s - 5/3\,m_\pi^6))\\
&+\overline{B}(m_\pi^2, m_K^2, s)\,((7/24\,m_\pi^2\,m_K^2 - 13/24\,m_\pi^2\,s + 7/12\,m_\pi^4 + 19/48\,m_K^2\,s\\
&-3/8\,m_K^4 - 1/48\,s^2) + P_{K\pi}\,(15/16\,m_\pi^2\,s^2 - 5/2\,m_\pi^4\,s + 5/3\,m_\pi^6))\\
&+\overline{B}(m_K^2, m_K^2, s)\,(-3/8\,m_\pi^2\,s - 3/8\,m_K^2\,s + 3/8\,s^2)
\end{aligned}
$$

$$
\begin{aligned}
&+\overline{B}(m_\eta^2, m_K^2, s)\,((-5/72\, m_\pi^2\, m_K^2 - 5/6\, m_\pi^2\, s + 5/9\, m_\pi^4\\
&-3/16\, m_K^2\, s - 7/72\, m_K^4 + 5/16\, s^2)\\
&+P_{K\pi}\,(5/16\, m_\pi^2\, s^2 - 5/6\, m_\pi^4\, s + 5/9\, m_\pi^6))\\
&+\overline{B}(m_\eta^2, m_\eta^2, s)\,((-13/36\, m_\pi^2\, m_K^2 + 5/12\, m_\pi^2\, s - 5/9\, m_\pi^4)\\
&+P_{K\pi}\,(5/12\, m_\pi^4\, s - 5/9\, m_\pi^6))\\
&+\overline{B_1}(m_\pi^2, m_K^2, s)\,(-13/24\, m_\pi^2\, m_K^2 + 1/12\, m_\pi^4 - 3/8\, m_K^4)\\
&+\overline{B_1}(m_\eta^2, m_K^2, s)\,(7/8\, m_\pi^2\, m_K^2 - 1/24\, m_K^4).
\end{aligned}
\tag{B.21}
$$

$$
\begin{aligned}
M_{12}^{27}(s) = \;&\\
&+\overline{B}(m_\pi^2, m_\pi^2, s)\,(-13/9\, m_\pi^2 + 13/36\, s)\\
&+\overline{B}(m_\pi^2, m_K^2, s)\,((-8/9\, m_\pi^2 - 41/144\, m_K^2 + 41/144\, s)\\
&+P_{K\pi}\,(5/144\, m_\pi^2\, s - 5/36\, m_\pi^4))\\
&+\overline{B}(m_K^2, m_K^2, s)\,((5/9\, m_\pi^2 - 5/18\, m_K^2 + 5/72\, s)\\
&+P_{K\pi}\,(-5/36\, m_\pi^2\, s + 5/9\, m_\pi^4))\\
&+\overline{B}(m_\eta^2, m_K^2, s)\,((-7/24\, m_\pi^2 - 55/48\, m_K^2 + 11/48\, s)\\
&+P_{K\pi}\,(5/48\, m_\pi^2\, s - 5/12\, m_\pi^4))\\
&+\overline{B_1}(m_\pi^2, m_K^2, s)\,(1/2\, m_\pi^2 - 41/72\, m_K^2)\\
&+\overline{B_1}(m_\eta^2, m_K^2, s)\,(-1/12\, m_\pi^2 + 11/72\, m_K^2).
\end{aligned}
\tag{B.22}
$$

References

[1] S. Weinberg, PhysicaA **96** (1979) 327.

[2] J. Gasser and H. Leutwyler, Annals Phys. **158** (1984) 142.

[3] J. Gasser and H. Leutwyler, Nucl. Phys. B **250** (1985) 465.

[4] Pich, A., Lectures at Les Houches Summer School in Theoretical Physics, Session 68: Probing the Standard Model of Particle Interactions, Les Houches, France, 28 Jul - 5 Sep 1997, [hep-ph/9806303];
Ecker, G., Lectures given at Advanced School on Quantum Chromodynamics (QCD 2000), Benasque, Huesca, Spain, 3-6 Jul 2000, [hep-ph/0011026].

[5] J. Kambor, J. Missimer and D. Wyler, Nucl. Phys. B **346** (1990) 17.

[6] J. Kambor, J. Missimer and D. Wyler, Phys. Lett. B **261** (1991) 496.

[7] J. Kambor, J. F. Donoghue, B. R. Holstein, J. Missimer and D. Wyler, Phys. Rev. Lett. **68** (1992) 1818.

[8] G. Ecker, Prog. Part. Nucl. Phys. **35** (1995) 1 [hep-ph/9501357];
A. Pich, Rept. Prog. Phys. **58** (1995) 563 [hep-ph/9502366];

E. de Rafael, Lectures given at Theoretical Advanced Study Institute in Elementary Particle Physics (TASI 94): CP Violation and the limits of the Standard Model, Boulder, CO, 29 May - 24 Jun 1994, hep-ph/9502254.

[9] J. A. Cronin, Phys. Rev. **161** (1967) 1483.

[10] B. R. Holstein, Phys. Rev. **183** (1969) 1228;
J. F. Donoghue, E. Golowich and B. R. Holstein, Phys. Rev. D **30** (1984) 587;
H. Y. Cheng, C. Y. Cheung and W. B. Yeung, Mod. Phys. Lett. A **4** (1989) 869; Z. Phys. C **43** (1989) 391;
S. Fajfer and J. M. Gerard, Z. Phys. C **42** (1989) 425.

[11] M. Knecht, B. Moussallam, J. Stern and N. H. Fuchs, Nucl. Phys. B **457** (1995) 513 [hep-ph/9507319].

[12] G. Esposito-Farese, Z. Phys. C **50** (1991) 255.

[13] G. Ecker, J. Kambor and D. Wyler, Nucl. Phys. B **394** (1993) 101.

[14] J. Bijnens, E. Pallante and J. Prades, Nucl. Phys. B **521** (1998) 305 [hep-ph/9801326].

[15] C. Zemach, Phys.Rev. **133** (1964) 1201.

[16] S. Weinberg, Phys. Rev. Lett. **17** (1966) 61.

[17] G. D'Ambrosio, G. Isidori, A. Pugliese and N. Paver, Phys. Rev. D **50** (1994) 5767 [Erratum-ibid. D **51** (1994) 3975] [hep-ph/9403235].

[18] T. J. Devlin and J. O. Dickey, Rev. Mod. Phys. **51** (1979) 237.

[19] C. Cheshkov, hep-ph/0105131.

[20] D. E. Groom *et al.* [Particle Data Group Collaboration], Eur. Phys. J. C **15** (2000) 1.

[21] R. Adler *et al.* [CPLEAR Collaboration], Phys. Lett. B **407** (1997) 193;
R. Adler *et al.* [CPLEAR Collaboration], Phys. Lett. B **374** (1996) 313;
A. Angelopoulos *et al.* [CPLEAR Collaboration], Eur. Phys. J. C **5** (1998) 389.

[22] S. Somalwar *et al.* [Fermilab E-731 Collaboration], Phys. Rev. Lett. **68** (1992) 2580.

[23] A. Lai *et al.* [NA48 Collaboration], Phys. Lett. B **515** (2001) 261 [hep-ex/0106075].

[24] G. B. Thomson *et al.*, Phys. Lett. B **337** (1994) 411;
Y. Zou *et al.*, Phys. Lett. B **369** (1996) 362.

[25] V. Y. Batusov *et al.*, Nucl. Phys. B **516** (1998) 3.

[26] V. N. Bolotov *et al.*, Sov. J. Nucl. Phys. **44** (1986) 73 [Yad. Fiz. **44** (1986) 117].

[27] G. Amoros, J. Bijnens and P. Talavera, Phys. Lett. B **480** (2000) 71 [hep-ph/9912398]; Nucl. Phys. B **585** (2000) 293 [Erratum-ibid. B **598** (2001) 665] [hep-ph/0003258]; Nucl. Phys. B **602** (2001) 87 [hep-ph/0101127].

[28] J. Bijnens and J. Gasser, "Eta decays at and beyond p^4 in chiral perturbation theory," [hep-ph/0202242], proceedings of the Workshop on Eta Physics: Prospects of Precision Measurements with the CELSIUS/WASA Facility, Uppsala, Sweden, 25-27 Oct 2001.

[29] G. Ecker, G. Isidori, G. Muller, H. Neufeld and A. Pich, Nucl. Phys. B **591** (2000) 419 [hep-ph/0006172];
V. Cirigliano, J. F. Donoghue and E. Golowich, Phys. Rev. D **61** (2000) 093002 [hep-ph/9909473]; Phys. Rev. D **61** (2000) 093001 [Erratum-ibid. D **63** (2000) 059903] [hep-ph/9907341];
S. Gardner and G. Valencia, Phys. Lett. B **466** (1999) 355 [hep-ph/9909202];
C. E. Wolfe and K. Maltman, Phys. Lett. B **482** (2000) 77 [hep-ph/9912254];
G. Ecker, G. Muller, H. Neufeld and A. Pich, Phys. Lett. B **477** (2000) 88 [hep-ph/9912264].

[30] G. Amoros, J. Bijnens and P. Talavera, Nucl. Phys. B **568** (2000) 319 [hep-ph/9907264].

Isospin Breaking in $K \to 3\pi$ Decays I: Strong Isospin Breaking

Paper II

Isospin Breaking in $K \to 3\pi$ Decays I: Strong Isospin Breaking[1,2]

Johan Bijnens and Fredrik Borg

Department of Theoretical Physics, Lund University
Sölvegatan 14A, S 22362 Lund, Sweden

Abstract:

The CP conserving amplitudes for the decays $K \to 3\pi$ are calculated in Chiral Perturbation Theory. The calculation is made at the next-to-leading order including strong and local electromagnetic isospin breaking. A comparison is made between the squared amplitudes with and without isospin violation to estimate the size of the effect. We find corrections of order five percent in the amplitudes.

[1]Reprinted from Nucl. Phys. B 697 (2004) 319, Johan Bijnens and Fredrik Borg, Isospin Breaking in $K \to 3\pi$ Decays I: Strong Isospin Breaking, Copyright (2004), with permission from Elsevier.

[2]LU TP 04-20, hep-ph/0405025, May 2004

2.1 Introduction

Chiral Perturbation Theory (ChPT) is the effective field theory of the low-energy strong interactions. It was introduced in its present form by Weinberg, Gasser and Leutwyler [1–3] and it has had many successes and applications. A pedagogical introduction can be found in [4]. The theory has been applied as well for nonleptonic weak decays. The main work of extending ChPT to the nonleptonic weak interaction was done by Kambor, Missimer and Wyler who worked out the general formalism [5] and applied it to $K \to 2\pi, 3\pi$ decays [6]. These results were then used to obtain directly relations between physical observables in [7]. Reviews of applications of ChPT to nonleptonic weak interactions are [8]. The expressions of Ref. [6] were never published and have been lost.

The next-to-leading order $K \to 2\pi$ amplitudes in the isospin limit were recalculated in [9, 10] and the $K \to 3\pi$ amplitudes in [10]. The latter have been confirmed in [11]. In [10] a full fit to all available $K \to 2\pi$ and $K \to 3\pi$ experimental results was performed and it was found that one could fit the decay rates and the slopes in the Dalitz plot. There was a discrepancy with the observed quadratic slopes or curvatures in the Dalitz plot and this can have several different origins. It could be an experimental problem (especially given the discrepancies between several experiments) or it could have a theoretical origin. In the latter the amplitudes calculated so far have three different types of corrections, isospin breaking, electromagnetic corrections or higher order ChPT corrections. In this paper we investigate the first class. Work is in progress to evaluate the electromagnetic corrections as well. More precisely, in this paper we investigate effects of the quark mass difference $m_u - m_d$ as well as the local electromagnetic effects. We have worked out all orders in $m_u - m_d$ to order four in the chiral expansion but we have found that the numerical difference between the all order isospin breaking and the first order effect was much smaller than the other uncertainties in the calculations. We therefore present results only to first order in $m_u - m_d$.

There exists very little work on isospin breaking in $K \to 3\pi$ decays and none that we know of within ChPT. The $K \to 2\pi$ case has been investigated more extensively since it has possibly strong effects on ϵ'/ϵ [12]. Recent works are [13–16].

The outline of this paper is as follows. The next section describes strong isospin breaking. Section 2.3 presents the Chiral Lagrangians needed for the calculation to next-to-leading order and section 2.4 specifies the decays and describes the relevant kinematics. The analytical results, the amplitudes for $K \to 3\pi$, are described in section 2.5 and in section 2.6 some numerical results are shown. The last section contains the conclusions.

2.2 Strong Isospin Breaking

Historically, the isospin approximation meant treating the proton and neutron in the same way. In a quark picture this corresponds to treating the up- and down-quark as being identical. This implies putting $m_u = m_d$ as well as neglecting electromagnetism. Obviously this is an approximation but since one can roughly estimate the corrections, and it greatly simplifies the calculations, its use is very common. However, to reduce the errors one has to quote, the isospin approximation has to be abandoned.

Isospin breaking is usually divided into two parts. Strong isospin breaking coming from the fact that $m_u \neq m_d$, and electromagnetic isospin breaking from including electromagnetic effects. In this paper we only take into account the strong part and the local part (the part which doesn't include explicit photons) of the EM isospin breaking. From now on we will use the name strong isospin breaking for the sum of these two effects.

The difference between m_u and m_d leads to mixing between π and η. This means changes in the formulas for both the physical masses of π and η as well as the amplitude for any process involving either of the two. For a detailed discussion see [17].

Including the local EM part means introducing new Lagrangians at each order, proportional to e^2 and $p^2\, e^2$ respectively.

2.3 The ChPT Lagrangians

The starting point of our ChPT calculation is the Lagrangians. The order parameters in the perturbation series are p, the momenta of, and m, the mass of the pseudoscalars. Including isospin breaking also e, the electron charge, is used as an order parameter. Leading order (order two) therefore means terms of order p^2, m^2, e^2, and next-to-leading order (order four) $p^4, p^2\, m^2, m^4, p^2\, e^2$ and $m^2\, e^2$ (e^4 is neglected).

2.3.1 Leading Order

Our leading order effective Lagrangian assumes the form

$$\mathcal{L}_2 = \mathcal{L}_{S2} + \mathcal{L}_{W2} + \mathcal{L}_{E2} \tag{2.1}$$

Here $\mathcal{L}_{S2}$ refers to the strong $\Delta S = 0$ part, $\mathcal{L}_{W2}$ the weak $\Delta S = \pm 1$ part, and $\mathcal{L}_{E2}$ the strong-electromagnetic and weak-electromagnetic parts combined. For the strong part we have [2]

$$\mathcal{L}_{S2} = \frac{F_0^2}{4}\,\langle u_\mu u^\mu + \chi_+ \rangle \tag{2.2}$$

Here $\langle A\rangle$ stands for the flavour trace of the matrix A, and F_0 is the pion decay constant in the chiral limit. We also define the matrices u_μ, u and $\chi_\pm$

$$u_\mu = iu^\dagger D_\mu U\, u^\dagger = u_\mu^\dagger\,, \quad u^2 = U\,, \quad \chi_\pm = u^\dagger\chi u^\dagger \pm u\chi^\dagger u\,, \tag{2.3}$$

where the special unitary matrix U contains the Goldstone boson fields

$$U = \exp\left(\frac{i\sqrt{2}}{F_0}M\right)\,, \quad M = \begin{pmatrix} \frac{1}{\sqrt{2}}\pi_3 + \frac{1}{\sqrt{6}}\eta_8 & \pi^+ & K^+ \\ \pi^- & \frac{-1}{\sqrt{2}}\pi_3 + \frac{1}{\sqrt{6}}\eta_8 & K^0 \\ K^- & \overline{K^0} & \frac{-2}{\sqrt{6}}\eta_8 \end{pmatrix}\,. \tag{2.4}$$

The formalism we use is the external field method of [2], but for our purpose it suffices to set

$$\chi = 2B_0 \begin{pmatrix} m_u & & \\ & m_d & \\ & & m_s \end{pmatrix} \quad \text{and} \quad D_\mu U = \partial_\mu U. \tag{2.5}$$

We diagonalize the quadratic terms in (2.2) by a rotation

$$\begin{aligned} \pi^0 &= \pi_3\cos\epsilon + \eta_8\sin\epsilon \\ \eta &= -\pi_3\sin\epsilon + \eta_8\cos\epsilon\,, \end{aligned} \tag{2.6}$$

where the lowest order mixing angle ϵ satisfies

$$\tan(2\epsilon) = \frac{\sqrt{3}}{2}\frac{m_d - m_u}{m_s - \hat{m}}\,, \tag{2.7}$$

with $2\hat{m} = m_u + m_d$.

For the weak part the Lagrangian has the form [18]

$$\mathcal{L}_{W2} = C\,F_0^4\left[G_8\langle\Delta_{32}u_\mu u^\mu\rangle + G_8'\langle\Delta_{32}\chi_+\rangle + G_{27}t^{ij,kl}\,\langle\Delta_{ij}u_\mu\rangle\langle\Delta_{kl}u^\mu\rangle\right] + \text{ h.c.}\,. \tag{2.8}$$

The tensor $t^{ij,kl}$ has as nonzero components

$$\begin{aligned} t^{21,13} = t^{13,21} = \frac{1}{3} \quad &; \quad t^{22,23} = t^{23,22} = -\frac{1}{6}\,; \\ t^{23,33} = t^{33,23} = -\frac{1}{6} \quad &; \quad t^{23,11} = t^{11,23} = \frac{1}{3}\,, \end{aligned} \tag{2.9}$$

and the matrix Δ_{ij} is defined as

$$\Delta_{ij} \equiv u\lambda_{ij}u^\dagger\,, \quad (\lambda_{ij})_{ab} \equiv \delta_{ia}\,\delta_{jb}\,. \tag{2.10}$$

The coefficient C is defined such that in the chiral and large N_c limits $G_8 = G_{27} = 1$,

$$C = -\frac{3}{5}\frac{G_F}{\sqrt{2}} V_{ud} V_{us}^* . \qquad (2.11)$$

Finally, the remaining electromagnetic part, relevant for this calculation, looks like (see e.g. [19])

$$\mathcal{L}_{E2} = e^2 F_0^4 Z \langle \mathcal{Q}_L \mathcal{Q}_R \rangle + e^2 F_0^4 \langle \Upsilon \mathcal{Q}_R \rangle \qquad (2.12)$$

where the strangeness-conserving term includes

$$\mathcal{Q}_L = u Q u^\dagger , \quad \mathcal{Q}_R = u^\dagger Q u \ \text{ with } \ Q = \begin{bmatrix} 2/3 & 0 & 0 \\ 0 & -1/3 & 0 \\ 0 & 0 & -1/3 \end{bmatrix} , \qquad (2.13)$$

and the weak-electromagnetic term is characterized by a constant G_E ($G_E = g_{\mathrm{ewk}} G_8$ in [19]),

$$\Upsilon = G_E F_0^2 \Delta_{32} + \text{h.c.} . \qquad (2.14)$$

2.3.2 Next-to-leading Order

Since ChPT is a non-renormalizable theory, new terms have to be added at each order to compensate for the loop-divergences. This means that the Lagrangians increase in size for every new order and the number of free parameters rise as well. At next-to-leading order we split the Lagrangian in four parts which, in obvious notation, are

$$\mathcal{L}_4 = \mathcal{L}_{S4} + \mathcal{L}_{W4} + \mathcal{L}_{S2E2} + \mathcal{L}_{W2E2}(G_8) . \qquad (2.15)$$

Here the notation (G_8) indicates that here only the dominant G_8-part is included in the Lagrangian, and therefore in the calculation. The strong part we need looks like [2, 20]

$$\begin{aligned} \mathcal{L}_{S4} \;=\; & L_1 \langle u_\mu u^\mu \rangle^2 + L_2 \langle u_\mu u^\nu \rangle \langle u^\mu u_\nu \rangle + L_3 \langle u_\mu u^\mu u_\nu u^\nu \rangle + L_4 \langle u_\mu u^\mu \rangle \langle \chi_+ \rangle \\ & + L_5 \langle u_\mu u^\mu \chi_+ \rangle + L_6 \langle \chi_+ \rangle^2 + L_7 \langle \chi_- \rangle^2 + L_8 \frac{1}{2} \left(\langle \chi_+^2 \rangle + \langle \chi_-^2 \rangle \right) , \end{aligned} \qquad (2.16)$$

and the weak part, quoting only the terms relevant for $K \to 3\pi$ decays, is [5, 21, 22],

$$\mathcal{L}_{W4} \;=\; C F_0^2 \Big\{ G_8 \Big[N_1 \mathcal{O}_1^8 + N_2 \mathcal{O}_2^8 + N_3 \mathcal{O}_3^8 + N_4 \mathcal{O}_4^8 + N_5 \mathcal{O}_5^8 + N_6 \mathcal{O}_6^8 + N_7 \mathcal{O}_7^8$$

$$
\begin{aligned}
&+N_8\mathcal{O}_8^8 + N_9\mathcal{O}_9^8 + N_{10}\mathcal{O}_{10}^8 + N_{11}\mathcal{O}_{11}^8 + N_{12}\mathcal{O}_{12}^8 + N_{13}\mathcal{O}_{13}^8\Big] \\
&+G_{27}\Big[D_1\mathcal{O}_1^{27} + D_2\mathcal{O}_2^{27} + D_4\mathcal{O}_4^{27} + D_5\mathcal{O}_5^{27} + D_6\mathcal{O}_6^{27} + D_7\mathcal{O}_7^{27} \\
&+D_{26}\mathcal{O}_{26}^{27} + D_{27}\mathcal{O}_{27}^{27} + D_{28}\mathcal{O}_{28}^{27} + D_{29}\mathcal{O}_{29}^{27} + D_{30}\mathcal{O}_{30}^{27} \\
&+D_{31}\mathcal{O}_{31}^{27}\Big]\Bigg\} + \text{h.c.}\,. \qquad (2.17)
\end{aligned}
$$

The octet operators are

$$
\begin{aligned}
&\mathcal{O}_1^8 = \langle\Delta_{32}u_\mu u^\mu u_\nu u^\nu\rangle && \mathcal{O}_2^8 = \langle\Delta_{32}u_\mu u_\nu u^\nu u^\mu\rangle \\
&\mathcal{O}_3^8 = \langle\Delta_{32}u_\mu u_\nu\rangle\langle u^\mu u^\nu\rangle && \mathcal{O}_4^8 = \langle\Delta_{32}u_\mu\rangle\langle u_\nu u^\mu u^\nu\rangle \\
&\mathcal{O}_5^8 = \langle\Delta_{32}(\chi_+ u_\mu u^\mu + u_\mu u^\mu \chi_+)\rangle && \mathcal{O}_6^8 = \langle\Delta_{32}u_\mu\rangle\langle u^\mu\chi_+\rangle \\
&\mathcal{O}_7^8 = \langle\Delta_{32}\chi_+\rangle\langle u_\mu u^\mu\rangle && \mathcal{O}_8^8 = \langle\Delta_{32}u_\mu u^\mu\rangle\langle\chi_+\rangle \qquad (2.18) \\
&\mathcal{O}_9^8 = \langle\Delta_{32}(\chi_- u_\mu u^\mu - u_\mu u^\mu \chi_-)\rangle && \mathcal{O}_{10}^8 = \langle\Delta_{32}\chi_+\chi_+\rangle \\
&\mathcal{O}_{11}^8 = \langle\Delta_{32}\chi_+\rangle\langle\chi_+\rangle && \mathcal{O}_{12}^8 = \langle\Delta_{32}\chi_-\chi_-\rangle \\
&\mathcal{O}_{13}^8 = \langle\Delta_{32}\chi_-\rangle\langle\chi_-\rangle\,,
\end{aligned}
$$

and the 27 operators are

$$
\begin{aligned}
\mathcal{O}_1^{27} &= t^{ij,kl}\langle\Delta_{ij}\chi_+\rangle\langle\Delta_{kl}\chi_+\rangle \\
\mathcal{O}_2^{27} &= t^{ij,kl}\langle\Delta_{ij}\chi_-\rangle\langle\Delta_{kl}\chi_-\rangle \\
\mathcal{O}_4^{27} &= t^{ij,kl}\langle\Delta_{ij}u_\mu\rangle\langle\Delta_{kl}(u^\mu\chi_+ + \chi_+u^\mu)\rangle \\
\mathcal{O}_5^{27} &= t^{ij,kl}\langle\Delta_{ij}u_\mu\rangle\langle\Delta_{kl}(u^\mu\chi_- - \chi_-u^\mu)\rangle \\
\mathcal{O}_6^{27} &= t^{ij,kl}\langle\Delta_{ij}\chi_+\rangle\langle\Delta_{kl}u_\mu u^\mu\rangle \\
\mathcal{O}_7^{27} &= t^{ij,kl}\langle\Delta_{ij}u_\mu\rangle\langle\Delta_{kl}u^\mu\rangle\langle\chi_+\rangle \\
\mathcal{O}_{26}^{27} &= t^{ij,kl}\langle\Delta_{ij}u_\mu u^\mu\rangle\langle\Delta_{kl}u_\nu u^\nu\rangle \\
\mathcal{O}_{27}^{27} &= t^{ij,kl}\langle\Delta_{ij}(u_\mu u_\nu + u_\nu u_\mu)\rangle\langle\Delta_{kl}u^\mu u^\nu\rangle \\
\mathcal{O}_{28}^{27} &= t^{ij,kl}\langle\Delta_{ij}(u_\mu u_\nu - u_\nu u_\mu)\rangle\langle\Delta_{kl}u^\mu u^\nu\rangle \\
\mathcal{O}_{29}^{27} &= t^{ij,kl}\langle\Delta_{ij}u_\mu\rangle\langle\Delta_{kl}u_\nu u^\mu u^\nu\rangle \\
\mathcal{O}_{30}^{27} &= t^{ij,kl}\langle\Delta_{ij}u_\mu\rangle\langle\Delta_{kl}(u^\mu u_\nu u^\nu + u_\nu u^\nu u^\mu)\rangle \\
\mathcal{O}_{31}^{27} &= t^{ij,kl}\langle\Delta_{ij}u_\mu\rangle\langle\Delta_{kl}u^\mu\rangle\langle u_\nu u^\nu\rangle\,. \qquad (2.19)
\end{aligned}
$$

The complete minimal Lagrangian of $\mathcal{O}(G_8e^2p^2)$ takes the form [19]

$$
\mathcal{L}_{W2E2}(G_8) = G_8e^2F_0^4\sum_{i=1}^{14} Z_iQ_i^w + \text{ h.c.} \qquad (2.20)
$$

with operators Q_i^w of $\mathcal{O}(p^2)$ and dimensionless coupling constants Z_i. A linear independent set of operators is given by

$$
\begin{aligned}
Q_1^w &= \langle \Delta_{32}\{\mathcal{Q}_R, \chi_+\}\rangle & Q_2^w &= \langle \Delta_{32}\mathcal{Q}_R\rangle\langle\chi_+\rangle \\
Q_3^w &= \langle \Delta_{32}\mathcal{Q}_R\rangle\langle\chi_+\mathcal{Q}_R\rangle & Q_4^w &= \langle \Delta_{32}\chi_+\rangle\langle\mathcal{Q}_L\mathcal{Q}_R\rangle \\
Q_5^w &= \langle \Delta_{32}u_\mu u^\mu\rangle & Q_6^w &= \langle \Delta_{32}\{\mathcal{Q}_R, u_\mu u^\mu\}\rangle \\
Q_7^w &= \langle \Delta_{32}u_\mu u^\mu\rangle\langle\mathcal{Q}_L\mathcal{Q}_R\rangle & Q_8^w &= \langle \Delta_{32}u_\mu\rangle\langle\mathcal{Q}_L u^\mu\rangle \\
Q_9^w &= \langle \Delta_{32}u_\mu\rangle\langle\mathcal{Q}_R u^\mu\rangle & Q_{10}^w &= \langle \Delta_{32}u_\mu\rangle\langle\{\mathcal{Q}_L, \mathcal{Q}_R\}u^\mu\rangle \\
Q_{11}^w &= \langle \Delta_{32}\{\mathcal{Q}_R, u_\mu\}\rangle\langle\mathcal{Q}_L u^\mu\rangle & Q_{12}^w &= \langle \Delta_{32}\{\mathcal{Q}_R, u_\mu\}\rangle\langle\mathcal{Q}_R u^\mu\rangle \\
Q_{13}^w &= \langle \Delta_{32}\mathcal{Q}_R\rangle\langle u_\mu u^\mu\rangle & Q_{14}^w &= \langle \Delta_{32}\mathcal{Q}_R\rangle\langle u_\mu u^\mu \mathcal{Q}_R\rangle \ .
\end{aligned}
\tag{2.21}
$$

Finally the strong-electromagnetic part, which looks like [20, 23]

$$
\mathcal{L}_{S2E2} = e^2 F_0^2 \sum_{i=1}^{11} K_i Q_i^s \tag{2.22}
$$

with

$$
\begin{aligned}
Q_1^s &= \tfrac{1}{2}\,\langle \mathcal{Q}_\mathrm{L}^2 + \mathcal{Q}_\mathrm{R}^2\rangle\,\langle u_\mu u^\mu\rangle & Q_2^s &= \langle \mathcal{Q}_\mathrm{L}\mathcal{Q}_\mathrm{R}\rangle\,\langle u_\mu u^\mu\rangle \\
Q_3^s &= (\langle \mathcal{Q}_\mathrm{L}u_\mu\rangle\,\langle \mathcal{Q}_\mathrm{L}u^\mu\rangle + \langle \mathcal{Q}_\mathrm{R}u_\mu\rangle\,\langle \mathcal{Q}_\mathrm{R}u^\mu\rangle) & Q_4^s &= \langle \mathcal{Q}_\mathrm{L}u_\mu\rangle\,\langle \mathcal{Q}_\mathrm{R}u^\mu\rangle \\
Q_5^s &= \langle (\mathcal{Q}_\mathrm{L}^2 + \mathcal{Q}_\mathrm{R}^2)\,u_\mu u^\mu\rangle & Q_6^s &= \langle (\mathcal{Q}_\mathrm{L}\mathcal{Q}_\mathrm{R} + \mathcal{Q}_\mathrm{R}\mathcal{Q}_\mathrm{L})\,u_\mu u^\mu\rangle \\
Q_7^s &= \tfrac{1}{2}\,\langle \mathcal{Q}_\mathrm{L}^2 + \mathcal{Q}_\mathrm{R}^2\rangle\,\langle\chi_+\rangle & Q_8^s &= \langle \mathcal{Q}_\mathrm{L}\mathcal{Q}_\mathrm{R}\rangle\,\langle\chi_+\rangle \\
Q_9^s &= \langle (\mathcal{Q}_\mathrm{L}^2 + \mathcal{Q}_\mathrm{R}^2)\chi_+\rangle & Q_{10}^s &= \langle (\mathcal{Q}_\mathrm{L}\mathcal{Q}_\mathrm{R} + \mathcal{Q}_\mathrm{R}\mathcal{Q}_\mathrm{L})\chi_+\rangle \\
Q_{11}^s &= \langle (\mathcal{Q}_\mathrm{R}\mathcal{Q}_\mathrm{L} - \mathcal{Q}_\mathrm{L}\mathcal{Q}_\mathrm{R})\chi_-\rangle \ .
\end{aligned}
\tag{2.23}
$$

The infinities appearing in the loop diagrams are canceled by replacing the coefficients in (2.16), (2.17), (2.20) and (2.22) by the renormalized coefficients and a subtraction part. The infinities needed in the strong sector were calculated first in [3] and those for the weak sector in [5]. The terms are all of the type

$$
X_i = (e^c\mu)^{-2\epsilon}\left(X_i^r + x_i\frac{1}{16\pi^2\epsilon}\right) , \tag{2.24}
$$

with the dimension of space-time $d = 4 - 2\epsilon$ and

$$
c = -\frac{1}{2}\left(\ln(4\pi) + \Gamma'(1) + 1\right) . \tag{2.25}
$$

For $X = L, N, D$ see [10], and for $X = Z, K$ see Table 2.1 [19, 23]. However, since the full e^2p^2-contribution is not included (the explicit photon diagrams

Z_i	z_i	K_i	k_i
1	$17/24 + 3/2\,Z - 3/4\,g_{\rm ewk}$	1	$-3/8$
2	$-1/2 - 8/3\,Z - 1/2\,g_{\rm ewk}$	2	$-1/2\,Z$
3	$-3/8 - 7/2\,Z$	3	$3/8$
4	$3/8 + 7/2\,Z$	4	$-Z$
5	1	5	$9/8$
6	$-7/4 - 5/2\,Z - 3/4\,g_{\rm ewk}$	6	$-3/4\,Z$
7	$-3/4 - 5/2\,Z$	7	0
8	$1/4$	8	$-1/2\,Z$
9	$11/12 - 2/3\,Z - g_{\rm ewk}$	9	$1/8$
10	$3/4 + 1/2\,Z$	10	$-1/8 - 3/4\,Z$
11	$3/4 + Z$	11	$-1/16$
12	$-3/4$		
13	$35/24 + 3/2\,Z - 1/2\,g_{\rm ewk}$		
14	$-3/2 - 15/2\,Z$		

Table 2.1: The coefficients of the subtraction of the infinite parts defined in Eq. (2.24).

are left out), the infinities don't cancel completely. They still provide a number of checks on the calculations though. Since contributions of order e^4 are neglected, Lagrangians allready containing e^2 will not add any explicit photon terms. Therefore the infinities proportional to Z and G_E cancel. Even more, since there are no explicit photon contributions to the decays involving only neutral particles, like $K_L \rightarrow \pi^0\pi^0\pi^0$, the infinities in that channel cancel completely.

2.4 Kinematics

There are five different CP-conserving decays of the type $K \rightarrow 3\pi$:

$$
\begin{aligned}
K_L(k) &\rightarrow \pi^0(p_1)\,\pi^0(p_2)\,\pi^0(p_3)\,, \quad [A^L_{000}]\,,\\
K_L(k) &\rightarrow \pi^+(p_1)\,\pi^-(p_2)\,\pi^0(p_3)\,, \quad [A^L_{+-0}]\,,\\
K_S(k) &\rightarrow \pi^+(p_1)\,\pi^-(p_2)\,\pi^0(p_3)\,, \quad [A^S_{+-0}]\,,\\
K^+(k) &\rightarrow \pi^0(p_1)\,\pi^0(p_2)\,\pi^+(p_3)\,, \quad [A_{00+}]\,,\\
K^+(k) &\rightarrow \pi^+(p_1)\,\pi^+(p_2)\,\pi^-(p_3)\,, \quad [A_{++-}]\,,
\end{aligned}
\tag{2.26}
$$

where we have indicated the four-momentum defined for each particle and the symbol used for the amplitude. The K^- decays are not treated separately since they are counterparts to the K^+ decays.

The kinematics is treated using

$$s_1 = (k - p_1)^2\ , \quad s_2 = (k - p_2)^2\ , \quad s_3 = (k - p_3)^2\ . \tag{2.27}$$

The amplitudes are expanded in terms of the Dalitz plot variables x and y defined as

$$y = \frac{s_3 - s_0}{m_{\pi^+}^2}\,, \quad x = \frac{s_2 - s_1}{m_{\pi^+}^2}\,, \quad s_0 = \frac{1}{3}\left(s_1 + s_2 + s_3\right)\,. \tag{2.28}$$

The amplitudes for $K_L \to \pi^+\pi^-\pi^0, K^+ \to \pi^+\pi^+\pi^-$ and $K^+ \to \pi^0\pi^0\pi^+$ are symmetric under the interchange of the first two pions because of CP or Bose-symmetry. The amplitude for $K_L \to \pi^0\pi^0\pi^0$ is of course symmetric under the interchange of all three final state particles and the one for $K_S \to \pi^+\pi^-\pi^0$ is antisymmetric under the interchange of π^+ and π^- because of CP.

The amplitudes to order four can be written in terms of single variable functions $M_i(s)$ [10] as

$$\begin{aligned}
A^L_{000}(s_1,s_2,s_3) &= M_0(s_1) + M_0(s_2) + M_0(s_3)\,,\\
A^L_{+-0}(s_1,s_2,s_3) &= M_1(s_3) + M_2(s_1) + M_2(s_2) + M_3(s_1)(s_2 - s_3)\\
&\quad +M_3(s_2)(s_1 - s_3)\,,\\
A^S_{+-0}(s_1,s_2,s_3) &= M_4(s_1) - M_4(s_2) + M_5(s_1)(s_2 - s_3) - M_5(s_2)(s_1 - s_3)\\
&\quad +M_6(s_3)(s_1 - s_2)\,,\\
A_{00+}(s_1,s_2,s_3) &= M_7(s_3) + M_8(s_1) + M_8(s_2) + M_9(s_1)(s_2 - s_3)\\
&\quad +M_9(s_2)(s_1 - s_3)\,,\\
A_{++-}(s_1,s_2,s_3) &= M_{10}(s_3) + M_{11}(s_1) + M_{11}(s_2) + M_{12}(s_1)(s_2 - s_3)\\
&\quad +M_{12}(s_2)(s_1 - s_3)\,.
\end{aligned} \tag{2.29}$$

The functions $M_i(s)$ are not unique. The full list of ambiguities can be found in App. A of [10].

2.5 Analytical Results

2.5.1 Lowest Order

The two diagrams that contribute to lowest order can be seen in Fig.2.1.

One of the problems in expressing the amplitudes is the various possible choices of masses to express the isospin conserving piece in. The simplest expressions usually follow when using a mixture of the neutral and charged masses and in the part that is obviously isospin violating we can use the neutral and charged masses interchangeably, denoted by m_K^2 and m_π^2.

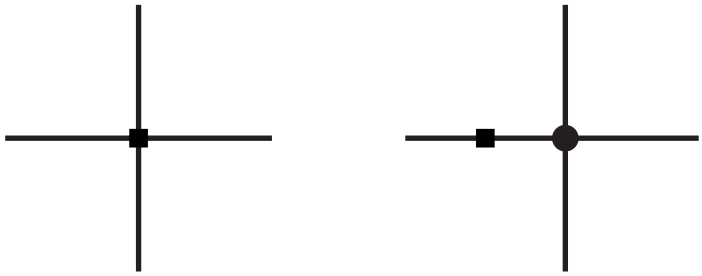

Figure 2.1: The tree level diagrams for $K \to 3\pi$. A filled square is a vertex from $\mathcal{L}_{W2}$ or $\mathcal{L}_{E2}(\Delta S = 1)$ and a filled circle from $\mathcal{L}_{S2}$ or $\mathcal{L}_{E2}(\Delta S = 0)$.

The simplest expressions for the lowest order we have found are

$$M_0(s)|_{p^2} = i\,\frac{C\,F_0^4}{F_\pi^3\,F_K}\,(G_8 - G_{27})\,\frac{1}{3}\,m_{K^0}^2\,\left(1+\sqrt{3}\,\sin\epsilon\right)\,. \tag{2.30}$$

$$\begin{aligned}
M_1(s)|_{p^2} &= i\frac{CF_0^4}{F_\pi^3 F_K}\Bigg\{(G_8 - G_{27})\,\frac{1}{3}m_{K^0}^2 + \frac{\sin\epsilon}{\sqrt{3}}\left(G_8 - \frac{13}{3}G_{27}\right)m_K^2\\
&\quad + Ze^2F_0^2\left(\frac{4}{3}G_8 + \frac{G_{27}}{3}\frac{6m_K^2 - 16m_\pi^2}{m_K^2 - m_\pi^2}\right)\Bigg\}\,,\\
M_2(s)|_{p^2} &= 0\,,\\
M_3(s)|_{p^2} &= i\frac{CF_0^4}{F_\pi^3 F_K}\Bigg\{-\frac{G_8}{3} + G_{27}\left(-\frac{1}{2} + \frac{1}{3}\frac{m_{\pi^+}^2}{m_{K^+}^2 - m_{\pi^+}^2} + \frac{1}{2}\frac{m_{\pi^0}^2}{m_{K^0}^2 - m_{\pi^0}^2}\right)\\
&\quad + \frac{\sin\epsilon}{\sqrt{3}}\left(-2G_8 + \frac{17}{6}G_{27}\frac{m_K^2}{m_K^2 - m_\pi^2}\right)\\
&\quad + \left(Z\,G_8 + \frac{1}{2}G_E\right)\frac{e^2F_0^2}{m_K^2 - m_\pi^2}\Bigg\}.
\end{aligned} \tag{2.31}$$

$$\begin{aligned}
M_4(s)|_{p^2} &= 0\,,\\
M_5(s)|_{p^2} &= 0\,,\\
M_6(s)|_{p^2} &= i\frac{CF_0^4}{F_\pi^3 F_K}\Bigg\{G_{27}\left(-\frac{5}{2} - \frac{1}{3}\frac{m_{\pi^+}^2}{m_{K^+}^2 - m_{\pi^+}^2} - \frac{1}{2}\frac{m_{\pi^0}^2}{m_{K^0}^2 - m_{\pi^0}^2}\right)
\end{aligned}$$

$$
\begin{aligned}
&+\frac{\sin\epsilon}{\sqrt{3}}\left(-G_8+\frac{G_{27}}{2}\frac{7m_K^2-6m_\pi^2}{m_K^2-m_\pi^2}\right)\\
&+\left(-Z\,G_8-\frac{1}{2}G_E\right)\frac{e^2F_0^2}{m_K^2-m_\pi^2}\Bigg\}\,.
\end{aligned}
\tag{2.32}
$$

This is in the isospin limit the same as (31) in [10] using Eq. (A.9) there.

$$
\begin{aligned}
M_7(s)|_{p^2} &= i\frac{CF_0^4}{F_\pi^3F_K}\Bigg\{\left(-\frac{1}{3}G_8-\frac{2}{9}G_{27}\right)m_{K^+}^2-\frac{10}{3}\frac{\sin\epsilon}{\sqrt{3}}m_K^2G_{27}\\
&\quad+Ze^2F_0^2\left(-\frac{8}{3}G_8+\frac{G_{27}}{9}\frac{-46m_K^2+16m_\pi^2}{m_K^2-m_\pi^2}\right)-G_Ee^2F_0^2\Bigg\}\,,\\
M_8(s)|_{p^2} &= 0\,,\\
M_9(s)|_{p^2} &= i\frac{CF_0^4}{F_\pi^3F_K}\Bigg\{\frac{G_8}{3}+G_{27}\left(\frac{19}{18}+\frac{1}{3}\frac{m_{\pi^+}^2}{m_{K^+}^2-m_{\pi^+}^2}+\frac{1}{2}\frac{m_{\pi^0}^2}{m_{K^0}^2-m_{\pi^0}^2}\right)\\
&\quad+\frac{\sin\epsilon}{\sqrt{3}}\left(G_8+\frac{G_{27}}{3}\frac{7m_K^2-6m_\pi^2}{m_K^2-m_\pi^2}\right)\\
&\quad+\left(Z\,G_8+\frac{1}{2}G_E\right)\frac{e^2F_0^2}{m_K^2-m_\pi^2}\Bigg\}\,.
\end{aligned}
\tag{2.33}
$$

This can be brought into the form of (32) of [10] using the equivalents of (A.3-A.5) there.

$$
\begin{aligned}
M_{10}(s)|_{p^2} &= i\frac{CF_0^4}{F_\pi^3F_K}\Bigg\{G_8\left(s-m_{K^+}^2-m_{\pi^+}^2\right)+G_{27}\left(-\frac{13}{3}s+m_{K^+}^2+\frac{13}{3}m_{\pi^+}^2\right)\\
&\quad-8Ze^2F_0^2\,G_8-\frac{16}{3}Ze^2F_0^2\,G_{27}-2\,G_Ee^2F_0^2\Bigg\}\,,\\
M_{11}(s)|_{p^2} &= 0\,,\\
M_{12}(s)|_{p^2} &= 0\,.
\end{aligned}
\tag{2.34}
$$

Here F_π and F_K are the pion and kaon decay constants respectively.

The terms proportional to G_E are published before in [11] and, after sorting out some misprints there, the results fully agree.

2.5.2 Next-to-leading Order

The results at next-to-leading order are a lot longer, and we decided to not include them all explicitely. A_{000}^L is however the full first order isospin breaking

$\tilde{K}_1$	$G_8\left(N_5^r - 2N_7^r + 2N_8^r + N_9^r\right) + G_{27}\left(-\frac{1}{2}D_6^r\right)$
$\tilde{K}_2$	$G_8\left(N_1^r + N_2^r\right) + G_{27}\left(\frac{1}{3}D_{26}^r - \frac{4}{3}D_{28}^r\right)$
$\tilde{K}_3$	$G_8\left(N_3^r\right) + G_{27}\left(\frac{2}{3}D_{27}^r + \frac{2}{3}D_{28}^r\right)$
$\tilde{K}_4$	$G_{27}\left(D_4^r - D_5^r + 4D_7^r\right)$
$\tilde{K}_5$	$G_{27}\left(D_{30}^r + D_{31}^r + 2D_{28}^r\right)$
$\tilde{K}_6$	$G_{27}\left(8D_{28}^r - D_{29}^r + D_{30}^r\right)$
$\tilde{K}_7$	$G_{27}\left(-4D_{28}^r + D_{29}^r\right)$
$\tilde{K}_8$	$G_8\left(2N_5^r + 4N_7^r + N_8^r - 2N_{10}^r - 4N_{11}^r - 2N_{12}^r\right) + G_{27}\left(-\frac{2}{3}D_1^r + \frac{2}{3}D_6^r\right)$
$\tilde{K}_9$	$G_8\left(N_5^r + N_8^r + N_9^r\right) + G_{27}\left(-\frac{1}{6}D_6^r\right)$
$\tilde{K}_{10}$	$G_{27}\left(2D_2^r - 2D_4^r - D_7^r\right)$
$\tilde{K}_{11}$	$G_{27}\left(D_7^r\right)$

Table 2.2: The independent linear combinations of the N_i^r and D_i^r that appear in the isospin invariant amplitudes.

amplitude (no explicit photon diagrams contribute) and we therefore present it in App. 2.A. The expressions for the remaining amplitudes are available on request from the authors or can be downloaded [24].

The diagrams contributing are the same as in [10], see figure there. Note however that vertices from $\mathcal{L}_{W4}$ can now also be from $\mathcal{L}_{W2E2}$, $\mathcal{L}_{S4}$ also from $\mathcal{L}_{S2E2}$ and vertices from $\mathcal{L}_{S2}$ or $\mathcal{L}_{W2}$ also from $\mathcal{L}_{E2}$.

The amplitudes at next-to-leading order can in principle include all the parameters from $\mathcal{L}_{W4}$, $\mathcal{L}_{S4}$, $\mathcal{L}_{W2E2}$ and $\mathcal{L}_{S2E2}$. The coefficients from the strong and electromagnetic Lagrangians are treated as known, which leaves G_8,G_{27},$N_1^r,\ldots,N_{13}^r$, D_1^r,D_2^r,$D_4^r,\ldots,D_7^r$, $D_{26}^r,\ldots,D_{31}^r$ and $Z_1^r,\ldots,Z_{14}^r$ as unknown. In total 41 undetermined parameters. However, all of these don't have to be independent in the sense that they multiply the same type of term, eg. m_K^4 or $e^2m_\pi^2$. It turns out that there are 30 independent combinations, denoted by $\tilde{K}_1\ldots\tilde{K}_{30}$. See Table 2.2 for the ones already present in the isospin limit [10] and Table 2.3 for the new isospin breaking combinations. $\tilde{K}_{12}$ to $\tilde{K}_{19}$ multiply terms including $\sin\epsilon$, $\tilde{K}_{20}$ to $\tilde{K}_{28}$ terms including e^2 and $\tilde{K}_{29}$ and $\tilde{K}_{30}$ terms including Ze^2.

The results proportional to G_E at next-to-leading order are also published in [11] and, after sorting out some misprints there, the results fully agree.

The corrections to the masses and decay constants including strong isospin breaking were also recalculated, and they were found to agree with the known results, see [20, 23] and references therein.

$\tilde{K}_{12}$	$G_8\,(3\,N_6^r - 4\,N_9^r - 5\,N_{10}^r - 6\,N_{11}^r - 7\,N_{12}^r - 6\,N_{13}^r)$
	$+G_{27}\,(23/3\,D_1^r - 5/3\,D_6^r)$
$\tilde{K}_{13}$	$G_{27}\,(10/3\,D_1^r - 11/12\,D_6^r)$
$\tilde{K}_{14}$	$G_{27}\,(5\,D_{27}^r + 5/2\,D_{31}^r)$
$\tilde{K}_{15}$	$G_{27}\,(-2/3\,D_{26}^r - 8/3\,D_{27}^r)$
$\tilde{K}_{16}$	$G_8\,(2\,N_9^r + 3\,N_{10}^r + 4\,N_{11}^r + N_{12}^r)$
	$+G_{27}\,(D_1^r - 1/3\,D_6^r)$
$\tilde{K}_{17}$	$G_{27}\,(D_6^r)$
$\tilde{K}_{18}$	$G_8\,(9/2\,N_4^r) + G_{27}\,(-2\,D_{26}^r - 6\,D_{27}^r + D_{31}^r)$
$\tilde{K}_{19}$	$G_8\,(3/2\,N_2^r) + G_{27}\,(3/2\,D_{26}^r + 4\,D_{27}^r - D_{31}^r)$
$\tilde{K}_{20}$	$G_8\,(-3\,Z_2^r + 2\,Z_3^r - 18/5\,Z_4^r + 3/4\,Z_5^r + 1/2\,Z_6^r + 1/2\,Z_7^r$
	$+3/4\,Z_8^r + 3/4\,Z_9^r + 1/2\,Z_{10}^r + 7/10\,Z_{11}^r + 7/10\,Z_{12}^r)$
$\tilde{K}_{21}$	$G_8\,(2\,Z_8^r + 2/3\,Z_{10}^r + 2/3\,Z_{11}^r - 2\,Z_{12}^r)$
$\tilde{K}_{22}$	$G_8\,(2\,Z_6^r + 2\,Z_8^r + 2\,Z_9^r + 4/3\,Z_{10}^r + 2/3\,Z_{11}^r$
	$+2/3\,Z_{12}^r + 2\,Z_{13}^r + 1/3\,Z_{14}^r)$
$\tilde{K}_{23}$	$G_8\,(Z_{12}^r)$
$\tilde{K}_{24}$	$G_8\,(Z_7^r + 3\,Z_8^r + Z_{10}^r + 3\,Z_{11}^r - Z_{12}^r)$
$\tilde{K}_{25}$	$G_8\,(-4\,Z_1^r - 2\,Z_2^r - 4/3\,Z_3^r + 4\,Z_4^r - 3/2\,Z_5^r + Z_6^r$
	$-Z_7^r + 1/2\,Z_8^r + 1/2\,Z_9^r + 1/3\,Z_{10}^r - 1/3\,Z_{11}^r - 1/3\,Z_{12}^r)$
$\tilde{K}_{26}$	$G_8\,(-12/5\,Z_4^r + 3/2\,Z_5^r - Z_6^r + Z_7^r - 3/2\,Z_8^r$
	$-3/2\,Z_9^r - Z_{10}^r - 1/5\,Z_{11}^r - 1/5\,Z_{12}^r)$
$\tilde{K}_{27}$	$G_8\,(8/5\,Z_4^r + 4/5\,Z_{11}^r + 4/5\,Z_{12}^r)$
$\tilde{K}_{28}$	$G_8\,(Z_3^r + Z_6^r + 3/2\,Z_8^r + 3/2\,Z_9^r + Z_{10}^r + 1/2\,Z_{11}^r + 1/2\,Z_{12}^r)$
$\tilde{K}_{29}$	$G_8\,(3\,N_{10}^r + 4\,N_{11}^r + N_{12}^r)$
	$+G_{27}\,(D_1^r + 2/3\,D_5^r - 1/3\,D_6^r)$
$\tilde{K}_{30}$	$G_8\,(8/3\,N_{11}^r + 8/3\,N_{12}^r) + G_{27}\,(16/9\,D_5^r + 4/9\,D_6^r)$

Table 2.3: The new independent linear combinations of the N_i^r, D_i^r and Z_i^r that appear in the isospin breaking amplitudes.

2.6 Numerical Results

2.6.1 Experimental Data and Fit

A full isospin limit fit was made in [10] taking into account all data published before May 2002. One of the reasons for this investigation of isospin breaking effects is to see whether isospin violation can solve the discrepancies in the quadratic slope parameters found there. A new full fit will be done after all the electromagnetic contributions have been included in the amplitudes (work in progress). The data from ISTRA+ [25] and KLOE [26], which appeared

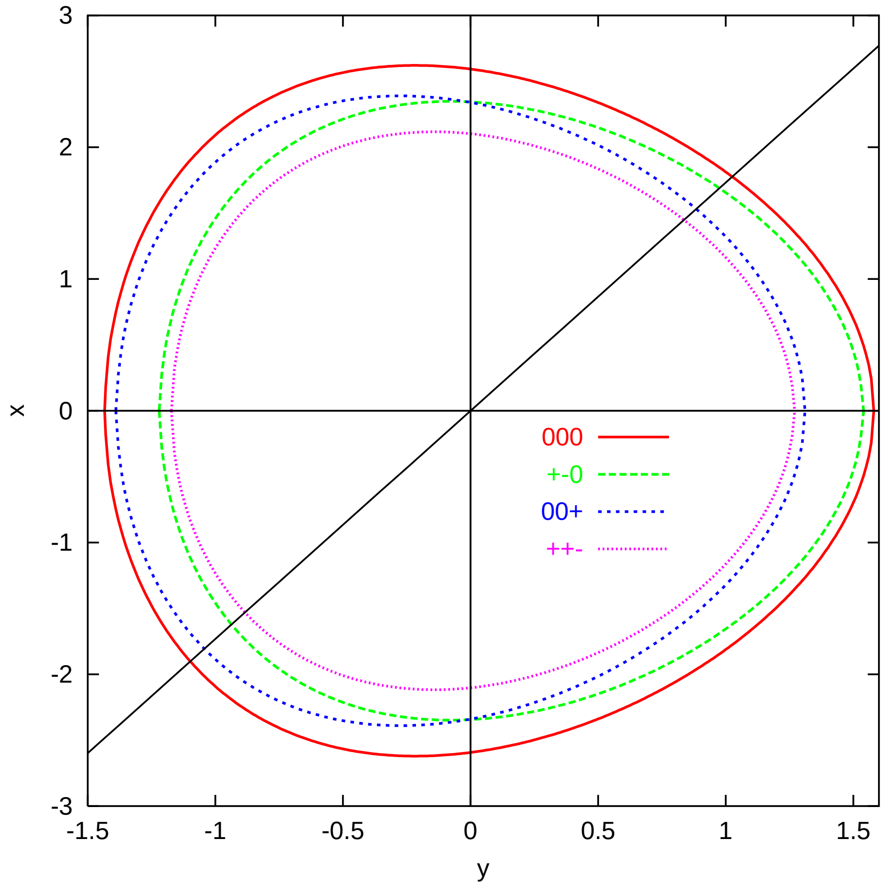

Figure 2.2: The phase space boundaries for the five different decays and the curves along which we will compare the amplitudes.

after [10], will then also be taken into account.

2.6.2 Results With and Without Strong Isospin Breaking

Our main result is the comparison between the amplitudes in the isospin limit and including first order strong isospin breaking. In Fig. 2.2 we show the phase space boundaries for the five different decays and the three curves along which we will show results for the squared amplitudes with and without first order

G_8	5.45	$L_1^r \cdot 10^3$	0.38	$\tilde{K}_1$	0
G_{27}	0.392	$L_2^r \cdot 10^3$	1.59	$\tilde{K}_2/G_8$	$5.19 \cdot 10^{-2}$
G_E	-0.4	$L_3^r \cdot 10^3$	-2.91	$\tilde{K}_3/G_8$	$3.77 \cdot 10^{-3}$
$\delta_2 - \delta_0$	-0.576	$L_4^r \cdot 10^3$	0	$\tilde{K}_4$	0
$\sin\epsilon$	$1.19 \cdot 10^{-2}$	$L_5^r \cdot 10^3$	1.46	$\tilde{K}_5/G_{27}$	$-4.25 \cdot 10^{-2}$
Z	0.805	$L_6^r \cdot 10^3$	0	$\tilde{K}_6/G_{27}$	$-1.66 \cdot 10^{-1}$
μ	0.77 GeV	$L_7^r \cdot 10^3$	-0.49	$\tilde{K}_7/G_{27}$	$1.20 \cdot 10^{-1}$
F_π	0.0924 GeV	$L_8^r \cdot 10^3$	1.0	$\tilde{K}_8 \ldots \tilde{K}_{11}$	0
F_K	0.113 GeV	$K_1 \ldots K_{11}$	0	$\tilde{K}_{12} \ldots \tilde{K}_{30}$	0

Table 2.4: The various input values used.

strong isospin breaking. The three curves are $x = 0$, $y = 0$ and $x = \sqrt{3}\,y$. In Fig. 2.3 to Fig. 2.7 we then plot the different squared amplitudes along these curves as a function of r, where $r = \pm\sqrt{y^2 + \frac{x^2}{3}}$ and the sign is chosen in the natural way,

$$r = \begin{cases} y, & x = 0 \\ x/\sqrt{3}, & y = 0 \\ y\,\sqrt{2}, & x = y\,\sqrt{3}\,. \end{cases} \tag{2.35}$$

Note that for all but A^S_{+-0} the squared amplitudes are normalized to their value at the center of the Dalitz plot. A comparison of the central values themselves is shown in Table 2.5 together with the decay rates integrated over the Dalitz region. In Fig. 2.3 one can clearly see the thresholds introduced by the difference between $m^2_{\pi^+}$ and $m^2_{\pi^0}$ induced by the breaking of strong isospin invariance. These thresholds correspond to a new process being allowed where two of the neutral pions are produced through an intermediate on shell state with one positive and one negative pion.

The input values used to get the results can be seen in Table 2.4. L_1^r to L_8^r come from a one-loop fit in [17], G_8, G_{27}, $\delta_2 - \delta_0$ and $\tilde{K}_1$ to $\tilde{K}_{11}$ from the isospin limit fit in [10], G_E from [27] and $\sin\epsilon$ from [17]. For Z we use the estimate

$$Z = \frac{1}{2\,F_\pi^2\,e^2}\,(m^2_{\pi^+} - m^2_{\pi^0}), \tag{2.36}$$

which corresponds to the value in Table 2.4. As usual, μ is chosen to be 0.77 GeV.

Very little knowledge exists of the values of $K_1 \ldots K_{11}$ and $\tilde{K}_{12} \ldots \tilde{K}_{30}$, so they are set equal to zero (tests were also made assigning order of magnitude estimates to them).

There are various ways to treat the masses, especially in the isospin limit case. In [10] the masses used in the phase space were the physical masses

	Centralvalue		Decay Rate	
	Iso limit [10]	Str iso-br	Iso limit [10]	Str iso-br
$K_L \to \pi^0\pi^0\pi^0$	$6.74 \cdot 10^{-12}$	$6.97 \cdot 10^{-12}$	$2.65 \cdot 10^{-18}$	$2.74 \cdot 10^{-18}$
$K_L \to \pi^+\pi^-\pi^0$	$7.46 \cdot 10^{-13}$	$7.66 \cdot 10^{-13}$	$1.63 \cdot 10^{-18}$	$1.67 \cdot 10^{-18}$
$K_S \to \pi^+\pi^-\pi^0$	0	0	$3.1 \cdot 10^{-21}$	$3.2 \cdot 10^{-21}$
$K^+ \to \pi^0\pi^0\pi^+$	$9.33 \cdot 10^{-13}$	$1.01 \cdot 10^{-12}$	$9.11 \cdot 10^{-19}$	$9.84 \cdot 10^{-19}$
$K^+ \to \pi^+\pi^+\pi^-$	$3.72 \cdot 10^{-12}$	$4.00 \cdot 10^{-12}$	$2.97 \cdot 10^{-18}$	$3.19 \cdot 10^{-18}$

Table 2.5: Comparison of the central values of the amplitudes squared and the decay rates.

occuring in the decays. However in the amplitudes the physical kaon mass of the kaon involved in the process was used and the pion mass was given by $m_\pi^2 = \frac{1}{3}\sum_{i=1,3} m_{\pi^i}^2$ with $i = 1, 2, 3$ being the three pions participating in the reaction. This allowed for the correct kinematical relation $s_1 + s_2 + s_3 = m_K^2 + 3m_\pi^2$ to be satisfied while having the isospin limit in the amplitude but the physical masses in the phase space. The results presented used the Gell-Mann-Okubo (GMO) relation for the eta mass in the loops. Results with the physical eta mass gave small changes within the general errors given in [10]. In the present isospin breaking calculation all the pion and kaon masses were used correctly in the amplitude, but for the eta we again use the GMO relation, but now including isospin breaking,

$$m_\eta^2 = \frac{2}{3}\,(m_{K^+}^2 + m_{K^0}^2 - m_{\pi^+}^2) + \frac{1}{3}\,m_{\pi^0}^2\,. \tag{2.37}$$

The possible lowest order contributions from the eta mass have been removed from the amplitudes using the corresponding next-to-leading order relation.

Here follows a discussion of the results in somewhat more detail. In general the results are of a size as can be expected from this type of isospin breaking. They are of order a few, up to 5% in the amplitudes. The isospin breaking corrections tend to increase all decay rates somewhat but this can be compensated by small changes in the values of the fitted $\tilde{K}_i$ compared to the results of [10]. The number of significant digits quoted in Table 2.5 is higher than the expected precision of our results, but the trend and the general size of the change compared to the isospin conserving results are stable with respect to variations in dealing with the eta mass (physical or GMO).

For $K_L \to \pi^0\pi^0\pi^0$ the central value of the amplitude squared increases by about 3%. The change in the quadratic slope is similar but the total variation over the Dalitz plot is small so the total decay rate increases by about 3% as well. This decay is the one which has most variation in the amplitude when changing how one deals with the eta mass. The extreme case we have found was

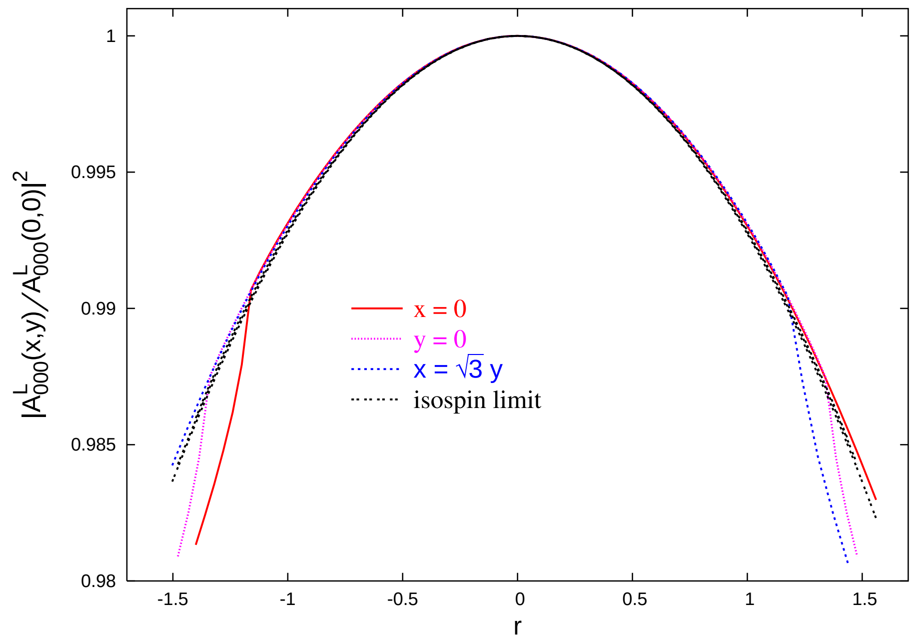

Figure 2.3: Comparison of $K_L \to \pi^0\pi^0\pi^0$ with and without strong isospin breaking.

that this effect completely cancelled the change from isospin violation. For this decay the amplitude as presented in the paper is also the final one. There are no contributions from loops with photons for this decay. It will only be indirectly affected when the $\tilde{K}_i$ are determined from the decays involving charged particles which do have contributions from loops and tree level diagrams with photons. Note the scale in Fig. 2.3 when viewing the result.

The squared amplitude $K_L \to \pi^+\pi^-\pi^0$ increases by about 2.5% with very little variation with the eta mass treatment. The decay rate increases by the same amount. The changes in the Dalitz plot slopes are similar as can be judged from Fig. 2.4.

For the decay $K_S \to \pi^+\pi^-\pi^0$ the amplitude in the center of the Dalitz plot vanishes because of the symmetries. The amplitude and the slopes increase by about 3% as can be seen in Fig. 2.5.

The decay $K^+ \to \pi^0\pi^0\pi^+$ has the largest increase. The squared amplitude in the center changes by about 11%. The linear slopes decrease somewhat leading to an increase of about 8% to the total decay rate when compared with the

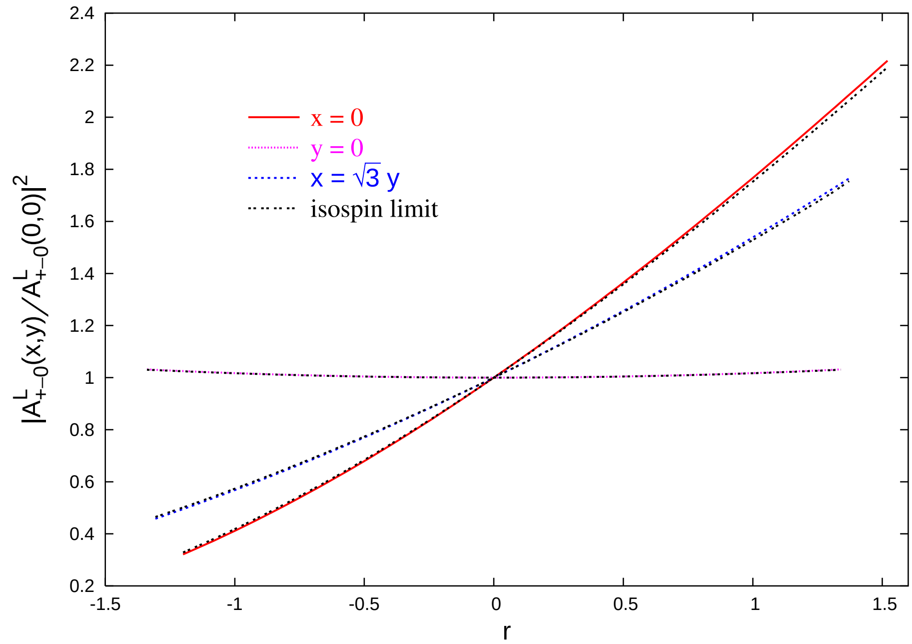

Figure 2.4: Comparison of $K_L \to \pi^+\pi^-\pi^0$ with and without strong isospin breaking.

isospin conserved case.

The decay $K^+ \to \pi^+\pi^+\pi^-$ has a change of about 7.5% upwards in the center of the Dalitz plot and a similar change in the decay rate. The slopes decrease somewhat.

The conclusions above do not seem to change qualitatively when we give the K_i^r a value of about 0.001 and the extra $\tilde{K}_i$ a value relative to G_8 and G_{27} of 0.01. However the changes induced by these values can be of the order of 10%, largest for $K_L \to \pi^0\pi^0\pi^0$.

It should be noted that the mentioned changes are with the values of $\tilde{K}_i$ determined using the isospin conserving fit. A new determination including isospin breaking effects is planned when the diagrams with photon propagators, both at tree level and one-loop level, have been taken into account. At present most of the changes found can probably be compensated by changes in the $\tilde{K}_i$.

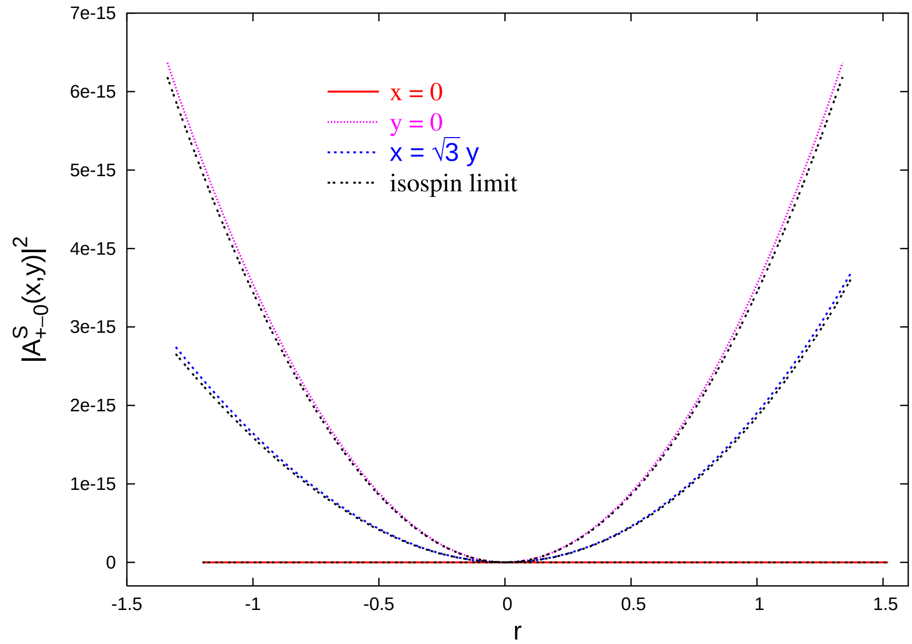

Figure 2.5: Comparison of $K_S \to \pi^+\pi^-\pi^0$ with and without strong isospin breaking.

2.7 Conclusions

We have calculated the $K \to 3\pi$ amplitudes to next-to-leading order (p^4, $p^2\,m^2$, m^4, $p^2\,e^2$) in Chiral Perturbation Theory. A similar calculation was done in [10] in the isospin limit, but we have now included strong isospin breaking ($m_u \neq m_d$) and local electromagnetic isospin breaking in the amplitudes . This was done partly because it is interesting in general to see the possible importance of isospin breaking in this process, but also to investigate whether isospin violation will improve the fit to experimental data. Discrepancies between data and the quadratic slopes from CHPT were found in [10], and isospin breaking may be the cause of this.

We have tried to estimate the effects of the breaking by comparing the squared amplitudes with and without isospin violation. The effect seems to be at a few percent level, and probably not quite enough to solve the dicrepancies. However, to really investigate this a new full fit has to be done also including the explicit photon diagrams and the new data [25,26] published after [10]. This

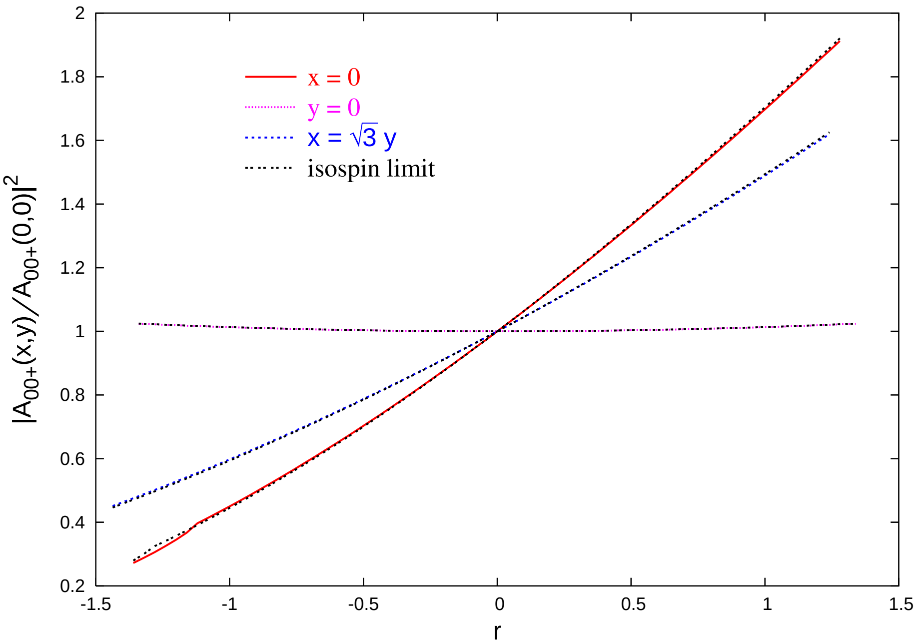

Figure 2.6: Comparison of $K^+ \to \pi^0\pi^0\pi^+$ with and without strong isospin breaking.

is work in progress and will be presented in the future papers Isospin Breaking in $K \to 3\pi$ Decays II and III.

Acknowledgments

The program FORM 3.0 has been used extensively in these calculations [28]. This work is supported in part by the Swedish Research Council and European Union TMR network, Contract No. HPRN-CT-2002-00311 (EURIDICE).

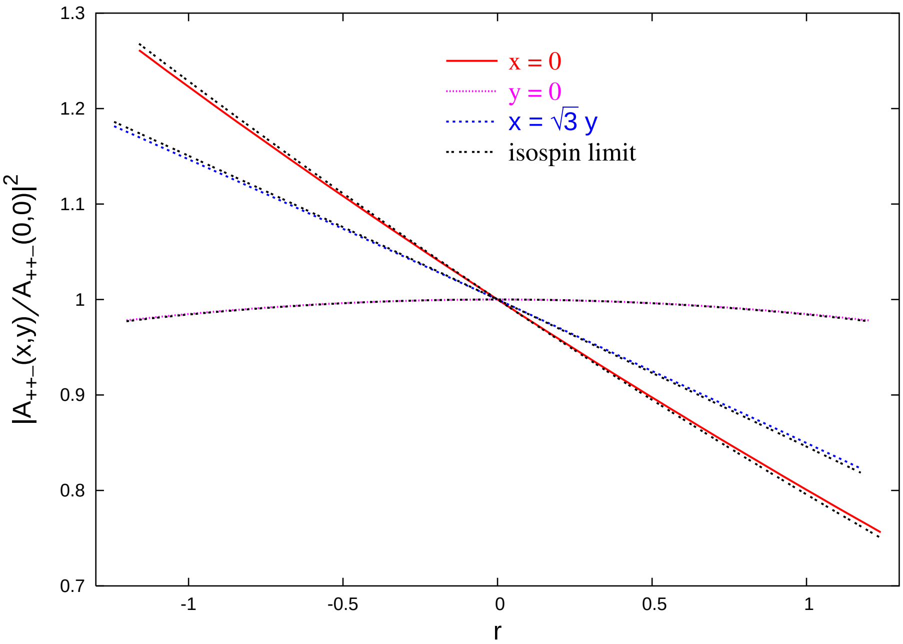

Figure 2.7: Comparison of $K^+ \to \pi^+\pi^+\pi^-$ with and without strong isospin breaking.

2.A The Amplitude for $K_L \to \pi^0\pi^0\pi^0$.

We divide the $M_0(s)$ function defined in Eq. (2.29) as

$$\begin{aligned} M_0(s) &= M_0(s)|_{p^2} + i\frac{CF_0^4}{F_\pi^3 F_K}\left\{\frac{G_8}{F_\pi^2}M_0^{8,F}(s) + \frac{G_8}{F_\pi^2}\frac{\sin\epsilon}{\sqrt{3}}M_0^{8,\epsilon}(s)\right. \\ &+ G_8\, e^2 M_0^{8,e}(s) + \frac{G_8'}{F_\pi^2}M_0^{8\prime}(s) + \frac{G_{27}}{F_\pi^2}M_0^{27,F}(s) + \frac{G_{27}}{F_\pi^2}\frac{\sin\epsilon}{\sqrt{3}}M_0^{27,\epsilon}(s) \\ &+ \left. G_{27}\, e^2 M_0^{27,e}(s)\right\}\,. \end{aligned} \tag{A.1}$$

The effect of G_8' cannot be distinguished from higher order coefficients in decays not involving external fields. This was known at tree level earlier and has been proven to one-loop in [5]. This means that terms proportinal to G_8' are effectively removed.

We have extensively used the first order isospin broken GMO relation,

$$m_\eta^2 = \frac{2}{3}\,(m_{K^+}^2 + m_{K^0}^2 - m_{\pi^+}^2) + \frac{1}{3}\,m_{\pi^0}^2\,, \tag{A.2}$$

in writing the amplitude in the form below.

The explicit expressions for $\overline{A}$, $\overline{B}$ and $\overline{B}_1$, the finite part of the loop functions, can be found in many places, e.g. [29].

The octet ones are:

$$
\begin{aligned}
&M_0^{8,F}(s) = \\
&\quad \Big(2\,L_1^r + 2\,L_2^r + L_3^r\Big)\Big(-8\,m_{\pi^0}^4 - 8/3\,m_{K^0}^4 + 8\,s^2\Big) \\
&\quad +\Big(4\,L_4^r + L_5^r\Big)\Big(-8/3\,m_{\pi^0}^2\,m_{K^0}^2\Big) \\
&\quad +\Big(N_1^r + N_2^r + 2\,N_3^r\Big)\Big(m_{\pi^0}^4 + 1/3\,m_{K^0}^4 - s^2\Big) \\
&\quad +N_5^r\Big(10/3\,m_{\pi^0}^2\,m_{K^0}^2 + 2/3\,m_{K^0}^4\Big) \\
&\quad +N_7^r\Big(4\,m_{\pi^0}^2\,m_{K^0}^2 - 4/3\,m_{K^0}^4\Big) + N_8^r\Big(10/3\,m_{\pi^0}^2\,m_{K^0}^2 + 4/3\,m_{K^0}^4\Big) \\
&\quad +N_9^r\Big(-2/3\,m_{\pi^0}^2\,m_{K^0}^2 + 2/3\,m_{K^0}^4\Big) + \Big(N_{10}^r + 2\,N_{11}^r + N_{12}^r\Big)\Big(-4\,m_{\pi^0}^2\,m_{K^0}^2\Big) \\
&\quad +\Big(\overline{A}(m_{K^0}^2) - \overline{A}(m_{K^+}^2)\Big)\left(\frac{1/4\,m_\pi^4}{m_\pi^2 - m_K^2}\right) \\
&\quad +\overline{A}(m_{\pi^+}^2)\Big(1/4\,m_{\pi^0}^2 - 1/2\,m_{K^0}^2\Big) + \overline{A}(m_{\pi^0}^2)\Big(17/24\,m_{K^0}^2\Big) \\
&\quad +\overline{A}(m_{K^+}^2)\Big(5/36\,m_{\pi^0}^2 + 25/36\,m_{K^0}^2\Big) + \overline{A}(m_{K^0}^2)\Big(-7/18\,m_{\pi^0}^2 - 1/36\,m_{K^0}^2\Big) \\
&\quad +\Big(\overline{A}(m_{K^0}^2) - \overline{A}(m_{K^+}^2)\Big)\Big(5/36\,m_\pi^2 + 5/18\,m_K^2\Big) + \overline{A}(m_\eta^2)\Big(1/8\,m_{K^0}^2\Big) \\
&\quad +\overline{B}(m_{\pi^+}^2, m_{\pi^+}^2, s)\Big(-2\,m_{\pi^0}^2\,s + m_{\pi^0}^4 + s^2\Big) + \overline{B}(m_{\pi^+}^2, m_{K^+}^2, s)\Big(5/4\,m_{\pi^0}^2\,m_{K^0}^2 \\
&\qquad -5/4\,m_{\pi^0}^2\,s - 1/2\,m_{K^0}^2\,s - 1/4\,m_{K^0}^4 + 3/4\,s^2\Big) \\
&\quad +\overline{B}(m_{\pi^0}^2, m_{\pi^0}^2, s)\Big(1/2\,m_{\pi^0}^2\,m_{K^0}^2\Big) \\
&\quad +\overline{B}(m_{\pi^0}^2, m_{K^0}^2, s)\Big(3/8\,m_{\pi^0}^2\,m_{K^0}^2 - 1/8\,m_{K^0}^2\,s + 1/8\,m_{K^0}^4\Big) \\
&\quad +\overline{B}(m_{K^+}^2, m_{K^+}^2, s)\Big(1/4\,m_{\pi^0}^2\,s + 1/4\,m_{K^0}^2\,s - 1/4\,s^2\Big) \\
&\quad +\overline{B}(m_{K^0}^2, m_\eta^2, s)\Big(1/24\,m_{\pi^0}^2\,m_{K^0}^2 + 1/8\,m_{K^0}^2\,s - 5/24\,m_{K^0}^4\Big) \\
&\quad +\overline{B}(m_\eta^2, m_\eta^2, s)\Big(1/18\,m_{\pi^0}^2\,m_{K^0}^2\Big) \\
&\quad +\overline{B}_1(m_{\pi^+}^2, m_{K^+}^2, s)\Big(-1/2\,m_{\pi^0}^2\,m_{K^0}^2 + 1/2\,m_{\pi^0}^4\Big)
\end{aligned}
$$

$$+\overline{B}_1(m_{\pi^0}^2, m_{K^0}^2, s)\Big(-1/4\,m_{\pi^0}^2\,m_{K^0}^2+1/4\,m_{K^0}^4\Big)$$
$$+\overline{B}_1(m_{K^0}^2, m_\eta^2, s)\Big(-1/4\,m_{\pi^0}^2\,m_{K^0}^2+1/4\,m_{K^0}^4\Big)$$

(A.3)

$$M_0^{8,\epsilon}(s)=$$
$$\Big(2\,L_1^r+2\,L_2^r+L_3^r\Big)\Big(-8\,m_\pi^4-8/3\,m_K^4+8\,s^2\Big)+L_4^r\Big(-32/3\,m_\pi^2\,m_K^2\Big)$$
$$+L_5^r\Big(-40/3\,m_\pi^2\,m_K^2+16/3\,m_K^4\Big)+L_7^r\Big(480\,m_\pi^2\,m_K^2-352\,m_K^4\Big)$$
$$+L_8^r\Big(224\,m_\pi^2\,m_K^2-160\,m_K^4\Big)$$
$$+\Big(N_1^r+N_2^r-2\,N_3^r+6\,N_4^r\Big)\Big(-m_\pi^4-1/3\,m_K^4+s^2\Big)$$
$$+N_5^r\Big(-26/3\,m_\pi^2\,m_K^2+10\,m_K^4\Big)$$
$$+N_6^r\Big(-48\,m_\pi^2\,m_K^2+40\,m_K^4\Big)+N_7^r\Big(4\,m_\pi^2\,m_K^2-4/3\,m_K^4\Big)$$
$$+N_8^r\Big(22/3\,m_\pi^2\,m_K^2+4/3\,m_K^4\Big)+N_9^r\Big(10/3\,m_\pi^2\,m_K^2-10/3\,m_K^4\Big)$$
$$+N_{10}^r\Big(20\,m_\pi^2\,m_K^2-16\,m_K^4\Big)+N_{11}^r\Big(-8\,m_\pi^2\,m_K^2\Big)$$
$$+N_{12}^r\Big(68\,m_\pi^2\,m_K^2-64\,m_K^4\Big)+N_{13}^r\Big(96\,m_\pi^2\,m_K^2-80\,m_K^4\Big)$$
$$+\frac{1}{m_\pi^2-m_K^2}\Big(\overline{A}(m_\pi^2)-\overline{A}(m_K^2)\Big)\Big(m_\pi^4\Big)+\overline{A}(m_\pi^2)\Big(-m_\pi^2+13/8\,m_K^2\Big)$$
$$+\overline{A}(m_K^2)\Big(m_\pi^2+3/4\,m_K^2\Big)+\overline{A}(m_\eta^2)\Big(5/8\,m_K^2\Big)$$
$$+\overline{B}(m_\pi^2, m_\pi^2, s)\Big(5/2\,m_\pi^2\,m_K^2-12\,m_\pi^2\,s+6\,m_\pi^4-m_K^2\,s+6\,s^2\Big)$$
$$+\overline{B}(m_\pi^2, m_K^2, s)\Big(-23/8\,m_\pi^2\,m_K^2-7\,m_\pi^2\,s+5\,m_\pi^4-3/8\,m_K^2\,s$$
$$+27/8\,m_K^4+3\,s^2\Big)$$
$$+\overline{B}(m_\pi^2, m_\eta^2, s)\Big(4/3\,m_\pi^2\,m_K^2-4/3\,m_K^4\Big)$$
$$+\overline{B}(m_K^2, m_K^2, s)\Big(-2\,m_\pi^2\,m_K^2+3\,m_\pi^2\,s+4\,m_K^2\,s-2\,m_K^4-3\,s^2\Big)$$
$$+\overline{B}(m_K^2, m_\eta^2, s)\Big(-11/24\,m_\pi^2\,m_K^2-3/8\,m_K^2\,s+23/24\,m_K^4\Big)$$
$$+\overline{B}(m_\eta^2, m_\eta^2, s)\Big(-5/18\,m_\pi^2\,m_K^2\Big)+\overline{B}_1(m_\pi^2, m_K^2, s)\Big(5/4\,m_\pi^2\,m_K^2-5/4\,m_K^4\Big)$$
$$+\overline{B}_1(m_K^2, m_\eta^2, s)\Big(3/4\,m_\pi^2\,m_K^2-3/4\,m_K^4\Big)$$

(A.4)

$$
\begin{aligned}
&M_0^{8,e}(s) = \\
&\quad \Big(3\,Z_5^r - 2\,Z_6^r + 2\,Z_7^r - 3\,Z_8^r - 3\,Z_9^r - 2\,Z_{10}^r + 2\,Z_{11}^r + 2\,Z_{12}^r\Big)\Big(1/9\,m_K^2\Big) \\
&\quad \Big(-2\,K_3^r + K_4^r\Big)\Big(1/2\,m_\pi^2 - m_K^2\Big) + \Big(K_5^r + K_6^r\Big)\Big(1/3\,m_\pi^2 + 2/9\,m_K^2\Big) \\
&\quad +\Big(K_9^r + K_{10}^r\Big)\Big(-1/3\,m_\pi^2\Big) + K_{12}^r\Big(8/3\,m_K^2\Big) \\
&\quad +\frac{m_\pi^4}{m_\pi^2 - m_K^2}\Big(K_3^r - 1/2\,K_4^r - 1/3\,K_5^r - 1/3\,K_6^r + 1/3\,K_9^r + 1/3\,K_{10}^r\Big) \\
&\quad +\frac{1}{m_\pi^2 - m_K^2}\Big(\overline{A}(m_\pi^2) - \overline{A}(m_K^2)\Big)\Big(-m_\pi^2\,Z - 1/2\,m_\pi^2\,\frac{G_E}{G_8}\Big) \\
&\quad +\frac{1}{m_\pi^2 - m_K^2}\,\overline{B}(m_\pi^2, m_\pi^2, s)\Big(-7\,m_\pi^2\,Z\,s - 7/2\,m_\pi^2\,\frac{G_E}{G_8}\,s \\
&\quad\quad +4\,m_\pi^4\,Z + 2\,m_\pi^4\,\frac{G_E}{G_8} + 3\,Z\,s^2 + 3/2\,\frac{G_E}{G_8}\,s^2\Big) \\
&\quad +\frac{1}{m_\pi^2 - m_K^2}\,\overline{B}(m_\pi^2, m_K^2, s)\Big(6\,m_\pi^2\,Z\,s + 3\,m_\pi^2\,\frac{G_E}{G_8}\,s - 4\,m_\pi^4\,Z \\
&\quad\quad -2\,m_\pi^4\,\frac{G_E}{G_8} - 9/4\,Z\,s^2 - 9/8\,\frac{G_E}{G_8}\,s^2\Big) \\
&\quad +\frac{1}{m_\pi^2 - m_K^2}\,\overline{B}(m_K^2, m_K^2, s)\Big(m_\pi^2\,Z\,s + 1/2\,m_\pi^2\,\frac{G_E}{G_8}\,s \\
&\quad -3/4\,Z\,s^2 - 3/8\,\frac{G_E}{G_8}\,s^2\Big) \\
&\quad +\Big(\overline{A}(m_\pi^2) - \overline{A}(m_K^2)\Big)\Big(-1/4\,Z - 1/8\,\frac{G_E}{G_8}\Big) \\
&\quad +\overline{B}(m_\pi^2, m_\pi^2, s)\Big(-m_\pi^2\,Z - 1/2\,m_\pi^2\,\frac{G_E}{G_8} + Z\,s + 1/2\,\frac{G_E}{G_8}\,s\Big) \\
&\quad +\overline{B}(m_\pi^2, m_K^2, s)\Big(7/2\,m_\pi^2\,Z + 7/4\,m_\pi^2\,\frac{G_E}{G_8} - 3/2\,m_K^2\,Z - 3/4\,m_K^2\,\frac{G_E}{G_8} \\
&\quad\quad -3/4\,Z\,s - 3/8\,\frac{G_E}{G_8}\,s\Big) + \overline{B}(m_K^2, m_K^2, s)\Big(-1/4\,Z\,s - 1/8\,\frac{G_E}{G_8}\,s\Big) \\
&\quad +\overline{B}_1(m_\pi^2, m_K^2, s)\Big(-5/2\,m_\pi^2\,Z - 5/4\,m_\pi^2\,\frac{G_E}{G_8} + 1/2\,m_K^2\,Z + 1/4\,m_K^2\,\frac{G_E}{G_8}\Big)
\end{aligned}
\tag{A.5}
$$

And the 27-plets are:

$$
\begin{aligned}
&M_0^{27,F}(s) = \\
&\quad \Big(2\,L_1^r + 2\,L_2^r + L_3^r\Big)\Big(8\,m_{\pi^0}^4 + 8/3\,m_{K^0}^4 - 8\,s^2\Big) + \Big(4\,L_4^r + L_5^r\Big)\Big(8/3\,m_{\pi^0}^2\,m_{K^0}^2\Big) \\
&\quad +\Big(D_1^r - 3\,D_2^r\Big)\Big(-4/3\,m_{\pi^0}^2\,m_{K^0}^2\Big) + D_4^r\Big(-11/3\,m_{\pi^0}^2\,m_{K^0}^2 - 1/3\,m_{K^0}^4\Big)
\end{aligned}
$$

$$
\begin{aligned}
&+D_5^r\Big(-1/3\,m_{\pi^0}^2\,m_{K^0}^2+1/3\,m_{K^0}^4\Big)+D_6^r\Big(7/9\,m_{\pi^0}^2\,m_{K^0}^2-1/3\,m_{K^0}^4\Big)\\
&+D_7^r\Big(-10/3\,m_{\pi^0}^2\,m_{K^0}^2-4/3\,m_{K^0}^4\Big)\\
&+\Big(D_{26}^r+4\,D_{27}^r-3\,D_{29}^r-6\,D_{30}^r-6\,D_{31}^r\Big)\Big(1/3\,m_{\pi^0}^4+1/9\,m_{K^0}^4-1/3\,s^2\Big)\\
&+\frac{1}{m_\pi^2-m_K^2}\Big(\overline{A}(m_{K^0}^2)-\overline{A}(m_{K^+}^2)\Big)\Big(7/12\,m_\pi^4\Big)\\
&+\frac{1}{m_{\pi^0}^2-m_{K^0}^2}\,\overline{A}(m_{\pi^+}^2)\Big(-5/6\,m_{\pi^0}^4\Big)+\frac{1}{m_{\pi^0}^2-m_{K^0}^2}\,\overline{A}(m_{K^+}^2)\Big(5/3\,m_{\pi^0}^4\Big)\\
&+\frac{1}{m_{\pi^0}^2-m_{K^0}^2}\,\overline{A}(m_{K^0}^2)\Big(-5/6\,m_{\pi^0}^4\Big)\\
&+\frac{1}{m_{\pi^0}^2-m_{K^0}^2}\,\overline{B}(m_{\pi^+}^2,m_{\pi^+}^2,s)\Big(5/2\,m_{\pi^0}^2\,s^2-35/6\,m_{\pi^0}^4\,s+10/3\,m_{\pi^0}^6\Big)\\
&+\frac{1}{m_{\pi^0}^2-m_{K^0}^2}\,\overline{B}(m_{\pi^+}^2,m_{K^+}^2,s)\Big(-15/8\,m_{\pi^0}^2\,s^2+5\,m_{\pi^0}^4\,s-10/3\,m_{\pi^0}^6\Big)\\
&+\frac{1}{m_{\pi^0}^2-m_{K^0}^2}\,\overline{B}(m_{K^+}^2,m_{K^+}^2,s)\Big(-5/8\,m_{\pi^0}^2\,s^2+5/6\,m_{\pi^0}^4\,s\Big)\\
&+\overline{A}(m_{\pi^+}^2)\Big(m_{\pi^0}^2-109/72\,m_{K^0}^2\Big)+\overline{A}(m_{\pi^0}^2)\Big(-17/24\,m_{K^0}^2\Big)\\
&+\overline{A}(m_{K^+}^2)\Big(-25/18\,m_{\pi^0}^2-25/72\,m_{K^0}^2\Big)+\overline{A}(m_{K^0}^2)\Big(7/18\,m_{\pi^0}^2+1/36\,m_{K^0}^2\Big)\\
&+\Big(\overline{A}(m_{K^0}^2)-\overline{A}(m_{K^+}^2)\Big)\Big(-5/36\,m_\pi^2-5/18\,m_K^2\Big)+\overline{A}(m_\eta^2)\Big(-1/8\,m_{K^0}^2\Big)\\
&+\overline{B}(m_{\pi^+}^2,m_{\pi^+}^2,s)\Big(5/6\,m_{\pi^0}^2\,m_{K^0}^2-13/6\,m_{\pi^0}^2\,s+2/3\,m_{\pi^0}^4\\
&\quad-5/6\,m_{K^0}^2\,s+3/2\,s^2\Big)\\
&+\overline{B}(m_{\pi^+}^2,m_{K^+}^2,s)\Big(25/6\,m_{\pi^0}^2\,m_{K^0}^2-35/6\,m_{\pi^0}^2\,s+10/3\,m_{\pi^0}^4\\
&\quad-53/24\,m_{K^0}^2\,s-1/6\,m_{K^0}^4+19/8\,s^2\Big)\\
&+\overline{B}(m_{\pi^0}^2,m_{\pi^0}^2,s)\Big(-1/2\,m_{\pi^0}^2\,m_{K^0}^2\Big)\\
&+\overline{B}(m_{\pi^0}^2,m_{K^0}^2,s)\Big(-3/8\,m_{\pi^0}^2\,m_{K^0}^2+1/8\,m_{K^0}^2\,s-1/8\,m_{K^0}^4\Big)\\
&+\overline{B}(m_{K^+}^2,m_{K^+}^2,s)\Big(-13/12\,m_{\pi^0}^2\,s-7/8\,m_{K^0}^2\,s+7/8\,s^2\Big)\\
&+\overline{B}(m_{K^0}^2,m_\eta^2,s)\Big(-1/24\,m_{\pi^0}^2\,m_{K^0}^2-1/8\,m_{K^0}^2\,s+5/24\,m_{K^0}^4\Big)\\
&+\overline{B}(m_\eta^2,m_\eta^2,s)\Big(-1/18\,m_{\pi^0}^2\,m_{K^0}^2\Big)\\
&+\overline{B}_1(m_{\pi^+}^2,m_{K^+}^2,s)\Big(-19/12\,m_{\pi^0}^2\,m_{K^0}^2+1/3\,m_{\pi^0}^4-5/12\,m_{K^0}^4\Big)
\end{aligned}
$$

$$+\Big(\overline{B}_1(m_{\pi^0}^2, m_{K^0}^2, s) + \overline{B}_1(m_{K^0}^2, m_\eta^2, s)\Big)\Big(1/4\, m_{\pi^0}^2\, m_{K^0}^2 - 1/4\, m_{K^0}^4\Big) \tag{A.6}$$

$$\begin{aligned}
M_0^{27,\epsilon}(s) =\ & \\
& \Big(2\, L_1^r + 2\, L_2^r + L_3^r\Big)\Big(8\, m_\pi^4 + 8/3\, m_K^4 - 8\, s^2\Big) \\
& + L_4^r \Big(32/3\, m_\pi^2\, m_K^2\Big) + L_5^r \Big(40/3\, m_\pi^2\, m_K^2 - 16/3\, m_K^4\Big) \\
& + L_7^r \Big(- 480\, m_\pi^2\, m_K^2 + 352\, m_K^4\Big) + L_8^r \Big(- 224\, m_\pi^2\, m_K^2 + 160\, m_K^4\Big) \\
& + D_1^r \Big(- 76/3\, m_\pi^2\, m_K^2 + 16\, m_K^4\Big) + D_2^r \Big(- 4\, m_\pi^2\, m_K^2 + 32/3\, m_K^4\Big) \\
& + D_4^r \Big(7/3\, m_\pi^2\, m_K^2 - 9\, m_K^4\Big) + D_5^r \Big(5/3\, m_\pi^2\, m_K^2 - 5/3\, m_K^4\Big) \\
& + D_6^r \Big(73/9\, m_\pi^2\, m_K^2 - 5\, m_K^4\Big) + D_7^r \Big(- 22/3\, m_\pi^2\, m_K^2 - 4/3\, m_K^4\Big) \\
& + \Big(7\, D_{26}^r + 28\, D_{27}^r - 3\, D_{29}^r - 6\, D_{30}^r - 6\, D_{31}^r\Big)\Big(1/3\, m_\pi^4 + 1/9\, m_K^4 - 1/3\, s^2\Big) \\
& + \frac{1}{m_\pi^2 - m_K^2}\Big(\overline{A}(m_\pi^2) - \overline{A}(m_K^2)\Big)\Big(- 41/6\, m_\pi^4\Big) \\
& + \frac{1}{m_\pi^2 - m_K^2}\,\overline{B}(m_\pi^2, m_\pi^2, s)\Big(25/2\, m_\pi^2\, s^2 - 175/6\, m_\pi^4\, s + 50/3\, m_\pi^6\Big) \\
& + \frac{1}{m_\pi^2 - m_K^2}\,\overline{B}(m_\pi^2, m_K^2, s)\Big(- 45/8\, m_\pi^2\, s^2 + 15\, m_\pi^4\, s - 10\, m_\pi^6\Big) \\
& + \frac{1}{m_\pi^2 - m_K^2}\,\overline{B}(m_K^2, m_K^2, s)\Big(- 55/8\, m_\pi^2\, s^2 + 85/6\, m_\pi^4\, s - 20/3\, m_\pi^6\Big) \\
& + \overline{A}(m_\pi^2)\Big(41/6\, m_\pi^2 + 43/12\, m_K^2\Big) + \overline{A}(m_K^2)\Big(- 41/6\, m_\pi^2 - 263/24\, m_K^2\Big) \\
& + \overline{A}(m_\eta^2)\Big(- 5/8\, m_K^2\Big) \\
& + \overline{B}(m_\pi^2, m_\pi^2, s)\Big(127/6\, m_\pi^2\, s - 38/3\, m_\pi^4 - 3/2\, m_K^2\, s - 17/2\, s^2\Big) \\
& + \overline{B}(m_\pi^2, m_K^2, s)\Big(- 101/24\, m_\pi^2\, m_K^2 - 59/3\, m_\pi^2\, s + 40/3\, m_\pi^4 + 7/2\, m_K^2\, s \\
& \quad - 71/24\, m_K^4 + 61/8\, s^2\Big) + \overline{B}(m_\pi^2, m_\eta^2, s)\Big(- 4/3\, m_\pi^2\, m_K^2 + 4/3\, m_K^4\Big) \\
& + \overline{B}(m_K^2, m_K^2, s)\Big(26/3\, m_\pi^2\, m_K^2 - 191/12\, m_\pi^2\, s + 20/3\, m_\pi^4 \\
& \quad - 311/24\, m_K^2\, s + 7\, m_K^4 + 69/8\, s^2\Big) \\
& + \overline{B}(m_K^2, m_\eta^2, s)\Big(11/24\, m_\pi^2\, m_K^2 + 3/8\, m_K^2\, s - 23/24\, m_K^4\Big) \\
& + \overline{B}(m_\eta^2, m_\eta^2, s)\Big(5/18\, m_\pi^2\, m_K^2\Big) + \overline{B}_1(m_\pi^2, m_K^2, s)\Big(- 5/2\, m_\pi^2\, m_K^2 + 25/6\, m_K^4\Big)
\end{aligned}$$

$$+\overline{B}_1(m_K^2, m_\eta^2, s)\,\Big(-3/4\,m_\pi^2\,m_K^2 + 3/4\,m_K^4\Big) \tag{A.7}$$

$$\begin{aligned}
M_0^{27,e}(s) = \\
&\Big(2\,K_3^r - K_4^r\Big)\Big(1/2\,m_\pi^2 - m_K^2\Big) + \Big(K_5^r + K_6^r\Big)\Big(-1/3\,m_\pi^2 - 2/9\,m_K^2\Big) \\
&+\Big(K_9^r + K_{10}^r\Big)\Big(1/3\,m_\pi^2\Big) + K_{12}^r\Big(-8/3\,m_K^2\Big) \\
&+\frac{m_\pi^4}{m_\pi^2 - m_K^2}\Big(-K_3^r + 1/2\,K_4^r + 1/3\,K_5^r + 1/3\,K_6^r - 1/3\,K_9^r - 1/3\,K_{10}^r\Big) \\
&+\frac{1}{m_\pi^2 - m_K^2}\Big(\overline{A}(m_\pi^2) - \overline{A}(m_K^2)\Big)\Big(-2/3\,m_\pi^2\,Z\Big) \\
&+\frac{1}{m_\pi^2 - m_K^2}\,\overline{B}(m_\pi^2, m_\pi^2, s)\Big(-14/3\,m_\pi^2\,Z\,s + 8/3\,m_\pi^4\,Z + 2\,Z\,s^2\Big) \\
&+\frac{1}{m_\pi^2 - m_K^2}\,\overline{B}(m_\pi^2, m_K^2, s)\Big(4\,m_\pi^2\,Z\,s - 8/3\,m_\pi^4\,Z - 3/2\,Z\,s^2\Big) \\
&+\frac{1}{m_\pi^2 - m_K^2}\,\overline{B}(m_K^2, m_K^2, s)\Big(2/3\,m_\pi^2\,Z\,s - 1/2\,Z\,s^2\Big) \\
&+\Big(\overline{A}(m_\pi^2) - \overline{A}(m_K^2)\Big)\Big(-1/6\,Z\Big) + \overline{B}(m_\pi^2, m_\pi^2, s)\Big(-2/3\,m_\pi^2\,Z + 2/3\,Z\,s\Big) \\
&+\overline{B}(m_\pi^2, m_K^2, s)\Big(7/3\,m_\pi^2\,Z - m_K^2\,Z - 1/2\,Z\,s\Big) + \overline{B}(m_K^2, m_K^2, s)\Big(-1/6\,Z\,s\Big) \\
&+\overline{B}_1(m_\pi^2, m_K^2, s)\Big(-5/3\,m_\pi^2\,Z + 1/3\,m_K^2\,Z\Big) \\
&-14/3\,m_K^2\,Z\left(\frac{1}{\epsilon} + \ln(4\pi) + \Gamma' + 1\right)\frac{1}{16\pi^2}\,.
\end{aligned} \tag{A.8}$$

The last term is the infinity remaining from the loops since we haven't included the $\mathcal{O}(G_{27}\,e^2p^2)$ Lagrangian.

References

[1] S. Weinberg, Physica A **96** (1979) 327.

[2] J. Gasser and H. Leutwyler, Annals Phys. **158** (1984) 142.

[3] J. Gasser and H. Leutwyler, Nucl. Phys. B **250** (1985) 465.

[4] Pich, A., Lectures at Les Houches Summer School in Theoretical Physics, Session 68: Probing the Standard Model of Particle Interactions, Les

Houches, France, 28 Jul - 5 Sep 1997, [hep-ph/9806303];
Ecker, G., Lectures given at Advanced School on Quantum Chromodynamics (QCD 2000), Benasque, Huesca, Spain, 3-6 Jul 2000, [hep-ph/0011026].

[5] J. Kambor, J. Missimer and D. Wyler, Nucl. Phys. B **346** (1990) 17.

[6] J. Kambor, J. Missimer and D. Wyler, Phys. Lett. B **261** (1991) 496.

[7] J. Kambor, J. F. Donoghue, B. R. Holstein, J. Missimer and D. Wyler, Phys. Rev. Lett. **68** (1992) 1818.

[8] G. Ecker, Prog. Part. Nucl. Phys. **35** (1995) 1, [hep-ph/9501357];
A. Pich, Rept. Prog. Phys. **58** (1995) 563, [hep-ph/9502366];
E. de Rafael, Lectures given at Theoretical Advanced Study Institute in Elementary Particle Physics (TASI 94): CP Violation and the limits of the Standard Model, Boulder, CO, 29 May - 24 Jun 1994, [hep-ph/9502254].

[9] J. Bijnens, E. Pallante and J. Prades, Nucl. Phys. B **521** (1998) 305, [hep-ph/9801326].

[10] J. Bijnens, P. Dhonte and F. Persson, Nucl. Phys. B 648 (2003) 317, [hep-ph/0205341].

[11] E. Gamiz, J. Prades and I. Scimemi, JHEP **0310** (2003) 042 [hep-ph/0309172].

[12] J. Bijnens and M. B. Wise, Phys. Lett. B **137** (1984) 245;
B. R. Holstein, Phys. Rev. D **20** (1979) 1187.

[13] S. Gardner and G. Valencia, Phys. Rev. D **62** (2000) 094024, [hep-ph/0006240], Phys. Lett. B **466** (1999) 355, [hep-ph/9909202].

[14] G. Ecker, G. Muller, H. Neufeld and A. Pich, Phys. Lett. B **477** (2000) 88, [hep-ph/9912264];
V. Cirigliano, A. Pich, G. Ecker and H. Neufeld, [hep-ph/0307030].

[15] C. E. Wolfe and K. Maltman, Phys. Lett. B **482** (2000) 77 [hep-ph/9912254], Phys. Rev. D **63** (2001) 014008, [hep-ph/0007319].

[16] V. Cirigliano, J. F. Donoghue and E. Golowich, Phys. Lett. B **450** (1999) 241, Eur. Phys. J. C **18** (2000) 83, [hep-ph/0008290], Phys. Rev. D **61** (2000) 093001, [Erratum-ibid. D **63** (2001) 059903], [hep-ph/9907341], Phys. Rev. D **61** (2000) 093002, [hep-ph/9909473].

[17] G. Amorós, J. Bijnens, P. Talavera Nucl. Phys. B 602 (2001) 87,[hep-ph/0101127].

[18] J. A. Cronin, Phys. Rev. **161** (1967) 1483.

[19] G. Ecker, G. Isidori, G. Muller, H. Neufeld and A. Pich, Nucl. Phys. B **591** (2000) 419, [hep-ph/0006172].

[20] V. Cirigliano, M. Knecht, H. Neufeld, H. Rupertsberger and P. Talavera, Eur. Phys. J. C **23**, 121 (2002) [hep-ph/0110153].

[21] G. Esposito-Farese, Z. Phys. C **50** (1991) 255.

[22] G. Ecker, J. Kambor and D. Wyler, Nucl. Phys. B **394** (1993) 101, [hep-ph/0006172].

[23] R. Urech, Nucl. Phys. B **433**, 234 (1995) [hep-ph/9405341].

[24] These can be downloaded from `http://www.thep.lu.se/~bijnens/chpt.html`.

[25] I. V. Ajinenko *et al.*, Phys. Lett. B **567**, 159 (2003) [hep-ex/0205027].

[26] A. Aloisio *et al.* [KLOE Collaboration], hep-ex/0307054.

[27] J. Bijnens and J. Prades, JHEP **0006** (2000) 035 [hep-ph/0005189].

[28] J. A. Vermaseren, math-ph/0010025.

[29] G. Amorós, J. Bijnens and P. Talavera, Nucl. Phys. B **568** (2000) 319, [hep-ph/9907264].

Isospin Breaking in $K \to 3\pi$ Decays II: Radiative Corrections

Paper III

Isospin Breaking in $K \to 3\pi$ Decays II: Radiative Corrections[1]

Johan Bijnens and Fredrik Borg

Department of Theoretical Physics, Lund University
Sölvegatan 14A, S 22362 Lund, Sweden

Abstract:

The five different CP conserving amplitudes for the decays $K \to 3\pi$ are calculated using Chiral Perturbation Theory. The calculation is made to next-to-leading order and includes full isospin breaking. The squared amplitudes are compared with the corresponding ones in the isospin limit to estimate the size of the isospin breaking effects. In this paper we add the radiative corrections to the earlier calculated $m_u - m_d$ and local electromagnetic effects. We find corrections of order 5–10 percent.

[1] LU TP 04-37, hep-ph/0410333, October 2004

3.1 Introduction

The non-perturbative nature of low-energy QCD calls for alternative methods of calculating processes including composite particles such as mesons and baryons. A method describing the interactions of the light pseudoscalar mesons (K, π, η) is Chiral Perturbation Theory (ChPT). It was introduced by Weinberg, Gasser and Leutwyler [1–3] and it has been very successful. Pedagogical introductions to ChPT can be found in [4]. The theory was later extended to also cover the weak interactions of the pseudoscalars [5], and the first calculation of a kaon decaying into pions $(K \to 2\pi, 3\pi)$ appeared shortly thereafter [6]. Reviews of other applications of ChPT to nonleptonic weak interactions can be found in [7].

A recalculation in the isospin limit of $K \to 2\pi$ to next-to-leading order was made in [8, 9] and of $K \to 3\pi$ in [9, 10]. In [9] also a full fit to all experimental data was made and it was found that the decay rates and linear slopes agreed well. However, a small discrepancy was found in the quadratic slopes and that is part of the motivation for this further investigation of the decay $K \to 3\pi$ in ChPT.

The discrepancies found can have several different origins. It could be an experimental problem or it could have a theoretical origin. In the latter case the corrections to the amplitude calculated in [9] are threefold: strong isospin breaking, electromagnetic (EM) isospin breaking or higher order corrections. These effects have been studied in many papers for the $K \to 2\pi$ decays, references can be traced back from [11]. For $K \to 3\pi$ less work has been done. In [12] the strong isospin and local electromagnetic corrections were investigated and it was found that the inclusion of those led to changes of a few percent in the amplitudes. The local electromagnetic part was also calculated in [10], in full agreement with our result after corrections of some misprints in [10].

In this paper we add also the radiative corrections, i.e. the nonlocal electromagnetic isospin breaking. The full (first order) isospin breaking amplitude to next-to-leading chiral order is thus calculated, and we will try to estimate the effect of this in the amplitudes. A new full fit, including also new experimental data [13, 14], has to be done to answer the question whether isospin breaking removes the problem of fitting the quadratic slopes. This, together with a study of models for the higher order coefficients, we plan to do in an upcoming paper.

Other recent results on $K \to 3\pi$ decays can be found in [15,16]. In [15] Nicola Cabibbo discusses the possibility of determining the $a_0 - a_2$ pion scattering length from the threshold effects of $K^+ \to \pi^0\pi^0\pi^+$. He gives an approximate theoretical result with very few unknown parameters. We have a possibly better theoretical description of these effects but it includes more unknown parameters. In [16] an attempt was made to calculate the virtual photon corrections to the $K^+ \to \pi^0\pi^0\pi^+$ decay. Our result disagrees with the result presented there.

The outline of this paper is as follows. The next section describes isospin breaking in more detail. In section 3.3 the basis of ChPT, the Chiral Lagrangians, are discussed. Section 3.4 specifies the decays and describes the relevant kinematics. The divergences appearing when including photons are discussed in section 3.5. In section 3.6 the analytical results are discussed, section 3.7 contains the numerical results and the last section contains the conclusions.

3.2 Isospin Breaking

Isospin symmetry is the symmetry under exchange of up- and down-quarks. Obviously this symmetry is only true in the approximation that $m_u = m_d$ and electromagnetism is neglected, i.e. in the isospin limit. Calculations are often performed in the isospin limit since this is simpler and gives a good first estimate of the result.

However, to get a precise result one has to include isospin breaking, i.e. the effects from $m_u \neq m_d$ and electromagnetism. Effects coming from $m_u \neq m_d$ we refer to as strong isospin breaking and include mixing between π^0 and η. This mixing leads to changes in the formulas for both the physical masses of π^0 and η as well as the amplitude for any process involving either of the two. For a detailed discussion see [17].

The other source is electromagnetic isospin breaking, coming from the fact that the up- and the down-quarks are charged, which implies different interactions with photons. This part can be further divided in local electromagnetic isospin breaking and explicit photon contributions (radiative corrections). The former are described by adding new Lagrangians at each order and the latter by introducing new diagrams including photons.

Our first calculation of $K \to 3\pi$ [9] was done in the isospin limit. In the next paper, [12], we included strong and local isospin breaking (there collectively referred to as strong isospin breaking) and we now present the calculation including all isospin breaking effects.

3.3 The ChPT Lagrangians

The basis of our ChPT calculation is the various Chiral Lagrangians. They can be divided in different orders and the order parameters in the perturbation series are p and m, the momenta and mass of the pseudoscalars. Including isospin breaking also e, the electron charge, is used as an order parameter. Leading order (order two) therefore means terms of order p^2, m^2, e^2 and next-to-leading order (order four) $p^4, p^2\, m^2, m^4, p^2\, e^2$ and $m^2\, e^2$ (e^4 is neglected).

3.3.1 Leading Order

The leading order Chiral Lagrangian is usually divided in three parts

$$\mathcal{L}_2 = \mathcal{L}_{S2} + \mathcal{L}_{W2} + \mathcal{L}_{E2}, \tag{3.1}$$

where $\mathcal{L}_{S2}$ refers to the strong $\Delta S = 0$ part, $\mathcal{L}_{W2}$ the weak $\Delta S = \pm 1$ part, and $\mathcal{L}_{E2}$ the strong-electromagnetic and weak-electromagnetic parts combined. For the strong part we have [2]

$$\mathcal{L}_{S2} = \frac{F_0^2}{4} \langle u_\mu u^\mu + \chi_+ \rangle \tag{3.2}$$

Here $\langle A \rangle$ stands for the flavour trace of the matrix A, and F_0 is the pion decay constant in the chiral limit. We define the matrices u_μ, u and $\chi_\pm$ as

$$u_\mu = i u^\dagger D_\mu U \, u^\dagger = u_\mu^\dagger \, , \quad u^2 = U \, , \quad \chi_\pm = u^\dagger \chi u^\dagger \pm u \chi^\dagger u \, , \tag{3.3}$$

where the special unitary matrix U contains the Goldstone boson fields

$$U = \exp\left(\frac{i\sqrt{2}}{F_0} M\right) \, , \quad M = \begin{pmatrix} \frac{1}{\sqrt{2}}\pi_3 + \frac{1}{\sqrt{6}}\eta_8 & \pi^+ & K^+ \\ \pi^- & \frac{-1}{\sqrt{2}}\pi_3 + \frac{1}{\sqrt{6}}\eta_8 & K^0 \\ K^- & \overline{K^0} & \frac{-2}{\sqrt{6}}\eta_8 \end{pmatrix} . \tag{3.4}$$

The formalism we use is the external field method of [2], and to include photons we set

$$\chi = 2B_0 \begin{pmatrix} m_u & & \\ & m_d & \\ & & m_s \end{pmatrix} \text{ and } D_\mu U = \partial_\mu U - ie\, Q A_\mu U - ie\, U Q A_\mu, \tag{3.5}$$

where A_μ is the photon field and

$$Q = \begin{pmatrix} 2/3 & & \\ & -1/3 & \\ & & -1/3 \end{pmatrix} . \tag{3.6}$$

We diagonalize the quadratic terms in (3.2) by a rotation

$$\begin{aligned} \pi^0 &= \pi_3 \cos\epsilon + \eta_8 \sin\epsilon \\ \eta &= -\pi_3 \sin\epsilon + \eta_8 \cos\epsilon \, , \end{aligned} \tag{3.7}$$

where the lowest order mixing angle ϵ satisfies

$$\tan(2\epsilon) = \sqrt{3} \frac{m_d - m_u}{2\, m_s - m_u - m_d} \, . \tag{3.8}$$

The weak part of the Lagrangian has the form [18]

$$\mathcal{L}_{W2} = C\, F_0^4 \left[G_8 \langle \Delta_{32} u_\mu u^\mu \rangle + G_8' \langle \Delta_{32} \chi_+ \rangle + G_{27} t^{ij,kl} \, \langle \Delta_{ij} u_\mu \rangle \langle \Delta_{kl} u^\mu \rangle \right] + \text{ h.c.} \,. \tag{3.9}$$

The tensor $t^{ij,kl}$ has as nonzero components

$$\begin{aligned} t^{21,13} = t^{13,21} = \frac{1}{3} \quad &; \quad t^{22,23} = t^{23,22} = -\frac{1}{6}\,; \\ t^{23,33} = t^{33,23} = -\frac{1}{6} \quad &; \quad t^{23,11} = t^{11,23} = \frac{1}{3}\,, \end{aligned} \tag{3.10}$$

and the matrix Δ_{ij} is defined as

$$\Delta_{ij} \equiv u \lambda_{ij} u^\dagger \,, \quad (\lambda_{ij})_{ab} \equiv \delta_{ia}\, \delta_{jb} \,. \tag{3.11}$$

The coefficient C is defined such that in the chiral and large N_c limits $G_8 = G_{27} = 1$,

$$C = -\frac{3}{5} \frac{G_F}{\sqrt{2}} V_{ud}\, V_{us}^* = -1.06 \cdot 10^{-6} \text{ GeV}^{-2} \,. \tag{3.12}$$

Finally, the remaining electromagnetic part, relevant for this calculation, looks like (see e.g. [19])

$$\mathcal{L}_{E2} = e^2 F_0^4 Z \langle \mathcal{Q}_L \mathcal{Q}_R \rangle + e^2 F_0^4 \langle \Upsilon \mathcal{Q}_R \rangle \tag{3.13}$$

where the weak-electromagnetic term is characterized by a constant G_E ($g_{\text{ewk}} G_8$ in [19]),

$$\Upsilon = G_E\, F_0^2 \Delta_{32} + \text{h.c.} \tag{3.14}$$

and

$$\mathcal{Q}_L = u Q u^\dagger \,, \ \ \mathcal{Q}_R = u^\dagger Q u \,. \tag{3.15}$$

3.3.2 Next-to-leading Order

The fact that ChPT is a non-renormalizable theory means that new terms have to be added at each order to compensate for the loop-divergences. This means that the Lagrangians increase in size for every new order and the number of free parameters rise as well. At next-to-leading order the Lagrangian is split in four parts which, in obvious notation, are

$$\mathcal{L}_4 = \mathcal{L}_{S4} + \mathcal{L}_{W4} + \mathcal{L}_{S2E2} + \mathcal{L}_{W2E2}(G_8) \,. \tag{3.16}$$

Here the notation (G_8) indicates that here only the dominant G_8-part is included in the Lagrangian and therefore in the calculation.

These Lagrangians are quite large and we choose not to write them explicitly here since they can be found in many places [2, 5, 19–23]. For a list of all the pieces relevant for this specific calculation see [12]. Note however that four terms producing photon interactions should be added to $\mathcal{L}_{W4}$ in [12]. The two new terms in the octet part are

$$N_{14}\, i\, \langle \Delta_{32} \{ f_+^{\mu\nu}, u_\mu u_\nu \} \rangle + N_{15}\, i\, \langle \Delta_{32}\, u_\mu f_+^{\mu\nu} u_\nu \rangle \tag{3.17}$$

and in the 27 part

$$D_{13}\, i\, t^{ij,kl} \langle \Delta_{ij}\, u_\mu \rangle \langle \Delta_{kl} [u_\nu, f_+^{\mu\nu}] \rangle + D_{15}\, i\, t^{ij,kl} \langle \Delta_{ij}\, u_\mu u_\nu \rangle \langle \Delta_{kl}\, f_+^{\mu\nu} \rangle, \tag{3.18}$$

where

$$f_+^{\mu\nu} = u F^{\mu\nu} u^\dagger + u^\dagger F^{\mu\nu} u, \quad F^{\mu\nu} = e\, Q\, (\partial^\mu A^\nu - \partial^\nu A^\mu). \tag{3.19}$$

3.3.2.1 Ultraviolet Divergences

The process $K \to 3\pi$ receives higher-order contributions from diagrams that contain loops. The study of these diagrams is complicated by the fact that they need to be defined precisely. The loop-diagrams involve an integration over the undetermined loop-momentum q, and the integrals are divergent in the $q \to \infty$ ultraviolet region. These ultraviolet divergences are canceled by replacing the coefficients in the next-to-leading order Lagrangians by the renormalized coefficients and a subtraction part, see [9, 12] and references therein. The divergences can be used as a check on the calculation and all our infinities (except the ones left since the G_{27}-part in $\mathcal{L}_{W2E2}$ is not known) cancel as they should.

3.3.2.2 Loop Integrals

The prescription we use for the loop integrals can be found in many places, e.g. [24]. The only one needed in addition to the ones given there is the one-loop three point function

$$C(m_1^2, m_2^2, m_3^3, p_1^2, p_2^2, p_3^2) = \int \frac{d^d p}{(2\pi)^d} \frac{-i}{(p^2 - m_1^2)\,((p-p_1)^2 - m_2^2)\,((p-p_3)^2 - m_3^2)}\,, \tag{3.20}$$

where $p_3 = p_1 + p_2$. For its numerical evaluation we use the program FF [25]. This program also deals with possible infrared divergences consistently.

3.4 Kinematics

There are five different CP-conserving decays of the type $K \to 3\pi$ (K^- decays are not treated separately since they are counterparts to the K^+ decays):

$$K_L(k) \quad \to \quad \pi^0(p_1)\, \pi^0(p_2)\, \pi^0(p_3)\,, \quad [A_{000}^L]\,,$$

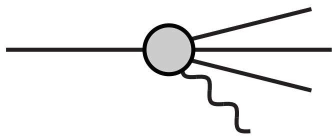

Figure 3.1: Bremsstrahlung, the emission of an extra final-state photon.

$$\begin{aligned}
K_L(k) &\rightarrow \pi^+(p_1)\,\pi^-(p_2)\,\pi^0(p_3)\,, \quad [A^L_{+-0}]\,,\\
K_S(k) &\rightarrow \pi^+(p_1)\,\pi^-(p_2)\,\pi^0(p_3)\,, \quad [A^S_{+-0}]\,,\\
K^+(k) &\rightarrow \pi^0(p_1)\,\pi^0(p_2)\,\pi^+(p_3)\,, \quad [A_{00+}]\,,\\
K^+(k) &\rightarrow \pi^+(p_1)\,\pi^+(p_2)\,\pi^-(p_3)\,, \quad [A_{++-}]\,,
\end{aligned} \tag{3.21}$$

where we have indicated the four-momentum defined for each particle and the symbol used for the amplitude.

The kinematics is treated using

$$s_1 = (k-p_1)^2\ , \quad s_2 = (k-p_2)^2\ , \quad s_3 = (k-p_3)^2\ . \tag{3.22}$$

The amplitudes are expanded in terms of the Dalitz plot variables x and y defined as

$$y = \frac{s_3 - s_0}{m^2_{\pi^+}}\,, \quad x = \frac{s_2 - s_1}{m^2_{\pi^+}}\,, \quad s_0 = \frac{1}{3}\left(s_1 + s_2 + s_3\right)\ . \tag{3.23}$$

The amplitude for $K_L \rightarrow \pi^0\pi^0\pi^0$ is symmetric under the interchange of all three final state particles and the one for $K_S \rightarrow \pi^+\pi^-\pi^0$ is antisymmetric under the interchange of π^+ and π^- because of CP. The amplitudes for $K_L \rightarrow \pi^+\pi^-\pi^0, K^+ \rightarrow \pi^+\pi^+\pi^-$ and $K^+ \rightarrow \pi^0\pi^0\pi^+$ are symmetric under the interchange of the first two pions because of CP or Bose-symmetry.

3.5 Infrared Divergences

In addition to the ultraviolet divergences which are removed by renormalization, diagrams including photons in the loops contain infrared (IR) divergences. These infinities come from the $q \rightarrow 0$ end of the loop-momentum integrals. They are canceled by including also the Bremsstrahlung diagram, where a real photon is radiated off one of the charged mesons, see Fig. 3.1. It is only the sum of the virtual loop corrections and the real Bremsstrahlung which is physically significant and thus needs to be well defined. We regulate the IR divergence in both the virtual photon loops and the real emission with a photon mass m_γ and keep only the singular terms plus those that do not vanish in the limit $m_\gamma \to 0$. We include the real Bremsstrahlung for photon energies up to a cut-off ω and treat it in the soft photon approximation.

The exact form of the amplitude squared for the bremsstrahlung diagram depends on which specific amplitude that is being calculated. For $K^+(k) \to \pi^0(p_1)\pi^0(p_2)\pi^+(p_3)$ it can be written in the soft photon limit (see e.g. [26])

$$|A|^2_{BS} = |A|^2_{LO}\, e^2 \int \frac{d^3q}{(2\pi)^3}\, \frac{1}{2q} \sum_{\lambda=0,1} \left[\frac{k\cdot\epsilon^{(\lambda)}}{q\cdot k} - \frac{p_3\cdot\epsilon^{(\lambda)}}{q\cdot p_3}\right]^2, \tag{3.24}$$

where $|A|_{LO}$ is the lowest order isospin limit amplitude. The number of terms inside the parentheses is the number of charged particles in the process and the sign of those terms depends both on the charge of the radiating particle and on whether it is incoming or outgoing. Writing out the square and using $\sum_{\lambda=0,1} \epsilon^{(\lambda)}_\mu \epsilon^{(\lambda)}_\nu = -g_{\mu\nu}$, you get

$$|A|^2_{BS} = -|A|^2_{LO}\, e^2 \int \frac{d^3q}{(2\pi)^3}\, \frac{1}{2q} \left[\frac{k^2}{(q\cdot k)^2} + \frac{p_3^2}{(q\cdot p_3)^2} - \frac{2\, p_3\cdot k}{(q\cdot k)(q\cdot p_3)}\right] \tag{3.25}$$

To solve the first integral term, place the vector k along the z-axis, i.e.

$$k = (k^0, 0, 0, k^z) \text{ and } (k\cdot q)^2 = (k^0 q^0 - k^z q^z)^2. \tag{3.26}$$

Changing to polar coordinates that part of the integral now looks like

$$-|A|^2_{LO}\, e^2\, \frac{m_k^2}{8\pi^2} \int dq\, d(\cos\theta)\, \frac{q}{(k^0 E_\gamma - k^z q\cos\theta)^2}, \tag{3.27}$$

where $k^2 = m_k$, $q_0 = E_\gamma$ and $q_z = q\cos\theta$ have been used. Solving the $d(\cos\theta)$ part is now straightforward and leads to

$$-|A|^2_{LO}\, e^2\, \frac{m_k^2}{8\pi^2} \int dq\, \frac{1}{k^z} \left(\frac{1}{k^0 E_\gamma - k^z q} - \frac{1}{k^0 E_\gamma + k^z q}\right), \tag{3.28}$$

Putting the two terms on a common denominator and changing variable to E_γ leads to

$$-|A|^2_{LO}\, e^2\, \frac{m_k^2}{4\pi^2} \int_{m_\gamma}^{\omega} dE_\gamma\, \frac{E_\gamma}{E_\gamma^2 (k^0)^2 - (E_\gamma^2 - m_\gamma^2)(k^z)^2}, \tag{3.29}$$

where ω is the photon energy above which the detector identifies it as a real external photon. We are only interested in the result in the limit $m_\gamma \to 0$, so it's enough to consider

$$-|A|^2_{LO}\, e^2\, \frac{m_k^2}{4\pi^2} \int_{m_\gamma}^{\omega} dE_\gamma\, \frac{1}{m_k^2 E_\gamma}, \tag{3.30}$$

which gives the result

$$-|A|^2_{LO}\,\frac{e^2}{4\pi^2}\log\frac{\omega^2}{m_\gamma^2}\,. \tag{3.31}$$

In a similar way one gets the result for the mixed term

$$\begin{aligned}\int\frac{d^3q}{(2\pi)^3}\,\frac{1}{2q}\left[2\frac{p_3\cdot k}{(q\cdot k)(q\cdot p_3)}\right] &= -\frac{x_s}{4\pi^2}\frac{s_3-m_K-m_\pi}{m_K m_\pi(1-x_s)}\log x_s\log\frac{\omega^2}{m_\gamma^2}\\ &\equiv I_{IR}(m_K^2,m_\pi^2,s_3)\,,\end{aligned} \tag{3.32}$$

where

$$x_s=\frac{\sqrt{1-4m_Km_\pi/(\bar s_3-(m_K-m_\pi)^2)}-1}{\sqrt{1-4m_Km_\pi/(\bar s_3-(m_K-m_\pi)^2)}+1}. \tag{3.33}$$

In order to obtain the correct imaginary part we use the $i\varepsilon$-prescription, which means $\bar s_3 = s_3 + i\varepsilon$.

For the other amplitudes the calculations are similar and the resulting bremsstrahlung amplitudes are

$$|A^L_{000}|^2_{BS}=0\,, \tag{3.34}$$

$$|A^L_{+-0}|^2_{BS}=-|A_{+-0}|^2_{LO}\,\frac{e^2}{4\pi^2}\left[2\log\frac{\omega^2}{m_\gamma^2}-I_{IR}(m_\pi^2,m_\pi^2,s_3)\right], \tag{3.35}$$

$$|A^S_{+-0}|^2_{BS}=-|A_{+-0}|^2_{LO}\,\frac{e^2}{4\pi^2}\left[2\log\frac{\omega^2}{m_\gamma^2}-I_{IR}(m_\pi^2,m_\pi^2,s_3)\right], \tag{3.36}$$

$$|A_{00+}|^2_{BS}=-|A_{00+}|^2_{LO}\,\frac{e^2}{4\pi^2}\left[2\log\frac{\omega^2}{m_\gamma^2}-I_{IR}(m_\pi^2,m_K^2,s_3)\right], \tag{3.37}$$

$$\begin{aligned}|A_{++-}|^2_{BS} &= -|A_{++-}|^2_{LO}\,\frac{e^2}{4\pi^2}\left[4\log\frac{\omega^2}{m_\gamma^2}-I_{IR}(m_\pi^2,m_K^2,s_1)\right.\\ &\quad -I_{IR}(m_\pi^2,m_K^2,s_2)+I_{IR}(m_\pi^2,m_K^2,s_3)-I_{IR}(m_\pi^2,m_\pi^2,s_1)\\ &\quad \left.-I_{IR}(m_\pi^2,m_\pi^2,s_2)+I_{IR}(m_\pi^2,m_\pi^2,s_3)\right].\end{aligned} \tag{3.38}$$

When using the above, the divergences from the explicit photon loops cancel exactly.

A similar problem shows up in the definition of the decay constants since we normalize the lowest order with F_{π^+} and F_{K^+}. Our prescription for the decay constants is described in App. 3.A.

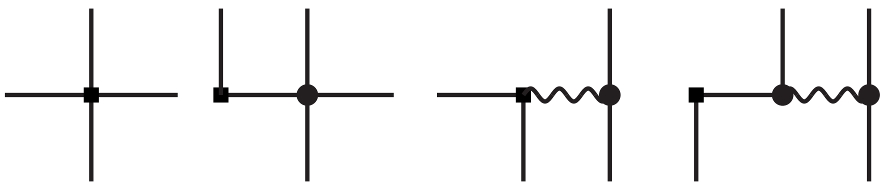

Figure 3.2: The tree level diagrams for $K \to 3\pi$. A filled square is a weak vertex, a filled circle a strong vertex, a straight line a pseudoscalar meson and a wiggly line a photon.

3.6 Analytical Results

3.6.1 Lowest Order

The four diagrams that could contribute to lowest order can be seen in Fig. 3.2.

However, the two diagrams including photons turn out to give zero. This is obviously so for $K^+ \to \pi^+\pi^0\pi^0$ and $K_L \to \pi^0\pi^0\pi^0$ since the $\gamma\pi^0\pi^0$ vertex vanishes as a consequence of charge conjugation.

The reason why it vanishes for the other decays is somewhat more subtle and is the same as why the lowest order result for $K \to \pi\ell^+\ell^-$ vanishes [27]. When doing a simultaneous diagonalization of the covariant kinetic and mass terms quadratic in the pseudoscalar fields, including those of the weak lagrangian $\mathcal{L}_{W2}$, p^2-terms of the form $\partial_\mu K \partial^\mu \pi$ are absent and all weak vertices involve at least three pseudoscalar fields. This result should not change as compared to our calculation where the weak Lagrangian was not included in the diagonalization. Thus in our case, the two diagrams on the right in Fig. 3.2 will together give zero contribution.

This means that the lowest order result in the full isospin case is the same as when just including strong and local EM isospin breaking. This result we published before, the full expressions can be found in [12].

3.6.2 Next-to-leading Order

There are 51 additional diagrams contributing to next-to-leading order. They can be divided in three different classes and examples will be shown of each class. It should be noted that the argument in the previous subsection is not valid at this order. There now exist $K\pi\gamma$ vertices. The reason for this is that one can not diagonalize simultaneously all terms with two pseudoscalar fields when going to next-to-leading order.

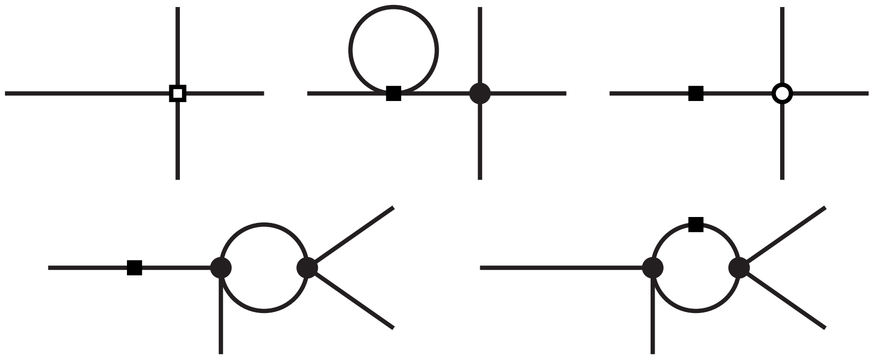

Figure 3.3: Examples of diagrams of next-to-leading order with no photons. An open square is a vertex from $\mathcal{L}_{W4}$ or $\mathcal{L}_{W2E2}$, an open circle a vertex from $\mathcal{L}_{S4}$ or $\mathcal{L}_{S2E2}$, a filled square a vertex from $\mathcal{L}_{W2}$ or $\mathcal{L}_{E2}$ ($\Delta S = 1$) and a filled circle a vertex from $\mathcal{L}_{S2}$ or $\mathcal{L}_{E2}$ ($\Delta S = 0$).

The first class of diagrams are the 13 which do not include explicit photons. They are the ones used in our earlier papers [9, 12] and a complete list of them can be found there. Some examples are shown in Fig. 3.3.

The second class of diagrams are the ones with a photon running in a loop. There are 18 of these and some examples can be found in Fig. 3.4. Their evaluation is the main new result of this paper. They are also responsible for the infrared divergences discussed in Sect. 3.5. The first diagram is an example where the photon is the only particle in the loop, a photon tadpole diagram. These vanish in dimensional regularization when only singular and nonzero terms in the limit $m_\gamma \to 0$ are kept.

The last class of diagrams is the ones with tree level photon propagators, 20 in total. They are photon reducible, i.e. if we cut the photon line the diagram falls apart. They are infrared finite and some examples can be seen in Fig. 3.5. It turns out that for realistic values of the input parameters this class of diagrams give a negligible contribution to all $K \to 3\pi$ processes.

We work to first order in isospin breaking, i.e. as soon as e^2 is present we set $m_u = m_d$, $m_{\pi^+} = m_{\pi^0} = m_\pi$ and $m_{K^+} = m_{K^0} = m_K$. Even then, the resulting amplitudes at next-to-leading order are rather long, and it does not seem very useful to present them here explicitly. However, the full expressions for the amplitudes are available on request from the authors or can be downloaded [28]. It should be noted that the amplitude for $K_L \to \pi^0\pi^0\pi^0$ was given in [12]. It was stated that it was the full isospin breaking amplitude since no explicit

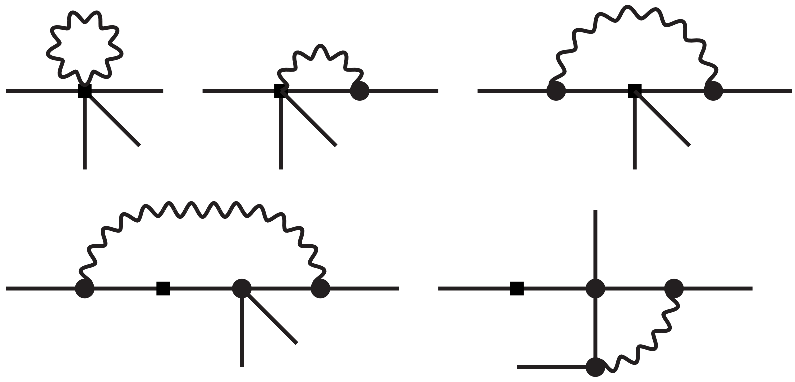

Figure 3.4: Examples of diagrams with photons in the loops. A filled square is a weak vertex, a filled circle a strong vertex, a straight line a pseudoscalar meson and a wiggly line a photon.

photon diagrams can contribute to this process. This is not completely true, the amplitude will change indirectly through the definition of F_{π^+} and F_{K^+}, see App. 3.A.

The next-to-leading order amplitudes can in principle include all the low-energy coefficients (LECs) from $\mathcal{L}_{W4}$, $\mathcal{L}_{S4}$, $\mathcal{L}_{W2E2}$ and $\mathcal{L}_{S2E2}$. The coefficients from the strong and electromagnetic part of the Lagrangian are treated as input, which leaves G_8,G_{27},$N_1^r,\ldots,N_{13}^r$, D_1^r,D_2^r,$D_4^r,\ldots,D_7^r$, $D_{26}^r,\ldots,D_{31}^r$ and $Z_1^r,\ldots,Z_{14}^r$ as undetermined. In total 41 unknown parameters. However, all of these do not appear independently, i.e. they multiply the same type of term, e.g. m_K^4 or $e^2m_\pi^2$. It turns out, as discussed in [12], that there are 30 independent combinations, denoted by $\tilde{K}_1\ldots\tilde{K}_{30}$. For the 11 combinations already appearing in the isospin limit see [9, 12] and the 19 additional ones for the isospin breaking case can be be found in [12]. In addition to the 30 combinations found in [12], four new coefficients show up when including photons: N_{14}^r, N_{15}^r, D_{13}^r and D_{15}^r. These all come from the third class of diagrams where a tree level photon is present. The four coupling constants show up in precisely the same combinations in $K\to\pi\ell^+\ell^-$ and can thus be determined experimentally in other decays. We therefore treat them as input.

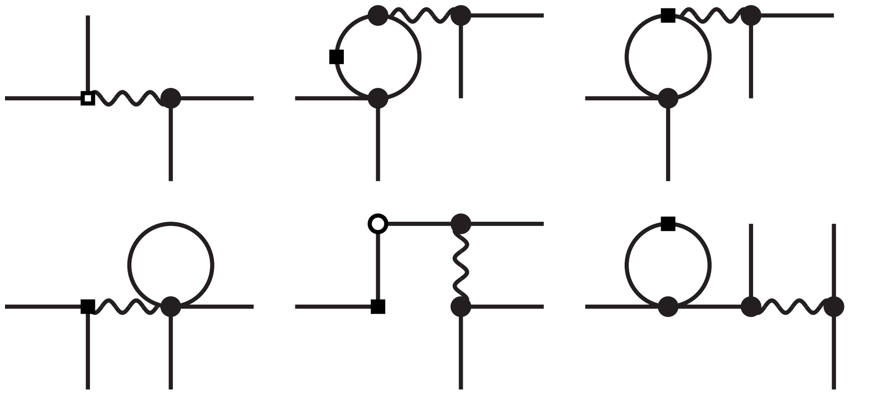

Figure 3.5: Examples of diagrams with photon propagators. An open square is a vertex from $\mathcal{L}_{W4}$ or $\mathcal{L}_{W2E2}$, an open circle a vertex from $\mathcal{L}_{S4}$ or $\mathcal{L}_{S2E2}$, a filled square a vertex from $\mathcal{L}_{W2}$ or $\mathcal{L}_{E2}$ ($\Delta S = 1$) and a filled circle a vertex from $\mathcal{L}_{S2}$ or $\mathcal{L}_{E2}$ ($\Delta S = 0$). A straight line is a pseudoscalar meson and a wiggly line a photon.

3.7 Numerical Results

3.7.1 Experimental Data and Fit

A full isospin limit fit was made in [9] taking into account all data published before May 2002. One of the motivations for this continued investigation of isospin breaking effects is to see whether isospin violation can solve the discrepancies in the quadratic slope parameters found there. A new full fit will be done in an upcoming paper. The data from ISTRA+ [13] and KLOE [14], which appeared after [9], will then also be taken into account. We do not present a new fit in this paper since estimates of the new combinations of constants should be done before attempting a full fit.

3.7.2 Inputs

The input values we use are presented in Table 3.1.

3.7.2.1 Strong and Electromagnetic Input

There are different ways to treat the masses, especially in the isospin limit case. In [9] the masses used in the phase space were obtained from the physical

G_8	5.45	$L_1^r \cdot 10^3$	0.38	$\tilde{K}_1$	0
G_{27}	0.392	$L_2^r \cdot 10^3$	1.59	$\tilde{K}_2/G_8$	$5.19 \cdot 10^{-2}$
G_E	-0.4	$L_3^r \cdot 10^3$	-2.91	$\tilde{K}_3/G_8$	$3.77 \cdot 10^{-3}$
$\delta_2 - \delta_0$	-0.576	$L_4^r \cdot 10^3$	0	$\tilde{K}_4$	0
$\sin\epsilon$	$1.19 \cdot 10^{-2}$	$L_5^r \cdot 10^3$	1.46	$\tilde{K}_5/G_{27}$	$-4.25 \cdot 10^{-2}$
Z	0.805	$L_6^r \cdot 10^3$	0	$\tilde{K}_6/G_{27}$	$-1.66 \cdot 10^{-1}$
μ	0.77 GeV	$L_7^r \cdot 10^3$	-0.49	$\tilde{K}_7/G_{27}$	$1.20 \cdot 10^{-1}$
F_π	0.0924 GeV	$L_8^r \cdot 10^3$	1.0	$\tilde{K}_8 \ldots \tilde{K}_{11}$	0
F_K	0.113 GeV	$L_9^r \cdot 10^3$	7.0	$\tilde{K}_{12} \ldots \tilde{K}_{30}$	0
N_{14}	$-10.4 \cdot 10^{-3}$	$K_1 \ldots K_{11}$	0	D_{13}	0
N_{15}	$5.95 \cdot 10^{-3}$			D_{15}	0

Table 3.1: The various input values used.

masses occuring in the decays. However in the amplitudes the physical mass of the kaon involved in the process was used and the pion mass was given by $m_\pi^2 = \frac{1}{3}\sum_{i=1,3} m_{\pi^i}^2$ with $i = 1,2,3$ being the three pions participating in the reaction. This allowed for the correct kinematical relation $s_1 + s_2 + s_3 = m_K^2 + 3m_\pi^2$ to be satisfied while having the isospin limit in the amplitude but the physical masses in the phase space. The results in [9] were obtained with the physical mass for the eta. Results with the Gell-Mann-Okubo (GMO) relation for the eta mass in the loops gave small changes within the general errors given in [9].

In the decays here, we work to first order in isospin breaking. We have rewritten explicit factors of $m_u - m_d$ in terms of $\sin\epsilon$ according to

$$m_u - m_d = -\frac{2}{\sqrt{3}}\,(2\,m_s - m_u - m_d)\,\sin\epsilon\,. \tag{3.39}$$

In general we use the physical masses of pions and kaons in the loops but as soon as a factor of $\sin\epsilon$ or e^2 is present we use a common kaon and a common pion mass. This simplifies the analytical formulas enormously. The kaon mass chosen is the mass from the kaon in the decay and the pion mass used is $3m_\pi^2 = \sum_i m_{\pi^i}^2$ with $i = 1,2,3$ the three pions in the final state, i.e. the mass we used in the isospin limit case. For the eta mass we use in general the GMO mass in the loops but with isospin violation included,

$$m_\eta^2 = \frac{2}{3}\,(m_{K^+}^2 + m_{K^0}^2 - m_{\pi^+}^2) + \frac{1}{3}\,m_{\pi^0}^2\,. \tag{3.40}$$

The possible lowest order contributions from the eta mass have been removed from the amplitudes using the corresponding next-to-leading order relation as described in [12].

The strong LECs L_1^r to L_8^r from $\mathcal{L}_{S4}$ as well as $\sin\epsilon$ come from the one-loop fit in [17].

The constant Z from $\mathcal{L}_{E2}$ we estimate via

$$Z = \frac{1}{2\,F_\pi^2\,e^2}\,(m_{\pi^+}^2 - m_{\pi^0}^2), \tag{3.41}$$

which corresponds to the value in Table 3.1. The higher order coefficients of $\mathcal{L}_{E4}$, $K_1 \ldots K_{11}$, are rather unknown. Some rough estimates exist but we put them to zero here.

The IR divergences are cancelled by adding the soft-photon Bremsstrahlung. We have used a 10 MeV cut-off in energy for this and used the same cut-off in the definition of F_{π^+} and F_{K^+}.

The subtraction scale μ is chosen to be 0.77 GeV.

3.7.2.2 Weak Inputs

The coefficients contributing in the isospin limit from $\mathcal{L}_{W2}$ and $\mathcal{L}_{W4}$ are taken from the fit in [9]. The values of G_8, G_{27} and $\delta_2 - \delta_0$ in Table 3.1 are taken from [9] as well. We use as a reasonable estimate for G_E the value presented in [29].

Very little knowledge exists of the values of $\tilde{K}_{12} \ldots \tilde{K}_{30}$, so they are set equal to zero at $\mu = 0.77$ GeV. Tests were also made assigning order of magnitude estimates to them. This imparted changes in the isospin breaking corrections similar in size to those of the loop contributions.

3.7.2.3 Input Relevant for the Photon Reducible Diagrams

The two new constants D_{13} and D_{15} are set to zero since no knowledge exist of their values. Note that in order to contribute at all, they have to get values orders of magnitude larger than the expected size.

The two other new constants, N_{14} and N_{15}, can be determined from $K \to \pi l^+ l^-$ decays. For these decays, the branching ratios can be expressed as [27]

$$\begin{aligned} \mathrm{BR}(K^+ \to \pi^+ e^+ e^-) &= (3.15 - 21.1 w_+ + 36.1 w_+^2) \cdot 10^{-20}\,|C\,G_8/(9\cdot\mathrm{GeV}^{-2})|^2 \\ \mathrm{BR}(K_S \to \pi^0 e^+ e^-) &= (3.07 - 18.7 w_S + 28.4 w_S^2) \cdot 10^{-22}\,|C\,G_8/(9\cdot\mathrm{GeV}^{-2})|^2 \end{aligned} \tag{3.42}$$

Using the measured central values [30]

$$\mathrm{BR}(K^+ \to \pi^+ e^+ e^-) = 2.88\cdot 10^{-7},\ \ \mathrm{BR}(K_S \to \pi^0 e^+ e^-) = 3.0\cdot 10^{-9} \tag{3.43}$$

one gets the results

$$w_+^{(1)} = 1.69,\ \ w_+^{(2)} = -1.10 \ \ \text{and}\ \ w_S^{(1)} = 1.93,\ \ w_S^{(2)} = -1.28. \tag{3.44}$$

	Centralvalue		
	Iso [9]	Strong [12]	Full
$K_L \to \pi^0\pi^0\pi^0$	$6.74 \cdot 10^{-12}$	$6.97 \cdot 10^{-12}$	$7.04 \cdot 10^{-12}$
$K_L \to \pi^+\pi^-\pi^0$	$7.46 \cdot 10^{-13}$	$7.66 \cdot 10^{-13}$	$7.88 \cdot 10^{-13}$
$K_S \to \pi^+\pi^-\pi^0$	0	0	0
$K^+ \to \pi^0\pi^0\pi^+$	$0.93 \cdot 10^{-13}$	$1.01 \cdot 10^{-12}$	$1.03 \cdot 10^{-12}$
$K^+ \to \pi^+\pi^+\pi^-$	$3.72 \cdot 10^{-12}$	$4.00 \cdot 10^{-12}$	$4.14 \cdot 10^{-12}$

Table 3.2: Comparison of the central values of the amplitudes squared in the isospin conserving case (Iso), including strong and local electromagnetic (Strong) and full (Full) isospin breaking.

These constants, w_+ and w_S, can then be written in terms of both strong and weak low-energy constants [27],

$$\begin{aligned} w_+ &= \frac{4}{3}(4\pi)^2[N_{14}^r(\mu) - N_{15}^r(\mu) + 3\,L_9^r(\mu)] - \frac{1}{3}\ln\frac{m_K m_\pi}{\mu^2} \\ w_S &= \frac{2}{3}(4\pi)^2[2\,N_{14}^r(\mu) + N_{15}^r(\mu)] - \frac{1}{3}\ln\frac{m_K^2}{\mu^2}, \end{aligned} \tag{3.45}$$

and from the knowledge of $L_9^r(\mu)$ [31], one gets the values listed in Table 3.1 for one choice of signs in eq. (3.44).

Note that the influence of this class of diagrams is not visible in the figures nor in the results shown in the tables for any of the possible signs chosen in eq. (3.44). The magnitude of these constants needs to be increased significantly in order to have a visible impact on our numerical results.

3.7.3 Results With and Without Isospin Breaking

The results we will present here is a comparison between the squared amplitudes and the decay rates in the isospin limit and including first order isospin breaking. The full squared amplitudes over the decay region is a 3-D plot with the two different cases plotted over phasespace. This is however very difficult to read, and instead we will present comparisons along three slices of these 3-D plots as explained below. We also present the corrections for the Dalitz plot parameters.

In Table 3.2 we present the values of the amplitudes squared in the center of the Dalitz plot, i.e. for $x = y = 0$. We show the results in the isospin limit from [9], with the strong and local electromagnetic isospin breaking included [12] and with full isospin breaking included.

Similarly, in Table 3.3 we present the integrated decay rates in the isospin conserving case [9], the one with strong and local electromagnetic isospin breaking included [12] and with all isospin breaking effects included. There are here

	Decay Rate			
	Iso [9]	Strong	Full	E_C [MeV]
$K_L \to \pi^0\pi^0\pi^0$	$2.65 \cdot 10^{-18}$	$2.74 \cdot 10^{-18}$	$2.77 \cdot 10^{-18}$	
$K_L \to \pi^+\pi^-\pi^0$	$1.63 \cdot 10^{-18}$	$1.67 \cdot 10^{-18}$	$1.72 \cdot 10^{-18}$	
$K_S \to \pi^+\pi^-\pi^0$	$3.1 \cdot 10^{-21}$	$3.2 \cdot 10^{-21}$	$3.3 \cdot 10^{-21}$	
$K^+ \to \pi^0\pi^0\pi^+$	$9.11 \cdot 10^{-19}$	$9.84 \cdot 10^{-19}$	$1.00 \cdot 10^{-18}$	
$K^+ \to \pi^+\pi^+\pi^-$	$2.97 \cdot 10^{-18}$	$3.19 \cdot 10^{-18}$	—	0
	$2.95 \cdot 10^{-18}$	$3.17 \cdot 10^{-18}$	$3.28 \cdot 10^{-18}$	1
	$2.91 \cdot 10^{-18}$	$3.13 \cdot 10^{-18}$	$3.24 \cdot 10^{-18}$	2
	$2.72 \cdot 10^{-18}$	$2.93 \cdot 10^{-18}$	$3.03 \cdot 10^{-18}$	5

Table 3.3: Comparison of the decay rates in the isospin conserving case (Iso), including strong and local electromagnetic (Strong) and full (Full) isospin breaking. The Coulomb cut-off used, E_C, is explained in the text.

in principle problems with an infinite correction when a charged two pion system is at rest. The effects of the electromagnetic interaction can then become very large from terms containing logarithms of the pion velocity. This is where the Coulomb interaction dominates and it should then really be resummed to all orders. In order to avoid this problem we have introduced the cut-off E_C. It means that we only integrate the phase space over the part where

$$\sqrt{s_i} \geq 2m_\pi + E_C \,. \tag{3.46}$$

Due to the way we have chosen the pion mass, the Coulomb problem only shows up for the decay $K^+ \to \pi^+\pi^+\pi^-$ where the systems of two charged pions can be at rest or at very low relative velocity at the edges of phase space. The places where this happens are indicated by the large dots in Fig. 3.6. The choice of the pion masses in $K_{L,S} \to \pi^+\pi^-\pi^0$ is such that the Coulomb threshold is slightly outside the physical phasespace. It turns out that in this case the part of the correction that includes the Coulomb singularity is rather small. We have therefore not included any corrections for it in the results presented.

In Fig. 3.6 we also show the phase space boundaries for the five different decays and the three curves along which we will show results for the squared amplitudes with and without isospin breaking. The three curves are $x = 0$, $y = 0$ and $x = \sqrt{3}\,y$. In Fig. 3.7 to Fig. 3.11 we then plot the five different squared amplitudes along these curves as a function of r, where $r = \pm\sqrt{y^2 + \frac{x^2}{3}}$ and the sign is chosen according to

$$r = \begin{cases} y, & x = 0 \\ x/\sqrt{3}, & y = 0 \\ y\,\sqrt{2}, & x = y\,\sqrt{3}\,. \end{cases} \tag{3.47}$$

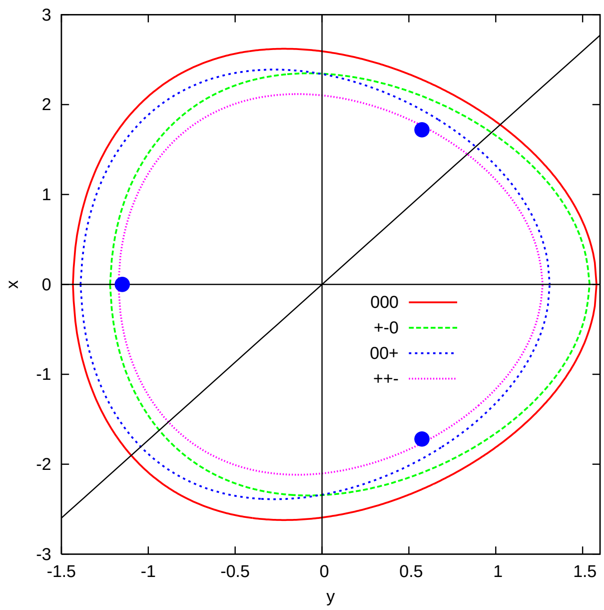

Figure 3.6: The phase space boundaries for the five different decays and the three curves along which we will compare the squared amplitudes. The points where two charged pions have low relative velocity for $K^+ \to \pi^+\pi^+\pi^-$ are indicated by the large dots.

Note that for all but A^S_{+-0} the squared amplitudes are normalized to their value at the center of the Dalitz plot. A comparison of the central values themselves is shown in Table 3.2.

We also calculate the changes in the Dalitz plot distribution parameters. These are defined by

$$\left|\frac{A(s_1,s_2,s_3)}{A(s_0,s_0,s_0)}\right|^2 = 1 + gy + hy^2 + kx^2\,. \tag{3.48}$$

The isospin breaking corrections to these parameters are given in Table 3.4. The amplitude for $K_S \to \pi^+\pi^-\pi^0$ is parametrized via

$$A^S_{+-0} = \gamma_S x - \xi_S xy\,. \tag{3.49}$$

We now discuss the results in somewhat more detail. In general the results are of a size as can be expected from this type of isospin breaking. They are of order a few, up to 11% in the amplitudes squared outside the Coulomb region.

Decay	Quantity	Iso [9]	Strong	Full
$K_L \to \pi^0\pi^0\pi^0$	h	-0.0072	-0.0068	-0.0068
$K_L \to \pi^+\pi^-\pi^0$	g	0.673	0.683	0.677
	h	0.085	0.089	0.088
	k	0.0055	0.0057	0.0057
$K_S \to \pi^+\pi^-\pi^0$	γ_S	$3.4 \cdot 10^{-8}$	$3.4 \cdot 10^{-8}$	$3.5 \cdot 10^{-8}$
	ξ_S	$-0.2 \cdot 10^{-8}$	$-0.2 \cdot 10^{-8}$	$-0.2 \cdot 10^{-8}$
$K^+ \to \pi^0\pi^0\pi^+$	g	0.635	0.619	0.619
	h	0.074	0.071	0.071
$K^+ \to \pi^+\pi^+\pi^-$	g	-0.215	-0.211	-0.201
	h	0.012	0.012	0.008
	k	-0.0052	-0.0050	-0.0037

Table 3.4: Comparison of the Dalitz plot distribution parameters in the isospin conserving case (Iso), including strong and local electromagnetic (Strong) and full (Full) isospin breaking.

The isospin breaking corrections tend to increase all decay rates somewhat and this will in a fit be compensated by small changes in the values of the $\tilde{K}_i$ compared to the results of [9]. The number of significant digits quoted in Table 3.2 is higher than the expected precision of our results, but the trend and the general size of the change compared to the isospin conserving results are stable with respect to variations in dealing with the eta mass (physical or GMO).

For $K_L \to \pi^0\pi^0\pi^0$ the central value of the amplitude squared increases by about 4.5%. In this case we have because of the symmetry of the final state that $g = 0$ and $k = h/3$. The quadratic slope decreases by about 5% but the total variation over the Dalitz plot is small so the total decay rate increases by about 4.5% as well. This decay is the one which has most variation in the amplitude when changing how one deals with the eta mass. The extreme case we have found was that this effect completely cancelled the change from isospin violation, but the relative change due to isospin breaking remained similar. Note the scale in Fig. 3.7 when viewing the result. The changes compared to [12] are entirely due to the photon loop corrections to F_{π^+} and F_{K^+}.

In Fig. 3.7 one can also clearly see the thresholds induced by the difference between $m^2_{\pi^+}$ and $m^2_{\pi^0}$ introduced when isospin invariance is broken. These thresholds correspond to a new process being allowed where two of the neutral pions are produced through an intermediate on shell state with one positive and one negative pion.

The squared amplitude $K_L \to \pi^+\pi^-\pi^0$ increases by about 5.5% with very little variation with the eta mass treatment. The decay rate increases by the same amount. The changes in the Dalitz plot slopes are rather small as can be

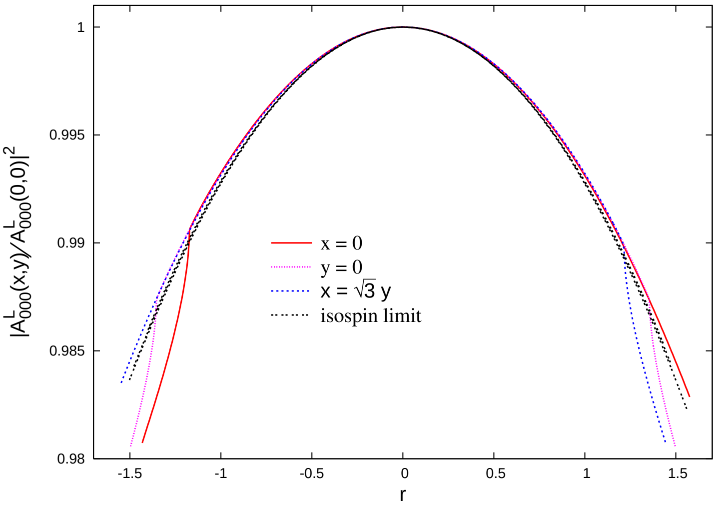

Figure 3.7: Comparison of $K_L \to \pi^0\pi^0\pi^0$ with and without isospin breaking.

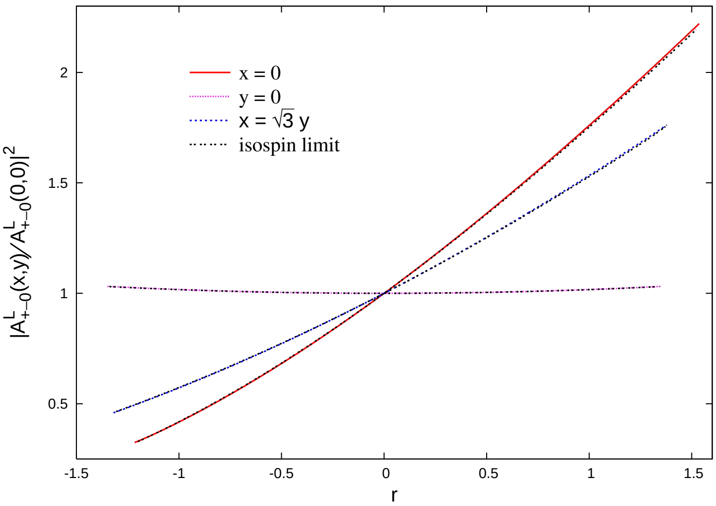

Figure 3.8: Comparison of $K_L \to \pi^+\pi^-\pi^0$ with and without isospin breaking.

judged from Fig. 3.8. The marginal differences compared to g quoted in [9] are due to a slightly different fitting procedure to the amplitudes squared.

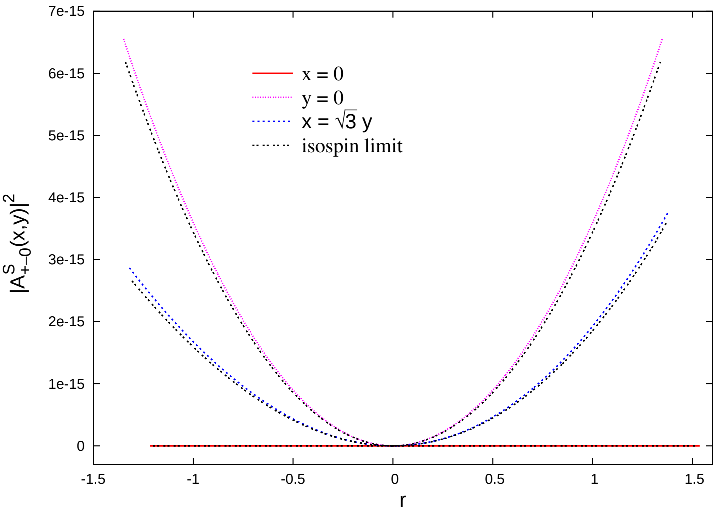

Figure 3.9: Comparison of $K_S \to \pi^+\pi^-\pi^0$ with and without isospin breaking.

For the decay $K_S \to \pi^+\pi^-\pi^0$ the amplitude in the center of the Dalitz plot vanishes because of the symmetries. The amplitude and the slopes increase by about 3% as can be seen in Fig. 3.9 and the tables.

The decay $K^+ \to \pi^0\pi^0\pi^+$ has a large increase. The squared amplitude in the center changes by about 11%. The linear slopes decrease somewhat leading to an increase of about 10% to the total decay rate when compared with the isospin conserved case. This is shown in Fig. 3.10.

The amplitude for $K^+ \to \pi^0\pi^0\pi^+$ is also calculated in [16]. Our result don't agree with the numerics presented there. We find an increase in the amplitude while there a decrease is found. In [16] a different lowest order is used than here and in [9, 12], but even after correcting for that we still disagree significantly with the results presented there.

The decay $K^+ \to \pi^+\pi^+\pi^-$ has a change of about 11% upwards in the center of the Dalitz plot. The slopes decrease somewhat. The decay rate can only be compared when the Coulomb region is excluded from the comparison but the total change is also about 11%.

The conclusions above do not change qualitatively when we give the K_i^r a value of about 0.001 and the new isospin breaking $\tilde{K}_i$ a value relative to G_8 and G_{27} of 0.01. However the changes induced by these values are numerically significant. They can be of the order of 10%, largest for $K_L \to \pi^0\pi^0\pi^0$.

It should be noted that the mentioned changes are with the values of $\tilde{K}_i$ determined from the isospin conserving fit in [9]. A new determination including

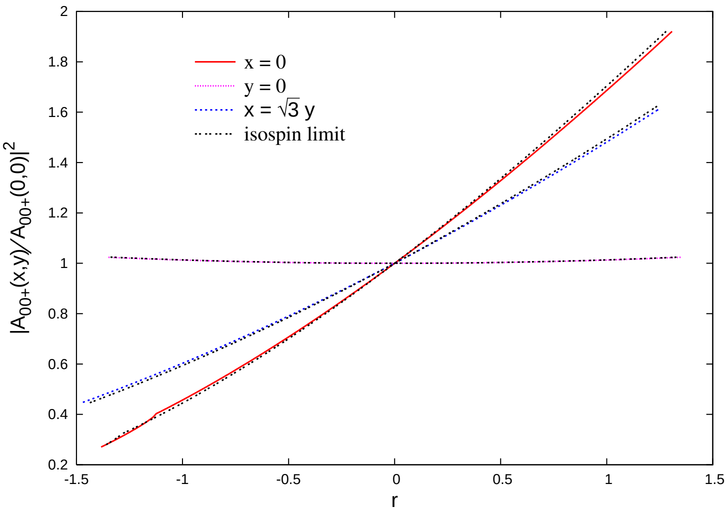

Figure 3.10: Comparison of $K^+ \to \pi^0\pi^0\pi^+$ with and without isospin breaking.

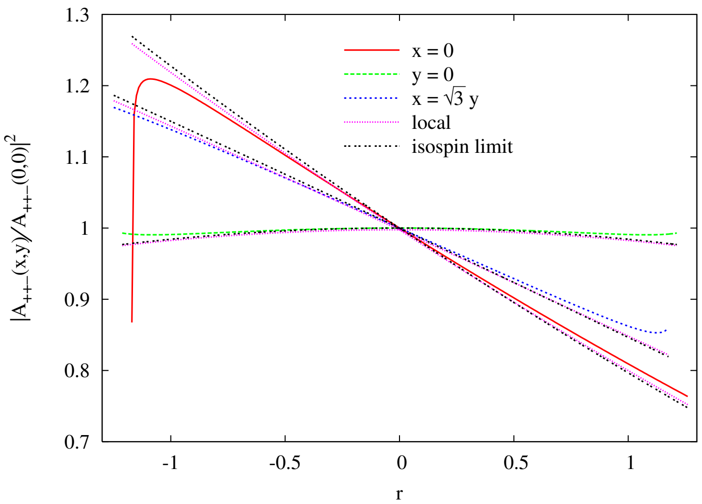

Figure 3.11: Comparison of $K^+ \to \pi^+\pi^+\pi^-$ with and without isospin breaking.

isospin breaking effects is planned in an upcoming paper.

3.8 Conclusions

We have calculated the $K \to 3\pi$ amplitudes to next-to-leading order (p^4, $p^2\,m^2$, m^4, $p^2\,e^2$) in Chiral Perturbation Theory. A similar calculation was done in [9] in the isospin limit, and in [12] including strong isospin breaking, but we have now included full isospin breaking. The motivations for this are both because it is interesting in general to see the importance of isospin breaking in this process, but also to investigate whether isospin violation will improve the fit to experimental data. Discrepancies between data and the quadratic slopes from ChPT were found in [9], and isospin breaking may be the cause of this.

We have estimated the effects of the isospin breaking by comparing the squared amplitudes with and without isospin violation. The effect seems to be at 5–10% percent level in the amplitudes squared. To investigate if this removes the discrepancies found in [9] a new full fit has to be done, also including the new data [13, 14] published after [9]. This is work in progress and will be presented in the future paper Isospin Breaking in $K \to 3\pi$ Decays III.

Acknowledgments

The program FORM 3.0 has been used extensively in these calculations [32]. This work is supported in part by the Swedish Research Council and European Union TMR network, Contract No. HPRN-CT-2002-00311 (EURIDICE).

3.A The Decay Constants F_{π^+} and F_{K^+}.

We have chosen to normalize our lowest order contribution with $F_0^4/(F_{\pi^+}^3 F_{K^+})$. F_{π^+} and F_{K^+} are the pion and kaon decay constants respectively. Including isospin breaking they are determined from the diagrams in Fig. 3.12 and the resulting expressions are

$$
\begin{aligned}
F_{\pi^+} = F_0 \Bigg\{ 1 + \frac{1}{F_0^2} \Bigg[& \\
& F_0^2 e^2 \Big(4/3\,K_1^r + 4/3\,K_2^r + 10/9\,K_5^r + 10/9\,K_6^r + 2\,K_{12}^r \\
& +2\,\frac{\partial}{\partial q^2}\overline{B}(m_\gamma^2, m_\pi^2, m_\pi^2)\,m_\pi^2 - \overline{B}_1(m_\gamma^2, m_\pi^2, m_\pi^2) - 2\,\frac{\partial}{\partial q^2}\overline{B}_1(m_\gamma^2, m_\pi^2, m_\pi^2)\,m_\pi^2 \Big) \\
& +L_4^r \Big(16\,m_\pi^2\,\frac{\sin\epsilon}{\sqrt{3}} - 16\,m_K^2\,\frac{\sin\epsilon}{\sqrt{3}} + 4\,m_{\pi^0}^2 + 8\,m_{K^0}^2 \Big) \\
& +L_5^r \Big(4\,m_{\pi^0}^2 \Big) + 1/2\,\overline{A}(m_{\pi^+}^2) + 1/2\,\overline{A}(m_{\pi^0}^2)
\end{aligned}
$$

Figure 3.12: Diagrams for the decay constants. An open square is a vertex from $\mathcal{L}_{W4}$ or $\mathcal{L}_{W2E2}$, a filled square a vertex from $\mathcal{L}_{W2}$ or $\mathcal{L}_{E2}\,(\Delta S = 1)$ and a filled circle a vertex from $\mathcal{L}_{S2}$ or $\mathcal{L}_{E2}\,(\Delta S = 0)$. A straight line is a pseudoscalar meson and a wiggly line a photon.

$$+1/4\,\overline{A}(m_{K^+}^2) + 1/4\,\overline{A}(m_{K^0}^2)\Big]\Big\} \tag{A.1}$$

and

$$\begin{aligned}
F_{K^+} = F_0\Bigg\{1 + \frac{1}{F_0^2}\Bigg[\\
& F_0^2\,e^2\Big(4/3\,K_1^r + 4/3\,K_2^r + 10/9\,K_5^r + 10/9\,K_6^r + 2\,K_{12}^r \\
& +2\,\frac{\partial}{\partial q^2}\overline{B}(m_\gamma^2, m_K^2, m_K^2)\,m_K^2 - \overline{B}_1(m_\gamma^2, m_K^2, m_K^2) \\
& -2\,\frac{\partial}{\partial q^2}\overline{B}_1(m_\gamma^2, m_K^2, m_K^2)\,m_K^2\Big) \\
& +L_4^r\Big(16\,m_\pi^2\,\frac{\sin\epsilon}{\sqrt{3}} - 16\,m_K^2\,\frac{\sin\epsilon}{\sqrt{3}} + 4\,m_{\pi^0}^2 + 8\,m_{K^0}^2\Big) \\
& +L_5^r\Big(16\,m_\pi^2\,\frac{\sin\epsilon}{\sqrt{3}} - 16\,m_K^2\,\frac{\sin\epsilon}{\sqrt{3}} + 4\,m_{K^0}^2\Big) \\
& +3/4\,\frac{\sin\epsilon}{\sqrt{3}}\,\overline{A}(m_\pi^2) + 1/4\,\overline{A}(m_{\pi^+}^2) + 1/8\,\overline{A}(m_{\pi^0}^2) \\
& +1/2\,\overline{A}(m_{K^+}^2) + 1/4\,\overline{A}(m_{K^0}^2) + \overline{A}(m_\eta^2)\Big(3/8 - 3/4\,\frac{\sin\epsilon}{\sqrt{3}}\Big)\Bigg]\Bigg\}.
\end{aligned} \tag{A.2}$$

These formulas agree with known results [3, 33].

The above formulas are infrared divergent when $m_\gamma \to 0$, and the standard way to deal with this is the same as in the amplitudes, i.e. adding a bremsstrahlung diagram. We have chosen to just add a term including a cut-off scale for the bremsstrahlung photon,

$$-|A|_{LO}\,\frac{e^2}{4\pi^2}\,\log\frac{\omega_F^2}{m_\gamma^2}\,, \qquad \text{(A.3)}$$

which cancels the dependence on the photon mass and therefore removes the divergence. The scale ω_F is set to 10 MeV.

References

[1] S. Weinberg, Physica A **96** (1979) 327.

[2] J. Gasser and H. Leutwyler, Annals Phys. **158** (1984) 142.

[3] J. Gasser and H. Leutwyler, Nucl. Phys. B **250** (1985) 465.

[4] Pich, A., Lectures at Les Houches Summer School in Theoretical Physics, Session 68: Probing the Standard Model of Particle Interactions, Les Houches, France, 28 Jul - 5 Sep 1997, [hep-ph/9806303];
Ecker, G., Lectures given at Advanced School on Quantum Chromodynamics (QCD 2000), Benasque, Huesca, Spain, 3-6 Jul 2000, [hep-ph/0011026].

[5] J. Kambor, J. Missimer and D. Wyler, Nucl. Phys. B **346** (1990) 17.

[6] J. Kambor, J. Missimer and D. Wyler, Phys. Lett. B **261** (1991) 496.

[7] G. Ecker, Prog. Part. Nucl. Phys. **35** (1995) 1, [hep-ph/9501357];
A. Pich, Rept. Prog. Phys. **58** (1995) 563, [hep-ph/9502366];
E. de Rafael, Lectures given at Theoretical Advanced Study Institute in Elementary Particle Physics (TASI 94): CP Violation and the limits of the Standard Model, Boulder, CO, 29 May - 24 Jun 1994, [hep-ph/9502254].

[8] J. Bijnens, E. Pallante and J. Prades, Nucl. Phys. B **521** (1998) 305, [hep-ph/9801326].

[9] J. Bijnens, P. Dhonte and F. Persson, Nucl. Phys. B 648 (2003) 317, [hep-ph/0205341].

[10] E. Gamiz, J. Prades and I. Scimemi, JHEP **0310** (2003) 042 [hep-ph/0309172].

[11] J. Bijnens and M. B. Wise, Phys. Lett. B **137** (1984) 245;
B. R. Holstein, Phys. Rev. D **20** (1979) 1187;
S. Gardner and G. Valencia, Phys. Rev. D **62** (2000) 094024, [hep-ph/0006240], C. E. Wolfe and K. Maltman, Phys. Lett. B **482** (2000) 77 [hep-ph/9912254]; V. Cirigliano, J. F. Donoghue and E. Golowich, Phys.

Lett. B **450** (1999) 24; V. Cirigliano, G. Ecker, H. Neufeld and A. Pich, Eur. Phys. J. C **33** (2004) 369 [arXiv:hep-ph/0310351].

[12] J. Bijnens and F. Borg, Nucl. Phys. B **697** (2004) 319 [arXiv:hep-ph/0405025].

[13] I. V. Ajinenko *et al.*, Phys. Lett. B **567**, 159 (2003) [hep-ex/0205027].

[14] A. Aloisio *et al.* [KLOE Collaboration], hep-ex/0307054.

[15] N. Cabibbo, [hep-ph/0405001].

[16] A. Nehme, [hep-ph/0406209].

[17] G. Amorós, J. Bijnens, P. Talavera Nucl. Phys. B 602 (2001) 87,[hep-ph/0101127].

[18] J. A. Cronin, Phys. Rev. **161** (1967) 1483.

[19] G. Ecker, G. Isidori, G. Muller, H. Neufeld and A. Pich, Nucl. Phys. B **591** (2000) 419, [hep-ph/0006172].

[20] V. Cirigliano, M. Knecht, H. Neufeld, H. Rupertsberger and P. Talavera, Eur. Phys. J. C **23**, 121 (2002) [hep-ph/0110153].

[21] G. Esposito-Farese, Z. Phys. C **50** (1991) 255.

[22] G. Ecker, J. Kambor and D. Wyler, Nucl. Phys. B **394** (1993) 101, [hep-ph/0006172].

[23] R. Urech, Nucl. Phys. B **433**, 234 (1995) [hep-ph/9405341].

[24] G. Amorós, J. Bijnens and P. Talavera, Nucl. Phys. B **568** (2000) 319, [hep-ph/9907264].

[25] G. J. van Oldenborgh, Comput. Phys. Commun. **66** (1991) 1; G. J. van Oldenborgh and J. A. M. Vermaseren, Z. Phys. C **46** (1990) 425.

[26] Peskin, Schroeder, "An Introduction to Quantum Field Theory "

[27] G. Ecker, A. Pich and E. de Rafael, Nucl. Phys. B **291** (1987) 692.

[28] These can be downloaded from `http://www.thep.lu.se/~bijnens/chpt.html`.

[29] J. Bijnens and J. Prades, JHEP **0006** (2000) 035 [hep-ph/0005189].

[30] S. Eidelman *et al.* [Particle Data Group Collaboration], Phys. Lett. B **592**, 1 (2004).

[31] J. Bijnens and P. Talavera, JHEP **0203** (2002) 046 [hep-ph/0203049].

[32] J. A. Vermaseren, math-ph/0010025.

[33] H. Neufeld and H. Rupertsberger, Z. Phys. C **71** (1996) 131 [hep-ph/9506448].

Isospin Breaking in $K \to 3\pi$ Decays III: Bremsstrahlung and Fit to Experiment

Paper IV

Isospin Breaking in $K \to 3\pi$ Decays III: Bremsstrahlung and Fit to Experiment[1]

Johan Bijnens and Fredrik Borg

Department of Theoretical Physics, Lund University
Sölvegatan 14A, S 22362 Lund, Sweden

Abstract:

We complete here our work on isospin violation in the $K \to 3\pi$ system. We first calculate $K \to 2\pi$ to the same order as we did $K \to 3\pi$ in papers I and II of this series. This adds effects of order $G_{27}\, p^2(m_u - m_d)$ and $G_{27}\, p^2 e^2$ to earlier work. We calculate also the lowest order Bremsstrahlung contributions, $K \to 2\pi\gamma, 3\pi\gamma$. With these and our earlier results we perform a full fit to all available CP conserving data in the $K \to 2\pi, 3\pi$ system including isospin violation effects. We perform these fits under various input assumptions as well as test the factorization and the vector dominance model for the weak NLO low energy constants.

[1]LU TP 04-40

4.1 Introduction

Low-energy QCD is non-perturbative, which calls for alternative methods of calculating processes including composite particles such as mesons and baryons. A method used to describe the interactions of the light pseudoscalar mesons (K, π, η) is Chiral Perturbation Theory (ChPT). It was first presented by Weinberg, Gasser and Leutwyler [1–3] and it has been very successful. Pedagogical introductions to ChPT can be found in [4]. The theory can be extended to also cover the weak interactions of the pseudoscalars, first done in [5].

The first calculation of a kaon decaying into pions $(K \to 2\pi, 3\pi)$ was presented in [6], and reviews of other applications of ChPT to nonleptonic weak interactions can be found in [7].

The details from [6] were lost, but a recalculation in the isospin limit of $K \to 2\pi$ to next-to-leading order was made in [8, 9] and of $K \to 3\pi$ in [9, 10]. In [9] a full fit to all experimental data existing at the time was made, and it was found that the decay rates and linear slopes agreed well. However, a small discrepancy was found in the quadratic slopes, and this can have several different origins. It could be an experimental problem or it could have a theoretical origin. In the latter case the corrections to the amplitude calculated in [9] are threefold: strong isospin breaking, electromagnetic (EM) isospin breaking or higher order corrections.

In [11] the strong isospin and local electromagnetic corrections were investigated and it was found that the inclusion of those led to changes of a few percent in the amplitudes. The local electromagnetic part was also calculated in [10], in full agreement with our result after sorting out some misprints in [10], corrected in [12]. In [13] the radiative corrections were added, which means that the full effects of isospin breaking were studied. This led to changes in the amplitudes of order 5–10 percent. Note that the results in [13] disagree numerically with the results for $K^+ \to \pi^0\pi^0\pi^+$ of [14].

To answer the question whether isospin breaking removes the problem of fitting the quadratic slopes, a new full fit has to be done. That is the main result in this paper, and in this new fit we also include new experimental data [15,16]. We also present recalculations of the amplitudes $K \to 2\pi$, $K \to 2\pi\gamma$ and $K \to 3\pi\gamma$, all calculated to next-to-leading order and including first order isospin breaking, i.e. we include contributions proportional to p^2, m^2, e^2, $m_u - m_d$ (leading order), and $p^2 e^2$, $m^2 e^2$, $p^2(m_u - m_d)$ and $m^2(m_u - m_d)$ (next-to-leading order). The corrections needed to be added to determine $\pi\pi$ scattering lengths from $K \to 3\pi$ [17] are beyond the order calculated in this paper.

The outline of this paper is as follows. The next section describes isospin breaking in more detail. In section 4.3 the basis of ChPT, the Chiral Lagrangians, are discussed. Section 4.4 specifies the decays and describes the relevant kinematics. The divergences appearing when including photons are discussed in section 4.5. In section 4.6 the analytical results are discussed, section

4.7 contains the numerical results and the last section contains the summary.

4.2 Isospin Breaking

Isospin symmetry is the SU(2) symmetry under the exchange of up- and down-quarks. This symmetry is only exact in the approximation that $m_u = m_d$ and electromagnetism is neglected, i.e. in the isospin limit. Calculations are sometimes performed in the isospin limit since this is simpler and gives a good first estimate of the result. However, to get a more accurate result one should include the effects from $m_u \neq m_d$ and electromagnetism, i.e. isospin breaking.

The two different sources of isospin breaking give rise to different effects. Strong isospin breaking, coming from $m_u \neq m_d$, include mixing between π^0 and η. This mixing leads to changes in the formulas for both the physical masses of π^0 and η as well as the amplitude for any process involving either of the two. For a detailed discussion see [18].

The other source, electromagnetic isospin breaking, coming from the fact that the up- and the down-quarks are charged, implies interactions with photons. This means both the addition of new Lagrangians at each order, as well as the introduction of new diagrams including explicit photons.

4.3 The ChPT Lagrangians

The basis of our ChPT calculation is the various Chiral Lagrangians of relevant orders. We work to leading order in $m_u - m_d$ and e^2 but next-to-leading order in p^2 and m^2. For simplicity we call in the remainder terms of order p^2, m^2, e^2, $m_u - m_d$ leading order and terms of order p^4 ,$p^2\, m^2$, m^4, $p^2\, e^2$, $m^2\, e^2$, $p^2(m_u - m_d)$ and $m^2(m_u - m_d)$ next-to-leading order.

4.3.1 Leading Order

The lowest order Chiral Lagrangian is divided in three parts

$$\mathcal{L}_2 = \mathcal{L}_{S2} + \mathcal{L}_{W2} + \mathcal{L}_{E2}, \tag{4.1}$$

where $\mathcal{L}_{S2}$ refers to the strong $\Delta S = 0$ part, $\mathcal{L}_{W2}$ the weak $\Delta S = \pm 1$ part, and $\mathcal{L}_{E2}$ the strong-electromagnetic and weak-electromagnetic parts combined. For the strong part we have [2]

$$\mathcal{L}_{S2} = \frac{F_0^2}{4} \langle u_\mu u^\mu + \chi_+ \rangle \,. \tag{4.2}$$

Here $\langle A \rangle$ stands for the flavour trace of the matrix A, and F_0 is the pion decay constant in the chiral limit. We define the matrices u_μ, u and $\chi_\pm$ as

$$u_\mu = i u^\dagger\, D_\mu U\, u^\dagger = u_\mu^\dagger \,, \quad u^2 = U \,, \quad \chi_\pm = u^\dagger \chi u^\dagger \pm u \chi^\dagger u \,, \tag{4.3}$$

where the special unitary matrix U contains the Goldstone boson fields

$$U = \exp\left(\frac{i\sqrt{2}}{F_0}M\right)\ ,\ M = \begin{pmatrix} \frac{1}{\sqrt{2}}\pi_3 + \frac{1}{\sqrt{6}}\eta_8 & \pi^+ & K^+ \\ \pi^- & \frac{-1}{\sqrt{2}}\pi_3 + \frac{1}{\sqrt{6}}\eta_8 & K^0 \\ K^- & \overline{K^0} & \frac{-2}{\sqrt{6}}\eta_8 \end{pmatrix}\ . \quad (4.4)$$

We use the formalism of the external field method [2], and to include photons we set

$$\chi = 2B_0 \begin{pmatrix} m_u & & \\ & m_d & \\ & & m_s \end{pmatrix} \quad \text{and} \quad D_\mu U = \partial_\mu U - ie\,QA_\mu U - ie\,UQA_\mu, \quad (4.5)$$

where A_μ is the photon field and

$$Q = \begin{pmatrix} 2/3 & & \\ & -1/3 & \\ & & -1/3 \end{pmatrix}. \quad (4.6)$$

The quadratic terms in (4.2) are diagonalized by a rotation

$$\begin{aligned} \pi^0 &= \pi_3 \cos\epsilon + \eta_8 \sin\epsilon \\ \eta &= -\pi_3 \sin\epsilon + \eta_8 \cos\epsilon\,, \end{aligned} \quad (4.7)$$

where the lowest order mixing angle ϵ satisfies

$$\tan(2\epsilon) = \sqrt{3}\frac{m_d - m_u}{2\,m_s - m_u - m_d}\,. \quad (4.8)$$

The weak, $\Delta S = 1$, part of the Lagrangian has the form [19]

$$\mathcal{L}_{W2} = C\,F_0^4 \left[G_8\langle\Delta_{32}u_\mu u^\mu\rangle + G_8'\langle\Delta_{32}\chi_+\rangle + G_{27}t^{ij,kl}\,\langle\Delta_{ij}u_\mu\rangle\langle\Delta_{kl}u^\mu\rangle\right] + \text{ h.c.}\,. \quad (4.9)$$

The tensor $t^{ij,kl}$ has as nonzero components

$$\begin{aligned} t^{21,13} = t^{13,21} &= \frac{1}{3}\,, \qquad t^{22,23} = t^{23,22} = -\frac{1}{6}\,, \\ t^{23,33} = t^{33,23} &= -\frac{1}{6}\,, \qquad t^{23,11} = t^{11,23} = \frac{1}{3}\,, \end{aligned} \quad (4.10)$$

and the matrix Δ_{ij} is defined as

$$\Delta_{ij} \equiv u\lambda_{ij}u^\dagger\,, \quad (\lambda_{ij})_{ab} \equiv \delta_{ia}\,\delta_{jb}\,. \quad (4.11)$$

The coefficient C is defined such that in the chiral and large N_c limits $G_8 = G_{27} = 1$,

$$C = -\frac{3}{5}\,\frac{G_F}{\sqrt{2}} V_{ud}\, V_{us}^* = -1.06 \cdot 10^{-6}\ \mathrm{GeV}^{-2}\,. \tag{4.12}$$

Finally, the remaining electromagnetic part, relevant for this calculation, looks like (see e.g. [20])

$$\mathcal{L}_{E2} = e^2 F_0^4 Z \langle \mathcal{Q}_L \mathcal{Q}_R \rangle + e^2 F_0^4 \langle \Upsilon \mathcal{Q}_R \rangle\,, \tag{4.13}$$

where the weak-electromagnetic term is multiplied by a constant G_E ($g_{\mathrm{ewk}} G_8$ in [20]),

$$\Upsilon = G_E\, F_0^2 \Delta_{32} + \mathrm{h.c.} \tag{4.14}$$

and

$$\mathcal{Q}_L = u Q u^\dagger\,,\ \ \mathcal{Q}_R = u^\dagger Q u\,. \tag{4.15}$$

4.3.2 Next-to-leading Order

Chiral Perturbation Theory is a non-renormalizable theory. This means that new terms have to be added at each order to compensate for the divergences coming from loop-diagrams. Thus the Lagrangians increase in size for every new order and the number of free parameters rises as well. At next-to-leading order the Lagrangian is split in four parts which, in obvious notation, are

$$\mathcal{L}_4 = \mathcal{L}_{S4} + \mathcal{L}_{W4} + \mathcal{L}_{S2E2} + \mathcal{L}_{W2E2}(G_8)\,. \tag{4.16}$$

The notation (G_8) indicates that here only the dominant G_8-part is included in the Lagrangian and therefore in the calculation.

The Lagrangians of next-to-leading order are quite large and we will not write them explicitly here since they can be found in many places [2, 5, 20–24]. For a list of all the pieces relevant for this specific calculation see [11, 13]. Note however that one contributing term was forgotten when writing $\mathcal{L}_{S2E2}$ in [11], namely

$$-i\, e^2\, F_0^2\, K_{12}\, \langle (\widehat{\nabla}_\mu \mathcal{Q}_L \mathcal{Q}_L - \mathcal{Q}_L \widehat{\nabla}_\mu \mathcal{Q}_L - \widehat{\nabla}_\mu \mathcal{Q}_R \mathcal{Q}_R + \mathcal{Q}_R \widehat{\nabla}_\mu \mathcal{Q}_R)\, u^\mu \rangle\,, \tag{4.17}$$

where

$$\begin{aligned} \widehat{\nabla}_\mu \mathcal{Q}_L &= \nabla_\mu \mathcal{Q}_L + \frac{i}{2}[u_\mu, \mathcal{Q}_L] = u D_\mu Q_L u^\dagger, \\ \widehat{\nabla}_\mu \mathcal{Q}_R &= \nabla_\mu \mathcal{Q}_R - \frac{i}{2}[u_\mu, \mathcal{Q}_R] = u^\dagger D_\mu Q_R u\,. \end{aligned} \tag{4.18}$$

It contributes to the calculation of the decay constants, F_{π^+} and F_{K^+}. It only contributes to the amplitudes of $K \to 2\pi$ and $K \to 3\pi$ via the rewriting of the lowest order in terms of F_{π^+} and F_{K^+} rather than F_0.

4.3.2.1 Ultraviolet Divergences

The processes $K \to 2\pi$ and $K \to 3\pi$ receives higher-order contributions from diagrams that contain loops. The study of these diagrams is complicated by the fact that they need to be precisely defined. The loop-diagrams involve an integration over the loop-momentum Q, and the integrals are divergent in the ultraviolet region, i.e. when $Q \to \infty$. These ultraviolet divergences are canceled by replacing the coefficients, X_i, in the next-to-leading order Lagrangians by the renormalized coefficients, X_i^r, and a subtraction part. See [9,11] and references therein.

4.4 Kinematics

4.4.1 $K \to 2\pi$ and $K \to 2\pi\gamma$

In the limit of CP-conservation, there are three different decays of the type $K \to 2\pi$ (K^- decays are not treated separately since they are counterparts to the K^+ decays):

$$\begin{aligned} K_S(k) &\to \pi^0(p_1)\,\pi^0(p_2)\,, \quad [A^S_{00}]\,, \\ K_S(k) &\to \pi^+(p_1)\,\pi^-(p_2)\,, \quad [A^S_{+-}]\,, \\ K^+(k) &\to \pi^+(p_1)\,\pi^0(p_2)\,, \quad [A_{+0}], \end{aligned} \tag{4.19}$$

where we have indicated the four-momentum defined for each particle and the symbol used for the amplitude. With an external photon it changes to:

$$\begin{aligned} K_S(k) &\to \pi^0(p_1)\,\pi^0(p_2)\,\gamma\,(q)\,, \quad [A^S_{00\gamma}]\,, \\ K_S(k) &\to \pi^+(p_1)\,\pi^-(p_2)\,\gamma\,(q)\,, \quad [A^S_{+-\gamma}]\,, \\ K^+(k) &\to \pi^+(p_1)\,\pi^0(p_2)\,\gamma\,(q)\,, \quad [A_{+0\gamma}]\,. \end{aligned} \tag{4.20}$$

The kinematics for $K \to 2\pi\gamma$ is treated using

$$r_0 \equiv -k \cdot q\,, \quad r_1 \equiv p_1 \cdot q\,, \quad r_2 \equiv p_2 \cdot q\,, \tag{4.21}$$

where

$$r_0 + r_1 + r_2 = 0\,. \tag{4.22}$$

4.4.2 $K \to 3\pi$ and $K \to 3\pi\gamma$

For the corresponding process $K \to 3\pi$, there are five different decays:

$$\begin{aligned} K_L(k) &\to \pi^0(p_1)\,\pi^0(p_2)\,\pi^0(p_3)\,, \quad [A^L_{000}]\,, \\ K_L(k) &\to \pi^+(p_1)\,\pi^-(p_2)\,\pi^0(p_3)\,, \quad [A^L_{+-0}]\,, \end{aligned}$$

$$
\begin{array}{rcll}
K_S(k) & \to & \pi^+(p_1)\,\pi^-(p_2)\,\pi^0(p_3)\,, & [A^S_{+-0}]\,,\\
K^+(k) & \to & \pi^0(p_1)\,\pi^0(p_2)\,\pi^+(p_3)\,, & [A_{00+}]\,,\\
K^+(k) & \to & \pi^+(p_1)\,\pi^+(p_2)\,\pi^-(p_3)\,, & [A_{++-}]\,,
\end{array}
\tag{4.23}
$$

and here the variables are

$$
s_1 \equiv (k-p_1)^2\;, \quad s_2 \equiv (k-p_2)^2\;, \quad s_3 \equiv (k-p_3)^2\;, \tag{4.24}
$$

where

$$
s_1 + s_2 + s_3 = k^2 + p_1^2 + p_2^2 + p_3^2\,. \tag{4.25}
$$

The amplitudes are expanded in terms of the Dalitz plot variables x and y defined as

$$
y = \frac{s_3 - s_0}{m^2_{\pi^+}}\,, \quad x = \frac{s_2 - s_1}{m^2_{\pi^+}}\,, \quad s_0 = \frac{1}{3}\left(s_1 + s_2 + s_3\right)\,. \tag{4.26}
$$

With an external photon the decays are:

$$
\begin{array}{rcll}
K_L(k) & \to & \pi^0(p_1)\,\pi^0(p_2)\,\pi^0(p_3)\,\gamma\,(q)\,, & [A^L_{000\gamma}]\,,\\
K_L(k) & \to & \pi^+(p_1)\,\pi^-(p_2)\,\pi^0(p_3)\,\gamma\,(q)\,, & [A^L_{+-0\gamma}]\,,\\
K_S(k) & \to & \pi^+(p_1)\,\pi^-(p_2)\,\pi^0(p_3)\,\gamma\,(q)\,, & [A^S_{+-0\gamma}]\,,\\
K^+(k) & \to & \pi^0(p_1)\,\pi^0(p_2)\,\pi^+(p_3)\,\gamma\,(q)\,, & [A_{00+\gamma}]\,,\\
K^+(k) & \to & \pi^+(p_1)\,\pi^+(p_2)\,\pi^-(p_3)\,\gamma\,(q)\,, & [A_{++-\gamma}]\,,
\end{array}
\tag{4.27}
$$

where the kinematics is treated using

$$
s_{1\gamma} \equiv (k-p_1)^2\;, \quad s_{2\gamma} \equiv (k-p_2)^2\;, \quad s_{3\gamma} \equiv (k-p_3)^2\;, \tag{4.28}
$$

$$
t_0 \equiv -k\cdot q\,, \quad t_1 \equiv p_1\cdot q\,, \quad t_2 \equiv p_2\cdot q\,, \quad t_3 \equiv p_3\cdot q\,, \tag{4.29}
$$

where

$$
t_0 + t_1 + t_2 + t_3 = 0 \quad \text{and} \quad s_{1\gamma} + s_{2\gamma} + s_{3\gamma} = k^2 + p_1^2 + p_2^2 + p_3^2 - 2\,t_0\,. \tag{4.30}
$$

4.5 Infrared Divergences

Beside the ultraviolet divergences which are removed by renormalization of the higher order coefficients, diagrams including photons in the loops contain infrared (IR) divergences. These infinities come from the $Q \to 0$ end of the loop-momentum integrals. They are handled by including also the Bremsstrahlung process, where a real photon is radiated off one of the charged mesons. It is only the sum of the virtual loop corrections and the real Bremsstrahlung which is physically significant and thus needs to be well defined.

We regulate the IR divergences in both the virtual photon loops and the real emission with a photon mass m_γ and keep only the singular terms plus those that do not vanish in the limit $m_\gamma \to 0$. We include the real Bremsstrahlung for photon energies up to a cut-off ω and treat it in the soft photon approximation.

The exact form of the amplitude squared for the Bremsstrahlung depends on which specific amplitude that is being calculated. For a detailed presentation of the calculation and resulting expressions for $K \to 3\pi$ see [13]. The corresponding amplitudes for $K \to 2\pi$ are

$$|A^S_{00}|^2_{BS} = 0\,, \tag{4.31}$$

$$|A^S_{+-}|^2_{BS} = -|A^S_{+-}|^2_{LO}\,\frac{e^2}{4\pi^2}\left[\log\frac{\omega^2}{m_\gamma^2} - I_{IR}(m_\pi^2, m_\pi^2, m_K^2)\right]\,, \tag{4.32}$$

$$|A_{+0}|^2_{BS} = -|A_{+0}|^2_{LO}\,\frac{e^2}{4\pi^2}\left[\log\frac{\omega^2}{m_\gamma^2} - I_{IR}(m_\pi^2, m_K^2, m_\pi^2)\right]\,. \tag{4.33}$$

When using these expressions, the divergences from the photon loops cancel exactly.

A similar problem shows up in the definition of the decay constants, since we normalize the lowest order with F_{π^+} and F_{K^+}. See [13] for details.

4.6 Analytical Results

4.6.1 $K \to 2\pi$

The most complete work on isospin violation in $K \to 2\pi$ is in [25], earlier work can be found in [26].

4.6.1.1 Lowest Order

There is only one diagram contributing to the decay $K \to 2\pi$ at lowest order, see top left in Fig. 4.1, and the resulting amplitudes are also quite simple. To first order in isospin they can be written

$$A^S_{00} = i\,F\,(G_8 - G_{27})\left(4\,\frac{\sin\epsilon}{\sqrt{3}}\,m_\pi^2 - 4\,\frac{\sin\epsilon}{\sqrt{3}}\,m_K^2 - 2\,m_{\pi^0}^2 + 2\,m_{K^0}^2\right)\,, \tag{4.34}$$

$$\begin{aligned} A^S_{+-} \;&=\; i\,F\,G_8\,(-2\,m_{\pi^+}^2 + 2\,m_{K^0}^2) + i\,F\,G_{27}\left(-\frac{4}{3}\,m_{\pi^+}^2 + \frac{4}{3}\,m_{K^+}^2\right) \\ &\quad -2\,i\,F^3\,e^2\,G_E\,, \end{aligned} \tag{4.35}$$

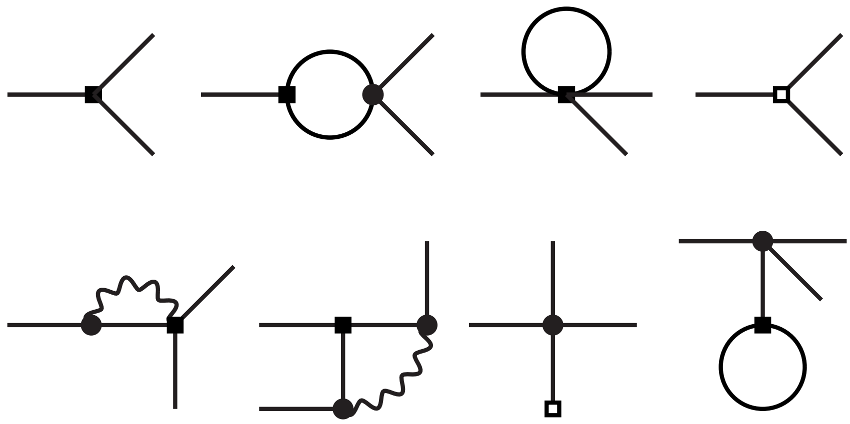

Figure 4.1: The diagrams for $K \to 2\pi$. An open square is a vertex from $\mathcal{L}_{W4}$ or $\mathcal{L}_{W2E2}$, a filled square a vertex from $\mathcal{L}_{W2}$ or $\mathcal{L}_{E2}$ ($\Delta S = 1$) and a filled circle a vertex from $\mathcal{L}_{S2}$ or $\mathcal{L}_{E2}$ ($\Delta S = 0$). A straight line is a pseudoscalar meson and a wiggly line a photon.

$$
\begin{aligned}
A_{+0} \quad = \quad & i\,F\,G_8 \left(-2\,\frac{\sin\epsilon}{\sqrt{3}}\,m_\pi^2 + 2\,\frac{\sin\epsilon}{\sqrt{3}}\,m_K^2 - m_{\pi^+}^2 + m_{\pi^0}^2\right) - i\,F^3\,e^2\,G_E \\
& + i\,F\,G_{27} \left(-3\,\frac{\sin\epsilon}{\sqrt{3}}\,m_\pi^2 + 3\,\frac{\sin\epsilon}{\sqrt{3}}\,m_K^2 - 7/3\,m_{\pi^+}^2 \right. \\
& \left. + 2/3\,m_{\pi^0}^2 + 5/3\,m_{K^+}^2\right) . \qquad (4.36)
\end{aligned}
$$

See section 4.7.1.1 for a discussion of the masses used.

4.6.1.2 Next-to-leading Order

There are seven more diagrams contributing to next-to-leading order, see Fig. 4.1. The resulting amplitudes are long, and we decided to not include them here but instead make them available for download [27]. Note that we have also included contributions proportional to G_{27}, not included in [25]. These are included for consistency between the $K \to 2\pi(\gamma)$ and $K \to 3\pi(\gamma)$ calculations.

4.6.2 $K \to 2\pi\gamma$

The amplitudes for the processes $K \to 2\pi\gamma$ have been calculated before. Here we only need the lowest order contribution to be consistent with the $K \to 2\pi$

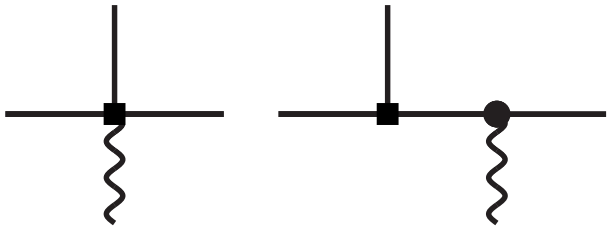

Figure 4.2: The diagrams for $K \to 2\pi\gamma$. A square is a weak vertex, a circle a strong vertex, a straight line a pseudoscalar meson and a wiggly line a photon.

calculation. This we recalculated and the starting point is the two diagrams that contribute to the process, shown in Fig. 4.2.

Since photons at this order only couple to charged particles, there are only two different amplitudes and the results are

$$\begin{aligned} A^S_{+-\gamma} &= e\,F\left(G_8 + \frac{2}{3}\,G_{27}\right)(m_K^2 - m_\pi^2)\left[-k.\varepsilon\left(\frac{1}{r_1} - \frac{1}{r_2}\right)\right. \\ &\qquad \left. + p_1.\varepsilon\left(-\frac{1}{r_1} - \frac{1}{r_2}\right) + p_2.\varepsilon\left(\frac{1}{r_1} + \frac{1}{r_2}\right)\right], \end{aligned} \tag{4.37}$$

and

$$\begin{aligned} A_{+0\gamma} &= e\,F\,\frac{5}{6}\,G_{27}\,(m_K^2 - m_\pi^2)\left[-k.\varepsilon\left(\frac{1}{r_0} + \frac{1}{r_1}\right)\right. \\ &\qquad \left. + p_1.\varepsilon\left(-\frac{1}{r_0} - \frac{1}{r_1}\right) + p_2.\varepsilon\left(-\frac{1}{r_0} + \frac{1}{r_1}\right)\right]. \end{aligned} \tag{4.38}$$

These amplitudes can be decomposed into an electric and a magnetic part:

$$A(K \to 2\pi\gamma) = e\,\varepsilon^\mu(k)\,(E_\mu + \varepsilon_{\mu\nu\rho\sigma}M^{\nu\rho\sigma}), \tag{4.39}$$

but at lowest order the magnetic amplitude $M^{\nu\rho\sigma}$ vanishes since there is no $\varepsilon_{\mu\nu\rho\sigma}$ tensor in the corresponding lowest order Lagrangian.

The electric amplitude, on the other hand, is completely determined by the corresponding non–radiative amplitude via Low's theorem [28].

4.6.3 $K \to 3\pi\gamma$

The decay $K \to 3\pi\gamma$ is discussed in detail in [29]. We only need the lowest order amplitude for consistency with the calculation of $K \to 3\pi$. We have

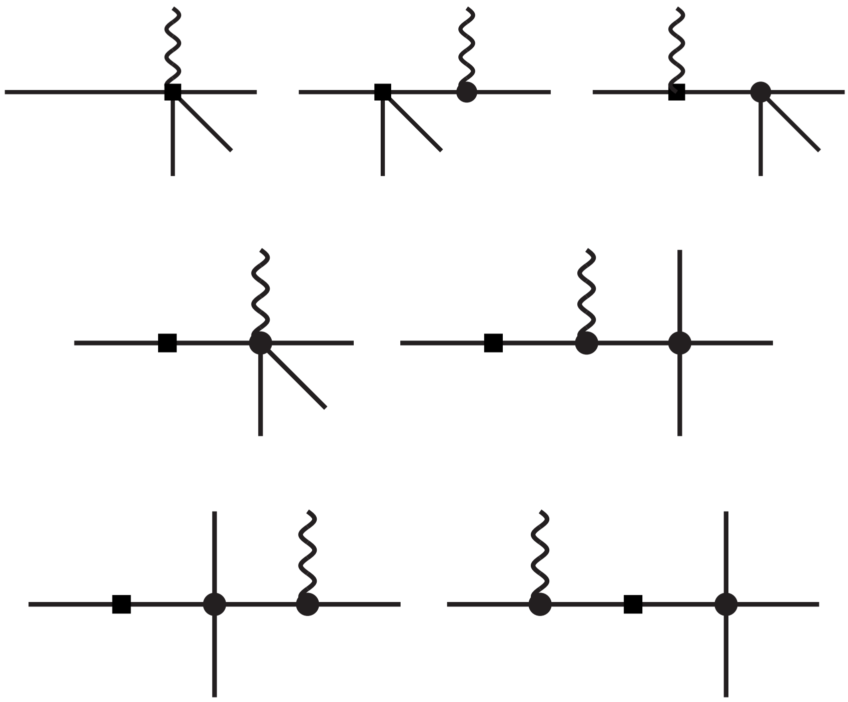

Figure 4.3: The diagrams for $K \to 3\pi\gamma$. A square is a weak vertex, a circle a strong vertex, a straight line a pseudoscalar meson and a wiggly line a photon.

calculated the four different amplitudes using Chiral Perturbation Theory, and checked that they agree with Low's theorem. The calculation is based on seven diagrams, see Fig. 4.3. The four amplitudes are

$$\begin{aligned} A^L_{+-0\gamma} \quad = \quad & i\,e\,\Bigg[\frac{G_8 - G_{27}}{3}\,m_K^2 + \left(-\frac{G_8}{3} - \frac{G_{27}}{6}\,\frac{-3\,m_K^2 + 8\,m_\pi^2}{m_\pi^2 - m_K^2}\right) \\ & (-3\,(s_{3\gamma} - 2\,t_1 - 2\,t_2) + m_K^2 + 3\,m_\pi^2)\left(\frac{p_1\cdot\varepsilon}{t_1} - \frac{p_2\cdot\varepsilon}{t_2}\right) \\ & -6\left(-\frac{G_8}{3} - \frac{G_{27}}{6}\,\frac{-3\,m_K^2 + 8\,m_\pi^2}{m_\pi^2 - m_K^2}\right)\times \\ & (t_2 + t_1)\left(\frac{p_1\cdot\varepsilon}{t_1} - \frac{p_2\cdot\varepsilon}{t_2}\right)\Bigg]\,, \end{aligned} \tag{4.40}$$

$$
\begin{aligned}
A^S_{+-0\gamma} &= i\,e\,\frac{5}{6}\left(-\frac{G_{27}}{m_\pi^2-m_K^2}\right)(2\,m_\pi^2-3\,m_K^2)\left[(s_{1\gamma}-s_{2\gamma})\left(\frac{p_1\cdot\varepsilon}{t_1}-\frac{p_2\cdot\varepsilon}{t_2}\right)\right.\\
&\left.+2\,t_0\left(\frac{p_1\cdot\varepsilon}{t_1}+\frac{k\cdot\varepsilon}{t_0}\right)+2\,t_0\left(\frac{p_2\cdot\varepsilon}{t_2}+\frac{k\cdot\varepsilon}{t_0}\right)\right], \qquad (4.41)
\end{aligned}
$$

$$
\begin{aligned}
A_{00+\gamma} &= i\,e\left[-\frac{G_8}{2}(m_K^2+m_\pi^2)+\frac{G_{27}}{m_\pi^2-m_K^2}(-5/3\,m_\pi^2\,m_K^2+13/6\,m_\pi^4\right.\\
&-1/2\,m_K^4)-\left(\frac{G_8}{2}+\frac{G_{27}}{m_\pi^2-m_K^2}(7/6\,m_\pi^2-17/6\,m_K^2)\right)\times\\
&(2\,(s_{3\gamma}-2\,t_1-2\,t_2)-m_K^2-3\,m_\pi^2)-\frac{G_{27}}{m_\pi^2-m_K^2}\,5/6\,(2\,m_\pi^2-3\,m_K^2)\\
&\left.\times(-(s_{3\gamma}-2\,t_1-2\,t_2)+m_K^2+3\,m_\pi^2)\right]\left(\frac{k\cdot\varepsilon}{t_0}+\frac{p_3\cdot\varepsilon}{t_3}\right), \qquad (4.42)
\end{aligned}
$$

$$
\begin{aligned}
A_{++-\gamma} &= i\,e\left[\left(-G_8\,(m_\pi^2+m_K^2)+G_{27}\,(m_K^2+13/3\,m_\pi^2)+(G_8-13/3\,G_{27})\times\right.\right.\\
&\left.(s_{3\gamma}-2\,t_1-2\,t_2)\right)\left(\frac{k\cdot\varepsilon}{t_0}+\frac{p_1\cdot\varepsilon}{t_1}+\frac{p_2\cdot\varepsilon}{t_2}-\frac{p_3\cdot\varepsilon}{t_3}\right)\\
&\left.+2\,(G_8-13/3\,G_{27})\,(t_2-t_1)\left(\frac{p_1\cdot\varepsilon}{t_1}-\frac{p_2\cdot\varepsilon}{t_2}\right)\right]. \qquad (4.43)
\end{aligned}
$$

Once again, these amplitudes can be decomposed into an electric and a magnetic part:

$$
A(K\to 3\pi\gamma)=e\,\varepsilon^\mu(k)\,(E_\mu+\varepsilon_{\mu\nu\rho\sigma}M^{\nu\rho\sigma}), \qquad (4.44)
$$

and the magnetic amplitude $M^{\nu\rho\sigma}$ vanishes for the reasons given above.

The electric amplitude at this order is again completely determined by the corresponding non–radiative amplitude $A(s,\nu)$ via Low's theorem [28, 29]:

$$
\begin{aligned}
E^\mu &= A(s,\nu)\,\Sigma^\mu\\
&\quad+2\frac{\partial A(s,\nu)}{\partial s}\Lambda^\mu_{12}+\frac{\partial A(s,\nu)}{\partial\nu}(\Lambda^\mu_{14}-\Lambda^\mu_{24})\\
&\quad+\mathcal{O}(k) \qquad (4.45)
\end{aligned}
$$

with (the meson charges in units of e are denoted q_i, with $\sum_{i=1}^4 q_i=0$)

$$
\begin{aligned}
s &= (p_1+p_2)^2\\
\nu &= k\cdot(p_1-p_2)
\end{aligned}
$$

G_E	-0.4	L_1^r	$0.38 \cdot 10^{-3}$
$\sin\epsilon$	$1.19 \cdot 10^{-2}$	L_2^r	$1.59 \cdot 10^{-3}$
Z	0.805	L_3^r	$-2.91 \cdot 10^{-3}$
F_π	0.0924 GeV	L_4^r	0
F_K	0.113 GeV	L_5^r	$1.46 \cdot 10^{-3}$
N_{14}	$-10.4 \cdot 10^{-3}$	L_6^r	0
N_{15}	$5.95 \cdot 10^{-3}$	L_7^r	$-0.49 \cdot 10^{-3}$
D_{13}	0	L_8^r	$1.0 \cdot 10^{-3}$
D_{15}	0	L_9^r	$7.0 \cdot 10^{-3}$

Table 4.1: The various input values used, LECs given at $\mu = 0.77$ GeV.

$$\begin{aligned}
\Sigma^\mu &= \sum_{i=1}^{4} \frac{q_i p_i^\mu}{t_i} \\
\Lambda_{ij}^\mu &= \Lambda_{ji}^\mu = (q_i t_j - q_j t_i) D_{ij}^\mu \\
D_{ij}^\mu &= -D_{ji}^\mu = \frac{p_i^\mu}{t_i} - \frac{p_j^\mu}{t_j} \ .
\end{aligned} \tag{4.46}$$

Since there are no terms of $\mathcal{O}(k)$ at lowest order in the chiral expansion, the leading–order electric amplitude is completely determined by the explicit terms in (4.45).

4.7 Numerical Results

4.7.1 Experimental Data and Input

For the numerical studies we use the input given in Table 4.1.

4.7.1.1 Strong and Electromagnetic Input

There are different ways to treat the masses, especially in the isospin limit case. In [9] the masses used in the phase space were obtained from the physical masses occurring in the decays. However, in the amplitudes the physical mass of the kaon involved in the process was used and the pion mass was given by $m_\pi^2 = \frac{1}{3}\sum_{i=1,3} m_{\pi^i}^2$ with $i = 1, 2, 3$ being the three pions participating in the reaction. This allowed for the correct kinematical relation $s_1 + s_2 + s_3 = m_K^2 + 3m_\pi^2$ to be satisfied while having the isospin limit in the amplitude but the physical masses in the phase space. The results in [9] were obtained with the physical mass for the eta. Results with the Gell-Mann-Okubo (GMO) relation for the eta mass in the loops gave small changes within the general errors given in [9].

In the decays here, we work to first order in isospin breaking. We have rewritten explicit factors of $m_u - m_d$ in terms of $\sin\epsilon$ according to

$$m_u - m_d = -\frac{1}{\sqrt{3}}\,(2\,m_s - m_u - m_d)\,\sin\epsilon\,. \tag{4.47}$$

In general we use the physical masses of pions and kaons in the loops but as soon as a factor of $\sin\epsilon$ or e^2 is present we use a common kaon and a common pion mass. This simplifies the analytical formulae enormously. The kaon mass chosen is the mass from the kaon in the decay and the pion mass used is $3m_\pi^2 = \sum_i m_{\pi^i}^2$ with $i = 1, 2, 3$ the three pions in the final state, i.e. the mass we used in the isospin limit case. For the eta mass we use in general the physical mass in the loop integrals. We have used the GMO mass relation with isospin violation included,

$$m_\eta^2 = \frac{2}{3}\,(m_{K^+}^2 + m_{K^0}^2 - m_{\pi^+}^2) + \frac{1}{3}\,m_{\pi^0}^2\,, \tag{4.48}$$

to simplify the amplitudes, except in the loops as stated above. The possible lowest order contributions from the eta mass have been removed from the amplitudes using the corresponding next-to-leading order relation as described in [11].

The strong LECs, L_1^r to L_8^r, as well as $\sin\epsilon$ come from the one-loop fit in [18], L_9^r from [30] and the G_E estimate is from [31].

The constant Z from $\mathcal{L}_{E2}$ we estimate via

$$Z = \frac{1}{2\,F_\pi^2\,e^2}\,(m_{\pi^+}^2 - m_{\pi^0}^2), \tag{4.49}$$

which corresponds to the value in Table 4.1. The higher order coefficients of $\mathcal{L}_{E4}$, $K_1^r \ldots K_{12}^r$, are rather unknown. Some rough estimates exist but we put them to zero here, at the relevant scale.

The IR divergences are canceled by adding the soft-photon Bremsstrahlung. We have used a 1 MeV cut-off in energy for this and used the same cut-off in the definition of F_{π^+} and F_{K^+}. We also use $m_\gamma = 1$ MeV, which effectively removes the infrared part.

The subtraction scale μ is chosen to be 0.77 GeV unless stated otherwise.

4.7.1.2 Input Relevant for the Photon Reducible Diagrams

The two constants D_{13} and D_{15} are set to zero since no knowledge exist of their values. One can determine the constants N_{14} and N_{15} from $K \to \pi l^+ l^-$ decays. For a detailed analysis, see [13]. The resulting values are given in Table 4.1. Note however, that as described in [13], D_{13}, D_{15}, N_{14} and N_{15} only contributes via the photon reducible diagrams. These diagrams are negligible numerically, unless the constants are orders of magnitude larger than expected.

4.7.2 Bremsstrahlung and Dependence on m_γ and ω

The isospin breaking amplitudes for $K \to 2\pi$ and $K \to 3\pi$ both depend on m_γ, introduced to regularize the infrared divergences coming from loops containing photons. This m_γ-dependence is canceled by adding the bremsstrahlung amplitudes, where a real soft photon is radiated off one of the mesons. This cancellation was checked for $K \to 3\pi$ in [13], and we have now also checked it for $K \to 2\pi$.

However, after the addition of bremsstrahlung the decay rates depend instead on ω, the cut-off energy of the radiated real photon. This is a parameter that should be set to a value depending on the experiment that one compares to.

Another possibility, which we use in this paper, is to add the full amplitudes with an extra radiated photon, $K \to 2\pi\gamma$ and $K \to 3\pi\gamma$. When doing that the decay rates should be independent of ω. We have checked this numerically and the results are presented in Table 4.2. For this comparison we have chosen $m_\gamma = 0.1$ MeV and varied omega over a large range. One can see that up to photon energies of 1 MeV, the sum is constant within the expected uncertainties. The different sum when including energies up to 10 MeV is an indication that the soft photon approximation, used in calculating the infrared contribution, is breaking down.

The way we treated the Bremsstrahlung contribution in the fits is as follows. We assume that the measured decay widths are including all photons. To compare to our amplitudes (calculated without hard photons), we therefore subtract numerically the calculated hard photon contributions from the experimental numbers.

4.7.3 Fit to $K \to 2\pi$

The process $K \to 2\pi$ in the presence of isospin breaking has been discussed in detail in [25]. We have reproduced that calculation but added in addition also all the isospin breaking contributions from the 27 amplitudes, except for the parts from the weak-electromagnetic 27 Lagrangian.

The isospin breaking corrections to the decay rates are rather small, but they have an impact on the phase shift between the $I = 2$ and $I = 0$ amplitudes, $\delta_2 - \delta_0$, as described in detail in [25]. Our results are compatible with the ones presented there. The phase shift we use here is defined via

$$\begin{aligned} A^S_{00} &= \frac{\sqrt{2}}{\sqrt{3}} A_0 - \frac{2}{\sqrt{3}} A_2 \,, \\ A^S_{+-} &= \frac{\sqrt{2}}{\sqrt{3}} A_0 + \frac{1}{\sqrt{3}} A_2 \,, \end{aligned}$$

ω (GeV)	IR photon (GeV)	Extra photon (GeV)	Sum (GeV)
	$K_S \to \pi^+\pi^-$		
0.01	$4.34 \cdot 10^{-17}$	$1.59 \cdot 10^{-17}$	$5.92 \cdot 10^{-17}$
0.001	$2.17 \cdot 10^{-17}$	$3.69 \cdot 10^{-17}$	$5.86 \cdot 10^{-17}$
0.0005	$1.52 \cdot 10^{-17}$	$4.34 \cdot 10^{-17}$	$5.85 \cdot 10^{-17}$
0.0001	0	$5.85 \cdot 10^{-17}$	$5.85 \cdot 10^{-17}$
	$K^+ \to \pi^+\pi^0$		
0.01	$4.30 \cdot 10^{-20}$	$1.54 \cdot 10^{-20}$	$5.84 \cdot 10^{-20}$
0.001	$2.15 \cdot 10^{-20}$	$3.61 \cdot 10^{-20}$	$5.77 \cdot 10^{-20}$
0.0005	$1.50 \cdot 10^{-20}$	$4.26 \cdot 10^{-20}$	$5.76 \cdot 10^{-20}$
0.0001	0	$5.77 \cdot 10^{-20}$	$5.77 \cdot 10^{-20}$
	$K_L \to \pi^+\pi^-\pi^0$		
0.01	$2.39 \cdot 10^{-21}$	$3.39 \cdot 10^{-22}$	$2.73 \cdot 10^{-21}$
0.001	$1.19 \cdot 10^{-21}$	$1.39 \cdot 10^{-21}$	$2.58 \cdot 10^{-21}$
0.0005	$8.34 \cdot 10^{-22}$	$1.74 \cdot 10^{-21}$	$2.58 \cdot 10^{-21}$
0.0001	0	$2.56 \cdot 10^{-21}$	$2.56 \cdot 10^{-21}$
	$K_S \to \pi^+\pi^-\pi^0$		
0.01	$5.88 \cdot 10^{-24}$	$8.93 \cdot 10^{-25}$	$6.77 \cdot 10^{-24}$
0.001	$2.94 \cdot 10^{-24}$	$3.43 \cdot 10^{-24}$	$6.37 \cdot 10^{-21}$
0.0005	$2.05 \cdot 10^{-24}$	$4.28 \cdot 10^{-24}$	$6.34 \cdot 10^{-21}$
0.0001	0	$6.29 \cdot 10^{-24}$	$6.29 \cdot 10^{-24}$
	$K^+ \to \pi^0\pi^0\pi^+$		
0.01	$3.77 \cdot 10^{-22}$	$4.03 \cdot 10^{-23}$	$4.18 \cdot 10^{-22}$
0.001	$1.89 \cdot 10^{-22}$	$1.98 \cdot 10^{-22}$	$3.86 \cdot 10^{-22}$
0.0005	$1.32 \cdot 10^{-22}$	$2.53 \cdot 10^{-22}$	$3.85 \cdot 10^{-22}$
0.0001	0	$3.83 \cdot 10^{-22}$	$3.83 \cdot 10^{-22}$
	$K^+ \to \pi^+\pi^+\pi^-$		
0.01	$5.05 \cdot 10^{-21}$	$5.86 \cdot 10^{-22}$	$5.63 \cdot 10^{-21}$
0.001	$2.52 \cdot 10^{-21}$	$2.73 \cdot 10^{-21}$	$5.25 \cdot 10^{-21}$
0.0005	$1.76 \cdot 10^{-21}$	$3.46 \cdot 10^{-21}$	$5.23 \cdot 10^{-21}$
0.0001	0	$5.19 \cdot 10^{-21}$	$5.19 \cdot 10^{-21}$

Table 4.2: $K \to 2, 3\pi$ decay rates calculated for different values on ω. Here we use $m_\gamma = 0.1$ MeV and the same value is used as a cut-off in the decay constants, see the appendix in [13].

$$
\begin{aligned}
A_{+0} &= \frac{\sqrt{3}}{2} A_2^+ \, , \\
\frac{A_2}{A_0} &= \left| \frac{A_2}{A_0} \right| e^{i(\delta_2 - \delta_0)} \, .
\end{aligned}
\tag{4.50}
$$

$K \to 2\pi$				
Order	μ [GeV]	G_8	G_{27}	$\delta_2 - \delta_0$
LO		10.4	0.55	$-60.3\,^\circ$
NLO	0.6	6.43	0.44	$-58.9\,^\circ$
NLO	0.77	5.39	0.36	$-58.0\,^\circ$
NLO	1.0	4.60	0.30	$-57.4\,^\circ$

Table 4.3: Quantities fitted from $K \to 2\pi$ only. The scale μ is the scale at which the unknown low energy constants are put to zero.

In the fits we have left $\delta_2 - \delta_0$ as an additional free parameter, as it is known that this phase is badly reproduced at one-loop order in ChPT. Note that because of the isospin breaking the A_2^+ amplitude is different from A_2.

We have performed a lowest order and a NLO fit to only the $K \to 2\pi$ amplitudes. In the NLO fit we set all the extra parameters, $\tilde{K}_i = K_i^r = Z_i^r = 0$ at the scale μ indicated. The Bremsstrahlung contribution has been subtracted as discussed above.

As can be seen in Table 4.3, there is a sizable variation depending on the input scale used. There is very little change in the absolute values of G_8 and G_{27} compared to the isospin limit fit of [9], where only the fit with $\mu = 0.77$ GeV was done. The angle is similar to the fit there, but this is a combination of two different effects. It was lowered because the new KLOE data have now been included in the PDG averaging, but the isospin breaking effects induced a positive correction as was also found in [25].

The values of G_8 and G_{27} are determined by fitting $CF_0^4 G_8$ and $CF_0^4 G_{27}$ and then setting $F_0 = F_\pi$ numerically to provide the numbers in the tables.

4.7.4 Fit to $K \to 2\pi$ and $K \to 3\pi$

The quantities we fit are the measured decay rates and the various parameters of the Dalitz plot distributions defined via

$$\left| \frac{A(s_1, s_2, s_3)}{A(s_0, s_0, s_0)} \right|^2 = 1 + gy + hy^2 + kx^2 \,. \tag{4.51}$$

For the decay $K_L \to 3\pi^0$, $k = h/3$ and $g = 0$. The decay $K_s \to \pi^+\pi^-\pi^0$ is included via

$$A^S_{+-0} = \gamma_S x - \xi xy \,. \tag{4.52}$$

The decay rates are included in the fit as follows. We subtract from the decay rates the Bremsstrahlung contributions as described above as a function of G_8 and G_{27}. We then convert the decay rate using the central values of

Decay	Width [GeV]	ChPT [GeV]	Fact. [GeV]
$K^+ \to \pi^+\pi^0$	$(1.1231 \pm 0.0078) \cdot 10^{-17}$	$1.123 \cdot 10^{-17}$	$1.127 \cdot 10^{-17}$
$K_S \to \pi^0\pi^0$	$(2.2828 \pm 0.0104) \cdot 10^{-15}$	$2.282 \cdot 10^{-15}$	$2.283 \cdot 10^{-15}$
$K_S \to \pi^+\pi^-$	$(5.0691 \pm 0.0108) \cdot 10^{-15}$	$5.069 \cdot 10^{-15}$	$5.069 \cdot 10^{-15}$
$K_L \to \pi^0\pi^0\pi^0$	$(2.6748 \pm 0.0358) \cdot 10^{-18}$	$2.618 \cdot 10^{-18}$	$2.698 \cdot 10^{-18}$
$K_L \to \pi^+\pi^-\pi^0$	$(1.5998 \pm 0.0271) \cdot 10^{-18}$	$1.658 \cdot 10^{-18}$	$1.711 \cdot 10^{-18}$
$K^+ \to \pi^0\pi^0\pi^+$	$(9.195 \pm 0.0213) \cdot 10^{-19}$	$8.934 \cdot 10^{-19}$	$8.816 \cdot 10^{-19}$
$K^+ \to \pi^+\pi^+\pi^-$	$(2.9737 \pm 0.0174) \cdot 10^{-18}$	$2.971 \cdot 10^{-18}$	$2.933 \cdot 10^{-18}$

Table 4.4: The various decay widths from the PDG tables [32], and our results from the main fit and the best factorization fit.

Decay	Quantity	Experiment	ChPT	Fact.
$K_L \to \pi^0\pi^0\pi^0$	h	-0.0050 ± 0.0014	-0.0062	-0.0025
$K_L \to \pi^+\pi^-\pi^0$	g	0.678 ± 0.008	0.678	0.654
	h	0.076 ± 0.006	0.088	0.083
	k	0.0099 ± 0.0015	0.0057	0.0068
$K_S \to \pi^+\pi^-\pi^0$	γ_S	$(3.3 \pm 0.5) \cdot 10^{-8}$	$3.0 \cdot 10^{-8}$	$2.9 \cdot 10^{-8}$
$K^\pm \to \pi^0\pi^0\pi^\pm$	g	0.638 ± 0.020	0.636	0.648
	h	0.051 ± 0.013	0.077	0.080
	k	0.004 ± 0.007	0.0047	0.0069
$K^+ \to \pi^+\pi^+\pi^-$	g	-0.2154 ± 0.0035	-0.215	-0.226
	h	0.012 ± 0.008	0.012	0.019
	k	-0.0101 ± 0.0034	-0.0034	-0.0033
$K^- \to \pi^-\pi^-\pi^+$	g	-0.217 ± 0.007		
	h	0.010 ± 0.006		
	k	-0.0084 ± 0.0019		

Table 4.5: Experimental values and the main fit and best factorization fit of the Dalitz plot distribution parameters. The data are from the PDG tables [32] except γ_S from [33].

the measured Dalitz plot distribution into a value for the amplitude squared at the center of the Dalitz plot. These squared amplitudes together with the parameters g, h, k and γ_S are used as the 18 experimental parameters to be fitted.

This means that the effect of Bremsstrahlung is included fully in the decay rates, but only via the soft photon approximation with a 1 MeV cut-off for the Dalitz plot distributions. We have not included the preliminary data from KTeV, NA48 and KLOE.

The number of free input parameters on the theory side is very large. Since it turns out that the isospin breaking effects are very small, we put those extra NLO parameters equal to zero at the scale μ indicated in the tables.

Let us repeat here the definitions of the various extra NLO parameters. The L_i^r are taken from the standard fit done at one loop to be compatible with the order of this calculation. The K_i^r are the extra parameters at NLO in the p^2e^2 sector. Those are always put to zero at the scale indicated. In the isospin limit 11 combinations of the weak NLO low-energy coefficients show up, as discussed in [9]. These are $\tilde{K}_i$, $i = 1, \ldots, 11$. In the presence of isospin breaking many more combinations of these, as well as from the weak octet order e^2p^2 Lagrangian, emerge and they were classified in [11]. The 27-part of the weak Lagrangian of order e^2p^2 has not been worked out and will lead to some more free parameters. We have not used any estimates of these extra parameters but set all of them to zero at the scale indicated, except for $\tilde{K}_i$, $i = 1, \ldots, 7$. The reason for this choice is that they are the leading contributions. $\tilde{K}_{1,2,3}$ are octet enhanced and come multiplied with factors of order m_K^4 and $\tilde{K}_{4,5,6,7}$ are 27-plets but also come multiplied with factors of order m_K^4. The neglected ones are thus suppressed by either isospin breaking, factors of m_π^2/m_K^2 or by the $\Delta I = 1/2$ rule, i.e. an extra factor of G_{27}/G_8.

4.7.4.1 General Fits

Here we perform the fits with similar assumptions as used in the isospin limit fit, as well as a few additional ones. First G_8 and G_{27} are extremely correlated with the values of $\tilde{K}_1$ and $\tilde{K}_4$ respectively. They are very difficult to obtain separately without additional assumptions. The main fit is therefore the one with

$$\tilde{K}_1 = \tilde{K}_4 = \tilde{K}_8 = \tilde{K}_9 = 0\,, \tag{4.53}$$

at a scale $\mu = 0.77$ GeV. The results are given in Table 4.6. This table is very similar to Table 6 in [9]. The large values of $\tilde{K}_6$ and the resulting large value of $\tilde{K}_7$ have the same origin as in that reference. In order to fit γ_S well, $\tilde{K}_6$ is put large because it gets multiplied there with a small factor and is the only one contributing. This in turn leads large values for $\tilde{K}_7$ to compensate in other places.

The fit with

$$\tilde{K}_6 = 0 \tag{4.54}$$

in addition has only a slightly larger χ^2 and a smaller $\tilde{K}_7$. The χ^2 is larger than in [9] because the experimental errors on several quantities have decreased since then. The overall fit is slightly better than the one of [9] because the newer measurements of the Dalitz distribution in $K^+ \to \pi^0\pi^0\pi^+$ agree better with the chiral expressions.

Constraint μ	Eq. (4.53) 0.77 GeV	Eq. (4.53) 1.0 GeV	Eq. (4.53) 0.6 GeV	Eq. (4.53,4.54) 0.77 GeV
G_8	5.39(1)	4.60(1)	6.43(1)	5.39(1)
G_{27}	0.359(2)	0.301(1)	0.438(2)	0.359(2)
$\delta_2-\delta_0$	$-57.(1.5)^o$	$-57.3(1.4)^o$	$-58.9(1.4)^o$	$-57.9(1.4)^o$
$10^3\tilde{K}_1/G_8$	$\equiv 0$	$\equiv 0$	$\equiv 0$	$\equiv 0$
$10^3\tilde{K}_2/G_8$	48.5(2.4)	56.5(2.4)	41.2(1.9)	46.6(1.6)
$10^3\tilde{K}_3/G_8$	2.6(1.2)	$-1.7(1.1)$	6.7(1.0)	3.5(0.8)
$10^3\tilde{K}_4/G_{27}$	$\equiv 0$	$\equiv 0$	$\equiv 0$	$\equiv 0$
$10^3\tilde{K}_5/G_{27}$	$-41.2(16.9)$	$-52.0(17.7)$	$-31.1(12.0)$	$-27.0(8.3)$
$10^3\tilde{K}_6/G_{27}$	$-102(105)$	$-114(105)$	$-93(76)$	$\equiv 0$
$10^3\tilde{K}_7/G_{27}$	78.6(33)	78.0(33.5)	79.6(22.7)	50.0(13.0)
$10^3\tilde{K}_8/G_8$	$\equiv 0$	$\equiv 0$	$\equiv 0$	$\equiv 0$
$10^3\tilde{K}_9/G_8$	$\equiv 0$	$\equiv 0$	$\equiv 0$	$\equiv 0$
χ^2/DOF	29.3/10	27.2/10	33.0/10	30.5/11

Table 4.6: The results for G_8 and G_{27} and the $\tilde{K}_i$ for the various constraints described in the text. In brackets are the MINUIT errors. The $\tilde{K}_i$ are quoted at the scale μ mentioned.

We get fits of roughly similar quality for all values of μ where the other parameters have been put to zero. The fits tend to be slightly better for the larger values of μ. The fitted values for the $\tilde{K}_i$ are μ-dependent, albeit not extremely strongly.

The $\tilde{K}_i$ themselves have a μ-dependence which is given by the cancellation of divergences, and this can be calculated from the known subtractions. We have shown the variation with μ from $\mu = 0.77\ GeV$, $\mu = 0.6$ GeV and $\mu = 1.0$ GeV for $\tilde{K}_i$, $i = 1,\ldots,11$ in Table 4.7

In order to compare with the factorization model of the weak low energy constants, we also perform a fit where all next-to-leading order LECs proportional to G_{27} are set to zero, but we keep in addition the sub-leading octet ones. This fit is shown for $\mu = 0.77$ GeV in Table 4.7. The fit is somewhat worse than those of Tab. 4.6 but not much. A very similar fit is obtained for $\mu = 1$ GeV with a χ^2 of 29.9. At $\mu = 0.6\ GeV$ the best solution found had a χ^2 of 57.8. This fit corresponds to

$$\tilde{K}_4 = \tilde{K}_5 = \tilde{K}_6 = \tilde{K}_7 = 0\,, \qquad (4.55)$$

and this type of fit is referred to below as an octet fit.

Constraint μ	Eq. (4.55) 0.77 GeV	μ variation 1.0 GeV	μ variation 0.6 GeV
G_8	4.84(1)	–	–
G_{27}	0.430(1)	–	–
$\delta_2 - \delta_0$	$-57.9(0.2)^o$	–	–
$10^3\tilde{K}_1/G_8$	2.0(1)	−5.88	5.61
$10^3\tilde{K}_2/G_8$	63.0(1.5)	−2.69	2.57
$10^3\tilde{K}_3/G_8$	−6.0(7)	0.159	−0.152
$10^3\tilde{K}_4/G_{27}$	$\equiv 0$	−9.93	9.48
$10^3\tilde{K}_5/G_{27}$	$\equiv 0$	0	0
$10^3\tilde{K}_6/G_{27}$	$\equiv 0$	27.0	−25.8
$10^3\tilde{K}_7/G_{27}$	$\equiv 0$	−21.5	20.5
$10^3\tilde{K}_8/G_8$	20.4(1)	−0.546	0.521
$10^3\tilde{K}_9/G_8$	9.1(1)	−2.92	2.79
$10^3\tilde{K}_{10}/G_8$	$\equiv 0$	11.6	−11.1
$10^3\tilde{K}_{11}/G_8$	$\equiv 0$	−1.66	1.58
χ^2/DOF	33.3/10	–	–

Table 4.7: The results for G_8 and G_{27} and the $\tilde{K}_i$ for the octet constraint described in the text. In brackets are the MINUIT errors. The $\tilde{K}_i$ are quoted at the scale μ mentioned. The last two columns are the values of the $\tilde{K}_i$ at the scale μ mentioned when they are zero at $\mu = 0.77\ GeV$ and run with $G_8 = 5.39$ and $G_{27} = 0.359$.

4.7.4.2 Fits to Factorization and other Models

Various models for the NLO weak constants exist. We will discuss here some of the ones which are presented in [23]. These have been discussed in that reference only for the pure octet case. So the quality of the models should be compared with the octet fit above.

A first choice is the resonance exchange domination of the weak constants. The problem here is that the weak decays of the resonances involve themselves many new unmeasured parameters and thus leads to fairly few general conclusions. If we assume that the vector octet exchange dominates, we get a relation between the octet NLO constants

$$N_1^r + N_2^r + 2N_3^r = 0\,, \tag{4.56}$$

which is a combination we can in fact determine. It translates for our parameters into

$$\tilde{K}_3 = -\frac{1}{2}\tilde{K}_2\,. \tag{4.57}$$

μ	0.77 GeV	0.9 GeV	0.842 GeV
G_8	4.18(1)	4.42	4.22(1)
G_{27}	0.360(2)	0.326(10)	0.339(10)
k_F	2.61(1)	4.94(2)	3.60(5)
χ^2/DOF	109/14	182/14	60.4/13

Table 4.8: The results for the fit with the factorization assumption for various values of μ including the optimal one.

It can be easily seen from Tables 4.6 and 4.7 that this is very far from being satisfied by our fits.

A very often used model is the factorization model. It corresponds to taking the underlying four quark operator and bosonizing separately the two quark currents present there. Looking at the dominant octet operators only for the cases that we need here, this leads to the relations [23]

$$\begin{aligned}
N_1^r &= 2k_f(32/3\,L_1^r + 4\,L_3^r + 2/3\,L_9^r)\,,\\
N_2^r &= 2k_f(16/3L_1^r + 4L_3^r + 10/3\,L_9^r)\,,\\
N_3^r &= 2k_f(8L_2^r - 2L_9^r)\,,\\
N_4^r &= 2k_f(-16/3\,L_1^r - 8/3\,L_3^r - 4/3\,L_9^r)\,,\\
N_5^r &= 2k_f(-L_5^r)\,,\\
N_6^r &= 2k_f(2/3\,L_5^r)\,,\\
N_7^r &= 2k_f(L_5^r)\,,\\
N_8^r &= 2k_f(4\,L_4^r + 2\,L_5^r)\,,\\
N_9^r &= N_{10}^r = N_{11}^r = N_{12}^r = N_{13}^r = 0\,.
\end{aligned} \tag{4.58}$$

The parameter k_f allows for some overall adjustment. The special value $k_f = 1/2$ is referred to as the Weak Deformation Model (WDM) [23, 34]. We have performed a fit leaving both k_f and μ free. Note that the scale μ is also the scale where we have put all the other NLO parameters equal to zero. The input values of the L_i^r have been scaled accordingly.

The fits done with k_f, G_8 and G_{27} as free parameters have χ^2 significantly larger than those reported above. Some representative values are shown in Table 4.8.

The fit with μ free gave a minimum at $\mu = 0.842$ GeV. The fits with μ outside the range of Table 4.8 had very large values of χ^2.

In order to show the quality of the fits we have given in Tables 4.4 and 4.5 also the values obtained for the quantities from the main fit and best factorization fit, labeled ChPT and Fact. respectively. Notice that the extrapolation to the full phase space here has been done from the amplitude squared in the center of the Dalitz plot using the experimental values for the distribution over the Dalitz plot.

4.8 Summary

We have recalculated in this paper the Bremsstrahlung amplitudes for $K \to 2\pi\gamma$ and $K \to 3\pi\gamma$. In addition we have calculated also the isospin violating effects to $K \to 2\pi$ including those with the 27-operators both for effects due to $m_u - m_d$ and electromagnetism. This we did to be consistent with the calculations of $K \to 3\pi$ done in [11, 13].

We have checked explicitly that the infrared divergences of the photon loops regulated by m_γ cancel between the virtual photon loops and the soft Bremsstrahlung. We checked in addition that the photon energy cut-off dependence cancels between the soft-photon Bremsstrahlung part and the part where hard photons are treated explicitly. We have not included the explicit expressions for the $K \to 2\pi$ amplitudes because they are rather long. They can be obtained from the authors or [27]. These amplitudes have passed all the standard tests, like cancellation of divergences from both NLO ChPT as well as the infrared singularities.

With these calculations and those published earlier in [11, 13], we have updated the fit to the CP conserving observables in the $K \to \pi\pi(\pi)(\gamma)$ system done in the isospin limit in [9]. As expected from the fairly small isospin violating effects found in [11, 13] and from the analysis of isospin breaking effects in the $K \to \pi\pi(\gamma)$ system of [25], the differences with the isospin conserving case are rather small. In addition we have studied the dependences on the subtraction scale μ, where the various assumptions are made. Our full amplitudes are μ independent as they should.

The fits show a similar quality to the ones performed earlier. The main differences are that the experimental Dalitz parameters have changed in $K^+ \to \pi^+\pi^+\pi^0$ and are now in better agreement with the ChPT fits. This is purely experimental and has nothing to do with the inclusion of isospin breaking effects. The total χ^2 is somewhat worse because the experimental errors on various partial widths have been reduced.

We also checked how well a few models of the NLO weak low energy constants work. The dominance by vectors and the weak deformation model gave a rather bad fit. The factorization model gave a somewhat better fit when an extra parameter, an overall scale factor, was allowed. The quality of this compared to the optimal ChPT fits can be judged from the tables giving the best fit values for the experimental quantities directly.

Acknowledgments

The program FORM 3.0 has been used extensively in these calculations [35]. This work is supported in part by the Swedish Research Council and European Union TMR network, Contract No. HPRN-CT-2002-00311 (EURIDICE).

References

[1] S. Weinberg, Physica A **96** (1979) 327.

[2] J. Gasser and H. Leutwyler, Annals Phys. **158** (1984) 142.

[3] J. Gasser and H. Leutwyler, Nucl. Phys. B **250** (1985) 465.

[4] A. Pich, Lectures at Les Houches Summer School in Theoretical Physics, Session 68: Probing the Standard Model of Particle Interactions, Les Houches, France, 28 Jul - 5 Sep 1997, hep-ph/9806303;
G. Ecker, Lectures given at Advanced School on Quantum Chromodynamics (QCD 2000), Benasque, Huesca, Spain, 3-6 Jul 2000, hep-ph/0011026.

[5] J. Kambor, J. Missimer and D. Wyler, Nucl. Phys. B **346** (1990) 17.

[6] J. Kambor, J. Missimer and D. Wyler, Phys. Lett. B **261** (1991) 496.

[7] G. Ecker, Prog. Part. Nucl. Phys. **35** (1995) 1, [hep-ph/9501357];
A. Pich, Rept. Prog. Phys. **58** (1995) 563, [hep-ph/9502366];
E. de Rafael, Lectures given at Theoretical Advanced Study Institute in Elementary Particle Physics (TASI 94): CP Violation and the limits of the Standard Model, Boulder, CO, 29 May - 24 Jun 1994, hep-ph/9502254.

[8] J. Bijnens, E. Pallante and J. Prades, Nucl. Phys. B **521** (1998) 305, [hep-ph/9801326].

[9] J. Bijnens, P. Dhonte and F. Persson, Nucl. Phys. B 648 (2003) 317, [hep-ph/0205341].

[10] E. Gamiz, J. Prades and I. Scimemi, JHEP **0310** (2003) 042, [hep-ph/0309172].

[11] J. Bijnens and F. Borg, Nucl. Phys. B **697** (2004) 319, [hep-ph/0405025].

[12] I. Scimemi, E. Gamiz and J. Prades, Invited talk at 39th Rencontres de Moriond on Electroweak Interactions and Unified Theories, La Thuile, Aosta Valley, Italy, 21-28 Mar 2004, hep-ph/0405204.

[13] J. Bijnens and F. Borg, hep-ph/0410333. To be published in Eur. Phys. J. C.

[14] A. Nehme, Phys. Rev. D **70**, 094025 (2004), [hep-ph/0406209].

[15] I. V. Ajinenko *et al.*, Phys. Lett. B **567**, 159 (2003), [hep-ex/0205027].

[16] A. Aloisio *et al.* [KLOE Collaboration], hep-ex/0307054.

[17] N. Cabibbo, Phys. Rev. Lett. **93** (2004) 121801, [hep-ph/0405001].

[18] G. Amorós, J. Bijnens, P. Talavera Nucl. Phys. B 602 (2001) 87, [hep-ph/0101127].

[19] J. A. Cronin, Phys. Rev. **161** (1967) 1483.

[20] G. Ecker, G. Isidori, G. Muller, H. Neufeld and A. Pich, Nucl. Phys. B **591** (2000) 419, [hep-ph/0006172].

[21] V. Cirigliano, M. Knecht, H. Neufeld, H. Rupertsberger and P. Talavera, Eur. Phys. J. C **23**, 121 (2002), [hep-ph/0110153].

[22] G. Esposito-Farese, Z. Phys. C **50** (1991) 255.

[23] G. Ecker, J. Kambor and D. Wyler, Nucl. Phys. B **394** (1993) 101, [hep-ph/0006172].

[24] R. Urech, Nucl. Phys. B **433**, 234 (1995), [hep-ph/9405341].

[25] V. Cirigliano, G. Ecker, H. Neufeld and A. Pich, Eur. Phys. J. C **33** (2004) 369, [hep-ph/0310351].

[26] J. Bijnens and M. B. Wise, Phys. Lett. B **137** (1984) 245;
B. R. Holstein, Phys. Rev. D **20** (1979) 1187;
S. Gardner and G. Valencia, Phys. Rev. D **62** (2000) 094024, [hep-ph/0006240],
C. E. Wolfe and K. Maltman, Phys. Lett. B **482** (2000) 77, [hep-ph/9912254];
V. Cirigliano, J. F. Donoghue and E. Golowich, Phys. Lett. B **450** (1999) 24,
V. Cirigliano, J. F. Donoghue and E. Golowich, Eur. Phys. J. C **18** (2000) 83, [hep-ph/0008290],
G. Ecker, G. Muller, H. Neufeld and A. Pich, Phys. Lett. B **477** (2000) 88, [hep-ph/9912264];

[27] These can be downloaded from `http://www.thep.lu.se/~bijnens/chpt.html`.

[28] F.E. Low, Phys. Rev. 110 (1958) 974.

[29] G. D'Ambrosio, G. Ecker, G. Isidori and H. Neufeld, Z. Phys. C **76** (1997) 301, [hep-ph/9612412].

[30] J. Bijnens and P. Talavera, JHEP **0203** (2002) 046, [hep-ph/0203049].

[31] J. Bijnens and J. Prades, JHEP **0006** (2000) 035, [hep-ph/0005189].

[32] S. Eidelman *et al.* [Particle Data Group Collaboration], Phys. Lett. B **592**, 1 (2004).

[33] R. Adler *et al.* [CPLEAR Collaboration], Phys. Lett. B **407** (1997) 193; R. Adler *et al.* [CPLEAR Collaboration], Phys. Lett. B **374** (1996) 313; A. Angelopoulos *et al.* [CPLEAR Collaboration], Eur. Phys. J. C **5** (1998) 389.

[34] G. Ecker, A. Pich and E. de Rafael, Nucl. Phys. B **291** (1987) 692.

[35] J. A. Vermaseren, math-ph/0010025.